



UNIVERSITY OF
KWAZULU-NATAL
—
INYUVESI
YAKWAZULU-NATALI

**Bio-inspired Solid Lipid Nanoparticles for therapeutic
siRNA Delivery: Targeting the LRRK2 G2019S Mutation
in a Parkinson's Disease cell model.**

by

Keelan Jagaran (215055447)

Discipline of Biochemistry, School of Life Science, College of Agriculture, Engineering and Science
at the University of KwaZulu-Natal (Westville)

2024

Supervisor:

Professor Moganavelli Singh

Abstract

Parkinson's disease (PD) is a progressive neurodegenerative disorder characterized by the loss of dopaminergic neurons and the presence of Lewy bodies. A significant genetic contributor to PD is the LRRK2 G2019S mutation, which leads to increased kinase activity and cellular dysfunction. Current treatments for PD are primarily palliative, necessitating an innovative gene delivery system adapted to a curative function. This study aimed to develop a therapeutic strategy using siRNA-mediated gene silencing to target the LRRK2 G2019S mutation and mitigate its pathogenic effects. A preliminary study demonstrated the proof of principle using *Ginkgo biloba* leaf extract (EGB)-functionalized sphingomyelin-cholesterol solid lipid nanoparticles (EGB-PLL-SLNPs). These SLNPs were successfully bio-synthesized using EGB, facilitating a dual therapy with favourable properties from the EGB and lipid components. Safety, biocompatibility, cytotoxicity, and cellular uptake efficiency were assessed through caspase and 3-[4,5-dimethylthiazol-2-yl]-2,5-diphenyltetrazolium bromide (MTT) cytotoxicity assays. The cellular uptake was assessed using the BLOCK-iT™ Fluorescent Oligo to provide a means of visualization through its ability to fluoresce on the wild-type SH-SY5Y (neuroblastoma) and embryonic kidney (HEK293) cells, confirming biocompatibility and efficient internalization, with cell viability exceeding 90%.

We further evaluated the therapeutic efficacy of EGB-PLL-SLNPs and compared them with the SLNPs without EGB (H₂O-PLL-SLNPs) in LRRK2 G2019S mutated SH-SY5Y cells. The EGB-PLL-SLNPs reduced ROS (+) levels by 51.39%, compared to a 31.27% reduction by their H₂O-based counterparts. The colour-based DNA damage assay showed that EGB-PLL-SLNPs decreased total DNA damage by 49.90%, whereas the H₂O-PLL-SLNPs achieved a 33.17% reduction. Additionally, EGB-PLL-SLNPs reduced kinase activity by 52.65%, surpassing the H₂O-PLL-SLNPs. The LRRK2 G2019S gene silencing efficiency of the siRNA complexed EGB-PLL-SLNPs was particularly notable, significantly decreasing the kinase activity and associated cellular dysfunction. The consistent efficacy of the EGB-PLL-SLNPs can be attributed to the bioactive components in EGB, which provided additional antioxidant and DNA repair benefits. These components enhance the LNPs' properties, facilitating better cellular uptake and siRNA delivery, highlighting the dual therapeutic capabilities of EGB and the therapeutic siRNA. The pathogenic effects of the LRRK2 G2019S mutation were effectively mitigated, with the findings suggesting that the EGB-PLL-SLNPs are highly effective nano vehicles for managing PD, particularly in cases involving the LRRK2 G2019S mutation. This study proposes a novel strategy for using EGB-PLL-SLNPs as a promising

treatment for PD and emphasizes the importance of natural products in advancing personalized medicine. The environmental safety, low toxicity, and cost-effectiveness of using EGB can make advanced therapeutics more accessible and sustainable for a broader range of neurodegenerative and genetic disorders.

Keywords: Parkinson's disease; gene therapy; siRNA; *Ginkgo biloba*; Solid lipid nanoparticles; sphingomyelin; cholesterol; nanomedicine; LRRK2 G2019S, kinase activity, gene silencing.

Preface

The experimental work described in this dissertation was carried out in the School of Life Sciences, University of KwaZulu-Natal, Westville campus, from January 2021 to November 2024, under the supervision of Professor Moganavelli Singh.

These studies represent original work by the author and have not otherwise been submitted in any form for any degree or diploma to any tertiary institution. Where use has been made of the work of others, it is duly acknowledged in the text.

Supervisors Declaration

The research contained in this dissertation was completed by the candidate while based in the Discipline of Biochemistry, School of Life Sciences, of the College of Agriculture, Engineering and Science, University of KwaZulu-Natal, Westville Campus, South Africa. The research was financially supported by the National Research Foundation (NRF).

The contents of this work have not been submitted in any form to another university and except where the work of others is acknowledged in the text, the results reported are due to investigations by the candidate.

As the candidate's supervisor I approve this thesis for submission.

A solid black rectangular box redacting the signature of the supervisor.

Signed: Prof Moganavelli Singh

Date:

Declaration 1: Plagiarism

I, Keelan Jagaran declare that:

1. The research reported in this thesis, except otherwise indicated, is my original research.
2. This thesis has not been submitted for any degree or examination at any other university.
3. This thesis does not contain any other persons' data, pictures graphs or other information, unless specifically acknowledged as being sourced from other persons.
4. This thesis does not contain other persons' writing unless specifically acknowledged as being sourced from other researchers. Where other written sources have been quoted, then:

A.Their words have been re-written but the general information attributed to them has been referenced.

B.Where their exact words have been used, then their writing has been placed in italics and inside quotation marks, and referenced.

5. This thesis does not contain text, graphics or tables copied and pasted from the internet, unless specifically acknowledged, and the source being detailed in the thesis and in the Reference Section.



Signed: Keelan Jagaran Date:

Declaration Plagiarism 22/05/08 FHDR Approved

Declaration 2: Publications

My role in each paper and presentation is indicated. The * indicates the corresponding author.

Published Papers

1. Jagaran, K., Singh, M*. Nanomedicine for Neurodegenerative Disorders: Focus on Alzheimer's and Parkinson's Diseases. *Int. J. Mol. Sci.*, **2021**, 22(16), 9082. DOI: <https://doi.org/10.3390/ijms22169082> (Appendix A1)
2. Jagaran, K., Singh, M*. Lipid Nanoparticles: Promising Treatment Approach for Parkinson's Disease. *Int. J. Mol. Sci.*, **2022**, 23(16), 9361. DOI: <https://doi.org/10.3390/ijms23169361> (Appendix A2)



Signed: Keelan Jagaran



Signed: Professor Moganavelli Singh

Date: October 2024

Dedications

To my loving parents, whose unwavering support and encouragement have been the foundation of my success. Your sacrifices, endless love, and resilience will always be my motivation.

To my late grandmother, though you are no longer with us, your memory, morals, and values live on in me and within my work. Your spiritual guidance and love are always felt.

To my dear grandmother, thank you for being a beacon of strength. Your hardworking attitude provides the motivation needed to succeed in every aspect of life.

Acknowledgments

I wish to extend my sincere appreciation and grateful to the people who have stood by me and allowed me to progress and complete this thesis, together with the institutions that have made this research possible.

- Firstly, I would like to give thanks to God for bestowing onto me the knowledge, protection, and guidance in all that I do and all that I am.

- Religious scriptures say that your first God is your teacher, and therefore, to Professor M Singh, thank you for all your support, guidance, and invaluable advice throughout this year of study. You have provided me with the opportunity to attain knowledge in such a vast and important field of study, with all your patience and time included. For that, I am eternally grateful.

- To my parents, family, and friends, thank you for always believing in me and being my motivators. No words can describe how thankful I am to you all.

- To all my colleagues at the Nano-gene and drug delivery lab for your kindness and willingness to help.

- To the **University of KwaZulu-Natal** for permitting this research and providing the facilities to achieve these goals.

- To the **BRICS STI Framework Programme and the National Research Foundation (NRF)** for funding this research initiative.

Contents

Abstract	I
Preface.....	III
Supervisors Declaration	IV
Declaration 1: Plagiarism.....	V
Declaration 2: Publications	VI
Dedications.....	VII
Acknowledgments.....	VIII
List of Tables	XVI
List of Figures	XVIII
List of Abbreviations	XXV
Chapter 1:.....	1
Introduction.....	1
1.1. Background.....	2
1.2. Rationale of the Study.....	4
1.3. Hypothesis.....	6
1.4. Aim and Objectives.....	6
1.4.1. Aim	6
1.4.2. Objectives	6
1.5. Outline of the Thesis.....	7
Chapter 2.....	11
Nanomedicine for Neurodegenerative Disorders: Focus on Alzheimer’s and Parkinson’s Diseases.....	11
Abstract:	12
2.1. Introduction.....	12
2.2. Neurodegenerative Diseases	14
2.2.1. Parkinson’s Disease (PD) and Implicated Genes.....	17
2.2.2. Alzheimer’s Disease (AD) and Implicated Genes	20

2.3. Nanoparticles and Nanomedicine	21
2.3.1. Challenges Facing Nanoparticles	24
2.3.2. Crossing the Blood–Brain Barrier	25
2.3.3. Gene Therapy	27
2.3.4. Nanomedicine in Clinical Trials—Update	30
2.4. Conclusions	31
Chapter 3	42
Lipid Nanoparticles: Promising Treatment Approach for Parkinson’s Disease	42
Abstract:	43
3.1. Introduction	44
3.2. Parkinson’s Disease	45
3.2.1. Neuropathological Hallmarks of Parkinson’s Disease	45
3.2.2. Clinical Manifestations and Determinants of Parkinson’s Disease	46
3.2.3. Current Therapeutics	48
3.3. Nanomedicine	49
3.3.1. Lipid Nanoparticles	51
3.3.2. Liposomes	53
3.3.3. Solid Lipid Nanoparticles and Nanostructured Lipid Carriers	54
3.4. LNPs and the Blood–Brain Barrier	55
3.4.1. LNPs for Parkinson’s Disease	57
3.4.2. An Update on Clinical Trials Using Lipid Nanoparticles	58
3.5. Conclusions and Future Perspectives	59
Chapter 4	67
The synergistic use of <i>Ginkgo biloba</i> in the biosynthesis of nanoparticles and as a therapeutic agent in Parkinson's Disease	67
Abstract.	68
4.1. Introduction	68

4.2. Parkinson's Disease: A Brief Overview	70
4.2.1. Current therapeutics	71
4.3. Traditional Therapeutics: <i>G. biloba</i> Extract	73
4.4. Merging Traditional with Modern Medicine: Biological Nanoparticle Synthesis	76
4.4.1. <i>Ginkgo biloba</i> as a Reducing Agent	77
4.4.2. General benefits of Plant Extracts.....	78
4.5. Traversing the Blood-Brain Barrier with <i>G. biloba</i> Synthesized Lipid Nanoparticles.....	79
4.5.1. Further enhancement of the BBB with EGB	82
4.6. Conclusions and Future Prospects	83
Chapter 5	92
Therapeutic Potential of Sphingomyelin-cholesterol based Solid Lipid Nanoparticles in Parkinson's Disease: Targeting the LRRK2 G2019S Mutation using therapeutic siRNA	92
Abstract	93
5.1. Introduction.....	93
5.2. The LRRK2 Mutation in Parkinson's Disease (PD).....	95
5.2.1. LRRK2 Associated Signalling Pathways.....	96
5.2.2. The Impact of the LRRK2 G2019S Mutation.....	97
5.2.3. Current Therapeutics.....	101
5.3. Solid Lipid Nanoparticles (SLNPs)	102
5.3.1. Sphingomyelin	104
5.3.2. Cholesterol	106
5.3.3. Synergism of Sphingomyelin-Cholesterol Solid Lipid Nanoparticles (SC-SLNPs).....	107
5.3.3.1. Synthesis and Characterization Approaches	107
5.3.3.2. SC-SLNPs Synergism Offering Enhanced Properties	109
5.3.3.3. Overcoming the Blood-Brain Barrier: SC-SLNPs for Neuroprotection and Gene silencing in PD.....	109
5.4. Applicability in RNA Interference (RNAi)	110
5.4.1. siRNA for targeting the LRRK2 G2019S Mutation	112

5.4.2. Optimizing siRNA Delivery	113
5.5. Conclusion	115
5.6. Future Recommendations	116
Chapter 6.....	128
Bio-inspired Polymeric Solid Lipid Nanoparticles for siRNA delivery: Cytotoxicity and Cellular Uptake <i>in vitro</i>	128
Abstract:	129
6.1. Introduction.....	129
6.2. Materials and Methods.....	132
6.2.1. Materials.....	132
6.2.2. Sample Collection and Preparation.....	132
6.2.3. Synthesis of Sphingomyelin-Cholesterol SLNPs (SC-SLNPs)	133
6.2.4. Functionalization of SC-SLNPs with Poly-L-lysine (PLL).....	134
6.2.5. Preparation of PLL-SC-SLNPs:siRNA nanocomplexes.....	134
6.2.6. Characterization	134
6.2.7. siRNA Binding Studies.....	135
6.2.7.1. Ethidium Bromide Intercalation Assay.....	135
6.2.7.2. Band Shift Assay.....	135
6.2.7.3. RNase A Protection Assay.....	136
6.2.8. Cell Culture.....	136
6.2.9. Cytotoxicity Studies.....	138
6.2.10. Caspase 3/7 Assay.....	139
6.2.11. Cellular Uptake Studies	139
6.2.12. Statistical Analysis.....	139
6.3. Results.....	140
6.3.1. Characterization	140
6.3.1.1. UV-visible (UV-vis) and FTIR Spectroscopy	140

6.3.1.2. Transmission Electron Microscopy (TEM) and Dynamic Light Scattering (DLS)	143
6.3.2. siRNA Binding Studies	145
6.3.2.1. Ethidium Bromide (EtBr) Intercalation Assay	145
6.3.2.2. Band Shift Electrophoresis	145
6.3.2.3. RNase A Protection Assay	147
6.3.3. Mycoplasma Detection	149
6.3.4. Cytotoxicity Assay	149
6.3.5. The Caspase 3/7 Assay	150
6.3.6. Cellular Uptake	152
6.4. Discussion	156
6.5. Conclusions	159
Chapter 7	164
Targeting the LRRK2 G2019S Mutation of Parkinson's Disease: The Therapeutic Efficiency of Bio-Synthesized Solid Lipid Nanoparticles for siRNA-Mediated Gene Therapy	164
Abstract	165
7.1. Introduction	165
7.2. Materials and Methods	167
7.2.1. Materials	167
7.2.2. PLL-SC-SLNPs: Synthesis	168
7.2.3. PLL-SC-SLNPs: Characterisation and Binding Studies	168
7.2.4. Cell Culture and LRRK2 G2019S Transfection	168
7.2.5. Cellular Uptake Studies	169
7.2.6. The 3-[4,5-dimethylthiazol-2-yl]-2,5-diphenyltetrazolium bromide (MTT) Assay	169
7.2.7. Caspase 3/7 Assay	170
7.2.8. NanoBRET [®] -TE Intracellular Kinase Assay	170
7.2.9. Oxidative Stress Assay	170

7.2.10. Multi-Colour DNA Damage Assay	171
7.2.11. Mitopotential Assay	171
7.3. Results.....	172
7.3.1. Synthesis, characterization and siRNA Binding Studies	172
7.3.2. Cellular Uptake Studies	173
7.3.2.1. BLOCK-iT™ Fluorescent Oligo Assay.....	173
7.3.3. siRNA:PLL-SLNPs Safety Profiles	176
7.3.3.1 The MTT Assay	176
7.3.3.2. Caspase 3/7 Assay.....	178
7.3.4. Gene Silencing Studies	180
7.3.4.1. Kinase Activity Assay.....	180
7.3.4.2. Oxidative Stress	182
7.3.4.3. Multi-colour DNA Damage Assay	185
7.3.4.4. Mitopotential Assay	189
7.3.4.5. Summary of inhibition of LRRK2 G2019S activity	193
7.4. Discussion	195
7.5. Conclusion	200
7.6. Future Recommendation.....	201
Chapter 8:.....	207
Summary, Conclusions, Limitations and Future Recommendations	207
8.1. Summary	208
8.3. Conclusion and future recommendations.....	210
Appendix B1	c
Appendix B2	d
Appendix B3	e
Appendix B4.....	f
Appendix B5	g

Appendix B6h
Appendix C1i

List of Tables

	Chapter 2	Pg.
Table 2.1.	Common drugs employed to treat the symptoms of Alzheimer's disease (adapted from [18]).	16
Table 2.2.	Common drugs used to treat the symptoms of Parkinson's disease (adapted from [19]).	17
Table 2.3.	Application of nanoparticles in neurodegenerative studies since 2017.	30
	Chapter 3	Pg.
Table 3.1.	Genes commonly implicated in the onset of Parkinson's disease.	48
Table 3.2.	The three broad classes of nanoparticles currently used in nanomedicine.	51
Table 3.3.	Some surface modifications to NPs for targeting the brain and increasing adsorption.	56
	Chapter 4	Pg.
Table 4.1.	Some approaches and drugs that are used for the treatment of PD.	72
	Chapter 5	Pg.
Table 5.1.	Neuronal implications associated with the hyperphosphorylation caused by the LRRK2 G2019S mutation.	98
Table 5.2.	Portraying the current research advancements in the therapeutic against the LRRK2 G2019S mutation.	101
Table 5.3.	The three structures of the SLNPs and their synthesis methods (Adapted from [72]).	103

Table 5.4. Portraying the chemical modification and their relevant benefits. 112

Table 5.5. Positive outcomes of various LNP formulations on Disorders presented. 114

Chapter 6 **Pg.**

Table 6.1. Absorbance peaks and troughs exhibited by the SLNPs. 141

Table 6.2. The wavenumbers (cm^{-1}) associated with the respective functional groups as confirmed by FTIR [30-32,34-39]. 142

Table 6.3 TEM and DLS nanoparticle and nanocomplex sizes and zeta potential and polydispersity index (PDI) obtained from DLS 144

Chapter 7 **Pg.**

Table 7.1. Caspase 3/7 analysis on the transfected SH-SY5Y and HEK293 cell lines outlining the apoptotic index and cell viability among all therapeutics 178

Table 7.2. Results obtained from the oxidative stress portraying the ROS (-) and ROS (+) cells in the wild type and transformed SH-SY5Y and HEK293 cells. 182

Table 7.3. Results obtained from the Multi-colour DNA damage assay portraying the level of DNA damage in the wild type and transformed SH-SY5Y and HEK293 cells. 186

Table 7.4. Results obtained from the MitoPotential assay depicting the levels of live and depolarized cells in wild-type and transformed SH-SY5Y and HEK293 cells. 190

List of Figures

Chapter 2:		Pg.
Figure 2.1.	The appearance of amyloid plaques in Alzheimer's disease and α -synuclein inclusions in the neocortical neurons in Parkinson's disease.	15
Figure 2.2	Broad classes of nanoparticles showing those commonly used in nanomedicine.	22
Figure 2.3.	Ideal criteria required for the development of a safe and efficient nanoparticle for use in nanomedicine.	24
Figure 2.4.	Common mechanisms for passage through the BBB. (A) Carrier-mediated transporter, (B) receptor-mediated transcytosis and (C) adsorptive-mediated transcytosis.	26
Chapter 3:		Pg.
Figure 3.1.	Commonly used drugs (shaded) are grouped with their functions (white) and PD therapeutics. Adapted from [33].	49
Figure 3.2.	An illustration of a lipid nanoparticle showing the outer phospholipid layer and the encapsulated therapeutics.	52
Figure 3.3.	Illustration of a liposome and encapsulation of hydrophilic and hydrophobic molecules.	53
Figure 3.4.	General structure of (A) solid lipid nanoparticles (SLNPs) and (B) nanostructured lipid carriers (NLCs).	54
Figure 3.5.	Important factors to consider when designing lipid nanoparticles for drug delivery. Adapted from [90].	57
Chapter 4:		Pg.
Figure 4.1.	An illustration of the symptoms associated with Parkinson's Disease.	71
Figure 4.2.	Chemical composition of <i>G.biloba</i> and their beneficial properties.	74
Figure 4.3.	Bottom-up biosynthesis process using plant extracts.	77
Figure 4.4.	The composition of the blood-brain barrier.	79
Figure 4.5.	Receptor-mediated transcytosis across the BBB utilizing LNPs synthesized with EGB.	82
Chapter 5:		Pg.
Figure 5.1.	The LRRK2 gene portraying the multidomain protein-protein interactions and the catalytic core with the potential pathogenic mutations (Adapted from [17]).	96

Figure 5.2.	Impact of the LRRK2 G2019S mutation on the phosphorylation of Rab GTPases in PD onset.	99
Figure 5.3.	Structure of Sphingomyelin	105
Figure 5.4.	Advantages of the incorporation of Cholesterols in SLNPs (Adapted from [100]).	107
Figure 5.5.	Schematic portraying the synthesis and characterization approaching in SLNPs.	108
Figure 5.6.	Disadvantages of unmodified and unconjugated naked siRNA molecules in circulation (Adapted from [104]).	111
Chapter 6:		Pg.
Figure 6.1.	<i>Ginkgo biloba</i> leaves used for the extraction process.	133
Figure 6.2.	Schematic illustration for the synthesis of the SC-SLNPs.	134
Figure 6.3.	Morphology of the (A) SH-SY5Y cells at 40x and 100x magnification; and (B) HEK293 cells at 100x magnification.	138
Figure 6.4.	UV-vis spectra of EGB-SLNPs, H ₂ O-SLNPs, EGB-PLL-SLNPs, and H ₂ O-PLL-SLNPs. The amplified 320-420 nm section shows the peak and trough variations.	141
Figure 6.5.	FTIR Analysis of: (A) EGB; (B) EGB-SLNPs; (C) EGB-PLL-SLNPs; (D) H ₂ O-SLNPs; (E) H ₂ O-PLL-SLNPs.	142
Figure 6.6.	TEM micrographs of the SLNPs. (A) H ₂ O-SLNPs, (B) H ₂ O-PLL-SLNPs, (C) EGB-SLNPs, (D) EGB-PLL-SLNPs. Scale Bar = 200 nm	143
Figure 6.7.	Ethidium bromide intercalation assay of (A) EGB- and H ₂ O-PLL-SC-SLNPs and (B) EGB- and H ₂ O-SC-SLNPs with siRNA (0.3 µg/µL). The stepwise addition of the SLNPs resulted in a drop in fluorescence until a plateau or point of inflection was reached as in A. Where no RNA was bound to the SLNPs (B), there was no drop in the fluorescence as in B. Arrows indicate the inflection point in A.	145

Figure 6.8. The band shift assay. (A) EGB-PLL-SLNPs: Lanes 1 – 8 (0, 0.2, 0.4, 0.6, 0.8, 0.10, 0.12, 0.14 μg) and (B) H₂O-PLL-SLNPs: Lanes 1-8 (0, 0.1, 0.2, 0.3, 0.4, 0.5, 0.6, 0.7 μg). The siRNA was maintained at 0.5 μg . The red boxes indicate the optimum binding ratios, superseded by the supra-optimum ratio and preceded by the sub-optimum ratio. 146

Figure 6.9. The band shift assay after 12 months of storage of the SLNPs at 4 °C. (A) EGB-PLL-SLNPs: Lanes 1 – 8 (0.2, 0.4, 0.6, 0.8, 0.10, 0.12, 0.14 μg) and (B) H₂O-PLL-SLNPs: Lanes 1-8 (0, 0.1, 0.2, 0.3, 0.4, 0.5, 0.6, 0.7 μg). The siRNA was kept constant at 0.5 μg . The red and yellow arrows indicate the optimum binding ratios, superseded by the supra-optimum ratio and preceded by the sub-optimum ratio. 147

Figure 6.10. The RNase protection assay. In both (A) and (B), Lanes 1 and 2 contain the positive (undigested siRNA) and negative (digested siRNA) controls. (A) EGB-PLL-SLNPs: Lane 3-5 (0.2, 0.4, 0.6 μg) and (B) H₂O-PLL-SLNPs: Lanes 3 – 5 (0.1, 0.2, 0.3 μg). All nanocomplexes were complexed with the targeted siRNA (0.5 μg). 148

Figure 6.11. Agarose gel images of the RNase protection assay after 12 months of storage of the SLNPs at 4 °C. In both (A) and (B), Lanes 1 and 2 contain positive and negative controls. (A) EGB-PLL-SLNPs: Lane 3-5 (0.2, 0.4, 0.6 μg) and (B) H₂O-PLL-SLNPs: Lanes 3 – 5 (0.1, 0.2, 0.3 μg). All nanocomplexes were complexed with targeted siRNA (0.5 μg). 148

Figure 6.12. Mycoplasma detection. A: The positive control portraying the morphological and optical features of mycoplasma using the mycoplasma MORFS stock suspension. B: The results for the mycoplasma detection in the HEK293 cells. C: The results for the mycoplasma detection in the SH-SY5Y cells. 149

Figure 6.13. The MTT cytotoxicity assay in (A) HEK293 and (B) SH-SY5Y cells. High viability was recorded for all tested ratios, indicating minimal cytotoxicity of the nanocomplexes to both cell lines. Data are presented as means \pm standard deviation (n = 3). A significant difference was observed between 150

the treated cells and the control group ($***p < 0.001$; Tukey's multiple comparisons test).

Figure 6.14. Caspase 3/7 activity induced by the nanocomplexes at the three studied ratios in the (A) HEK293 and (B) SH-SY5Y cells. The cytographs depict the apoptotic responses of the HEK293 (A) and SH-SY5Y (B) cells following treatment with the PLL-SLNPs at the sub-optimum, optimum, and supra-optimum ratios. High cell viability (>75%), with minimal apoptosis induction, was noted.

151

Figure 6.15. Apoptosis Rates in HEK293 and SH-SY5Y cells following treatment with the siRNA: PLL-SLNP nanocomplexes at the sub-optimum, optimum, and supra-optimum (w/w) ratios. Apoptosis levels were determined from the caspase 3/7 activity recorded. No statistical significance (ns) was observed among all groups, indicating that each treatment maintained the initial apoptosis rate, supporting the safety of the treatments.

152

Figure 6.16. Fluorescent images showing cellular uptake in the HEK293 cells. (A) Control of HEK293 cells not treated with the fluorescent oligo, (B) Control of naked Block-IT™ oligo not complexed to the SLNPs, (C) Oligo: EGB-PLL-SLNPs in a 1:1 (w/w) ratio; (D) Oligo: EGB-PLL- SLNPs in a 2:1 (w/w) ratio; (E) Oligo:H₂O-PLL-SLNPs in a 1:1 (w/w) ratio; (F) Oligo:H₂O- PLL-SLNPs in a 2:1 (w/w) ratio. The cells were visualized at 100x magnification. Scale Bar = 200 μm.

153

Figure 6.17. HEK293 cells treated with BLOCK-iT™ fluorescent oligo (0.5 and 1.0 μg) conjugated to PLL-SLNPs at 1:1 and 2:1 (w/w) ratios. Intracellular fluorescence was measured after 24 hours. Control 1 = HEK293 cells only, and control 2 = naked/uncomplexed BLOCK-iT™ fluorescent oligo. Controls were compared to the nanocomplexes ($*** p < 0.001$).

154

Figure 6.18. Fluorescent images showing cellular uptake in the SH-SY5Y cells. (A) Control of SH-SY5Y cells not treated with the fluorescent oligo, (B) Control of naked Block-IT™ oligo not complexed to the SLNPs, (C) Oligo:EGB-PLL-SLNPs in a 1:1 (w/w) ratio; (D) Oligo:EGB-PLL- SLNPs in a 2:1 (w/w) ratio; (E) Oligo:H₂O-PLL-SLNPs in a 1:1 (w/w) ratio; (F)

Oligo:H₂O- PLL-SLNPs in a 2:1 (w/w) ratio. The cells were visualized at 100x magnification. Scale Bar = 200 μm. 154

Figure 6.19. SH-SY5Y cells treated with PLL-SLNPs conjugated to BLOCK-iT™ fluorescent oligo (0.5 and 1.0 μg) at 1:1 and 1:2 (w/w) ratios. Intracellular fluorescence was measured after 24 hours. Control 1 = SH-SY5Y cells only, and control 2 = naked BLOCK-iT™ fluorescent oligo. Controls were compared to the nanocomplexes (***) $p < 0.001$. 155

Chapter 7: Pg.

Figure 7.1. Fluorescent images showing cellular uptake in the SH-SY5Y cells. (A1) Control of SH-SY5Y cells not treated with the fluorescent oligo, (A2) Control of naked Block-IT™ oligo not complexed to the SLNPs, (B1 & 2) Oligo: EGB-PLL-SLNPs in a 1:1 (w/w) ratio; (B3 & 4) Oligo: EGB-PLL-SLNPs in a 2:1 (w/w) ratio; (B5 & 6) Oligo:H₂O-PLL-SLNPs in a 1:1 (w/w) ratio; (B7 & 8) Oligo:H₂O- PLL-SLNPs in a 2:1 (w/w) ratio. The cells were visualized at 100x magnification. Scale Bar = 200 μm. 174

Figure 7.2. Fluorescent images showing cellular uptake in the HEK293 cells. (A1) Control of HEK293 cells not treated with the fluorescent oligo, (A2) Control of naked Block-IT™ oligo not complexed to the SLNPs, (B1 & 2) Oligo: EGB-PLL-SLNPs in a 1:1 (w/w) ratio; (B3 & 4) Oligo: EGB-PLL-SLNPs in a 2:1 (w/w) ratio; (B5 & 6) Oligo:H₂O-PLL-SLNPs in a 1:1 (w/w) ratio; (B7 & 8) Oligo:H₂O- PLL-SLNPs in a 2:1 (w/w) ratio. The cells were visualized at 100x magnification. Scale Bar = 200 μm. 175

Figure 7.3. The transfection analysis portraying the Control 1 (Transformed HEK293 and SH-SY5Y cells only), control 2 (Naked BLOCK-iT™ Fluorescent Oligo) and the two ratios per PLL-SLNPs therapeutics (***) $p < 0.001$. 176

Figure 7.4. The MTT cytotoxicity in the transformed (A) SH-SY5Y and (B) HEK293 cells. Data are represented as means ± standard deviation (n = 3). ***) $p < 0.001$ are considered statistically significant between the corresponding means of each suboptimum, optimum, and supra-optimum nanocomplexes and the positive control (Tukey's multiple comparisons test). 177

- Figure 7.5.** Caspase 3/7 Assay of Therapeutic Nanocomplexes in (A) HEK293 and (B) SH-SY5Y Cells. The graph illustrates the apoptotic response of HEK293 and SH-SY5Y cells after treatment with EGB-PLL-SLNPs and H₂O-PLL-SLNPs. 179
- Figure 7.6.** Apoptosis Rates in HEK293 and SH-SY5Y cells following treatment with the siRNA: PLL-SLNP nanocomplexes (*w/w*) ratios. Apoptosis levels were determined from the caspase 3/7 activity recorded. No statistical significance (ns) was observed among all groups. 180
- Figure 7.7.** Impact of Therapeutic siRNA-Conjugated EGB-PLL-SLNPs and H₂O-PLL-SLNPs on Kinase Activity in Wild-Type and LRRK2 G2019S Transformed SH-SY5Y and HEK293 Cells. 181
- Figure 7.8.** The oxidative stress analysis of the therapeutic nanocomplexes on the wild type and transformed SH-SY5Y cells; (B) The normalization studies portraying the comparison of ROS (+) cells between the post-treated transformed SH-SY5Y cells and the wild-type control baseline. 183
- Figure 7.9.** The oxidative stress analysis pertaining to the various therapeutic groups on the wild type and transformed HEK293 cell lines; (B) The normalization studies portraying the comparison of ROS (+) cells between the post-treated transformed HEK293 cells and the wild-type control baseline. 184
- Figure 7.10.** The multi-colour DNA damage analysis pertaining to the various therapeutic groups on the wild type and transformed SH-SY5Y cells. (B) The normalization studies portraying the comparison of total DNA damaged (%) cells between the post-treated transformed SH-SY5Y cells and the wild-type control baseline 187
- Figure 7.11.** The multi-colour DNA damage analysis pertaining to the various therapeutic groups on the wild type and transformed HEK293 cells. (B) The normalization studies portraying the comparison of total DNA damaged (%) cells between the post-treated transformed HEK293 cells and the wild-type control baseline. 188

Figure 7.12. (A) The MitoPotential analysis pertaining to the various therapeutic groups on the wild type and transformed SH-SY5Y cell lines; (B) The normalization studies portraying the comparison of total depolarized (%) cells between the post-treated transformed SH-SY5Y cells and the wild-type control baseline. 191

Figure 7.13. The MitoPotential analysis pertaining to the various therapeutic groups on the wild type and transformed HEK293 cell lines; (B) The normalization studies portraying the comparison of total depolarized (%) cells between the post-treated transformed HEK293 cells and the wild-type control baseline. 192

Figure 7.14. A comprehensive overview of the therapeutic efficiency to silence the LRRK2 G2019S by assessing various pivotal indicators of cellular health in PD, including kinase activity, oxidative stress, DNA damage and MitoPotential and shown as (A) Percentage reduction and (B) Fold change. These were generated through the comparison of the post-treated cells with the control of untreated cells. 194

List of Abbreviations

Abbreviation	Full Name
PD	Parkinson's Disease
BBB	Blood-Brain Barrier
SN	Substantia Nigra
LSVT	Lee Silverman Voice Treatment
L-DOPA	Levodopa
CNS	Central Nervous System
LRRK2	Leucine-Rich Repeat Kinase 2
G2019S	Glycine-to-Serine mutation at codon 2019 in LRRK2
DJ-1	Protein associated with PD
siRNA	Small Interfering RNA
RISC	RNA-Induced Silencing Complex
ER	Endoplasmic Reticulum
HEK293	Human Embryonic Kidney 293 Cells
SLNPs	Solid Lipid Nanoparticles
LDH	Lactate Dehydrogenase
ROS	Reactive Oxygen Species
RNAi	RNA Interference
MTT	3-[4,5-Dimethylthiazol-2-yl]-2,5-diphenyltetrazolium bromide
TEM	Transmission Electron Microscopy
FTIR	Fourier Transform Infrared Spectroscopy
MLi-2	LRRK2 Inhibitor (MLi-2)
MOA-B	Monoamine Oxidase B
SNCA	Alpha-Synuclein (gene associated with PD)
GPCRs	G Protein-Coupled Receptors
ARs	Adenosine Receptors
UV-vis	Ultraviolet-Visible Spectroscopy

Chapter 1:
Introduction

1.1. Background

Parkinson's disease (PD) is a debilitating neurodegenerative disorder and the fastest-growing of its kind, affecting 6.1 million people in 2016 (Barnish and Barran, 2020). This was drastically increased in 2021, to 11.77 million people being affected globally (Luo et al., 2025). PD patients suffer from progressive movement disorders and various non-motor symptoms, including anosmia, sleep disturbances, depression, anxiety, and constipation (Schrag *et al.*, 2018; Noyce *et al.*, 2016). The disease, associated with dopamine deficiency and motor as well as non-motor deficits, necessitates ongoing remediation and therapeutic strategies. Current therapeutic options, such as dopamine agonists and replacements, monoamine oxidase-B inhibitors, and catechol-O-methyl transferase (COMT) inhibitors, remain palliative and are administered only after symptom onset (Jagaran and Singh, 2023).

The etiology of PD is not fully elucidated; however, a synergistic combination of genetic and environmental factors plays a pivotal role in its development. Genes such as the LRRK2 G2019S mutation should be extensively studied to determine, correct, and treat the root cause of PD (Lill, 2016). PD cases can be idiopathic or familial, with 5-10% of cases being familial. Familial cases are linked to mutations in multiple genes such as Parkin (PRKN), α -synuclein (SNCA), glucocerebrosidase (GBA), DJ-1, VPS35, and leucine-rich repeat kinase 2 (LRRK2) (Bandres-Ciga *et al.*, 2020). Among these, the LRRK2 G2019S mutation is the most common, accounting for 6-40% of familial cases. This large, multidomain protein (280 kDa) belongs to the ROCO superfamily, with G2019S being part of the kinase domain (Lee *et al.*, 2012; Jeong and Lee, 2020). LRRK2 plays a pivotal role in autophagy, lysosomal degradation, and vesicular trafficking (Hu *et al.*, 2023).

Currently, there is a lack of comprehensive knowledge about the molecular mechanisms regulating the kinase and GTPase activities of LRRK2. However, inter- and intra-molecular regulation is known to control its enzymatic activity (Jeong and Lee, 2020). The LRRK2 G2019S mutation has been identified to increase kinase activity compared to the wild type (WT). Studies on primary neuronal cultures show that overexpression of this gene consistently induces neuronal toxicity, impairing intracellular organelle functions, causing cell death, and shortening neurites (Madureira et al., 2020). Furthermore, LRRK2 transgenic (Tg) animal models have been developed to elucidate its role in PD further. For instance, *Drosophila* Tg models link LRRK2-G2019S mutations to age-dependent DA neuronal loss, locomotor defects, dopamine homeostasis dysregulation, and significantly reduced survival (Seegobin et al., 2020). *Caenorhabditis elegans* (*C. elegans*) Tg models show resultant neurodegeneration of

DA neurons, significant reduction in dopamine levels, and locomotor dysfunction (Caldwell et al., 2020). While LRRK2 inhibitors like MLI-2 have been utilized to treat familial cases by inducing protective effects on cellular senescence, lysosomal function, endosome maturation, and the axonal transport and localization of α -synuclein, reduced levels of LRRK2 lead to pulmonary fibrosis (Hu et al., 2023). Thus, exploring other therapeutic avenues is imperative.

In addition to the incomplete elucidation of familial case mechanisms, a major hindrance to PD therapeutics is the protective blood-brain barrier (BBB). This barrier, composed of pericytes and neural endothelial cells, tightly regulates and inhibits the entry of foreign substances, such as drugs, resulting in treatment being administered at lower dosages (Preetam et al., 2023). Consequently, an efficient delivery system to traverse the BBB is crucial. Nanomedicine has been extensively studied, with lipid nanoparticles (LNPs), particularly solid lipid nanoparticles (SLNPs), at the forefront. SLNPs exhibit high loading capacity, low cytotoxicity, increased permeability, bioavailability, and ease of surface modification for successful nucleic acid conjugation for gene therapy (Hangargekar et al., 2019). Their size range of 50-1000 nm makes them suitable for pharmaceutical transport.

Various lipids can be employed; however, sphingomyelin (SM) portrays advantageous properties against PD and crossing the BBB. SM, a phospholipid and sphingolipid, is highly concentrated in the plasma membrane and the myelin sheath surrounding nerve cell axons. These lipids are essential for impulse transmission, neurotransmitter receptor location, myelin sheath integrity, and BBB maintenance. Thus, SM containing SLNPs can serve as medicaments. Kim et al. (2020) elucidated the role of SM as an efficient carrier system due to its ability to cross the BBB and be metabolized by the spleen and liver, permitting clearance. In addition to SM, cholesterol (Chol) is added to enhance circulatory time *in vivo*, with improved pharmacokinetics and therapeutic properties. SM-Chol establishes cholesterol/sphingomyelin-enriched nanodomains in organelle membranes (e.g., golgi), which play a pivotal role in neurotransmitter release, synaptic plasticity, and regulating synaptic functions (Ariga, 2017). These properties are beneficial for developing efficacious therapeutic systems with excellent loading capabilities.

One promising approach is the biological synthesis of Chol-SM containing SLNPs using *Ginkgo biloba* (*G. biloba*) leaf extracts (EGB). The BBB comprises a class of G protein-coupled receptors (GPCRs) known as adenosine receptors (ARs), which regulate BBB permeability (Cheng et al., 2016). EGB contain ginkgolides A, B, C, bilobalide, and

kaempferol, which can effectively activate the A1R, making the BBB more permeable and inducing cellular changes such as decreased transendothelial electrical resistance, increased actinomyosin stress fiber formation, and altered tight junctions (Liang *et al.*, 2019). Furthermore, EGB provides a reversible opening of the BBB for four hours, preventing dysregulation in brain homeostasis (Liang *et al.*, 2019). It also serves as a monoamine oxidase-B (MOA-B) inhibitor, preventing the conversion of 1-methyl-4-phenyl-1,2,3,6-tetrahydropyridine (MPTP) to MPP⁺, thereby preventing decreased ATP production, oxidative stress, inhibition of cellular respiration, and cellular demise associated with PD (Taib and Mustapha, 2020; Wu *et al.*, 2021; Haga *et al.*, 2019; Prasad and Hung, 2020). This inhibition reduces the loss and minimizes the damage to dopaminergic neurons in the substantia nigra pars compacta (SNPC). Overall, the advantageous properties of EGB against PD include inhibiting disease development in A53T α -synuclein transgenic mice, maintaining dopamine homeostasis, decreasing oxidative damage, and improving locomotor activity (Kuang *et al.*, 2018).

While these approaches show high potential, treating the cause of PD is imperative. One therapeutic approach is RNA interference (RNAi), a post-transcriptional gene regulatory mechanism (Haiyong, 2019). This process is activated by double-stranded RNA molecules, comprising 21-25 nucleotides that are referred to as small interfering RNA (siRNA). These molecules can target specific mRNA sequences in mammalian cells, resulting in sequence-specific gene silencing through the degradation of target mRNA and suppression of gene expression (Jung *et al.*, 2021). However, siRNA requires a suitable vehicle for transport due to its high molecular weight, polyanionic behavior, and hydrophilic nature (Daniels and Singh, 2019). Therefore, conjugating siRNA to SLNPs ensures efficient and safe delivery to the targeted sequence and effective gene silencing.

This study aims to exploit these beneficial properties by developing a siRNA-based therapeutic to suppress the expression of LRRK2-G2019S using SLNPs reduced and loaded with EGB. This approach enables dual therapy for PD at both genetic and symptomatic levels.

1.2. Rationale of the Study

The novelty of this study lies in the innovative use of the EGB-based and poly-L-lysine (PLL) functionalized SLNPs (EGB-PLL-SLNPs) for targeted gene silencing in a PD cell model, specifically addressing the LRRK2 G2019S mutation. This approach showcases a significant

advancement in nanomedicine and sets a precedent for developing natural extract-based nanoparticle therapies. By demonstrating substantial reductions in oxidative stress, DNA damage, and kinase activity in mutated SH-SY5Y cells, this study provides a compelling proof-of-concept for the therapeutic potential of EGB-PLL-SLNPs. The implications for PD research are profound, offering a new avenue for mitigating the pathogenic effects of genetic mutations contributing to the disease. This study's findings can significantly improve the quality of life for PD patients by potentially slowing disease progression and alleviating symptoms.

siRNA delivery using SLNs has been widely explored due to their biocompatibility, ability to cross the BBB, and capacity for controlled release. Various SLN formulations have been developed using cationic lipids, PEGylation, and surface modifications with targeting ligands to enhance delivery efficiency. However, many existing approaches face challenges such as rapid clearance, low transfection efficiency, and toxicity concerns due to excessive cationic charges (Prabhakar and Banerjee, 2024). This study addresses these gaps by utilizing bio-inspired SC-SLNPs synthesized with Ginkgo biloba extract to enhance BBB penetration, improve biocompatibility, and provide additional neuroprotective benefits. The incorporation of poly-L-lysine (PLL) functionalization further stabilizes the siRNA complexes, improving their cellular uptake and gene silencing efficiency. This novel approach distinguishes itself from previous work by integrating a natural bioactive component to enhance therapeutic efficacy while maintaining safety and stability.

Furthermore, this research exemplifies the shift towards personalized medicine, where treatments are tailored to the genetic makeup of individual patients, enhancing therapeutic efficacy and minimizing adverse effects. Using bioactive natural extracts in a nanoparticle formulation represents a paradigm shift in nanomedicine, promoting safer and more effective treatments. EGB, being a natural product, is likely to offer better biocompatibility and reduced toxicity compared to synthetic compounds, ensuring environmental safety and reducing the risk of long-term adverse effects.

From an economic perspective, utilizing readily available natural extracts can lower production costs, making advanced therapies more accessible. The principles and methodologies established in this research can be extrapolated to other neurodegenerative diseases and genetic disorders, broadening the scope of gene-silencing technologies. This innovative approach can encourage further research and development, leading to new therapeutic strategies that harness the power of natural compounds and advanced drug delivery systems.

This study advances PD research and paves the way for transformative applications that enhance the potential for targeted, efficient, and biocompatible treatments for various diseases. The commitment to environmental safety, reduced toxicity, and cost-effectiveness underscores the broader impact of this research, highlighting its potential to revolutionize the future of personalized medicine and healthcare.

1.3. Hypothesis

This study hypothesizes that EGB-PLL-SLNPs loaded with small interfering RNA (siRNA) targeting the LRRK2 G2019S mutation will effectively deliver the siRNA to a PD cell model, resulting in significant gene silencing and neuroprotection, thereby mitigating the progression of Parkinson's disease (PD) at both genetic and symptomatic levels.

1.4. Aim and Objectives

1.4.1. Aim

This study aims to develop and evaluate the efficacy of EGB-PLL- SLNPs as a delivery system for siRNA targeting the LRRK2 G2019S mutation to achieve both gene silencing and neuroprotective effects in a PD cell model.

1.4.2. Objectives

- ❖ To synthesize sphingomyelin-cholesterol-containing SLNPs biologically, using *Gingko biloba* leaf extracts, using distilled water-suspended SLNPs (H₂O-SLNPs) as a comparator.
- ❖ To functionalize the SLNPs with poly-L-lysine and conjugate this to a therapeutic siRNA.
- ❖ To characterize SLNPs and nanocomplexes using UV-vis and FTIR spectroscopy, transmission electron microscopy (TEM) and dynamic light scattering (DLS).
- ❖ To determine the siRNA binding and compaction ability of these SLNPs.
- ❖ To determine the cellular uptake efficiency of the formulated therapeutics.
- ❖ To assess the *in vitro* cytotoxicity of the nanocomplexes using the MTT and caspase 3/7 assays.
- ❖ To determine the efficacy of the therapeutic nanosystem in mitigating the effects of the LRRK2 G2019S mutation by assessing their kinase activity, oxidative stress, DNA damage, and mitopotential assays.

1.5. Outline of the Thesis

- ❖ **Chapter One** provides a background and rationale for the study, including the aim and objectives.
- ❖ **Chapter Two** details the published review paper titled ‘Nanomedicine for Neurodegenerative Disorders: Focus on Alzheimer’s and Parkinson’s Diseases’
- ❖ **Chapter Three** details the published review paper titled ‘Lipid-based Nanoparticles: Promising Treatment strategies for Parkinson's Disease’.
- ❖ **Chapter Four** describes a submitted manuscript: “The synergistic use of *Ginkgo biloba* in the biosynthesis of nanoparticles and as a therapeutic agent in Parkinson's Disease.”
- ❖ **Chapter Five** discusses the prepared manuscript: “Therapeutic Potential of Sphingomyelin-cholesterol Solid Lipid Nanoparticles in Parkinson's Disease: Targeting the LRRK2 G2019S Mutation using therapeutic siRNA”.
- ❖ **Chapter Six** details the submitted manuscript: “Bio-inspired polymeric Solid Lipid Nanoparticles for siRNA delivery: Cytotoxicity and Cellular Uptake in a Parkinson's cell model.”.
- ❖ **Chapter Seven** discusses the prepared manuscript: “Targeting the LRRK2 G2019S Mutation of Parkinson’s Disease: The Therapeutic Efficiency of *Bio*-Synthesized Solid Lipid Nanoparticles for siRNA-Mediated Gene Therapy.”.
- ❖ **Chapter Eight** summarizes and provides the overall conclusion of the conducted research, together with future recommendations.

References

1. Barnish, M.S., Barran, S.M. A systematic review of active group-based dance, singing, music therapy and theatrical interventions for quality of life, functional communication, speech, motor function and cognitive status in people with Parkinson's disease. *BMC Neurol.*, **2020**, 20, 371. DOI: 10.1186/s12883-020-01938-3.
2. Luo, Y., Qiao, L., Li, M., Wen, X., Zhang, W., Li, X. Global, regional, national epidemiology and trends of Parkinson's disease from 1990 to 2021: findings from the Global Burden of Disease Study 2021. *Front. Aging Neurosci.*, **2025**, 16. DOI: 10.3389/fnagi.2024.1498756
3. Schrag, A., Anastasiou, Z., Ambler, G., Noyce, A., Walters, K. Predicting diagnosis of Parkinson's disease: a risk algorithm based on primary care presentations. *Mov. Disord.*, **2019**, 34, 480-486. DOI: 10.1002/mds.27616.
4. Noyce, A.J., Lees, A.J., Schrag, A.E. The prediagnostic phase of Parkinson's disease. *J Neurol Neurosurg Psychiatry*, **2016**, 87, 871-878. DOI: 10.1136/jnnp-2015-311890.
5. Lill, C.M. Genetics of Parkinson's disease. *Mol Cell Probes*, **2016**, 30, 386–96. DOI: 10.1016/j.mcp.2016.11.001.
6. Bandres-Ciga, S., Diez-Fairen, M., Kim, J.J., Singleton, A.B. Genetics of Parkinson's disease: An introspection of its journey towards precision medicine. *Neurobiol. Dis.*, **2020**, 137, 104782. DOI: 10.1016/j.nbd.2020.104782.
7. Lee, B.D., Dawson V.L., Dawson T.M. Leucine-rich repeat kinase 2 (LRRK2) as a potential therapeutic target in Parkinson's disease. *Trends Pharmacol. Sci.*, **2012**, 33, 365–373. DOI: 10.1016/j.tips.2012.04.001.
8. Jeong, G.R., Lee, B.D. Pathological Functions of LRRK2 in Parkinson's Disease. *Cells*, **2020**, 9, 2565. DOI: 10.3390/cells9122565
9. Madureira, M., Connor-Robson, N., & Wade-Martins, R. LRRK2: Autophagy and Lysosomal Activity. *Front. Neurosci.*, **2020**, 14. DOI: 10.3389/fnins.2020.00498.
10. Seegobin, S. P., Heaton, G. R., Liang, D., Choi, I., Ramirez, M. B., Tang, B., & Yue, Z. Progress in LRRK2-Associated Parkinson's Disease Animal Models. *Front. Neurosci.*, 2020, 14. DOI: 10.3389/fnins.2020.00674
11. Caldwell, K. A., Willicott, C. W., & Caldwell, G. A. Modeling neurodegeneration in *Caenorhabditis elegans*. *Dis. Model. Mech.*, 2020, 13(10). DOI: 10.1242/dmm.046110.
12. Hu, J., Zhang, D., Tian, K., Ren, C., Li, H., Lin, C., Huang, X., Liu, J., Mao, W., Zhang, J. Small-molecule LRRK2 inhibitors for PD therapy: Current achievements and future perspectives. *European Journal of Medicinal Chemistry*, **2023**, 256, 115475. DOI: <https://doi.org/10.1016/j.ejmech.2023.115475>.

13. Kim, J.K., Ahn, S.I., Kim, Y. Nanotherapeutics Engineered to Cross the Blood-Brain Barrier for Advanced Drug Delivery to the Central Nervous System. *J Ind Eng Chem.*, **2020**, 73, 8-18. DOI: 10.1016/j.jiec.2019.01.021
14. Ariga, T. The Pathogenic Role of Ganglioside Metabolism in Alzheimer's Disease-Cholinergic Neuron-Specific Gangliosides and Neurogenesis. *Mol Neurobiol.*, **2017**, 54, 623-638. DOI: 10.1007/s12035-015-9641-0.
15. Cheng, C.-C., Yang, Y.L., Liao, K.H., Lai, T.W. Adenosine receptor agonist 524 NECA increases cerebral extravasation of fluorescein and low molecular weight 525 dextran independent of blood-brain barrier modulation. *Sci Rep* 6, **2016**, 23882. Doi: 10.1038/srep23882.
16. Liang, W., Xu, W., Zhu, J., Zhu, Y., Gu, Q., Li, Y., Guo, C., Huang, Y., Yu, J., Wang, W., Hu, Y., Zhao, Y., Han, B., Bei, W., Guo, J. *Ginkgo biloba* extract improves brain uptake of ginsenosides by increasing blood-brain barrier permeability via activating A1 adenosine receptor signaling pathway. *Journal of Ethnopharmacology*, **2019**. Doi: <https://doi.org/10.1016/j.jep.2019.112243>.
17. Taib, C.N.M., Mustapha, M. MPTP-induced mouse model of Parkinson's disease: A promising direction of therapeutic strategies. *Bosn. J. Basic Med. Sci.*, **2020**, 21, 422–433. Doi: 10.17305/bjbms.2020.5181.
18. Wu, W.J., Lu, C.W., Wang, S.E., Lin, C.L., Su, L.Y., Wu, C.H. MPTP toxicity causes vocal, auditory, orientation and movement defects in the echolocation bat. *Neuroreport.*, **2021**, 32, 125–134. Doi: 10.1097/WNR.0000000000001574.
19. Haga H., Matsuo K., Yabuki Y., Zhang C., Han F., Fukunaga K. Enhancement of ATP production ameliorates motor and cognitive impairments in a mouse model of MPTP-induced Parkinson's disease. *Neurochem. Int.*, 2019, 129, 104492. Doi: 10.1016/j.neuint.2019.104492.
20. Prasad, E.M., Hung, S.Y. Behavioral Tests in Neurotoxin-Induced Animal Models of Parkinson's Disease. *Antioxidants.*, **2020**, 9, 1007. Doi: 10.3390/antiox9101007
21. Kuang, S., Yang, L., Rao, Z., *et al.* Effects of *Ginkgo biloba* Extract on A53T α -Synuclein Transgenic Mouse Models of Parkinson's Disease. *Canadian Journal of Neurological Sciences*, **2018**, 45, 182–187. DOI: 10.1017/cjn.2017.268.
22. Haiyong, H. RNA Interference to Knock Down Gene Expression. *Methods Mol Biol.*, **2019**, 1706, 293-302. DOI: 10.1007/978-1-4939-7471-9_16
23. Jung, J.Y., Ryu, H.J., Lee, S., Kin, D., Kim, M.J., Lee, E.J., Ryu, Y., Kim, S., Kim, K., Choi, E.Y., Ahn, H.J., Chang, S. siRNA Nanoparticle Targeting PD-L1 Activates Tumor Immunity and Abrogates Pancreatic Cancer Growth in Humanized Preclinical Model. *Cells*, **2021**, 10, 2734. DOI: 10.3390/cells10102734

24. Daniels, A.N., Singh, M. Sterically stabilized siRNA:gold nanocomplexes enhance c-MYC silencing in a breast cancer cell model. *Nanomedicine*, **2019**, 14, 1387-1401. DOI: 10.2217/nmm-2018-0462
25. Prabhakar, P., Banerjee, M. Nanotechnology in Drug Delivery System: Challenges and Opportunities. *Journal of Pharmaceutical Sciences and Research*, 2024, 12(4), 1-10.

Refer to Appendix C1 for the Turnitin Report.

Chapter 2

Nanomedicine for Neurodegenerative Disorders: Focus on Alzheimer's and Parkinson's Diseases

Nanomedicine for Neurodegenerative Disorders: Focus on Alzheimer's and Parkinson's Diseases

This chapter has been published in the *International Journal of Molecular Sciences*.

Jagaran, K.; Singh, M. Nanomedicine for Neurodegenerative Disorders: Focus on Alzheimer's and Parkinson's Diseases. *Int. J. Mol. Sci.* 2021, 22, 9082.

<https://doi.org/10.3390/ijms22169082>

Abstract: Neurodegenerative disorders involve the slow and gradual degeneration of axons and neurons in the central nervous system (CNS), resulting in abnormalities in cellular function and eventual cellular demise. Patients with these disorders succumb to the high medical costs and the disruption of their normal lives. Current therapeutics employed for treating these diseases are deemed palliative. Hence, a treatment strategy that targets the disease's cause, not just the symptoms exhibited, is desired. The synergistic use of nanomedicine and gene therapy to effectively target the causative mutated gene/s in the CNS disease progression could provide the much-needed impetus in this battle against these diseases. This review focuses on Parkinson's and Alzheimer's diseases, the gene/s and proteins responsible for the damage and death of neurons, and the importance of nanomedicine as a potential treatment strategy. Multiple genes were identified in this regard, each presenting with various mutations. Hence, genome-wide sequencing is essential for specific treatment in patients. While a cure is yet to be achieved, genomic studies form the basis for creating a highly efficacious nanotherapeutic that can eradicate these dreaded diseases. Thus, nanomedicine can lead the way in helping millions of people worldwide to eventually lead a better life.

Keywords: neurodegenerative disorders; gene therapy; nanomedicine; Parkinson's disease; Alzheimer's disease

2.1. Introduction

Neurodegenerative disorders, through the subsequent immune activation of the central nervous system (CNS), impose substantial burdens on the public and health sectors. While immune activation may aid in regeneration and repair, together with various other mechanisms such as the limitation of neurotropic viral infections and the removal of necrotic cells, it can also lead to the development of neurodegeneration, ischaemia, infections, and immune-mediated

disorders. Neurodegeneration is defined as the slow but gradual degeneration of neurons and axons in the CNS that results in abnormalities in cellular function and, consequently, cellular demise [1]. The ensuing symptoms stem from the degeneration stage, beginning with a loss of coordination and memory, to a complete loss of the ability to function as a normal healthy individual. The three major neurodegenerative disorders have been identified as Alzheimer's disease (AD), Parkinson's disease (PD), and amyotrophic lateral sclerosis (ALS) [2]. These diseases are closely linked to environmental cues, disordered immunity, advancing age, and the genetic make-up of the affected individual [3].

Although over 50 million people are believed to be affected by AD globally, these numbers are progressively increasing due to the increased average lifespan and genetic and environmental factors. An estimated 152 million of the population are projected to be affected by the year 2050 [4]. This will create an immense global economic strain in the years to come. Beyond AD, and based on the Parkinson's Foundation Prevalence Project, approximately 10 million individuals have presented with PD, with about one million belonging to the United States of America (USA) alone. These patients succumb to the high costs involved in their treatment over and above the complete alteration of their normal lives. This economic burden is estimated to be close to USD 52 billion per year in the USA [5]. The pathogenesis of the diseases above is initiated through the accretion, aggregation and alteration of the normal host proteins, the modification of tissue homeostasis, disrupted blood flow, and immunological damage [6,7]. To date, treatment of these diseases remains palliative, majorly as a result of the inability of therapeutic drugs and biomolecules to effectively traverse the blood–brain barrier (BBB) [8]. The limitations arise through the brain microvessel endothelial cells (BMVECs), creating brain capillaries. The high concentrations of drug-metabolizing enzymes and the expression of outward drug efflux transporters, together with low pinocytic potential and close intercellular junctions, restricts the passage of biomacromolecules and low molecular weight compounds from the blood to the brain [3]. The goal of optimal therapeutic outcomes stands firm in creating site-specific and safe therapeutic means of treating these life-changing diseases effectively.

This challenge of crossing the BBB could potentially be overcome via the utilization of novel therapeutic nano-delivery systems. Nanomedicine, the amalgamation of nanotechnology and medicine, involves the use of nanoscale-sized particles to safely and efficiently transport pharmacologically active agents (therapeutic drugs or genes) to diseased sites in the body, including the brain. Furthermore, exploiting the synergy between nanomedicine and gene

therapy may hold greater promise in treating various diseases, including monogenic disorders. Genetic alterations can characterize the onset of AD and PD. Comprehensive knowledge of these genetic aberrations is imperative in creating a treatment strategy that is both effective and specific to the type of the disease without harming normal body cells. Several genetic disorders, including cancer therapy, are being investigated by nanomedicine-based interventions, the clinical success of which will be determined in time. This review paper explores the possibility of utilizing nanomedicine and its potential role as an effective therapeutic strategy against two selected neurodegenerative disorders, Alzheimer's and Parkinson's disease.

2.2. Neurodegenerative Diseases

Neurodegenerative diseases form part of a heterogeneous group of disorders characterized primarily by the progressive and slow degeneration of the structure and function of the CNS. The classification of the various disease types is due to their clinical manifestations, such as cognitive and behavioural disorders, with pyramidal and extrapyramidal movement disorders being the most common [9]. There is gradual neuronal dysfunction and death due to oxidative stress, neuroinflammation, programmed cell death and proteotoxic stress, with abnormalities noted in the lysosomal/autophagosomal and ubiquitin– proteasomal systems [9].

While protein abnormalities define most neurodegenerative disorders, the clinical manifestations often only present themselves a while later, with more than one disease process being observed in a patient [10]. Furthermore, diagnostics are hindered due to a lack of available biomarkers, with the exception of rare cases where genetic mutations are identified as the causative agents [11]. The most common protein abnormality disorders are tauopathies, transactivation response DNA binding protein 43 (TDP-43) proteinopathies, amyloidosis, and α -synucleinopathies. The neuroanatomical and cellular distribution, together with abnormalities present in the protein conformations of the relevant disorders, constitute the histopathological features that allow for the neuropathological diagnosis of the disorder [9]. In AD, amyloid- β deposits (senile plaques) (Figure 2.1) are often seen in the neocortex, while tau inclusions such as a neurofibrillary tangle manifest in a neocortical neuron. In PD, α -synuclein inclusions (Figure 2.1) are commonly found in the neocortical neurons [12]. Unlike neuronal inclusions present in viral infections that contain foreign viral proteins, the aggregation of the abnormal proteins is composed of various cellular components and intrinsic neuronal proteins. These abnormalities have more amyloid-like properties, with filament formations and β -pleated sheet-enriched secondary structures [9]. The aggregation of proteins in these disparate

disorders portray templating, nucleation, multiplication, growth and spread. A reduction in these amyloidogenic proteins can regulate the concentration of the targeted proteins, thereby effectively impeding the growth and nucleation [13]. Since amyloid- β and tau proteins are reportedly discharged into the extracellular space, which is regulated by the activity of the neurons, targeting the cause of the disease progression, they may abrogate this discharge by halting their cellular release, transport, and uptake into cells, or by arresting their movement between cells. Hence, novel nano-therapeutics can be formulated to overcome the limitations of the current therapy while incorporating gene therapy to restrict the disease progression.

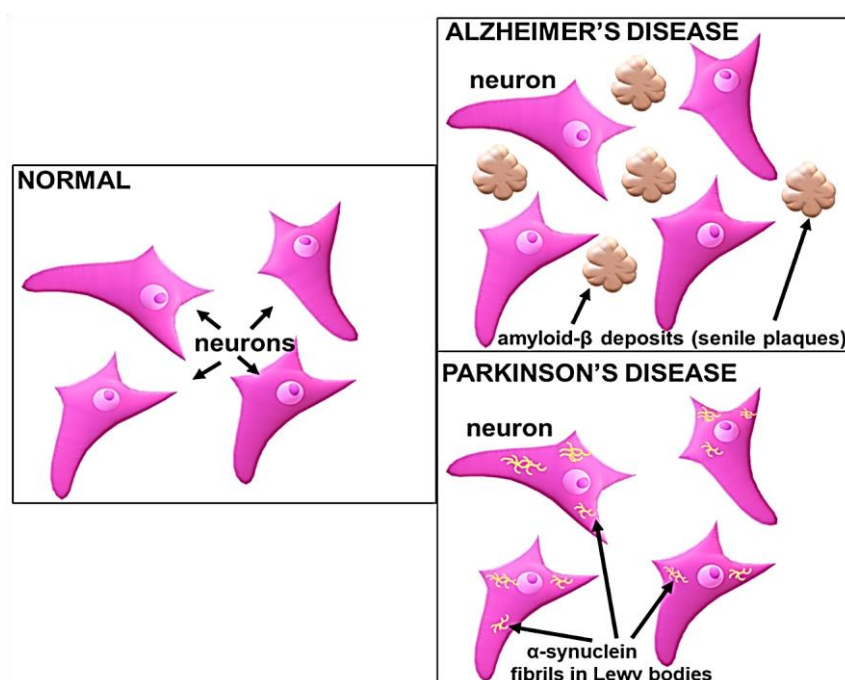


Figure 2.1. The appearance of amyloid plaques in Alzheimer’s disease and α -synuclein inclusions in the neocortical neurons in Parkinson’s disease.

To date, there is no cure available for these neurodegenerative disorders, with current treatment remaining palliative. Western medicine has provided relief to the symptoms experienced by patients suffering from these disorders, ranging from dopaminergic treatment for movement disorders related to PD to antipsychotic medication prescribed for dementia/AD to treat the psychological and behavioural symptoms [14,15]. To date, there are several drugs available that treat the symptoms of AD and PD (Tables 2.1 and 2.2). While some relief is noted in patients, the ever-progressing disease renders the drug therapy inadequate and ineffective [15]. Beyond this, the major limitation in drug therapy is the unfavourably low concentration of the drug that eventually localizes in the CNS following the systemic administration. This is

primarily due to the blood–brain barrier (BBB), which hinders the effective transport of the drugs to the brain [16].

While there are many neurodegenerative disorders that affect individuals, AD and PD are two of the most highly prevalent disorders, accounting for a significant portion of the global burden in respect to CNS disorders. These diseases can occur through genetic predisposition or sporadically through the interaction of genes with the environment. Genes involved in neurodegeneration, the metabolism of xenobiotics and the function of dopaminergic neurons have been observed to be associated with PD. In contrast, a polymorphism on the susceptibility gene of the epsilon 4 allele, apolipoprotein E gene (APOE), is strongly related to the onset of AD [17]. The use of nanomedicine and gene therapy could pave the way for novel treatment strategies for CNS-related diseases.

Table 2.1. Common drugs employed to treat the symptoms of Alzheimer’s disease (adapted from [18]).

Drug	Function
Donepezil (Aricept)	Cholinesterase Inhibitor
Galantamine (Razadyne)	Cholinesterase inhibitor
Tacrine (Cognex)	Cholinesterase inhibitor
Memantine (Namenda)	N-methyl-d-aspartate receptor blocker
Rivastigmine (Exelon)	Cholinesterase inhibitor
Memantine extended-release and donepezil (Namzaric)	N-methyl-d-aspartate receptor and acetylcholinesterase inhibitor

Table 2.2. Common drugs used to treat the symptoms of Parkinson’s disease (adapted from [19]).

Drug	Function
Carbidopa-levodopa (Sinemet, Parcopa, Rytary, Duopa)	Dopamine decarboxylase inhibitor/DA precursor
Levodopa (Inbrija)	Dopamine precursor
Entacapone (Comtan)	Catechol-o-methyltransferase inhibitor inhibits the breakdown of Levodopa
Tolcapone (Tasmar)	Catechol-o-methyltransferase inhibitor inhibits the breakdown of Levodopa
Opicapone (Ongentys)	Catechol-o-methyltransferase inhibitor inhibits the breakdown of Levodopa
Carbidopa/Levodopa Entacapone (Stalevo)	Dopamine decarboxylase inhibitor/DA precursor/COMT inhibitor
Pramipexole (Mirapex)	Dopamine agonist
Ropinirole (Requip)	Dopamine agonist
Apomorphine (Apokyn, Kynmobi)	Dopamine agonist
Rotigotine (Neupro)	Dopamine agonist
Selegiline (Eldepryl, Zelapar)	Monoamino oxidase-B inhibitor; inhibits breakdown of dopamine
Rasagiline (Azilect)	Monoamino oxidase B inhibitor; inhibits breakdown of dopamine
Safinamide (Xadago)	Monoamino oxidase-B inhibitor; inhibits breakdown of dopamine
Amantadine (Symmetrel, Gocovri, Osmolex)	Mixed mechanisms, including N-methyl-D-aspartate antagonism
Istradefylline (Nourianz)	Adenosine 2A antagonist
Trihexyphenidyl (Artane)	Anticholinergic
Benzotropine (Cogentin)	Anticholinergic

2.2.1. Parkinson’s Disease (PD) and Implicated Genes

In contrast to diseases such ALS, leukodystrophies, and lipid storage diseases, PD exhibits a confined, well-defined, and compact group of affected neurons. Studies pertaining to PD have

been made simpler due to the readily available rodent and primate models. Knowledge of the survival, function, and development of dopamine neurons is also well understood [20]. PD is primarily caused by neuronal damage in the substantia nigra (SN) of the brainstem, diminution of the nigrostriatal neurotransmitter and dystrophy of the associated projection fibres to the corpus striatum, leading to motor system malfunction that progresses to non-motor symptoms [20–22]. These affected cells are responsible for synthesizing dopamine and the control of movement via the innervation of the large area of the forebrain. Manifestations of symptoms are underappreciated prior to 60% loss of the substantia nigra pars compacta (SNpc) dopamine neurons, which causes a drastic loss (80%) of dopamine [23,24]. Early symptoms present as tremors, slowness of movement, rigidity, and walking difficulties, together with apathy, anxiety, and depression [25].

Genetic links in PD have been previously elucidated, with the first discovered genetic defect or mutation being present on the SNCA gene on chromosome 4, encoding for α -synuclein [26]. Further investigation revealed a duplication or triplication of SNCA that suggested that overexpression of α -synuclein could lead to toxicity and PD [27]. Other genes that have been identified include Leucine-Rich Repeat Kinase 2 (LRRK2), DJ-1, ubiquitin carboxyl-terminal esterase L1 (UCHL 1), phosphatase and tensin homolog (PTEN), and Parkin [21]. The most common monogenic mutation noted is in the LRRK2 gene, particularly mutations in Gly2019Ser, observed in patients presenting with autosomal dominant PD. This mutation type accounts for 1% of sporadic and 4% of familial PD worldwide. Apart from mutations in the Gly2019Ser, other mutations were noted in Arg1441His, Arg1441Cys, Arg1441Gly, Ile2020Thr, Tyr1699Cys and Asn1437His. This particular gene has various protein–protein interaction domains, together with an enzymatic core that brings about GTPase and serine–threonine kinase activities. The gene possesses the Gly2019Ser mutation in the kinase domain, adjacent to the Ras-of-complex (Roc) GTPase domain, which results in an unfavourable increase in the LRRK2 kinase activity [28]. It is due to this that current gene therapy techniques utilize this domain as a target for LRRK2 kinase inhibitors.

DJ-1, encoded by the PARK7 gene, is a highly conserved protein made up of 189 amino acids that are expressed under physiological conditions, initially linked to early-onset PD of a familial nature [29]. It was earlier reported that a mutation in the DJ-1 protein resulted in a disease with parkinsonian clinical manifestations such as tremors, dyskinesia, and rigidity [30]. Hence, the PARK7 gene serves as an interesting target for gene therapy, since it functions to protect against oxidative stress and is under-expressed in PD. Studies related to increasing DJ-

1 levels to obtain neuroprotection of the dopaminergic neurons have been verified using rat PD models [31]. Alternatively, recombinant fused TAT cells have also been used to cross the BBB and reduce 6-hydroxydopamine (6-OHDA) toxicity during intrastriatal administration [32].

Functions of the ubiquitin–proteasome system (UPS) are maintained by ubiquitin, and mutations therein are suggested to be involved in PD. This was observed in a study of Lewy bodies of the nerve cells in PD patients, identifying mutations in the UCHL1 gene as being the cause [33]. The decreased expression of this gene resulted in the degradation of axons, motor ataxia, and instability of the free ubiquitin levels. This gene, containing 223 amino acids and accounting for 1–2% of human brain protein, is majorly expressed in the peripheral nervous system [34]. In contrast, mutations in the UCH-L1S18Y gene portray specific antioxidant protective functions that potentially decrease the risk of developing PD. Hence, there is a strong potential for the application of gene therapy and/or nanomedicine in patients presenting with UCHL1-related PD [35,36].

Phosphatase and tensin homolog (PTEN) with tumour suppressor properties serves as a dual-specificity phosphatase with lipid and protein phosphatase activities. It is also a regulator of the PI3K/AKT pathway [37]. However, cells with the overexpression of PTEN portray an activation in the proteolytic cascade for apoptosis, which has been correlated to a decline in cell survival kinase AKT, leading to neuronal damage and death [38]. It is important to note that increased AKT can reduce oxidative stress levels and cell death, and therefore serves a therapeutic role in reducing neuronal damage. Furthermore, PTEN-induced kinase 1 (PINK1) has portrayed a significant role in oxidative DNA damage, preventing mitochondrial oxidative stress, autophagy, and mitochondrial conservation. It, therefore, reverses the apoptotic function of overexpressed PTEN in neuronal cell damage [39,40].

The PARK2 gene is noted as the most common autosomal recessive juvenile form of PD and is a significant contributor to sporadic and familial early-onset PD [41]. Parkin is encoded by the PARK2 gene and is characterized by a ring-between-ring domain E3 ubiquitin ligase, which is responsible for the catalysis of covalently attached ubiquitin to specific substrates and the regulation of vital cellular processes such as apoptosis and mitochondrial quality control [42–44]. A loss of Parkin function results in the ubiquitination of mitochondrial proteins downstream of the PINK1 kinase, resulting in mitophagy [45]. The build-up of these dysfunctional and damaged mitochondria causes oxidative stress, resulting in the loss of dopaminergic neurons and the occurrence of the motor symptoms of PD [41].

Hence, gene knockdown of overexpressed genes or the expression of under-expressed genes (in the case of Parkin) may be possible using nanoparticles to carry the gene of interest or therapeutic gene to target specific areas of the brain. While it may be complex, understanding the genetics pertaining to PD is highly imperative in designing an efficacious treatment at the genetic level. Since individuals present with varied genetics, ‘personalized medicine’ using therapeutic gene strategies holds great promise, especially for reducing side effects.

2.2.2. Alzheimer’s Disease (AD) and Implicated Genes

AD is one of the most common irreversible causes of dementia, a progressive neurodegenerative disease that manifests as a gradual loss of cognitive skills and memory. AD accounts for 60–80% of dementia cases [46]. The neurodegeneration occurs as a result of extracellular β -amyloid plaque deposition and intracellular neurofibrillary tangle deposition that cause neurotoxicity and synaptic loss [47]. The amyloid precursor protein (APP), presenilin 1 (PSEN1), and presenilin 2 (PSEN2) genes are predominant in the autosomal dominant forms of AD, while apolipoprotein E (ApoE) is evident in sporadic AD. The pathogenesis of AD exhibits various mechanisms, with APP processing into amyloid-beta peptide ($A\beta$) via the β -secretase and γ -secretase complexes being identified as the main mechanism and a potential target for therapeutics [48]. This could involve the use of inhibitors of APP-cleaving enzymes, such as caspases, meprin- β , rhomboid-like protein4 (RHBDL4), membrane-type matrix metalloproteinases (MT-MMPs/ η -secretases) and legumain (δ -secretase) [48,49].

Mutations in the PSEN1 gene are the most common cause of familial AD (FAD). This gene encodes for presenilin-1 (PS1), which is responsible for the catalysis of γ -secretase, which cleaves some type 1 transmembrane proteins, such as Notch and APP [50]. Before the cleavage mentioned above, cleavage occurs via the β -secretase to generate $A\beta$. This results in the production of $A\beta_{40}$ and $A\beta_{42}$, with the latter product being hydrophobic and nucleating $A\beta$ aggregation in the brain, leading to amyloid plaque deposition. This has been reported as the pathogenetic mechanism causing FAD [51]. Since the natural properties of presenilin are involved in memory and learning, together with neuronal survival following age progression, it was suggested that a mutation in PSEN1 leads to the loss of presenilin function, resulting in dementia and neurodegeneration in FAD [50].

In contrast to PSEN1, PSEN2 mutations are rare, with less than 40 mutations identified. Besides the progression of AD with age, environmental aspects are proposed to play a major

role in the autosomally inherited form of AD [51]. Mutations in this gene are responsible for early-onset AD (EOAD), late-onset AD (LOAD), frontotemporal dementia (FTD) and dementia with Lewy bodies (DLBs), together with other diseases such as dilated cardiomyopathy (DCM) and breast cancer [37,52]. The pathogenetic mechanism related to mutations in PSEN2 and PSEN1 are similar, but with A β 42 aggregation occurring to a lesser extent for PSEN2 [53]. Both PSEN 1 and PSEN2 may be ideal candidates for therapeutic intervention via gene therapy and nanomedicine.

ApoE is responsible for lipid transport and injury repair in the brain. Polymorphisms related to this gene predispose an individual to AD [54]. Although most mutations occur at the ϵ 3 allele, the ϵ 4 allelic mutations pose a greater risk to AD and present an increased risk for age-related cognitive decline and cerebral amyloid angiopathy [55]. ApoE permits the delivery of lipids and A β through the subsequent binding to cell-surface receptors on the brain. Hence, mutations result in the initiation of toxic events leading to neurodegeneration through synaptic dysfunction. Furthermore, ApoE is responsible for the regulation and clearance of A β aggregation, glucose metabolism, mitochondrial function, brain lipid transport, neuroinflammation and neuronal signalling, with mutations significantly affecting individuals [54].

2.3. Nanoparticles and Nanomedicine

The use of nanoscale particles in medicine, especially as carriers of therapeutics, holds great potential for treating many diseases, owing to their many favourable properties such as size, shape, and surface morphology [56]. Nanotechnology further permits intentional design variations, providing the ability to control their properties [37]. This malleability of nanoparticles (NPs) allows for the attachment of various biomolecules, thereby allowing for the efficient and safe transportation of pharmacologically active agents, such as genes or drugs. NP delivery vehicles of 1–100 nm in size have the ability to penetrate significant physiological barriers such as those found in the lungs, liver, gastrointestinal fluid, blood, tumour vasculature, mucosal membranes, and the blood–brain barrier [57–59]. Various NPs have been utilized in this regard, each portraying their unique characteristics as a therapeutic, diagnostic or theranostic tool. The ability to conjugate therapeutic nucleic acids and drugs to NPs has opened up avenues in target-specific nanomedicine. Apart from medicine, NPs can be employed in cosmetics, packaging, electronics, and biotechnology. NPs can be broadly classed as organic, carbon-based, or inorganic NPs (Figure 2.2).

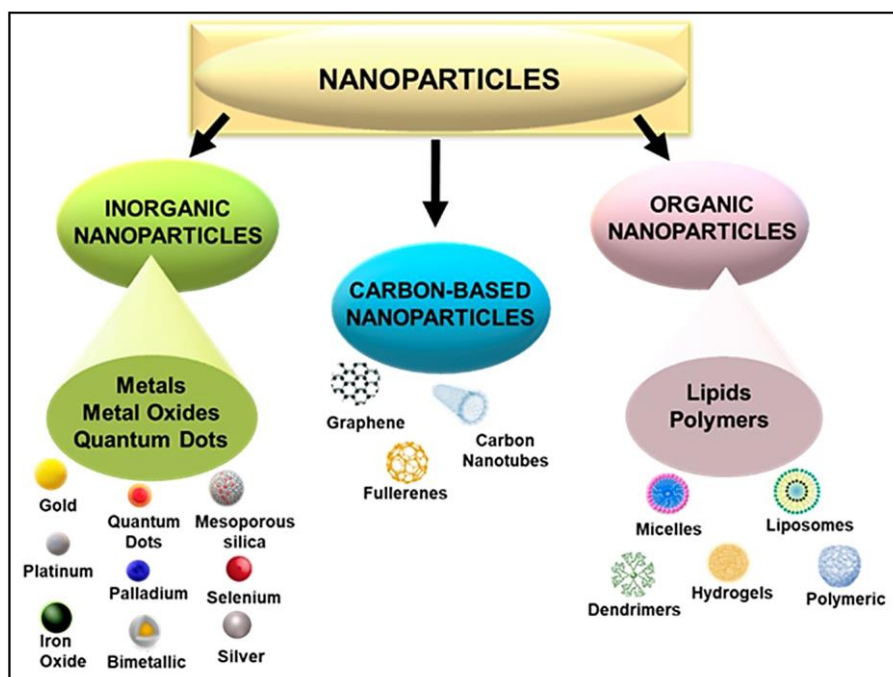


Figure 2.2. Broad classes of nanoparticles showing those commonly used in nanomedicine.

Biocompatibility relies on the physicochemical properties of the NPs, with each NP displaying distinctive properties. The modification of NPs with polymers and targeting ligands can enhance binding affinities with the gene or drug being conjugated [60], in addition to cell-specific uptake. The noble metals, gold (Au), silver (Ag), platinum (Pt), and palladium (Pd), have been commonly employed due to their favourable physicochemical, biological, and optical properties [58,61]. The physicochemical properties of AuNPs are easily tunable for clinical application [62]. They have demonstrated promising results in various diseases, including smallpox, cancer, syphilis, AIDS, and skin ulcers [63], and have also been used to detect copper ion-induced aggregated A β peptides [64]. AgNPs possess anti-microbial and anti-viral properties that have been exploited as a pre-treatment for wound infections [65]. The use of unmodified AgNPs as delivery vehicles has been hindered by their propensity to aggregate and increase in size [66]. Pd is more commonly used in dentistry, where it is part of the composition of electrical equipment [61,67]. Bimetallic Au-Pd NPs modified with quercetin have been studied as possible inducers of autophagy in Alzheimer's disease [68]. Pt is a good antioxidant for the reduction in free radicals [58] and is part of the anticancer drugs cisplatin and oxaliplatin, which have reported some neurotoxicity [69].

Selenium (Se), an essential micro-element, is required by all organisms for various biological functions, with the supplementation of Se being reported to reduce the incidence of cardiovascular diseases, osteoarthritis, type 2 diabetes, and neurodegenerative diseases such as

AD [70,71]. Se NPs possess favourable properties, including anticancer and antioxidant properties of Se, while exhibiting lower cytotoxicity, better bioavailability, biocompatibility, and biodegradability in vivo [71,72]. Due to their potential synergistic effect with the therapeutic gene or drug, these NPs are becoming increasingly popular. The application of mesoporous silica NPs (MSNs) as nano-delivery vehicles has gained significant momentum due to their porous structures that offer both inner and outer increased surface areas for therapeutic cargo [73,74]. This porous nature of MSNs allows for the possible combination delivery of therapeutic genes and drugs, which can improve biological activity [75]. Quercetin-encapsulated silica NPs have demonstrated potential against Cu-induced oxidative stress observed in neurodegenerative diseases [76]

Iron oxides, commonly referred to as magnetic NPs (MNPs), including maghemites, magnetites and ferrites, have been widely studied in nanomedicine due to their low cytotoxicity, biodegradability, stability, magnetization, biocompatibility, low sensitivity to oxidation and reactive surfaces, non-carcinogenicity, and ease of synthesis and modification [77]. The target-specific delivery of MNPs can be achieved by the process of magnetofection that uses an external magnetic field to guide their delivery. Their application has been extended to magnetic hyperthermia, magnetic resonance imaging (MRI), and delivery systems [78,79]. However, unmodified MNPs are hydrophobic, and can aggregate and generate reactive oxygen species, limiting their in vivo efficacy [80].

Quantum dots (QDs) have unique optical properties, but due to their composition, which often includes metals such as cadmium and zinc, they tend to be toxic. This could be overcome using modified core-shell QDs or coated QDs [75]. Carbon nanotubes, either single-walled or multi-walled, can readily enter cells. However, without either internal or external functionalization, they are insoluble, cytotoxic, hydrophobic, and immunogenic [81]. The use of polymeric delivery systems has evolved over the years, with cationic polymers being favoured due to their ability to bind anionic molecules such as nucleic acids. In addition, the chosen polymers must be biocompatible, biodegradable, and stable in vivo [75]. Hence, polymers such as dendrimers have been popular due to their many cationic groups. They have been further utilized as suitable stabilizers of metallic NPs such as AuNPs [82,83]. Poly (lactic-co-glycolic acid), a polymer approved by the Food and Drug Administration (FDA), has shown good properties for use in drug delivery in combination with Au [84], while its PEGylated derivatives have been investigated in AD [85]. From the lipid-based NPs, liposomes have been commonly used for

the delivery of bio-active compounds, with some positive results noted in animal models for AD [86,87].

Overall, inorganic NPs in most cases possess an advantage over their organic counterparts, especially with regard to the ease of synthesis and functionalization approaches, size, stability, and their theranostic potential. All the NPs mentioned above have shown potential in nanomedicine and may be extended to neurological disorders such as AD and PD. Overall, for these nanosystems to be suitable, predetermined properties of the NP needs to be addressed and prioritized [88], as illustrated in Figure 2.3.

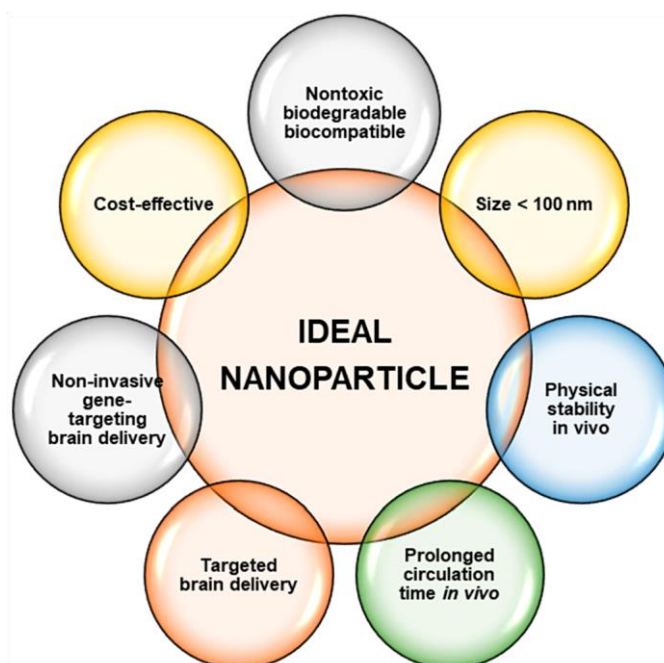


Figure 2.3. Ideal criteria required for the development of a safe and efficient nanoparticle for use in nanomedicine.

2.3.1. Challenges Facing Nanoparticles

The use of NPs does not come without challenges, especially when considering their use as therapeutic delivery vehicles for neurodegenerative diseases. Besides the BBB, which poses the greatest hindrance to therapeutics, neurotoxicity due to nano-delivery systems also raises safety concerns [89]. This neurotoxicity is commonly noted by the generation of oxidative stress, and predominantly depends upon the morphology, size, surface area, solubility, concentration, and the duration and mode of the nanotherapeutic administration [90]. Although some metals play pivotal roles in the human body, the accumulation and aggregation of metal NPs may be a cause for concern. Using the neuronal model of PC12 cells, it was earlier reported that iron NPs produced significant cytotoxicity [91], while manganese and Cu NPs generated

reactive oxygen species [92]. The use of zinc oxide NPs induced apoptosis in neural stem cells [93], while the oral administration of Ag NPs was toxic and accumulated in the kidney, liver, and brain in Sprague Dawley rats [94]. In addition, the administration of iron oxide NPs to mice models produced oxidative stress, neurodegeneration [95], cell-cycle-dependent neuronal apoptosis [96], and neurobehavioural toxicity [97].

Despite these challenges, the physicochemical properties of NPs, as mentioned previously, make them attractive candidates in nanomedicine. To overcome some of these challenges, the NP formulations must encompass biocompatible materials that are also biodegradable and readily excreted from the system [98]. Their ability to cross the BBB is further described in Chapter 3, section 3.2. In addition, the toxicities evidenced are often dependent on the type of NP used, with surface functionalizations being a way forward in reducing adverse effects and interactions. Hence, there is no “one size fits all” regarding the choice of a NP and its application. It is essential to identify the advantages and disadvantages related to the use primarily of metals and non-metal carriers, bearing in mind that many metals are required in the body, as mentioned previously. Hence, the concentration utilized will be critical to maintaining homeostatic equilibrium. The use of targeted approaches in treating AD and PD will be crucial, as cell-specific targeting is essential for treating damaged or mutated genes while upholding the integrity of normal functioning genes and cells. However, it is clear that a deeper investigation of NPs is warranted when formulating therapeutics for the CNS. Presently, there is a dearth of information on NP neurotoxicity, suggesting an urgent need for further *in vitro* and *in vivo* studies to provide a foundation for future studies. Using emerging technologies, especially *in silico* studies, computer and mathematical modelling, and greater knowledge in bioinformatics, may assist in the challenges facing nanomedicine in formulating an ideal NP.

2.3.2. Crossing the Blood–Brain Barrier

The blood–brain barrier (BBB) is a dynamic boundary that serves a self-protective role in modulating the transport of biomolecules from the blood into the brain while obstructing the ingress of toxic chemicals and larger drugs. While this role is greatly beneficial, it serves as an obstacle to current therapeutics. The BBB, a specialized part of the vascular system, is made up of a basal lamina comprising extracellular matrix proteins (laminin, heparan sulfate, or collagen), together with endothelial cells, pericytes, astrocyte endfeet, and interneurons [99]. The vascular, neuronal, and glial cells are known to interact, forming a cellular network appropriately termed the neurovascular unit that is involved in the maintenance of tissue

homeostasis [100]. The BBB is the largest barrier in the CNS and has a surface area of 20 m². It is considered a critical site for the exchange of molecules between the blood and the CNS [101]. Since NPs are small (mostly <200 nm) molecules, they have the advantage of being able to traverse this BBB. Apart from size, properties such as charge, especially a positive charge, suitable surface functionalizations, the addition of targeting ligands such as cell-penetrating peptides and polyethylene glycol for improved circulation time in vivo imbue NPs with the capacity to successfully cross the BBB [99]. It has been observed that molecules penetrate the brain via the carrier-mediated transporter (CMT) (Figure 2.4), which includes the glucose transporter (GLUT1), adenosine transporters (CNT2), large neutral amino-acid transporters (LAT1), and monocarboxylic acid (MCT1) [8]. Drug delivery of chemo-nanotherapeutics in the treatment of brain diseases portrayed the use of circulating cells, such as exosomes, erythrocytes, neutrophils, and leukocytes, which possess the ability to spontaneously cross the BBB [102].

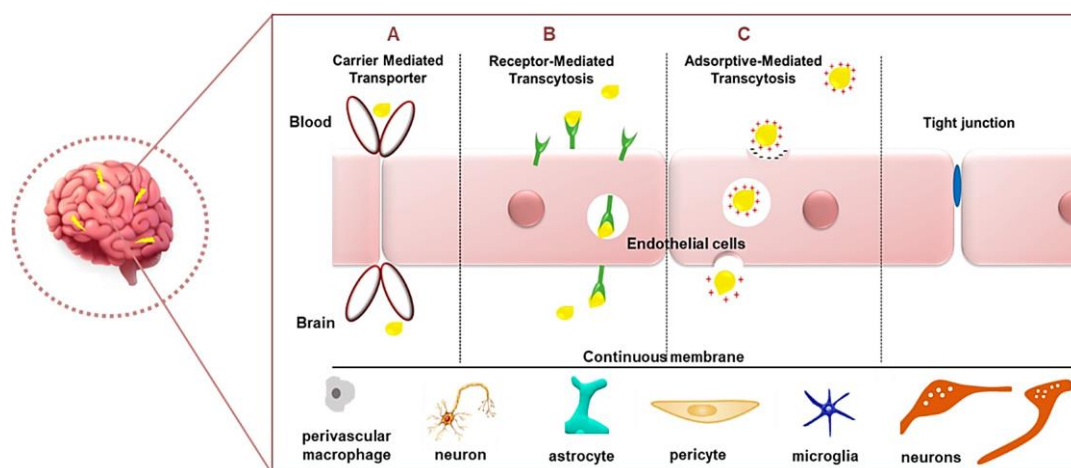


Figure 2.4. Common mechanisms for passage through the BBB. (A) Carrier-mediated transporter, (B) receptor-mediated transcytosis and (C) adsorptive-mediated transcytosis.

Other means of entry can be seen in receptor-mediated transcytosis (RMT) and adsorptive-mediated transcytosis (AMT) (Figure 2.4) [103]. The former transport system relies on the NPs' ability to be modified to possess ligands permitting the efficient binding to receptors present at the BBB. Ligands can be directed to targets such as GLUT1 or albumin transporters [104], lactoferrin (Lf) receptors, LRP1 (using angiopep-2) [105], or transferrin receptors (TfR) (using transferrin ligand) [106]. TfR has been identified to be sometimes overexpressed in neuronal [107] and glioma cells [108]. However, the levels of brain transferrin decrease with age and a dramatic reduction is observed in neurodegenerative diseases such as AD or PD

[109]. However, the TfR does offer great promise in the delivery of therapeutic agents across the blood–brain barrier to the brain [110]. RMT thereby exploits the role of surface-labelled nanocarriers for the efficient entry of the nanocomplexes into the brain. However, the choice and concentration of the attached ligand will be limiting factors that will determine the success of endocytosis. Gold nanospheres [111] and gold nanostars conjugated to a cell-penetrating peptide demonstrated the ability to cross the BBB [112].

AMT, however, portrays a slightly varied mechanism of action in that it utilizes electrostatic interactions between the negatively charged BBB and the positively charged NPs [91]. It was reported that gold-NP-decorated wheat germ agglutinin was taken up by nerve terminals and retrogradely transported by the axons to the CNS [113]. These carrier transporters all allow for the slackening of the BBB surfactants, thereby disrupting the endothelial cell junctions and allowing for the entry of the NPs into the brain. Studies in mice models have reported a lack of damage to the brain [114,115]. However, it has been noted that the choice of the in vivo disease model for testing the NPs' ability to cross the BBB is crucial, since BBB permeability may differ from rodents to humans [99]. Extensive studies on transport molecules enable researchers to create therapeutics that can exploit the natural physiological barriers for the safe and efficient delivery of pharmacologically active agents to the brain. The optimal parameters for a nanocomposite to be able to pass through the BBB were proposed to be a low molecular weight (<400 Da), a suitable charge, $\log p < 2$, non-ionization, the presence of hydrogen bonds (8–10), and lipophilicity [100].

Besides the use of NPs in drug delivery, which has shown some in vivo instability and immune reactions due to the intravenous administration of the nanosystem, the employment of gene therapy utilizing NP carriers can be considered.

2.3.3. Gene Therapy

The idea of gene therapy dates back to the 1960s and is the treatment or prevention of a disease or a genetic disorder using therapeutic nucleic acids [116]. Despite the high transfection rates obtained using viral delivery vehicles, the disadvantages relating to a low loading capacity, large-scale manufacturing, the size of gene it can carry, and the safety factors of potential oncogenicity and immunogenicity prompted the development of non-viral methods. Non-viral gene delivery systems have a greater ability to target cells/tissues, a significantly lowered oncogenic and immunogenic nature, an enhanced efficacy of preparation at low cost, no limitation on the size of the genetic cargo, and amenability to structural manipulations [117].

From the non-viral delivery vehicles, cationic polymers and lipid-based constructs, especially cationic liposomes, have been the most studied to date, with the use of inorganic NPs now gaining momentum.

NPs can overcome both intracellular and extracellular barriers that hinder gene delivery. These barriers include nuclear uptake, the avoidance of clearance by the reticuloendothelial system (RES), endosomal and lysosomal escape, the protection of genetic cargo from degradation, nucleic acid release, and the targeting of specific cells [118]. Due to inorganic NPs portraying greater surface area to volume ratios with tunable magnetic, optical, and biological properties, they can be engineered to deliver genes with enhanced efficacy by modifying the shape, chemical composition, and size. An ideal gene delivery vehicle should possess properties such as the ability to disrupt the endosomal membrane, to cross the plasma membrane, to bind, condense and protect the nucleic acid cargo, to ensure target specific delivery, have stability in circulation, and be able to evade the immune system [118,119].

The extensive research about the pathogenetic mechanisms of neurodegenerative disorders has led to the identification of specific genetic defects implicated in the progression of diseases. Gene therapy permits the delivery of genomic cargo, which includes microRNA (miRNA), small interfering RNA (siRNA), guide RNA (gRNA), and messenger RNA (mRNA). Studies portrayed success in gene silencing strategies via RNA interference (RNAi), which utilizes siRNA, miRNA and piwi-interacting RNA to decrease the synthesis of the targeted mRNA molecules [120]. When synthetic double-stranded siRNAs (21–25 nucleotides in size) are transfected into mammalian cells, they target the specific mRNA sequences with a high degree of specificity, which leads to gene silencing [75]. The RNAi revolution has opened up a novel avenue for therapeutic intervention in a wide array of disorders, from cancer to neurodegenerative diseases [75,121]. Overall, the successful application of siRNA-mediated gene silencing in medicine would require a suitable delivery vehicle, preferably a nanocarrier, that would ensure the safe and efficient delivery of the siRNA. Genome editing has been recently introduced into gene therapy and heralds a technique that can directly target aberrant genetic changes at diseased sites [122].

A potential target in gene therapy is the abnormal accumulation of misfolded proteins such as amyloid β -oligomers and α -synuclein (Figure 2.1), which generate endoplasmic reticulum (ER)-associated degradation and ER stress [123]. The aggregation of these proteins in the ER lumen consequentially causes a destabilization of the ER calcium homeostasis and distortion

in the unfolded protein response (UPR) signalling, resulting in neuron death via pro-apoptotic responses [124,125]. This can be overcome by targeting the UPR signalling to enhance protein folding, as seen when PD was treated by targeting the reduction in dopaminergic neuron apoptosis and improving the motor performance, thereby delaying the disease progression. This was permitted via gene therapy, which involved targeting the overexpression of the BiP (glucose-regulated protein 78) gene, which is linked to a reduction in the unfolded protein response [126]. Hence, gene silencing strategies can be successful in such cases.

Furthermore, mitochondrial respiratory dysfunction has been noted in diseases such as Huntington disease (HD), AD, PD, and ALS, resulting in the limited regulation of mitochondrial quality, NAD⁺ depletion, oxidative damage, protein aggregations, disrupted ATP synthesis and unbalanced mitochondrial calcium homeostasis [127–129]. Gene therapy has been seen to overcome this phenomenon via either inhibiting the mitochondrial damage or promoting mitochondrial biogenesis. Alternatively, neurotoxicity in experimental HD and PD can be regulated by the overexpression of regulators of mitochondrial oxidative stress and dynamics, including PGC-1 α , HSP70, TFEB [130,131].

Other mechanisms of pathogenesis are seen in abnormal rapamycin (mTOR) signalling in PD, AD and HD, together with epigenetic dysregulation, autophagy, and microglial and astrocyte dysfunction [132]. Each mechanism exhibits unique modes of dysfunction owing to the progression of the disease, and it is therefore important to understand which mechanism is involved in a patient presenting with these diseases to administer the appropriate treatment with maximum efficacy. Furthermore, gene therapy has proved its efficacy in various other diseases. It, therefore, is a great contender for neurodegenerative therapeutics, following research on genetic aberrations in patients with PD and AD.

Table 2.3 highlights a few of the NPs used for gene therapy of the CNS from 2017 to 2020. The success of such experiments has expanded the knowledge of nanomedicine in neurodegenerative disorders, aiding in the specific targeting of the causative genes or aggregated proteins. Gene therapy strategies delivered using nanoparticle vectors are attractive alternatives as they can potentially satisfy many requirements for safe and efficient delivery across biological barriers, especially the blood–brain barrier. Aside from the advantages portrayed in gene therapy, the biological synthesis of NPs vaunts its own array of benefits with regard to specific extracts utilized [133] that may work synergistically with the therapeutic gene.

Table 2.3. Application of nanoparticles in neurodegenerative studies since 2017.

Nanoparticle	Disease	Therapeutic	Therapeutic Effect	Cell Entry	Ref
Gold	PD	<i>pDNA</i> incorporated exogenous interfering RNA (RNAi) and Nerve growth factor (NGF)	Inhibition of PC12 cells and substantia nigra striatum dopaminergic neuronal apoptosis	Nerve growth factor (NGF) endocytosis	[134]
Gold	AD	3.3 nm L- and D-glutathione	Inhibition of A β 42 aggregation	Chiral nanoparticle endocytosis across the BBB	[133]
Silver	PD	Citrate cap	Up-regulation of hydrogen sulphide (H ₂ S) and Ag ₂ S—reducing neurotoxicity	Natural properties of silver penetrate the brain	[135]
Silver	AD	<i>Lampranthus coccineus</i> and <i>Malephora lutea</i> F. Aizoaceae plant extract	Anticholinesterase and antioxidant activity as a plant-based anti-Alzheimer drug	Natural properties of silver penetrate the brain	[136]
Selenium	AD	Curcumin-loaded nanospheres	Decrease in amyloid- β plaques in AD lesions	Curcumin's capability to bind with amyloid b and iron in plaques by intermolecular hydrogen bonds without any additional chemical linkers.	[137]

2.3.4. Nanomedicine in Clinical Trials—Update

Several clinical trials using drugs as secretase inhibitors and therapeutic antibodies in AD have been conducted, with only a few completed and the majority discontinued [8]. Interestingly, there has been a global lack of novel drug development for AD since 2003 [138]. This was also evident in a recent search of the NIH library, with only two studies related to NP delivery. One entitled “Safety, tolerability and efficacy assessment of intranasal nanoparticles of APH-1105, a novel alpha-secretase modulator for mild to moderate cognitive impairment due to

Alzheimer's disease" is only due to start in 2023. The second trial, "A Phase 2, pilot open-label, sequential group, investigator blinded study of magnetic resonance spectroscopy (31P-MRS) to assess the effects of CNM-Au8 for the bioenergetic improvement of impaired neuronal redox state in Parkinson's disease", began in December 2019, and was scheduled to be completed in July 2021 [139]. This study utilized gold nanocrystals. Although gold nanocrystals have been approved recently for treating multiple sclerosis [140], updates on the current study are awaited. Positive results can only propel the use of NPs in future investigations.

2.4. Conclusions

Nanomedicine is emerging as a highly efficacious tool to overcome barriers that still challenge traditional medicine. The combination of nanomedicine and gene therapy can be exploited for greater therapeutic benefits. This review highlighted some of the genes involved in the disease progression of PD and AD that may open the prospect of gene therapy studies. A greater understanding of the causes of genetic aberrations and how they lead to neurodegeneration can lead to tailored therapeutics in response to a specific mutation type presented by an individual. While a cure may not be immediate, such research studies form the stepping stones to ultimately create a treatment strategy that would one day eradicate diseases linked to neuronal damage and help millions of patients worldwide to live normal and healthy lives. The combination of nanomedicine and neuroscience can potentially provide novel solutions to many CNS-related disorders, including AD and PD. The array of nanoparticles currently available needs to undergo stringent testing to determine their toxicity and stability, and they must be optimized for gene or drug delivery to the CNS.

References

1. Amor, S.; Puentes, F.; Baker, D.; Van Der Valk, P. Inflammation in neurodegenerative diseases. *Immunology* **2010**, *129*, 154–169.
2. Checkoway, H.; Lundin, J.L.; Kelada, S.N. Neurodegenerative diseases. *IARC Sci. Publ.* **2011**, *163*, 407–419.
3. Kabanov, A.V.; Gendelman, H.E. Nanomedicine in the diagnosis and therapy of neurodegenerative disorders. *Prog. Polym. Sci.* **2007**, *32*, 1054–1082.

4. Patterson, C. *The State of the Art of Dementia Research: New Frontiers*; World Alzheimer Report 2018; Alzheimer's Disease International: London, UK, 2018. Available online: <https://www.alz.co.uk/research/WorldAlzheimerReport2018.pdf> (accessed on 8 March 2021).
5. Parkinson's Foundation. 2021 Statistics. Available online: <https://www.parkinson.org/Understanding-Parkinsons/Statistics#:~:text=More%20than%2010%20million%20people,have%20Parkinson\T1\textquoterights%20disease%20than%20women> (accessed on 8 March 2021).
6. Gendelman, H.E. Neural immunity: Friend or foe? *J. Neurovirol.* **2002**, *8*, 474–479.
7. Liu, B.; Hong, J.S. Role of microglia in inflammation-mediated neurodegenerative diseases: Mechanisms and strategies for therapeutic intervention. *J. Pharmacol. Exp. Ther.* **2003**, *304*, 1–7.
8. Pardridge, W.M. Treatment of Alzheimer's disease and Blood-Brain barrier drug delivery. *Pharmaceuticals* **2020**, *13*, 394. [CrossRef]
9. Dugger, B.N.; Dickson, D.W. Pathology of Neurodegenerative Diseases. *Cold Spring Harb. Perspect. Biol.* **2017**, *9*, a028035.
10. Uchikado, H.; DelleDonne, A.; Ahmed, Z.; Dickson, D.W. Lewy bodies in progressive supranuclear palsy represent an independent disease process. *J. Neuropathol. Exp. Neurol.* **2006**, *65*, 387–395.
11. Ghasemi, M.; Brown, R.H.J. Genetics of Amyotrophic Lateral Sclerosis. *Cold Spring Harb. Perspect. Med.* **2018**, *8*, a024125.
12. Jucker, M.; Walker, L.C. Self-propagation of pathogenic protein aggregates in neurodegenerative diseases. *Nature* **2013**, *501*, 45–51.
13. Eisenberg, D.; Jucker, M. The amyloid state of proteins in human diseases. *Cell* **2012**, *148*, 1188–1203.
14. Desai, A.K.; Grossberg, G.T. Diagnosis and treatment of Alzheimer's disease. *Neurology* **2005**, *64*, S34–S39.
15. Mizuno, Y. Recent research progress in and future perspective on treatment of Parkinson's disease. *Integr. Med. Int.* **2014**, *1*, 67–79.
16. Chiara, T.; Origlia, N.; Mattu, C.; Accorroni, A.; Chiono, V. Current Limitations in the Treatment of Parkinson's and Alzheimer's Diseases: State-of-the-Art and Future Perspective of Polymeric Carriers. *Curr. Med. Chem.* **2018**, *25*, 5755–5771.
17. Elbaz, A.; Dufouil, C.; Alperovitch, A. Interaction between genes and environment in neurodegenerative diseases. *C. R. Biol.* **2007**, *330*, 318–328.
18. Drugs for Alzheimer's Disease: Current and in Development. Available online: <https://www.healthline.com\T1\guilsinglrightalzheimers-disease-drugs> (accessed on 20 July 2021).

19. American Parkinson's Disease Association. Available online: <https://www.apdaparkinson.org/what-is-parkinsons/treatmentmedication/medication/> (accessed on 20 July 2021).
20. Bohn, M.C. Parkinson's Disease: A neurodegenerative disease particularly amenable to gene therapy. *Cell* **2000**, *1*, 494–496.
21. Feng, L.R.; Maguire-Zeiss, K.A. Gene Therapy in Parkinson's Disease: Rationale and Current Status. *CNS Drugs* **2010**, *24*, 177–192.
22. Kalia, L.V.; Lang, A.E. Parkinson's disease. *Lancet* **2015**, *386*, 896–912.
23. Greffard, S.; Verny, M.; Bonnet, A.M.; Beinis, J.Y.; Gallinari, C.; Meaume, S.; Piette, F.; Hauw, J.J.; Duyckaerts, C. Motor score of the Unified Parkinson Disease Rating Scale as a good predictor of Lewy body-associated neuronal loss in the substantia nigra. *Arch. Neurol.* **2006**, *63*, 584–588.
24. Toulouse, A.; Sullivan, A.M. Progress in Parkinson's disease-where do we stand? *Prog. Neurobiol.* **2008**, *85*, 376–392.
25. Han, J.W.; Ahn, Y.D.; Kim, W.; Shin, C.M.; Jeong, S.J.; Song, Y.S.; Bae, Y.J.; Kim, J. Psychiatric Manifestation in Patients with Parkinson's Disease. *J. Korean Med. Sci.* **2018**, *33*, 300.
26. Nussbaum, R.L.; Polymeropoulos, M.H. Genetics of Parkinson's disease. *Hum. Mol. Genet.* **1997**, *6*, 1687–1691. [CrossRef] 27.Nishioka, K.; Hayashi, S.; Farrer, M.J.; Singleton, A.B.; Yoshino, H.; Imai, H.; Kitami, T.; Sato, K.; Kuroda, R.; Tomiyama, H.; *et al.* Clinical heterogeneity of alpha-synuclein gene duplication in Parkinson's disease. *Ann. Neurol.* **2006**, *59*, 298–309.
28. Tolosa, E.; Vila, M.; Klein, C.; Rascol, O. LRRK2 in Parkinson disease: Challenges of clinical trials. *Nat. Rev. Neurol.* **2020**, *16*, 97–107.
29. Bonifati, V.; Rizzu, P.; van Baren, M.J.; Schaap, O.; Breedveld, G.J.; Krieger, E.; Dekker, M.C.; Squitieri, F.; Ibanez, P.; Joosse, M.; *et al.* Mutations in the DJ-1 gene associated with autosomal recessive early-onset parkinsonism. *Science* **2003**, *299*, 256–259.
30. Abou-Sleiman, P.M.; Healy, D.G.; Quinn, N.; Lees, A.J.; Wood, N.W. The role of pathogenic DJ-1 mutations in Parkinson's disease. *Ann. Neurol.* **2003**, *54*, 283–286.
31. Repici, M.; Giorgini, F. DJ-1 in Parkinson's Disease: Clinical Insights and Therapeutic Perspectives. *J. Clin. Med.* **2019**, *8*, 1377.
32. Batelli, S.; Invernizzi, R.W.; Negro, A.; Calcagno, E.; Rodilossi, S.; Forloni, G.; Albani, D. The Parkinson's disease-related protein DJ-1 protects dopaminergic neurons in vivo and cultured cells from alpha-synuclein and 6-hydroxydopamine toxicity. *Neurodegener. Dis.* **2015**, *15*, 13–23.

33. Lowe, J.; McDermott, H.; Landon, M.; Mayer, R.J.; Wilkinson, K.D. Ubiquitin carboxyl-terminal hydrolase (PGP 9.5) is selectively present in ubiquitinated inclusion bodies characteristic of human neurodegenerative diseases. *J. Pathol.* **1990**, *161*, 153–160.
34. Wilkinson, K.D.; Lee, K.M.; Deshpande, S.; Duerksen-Hughes, P.; Boss, J.M.; Pohl, J. The neuron-specific protein PGP 9.5 is a ubiquitin carboxyl-terminal hydrolase. *Science* **1989**, *246*, 670–673.
35. Carmine, B.A.; Westerlund, M.; Bergman, O.; Nissbrandt, H.; Lind, C.; Sydow, O.; Galter, D. S18Y in ubiquitin carboxy-terminal hydrolase L1 (UCH-L1) associated with decreased risk of Parkinson's disease in Sweden. *Parkinsonism Relat. Disord.* **2007**, *13*, 295–298.
36. Maraganore, D.M.; Lesnick, T.G.; Elbaz, A.; Chartier-Harlin, M.C.; Gasser, T.; Kruger, R.; Hattori, N.; Mellick, G.D.; Quattrone, A.; Satoh, J.-I.; *et al.* UCHL1 Global Genetics Consortium. UCHL1 is a Parkinson's disease susceptibility gene. *Ann. Neurol.* **2004**, *55*, 512–521.
37. Chen, W.; Ouyang, J.; Yi, X.; Xu, Y.; Niu, C.; Zhang, W.; Wang, L.; Sheng, J.; Deng, L.; Liu, Y.N.; *et al.* Black Phosphorus Nanosheets as a Neuroprotective Nanomedicine for Neurodegenerative Disorder Therapy. *Adv. Mater.* **2018**, *30*, 1703458.
38. Ogino, M.; Ichimura, M.; Nakano, N.; Minami, A.; Kitagishi, Y.; Matsuda, S. Roles of PTEN with DNA Repair in Parkinson's Disease. *Int. J. Mol. Sci.* **2016**, *17*, 954.
39. Devireddy, S.; Liu, A.; Lampe, T.; Hollenbeck, P.J. The Organization of Mitochondrial Quality Control and Life Cycle in the Nervous System in Vivo in the Absence of PINK1. *J. Neurosci.* **2015**, *35*, 9391–9401.
40. Li, L.; Hu, G.K. Pink1 protects cortical neurons from thapsigargin-induced oxidative stress and neuronal apoptosis. *Biosci. Rep.* **2015**, *5*, e00174.
41. Zhu, M.; Cortese, G.P.; Waites, C.L. Parkinson's disease-linked Parkin mutations impair glutamatergic signaling in hippocampal neurons. *BMC Biol.* **2018**, *16*, 100.
42. Charan, R.A.; LaVoie, M.J. Pathologic and therapeutic implications for the cell biology of Parkin. *Mol. Cell. Neurosci.* **2015**, *66*, 62–71.
43. Hattori, N.; Mizuno, Y. Twenty years since the discovery of the parkin gene. *J. Neural Transm. (Vienna)* **2017**, *124*, 1037–1054.
44. Zhang, C.W.; Hang, L.; Yao, T.P.; Lim, K.L. Parkin regulation and neurodegenerative disorders. *Front. Aging Neurosci.* **2015**, *7*, 248.
45. Jacoupy, M.; Hamon-Keromen, E.; Ordureau, A.; Erpapazoglou, Z.; Coge, F.; Corvol, J.-C.; Nosjean, O.; la Cour, C.M.; Millan, M.J.; Boutin, J.A.; *et al.* The PINK1 kinase-driven ubiquitin ligase Parkin promotes mitochondrial protein import through the presequence pathway in living cells. *Sci. Rep.* **2019**, *9*, 11829.

46. 2020 Alzheimer's Disease Facts and Figures. *Alzheimers Dementia*. 2020. Available online: <https://alz-journals.onlinelibrary.wiley.com/doi/full/10.1002/alz.12068> (accessed on 8 March 2021).
47. Sanabria-Castro, A.; Alvarado-Echeverria, I.; Monge-Bonilla, C. Molecular pathogenesis of Alzheimer's disease: An update. *Ann. Neurosci.* **2017**, *24*, 46–54.
48. García-González, L.; Pilat, D.; Baranger, K.; Rivera, S. Emerging Alternative Proteinases in APP Metabolism and Alzheimer's Disease Pathogenesis: A Focus on MT1-MMP and MT5-MMP. *Front. Aging Neurosci.* **2019**, *11*, 244. [CrossRef]
49. Agatonovic-Kustrina, S.; Kettle, C.; Morton, D.W. A molecular approach in drug development for Alzheimer's disease. *Biomed. Pharmacother.* **2018**, *106*, 553–565.
50. Kelleher, R.J.; Shen, J. Presenilin-1 mutations and Alzheimer's disease. *Proc. Natl. Acad. Sci. USA* **2017**, *114*, 629–631.
51. Sun, L.; Zhou, R.; Yang, G.; Shi, Y. Analysis of 138 pathogenic mutations in presenilin-1 on the in vitro production of A β 42 and A β 40 peptides by γ -secretase. *Proc. Natl. Acad. Sci. USA* **2017**, *114*, E476–E485.
52. Cai, Y.; An, S.S.A.; Kim, S. Mutations in presenilin 2 and its implications in Alzheimer's disease and other dementia-associated disorders. *Clin. Interv. Aging* **2015**, *10*, 1163–1172.
53. Larner, A.J. Presenilin-1 mutation Alzheimer's disease: A genetic epilepsy syndrome? *Epilepsy Behav.* **2011**, *21*, 20–22.
54. Liu, C.; Kanekiyo, T.; Xu, H.; Bu, G. Apolipoprotein E and Alzheimer disease: Risk, mechanisms, and therapy. *Nat. Rev. Neurol.* **2013**, *9*, 106–118.
55. Chartier-Harlin, M.C.; Parfitt, M.; Legrain, S.; Pérez-Tur, J.; Brousseau, T.; Evans, A.; Berr, C.; Vidal, O.; Roques, P.; Gourlet, V. Apolipoprotein E, epsilon 4 allele as a major risk factor for sporadic early and late-onset forms of Alzheimer's disease: Analysis of the 19q13.2 chromosomal region. *Hum. Mol. Genet.* **1994**, *3*, 569–574.
56. Maney, V.; Singh, M. The synergism of Platinum-Gold bimetallic nanoconjugates enhance 5-Fluorouracil delivery in vitro. *Pharmaceutics* **2019**, *11*, 439.
57. Von Roemeling, C.; Jiang, W.; Chan, C.K.; Weissman, I.L.; Kim, B.Y. Breaking down the barriers to precision cancer nanomedicine. *Trends Biotechnol.* **2017**, *35*, 159–171.
58. Maney, V.; Singh, M. An in vitro assessment of Chitosan/Bimetallic PtAu nanocomposites as delivery vehicles for Doxorubicin. *Nanomedicine* **2017**, *12*, 2625–2640.
59. Venkatas, J.; Singh, M. Nanomedicine-mediated optimization of Immuno-therapeutic approaches in Cervical cancer. *Nanomedicine* **2021**, *16*, 1311–1328.
60. AderibiEGB, B.A. Metal-based nanoparticles for the treatment of infectious diseases. *Molecules* **2017**, *22*, 1370.
61. Yaqoob, S.B.; Adnan, R.; Khan, A.M.R.; Rashid, M. Gold, Silver, and Palladium Nanoparticles: A Chemical Tool for Biomedical Applications. *Front. Chem.* **2020**, *8*, 376.

62. Oladimeji, O.; Akinyelu, A.; Singh, M. Co-polymer Functionalised Gold Nanoparticles show efficient Mitochondrial Targeted Drug Delivery in Cervical Carcinoma Cells. *J. Biomed. Nanotechnol.* **2020**, *16*, 853–866.
63. Chitra, M.A. Rapid detection of staphylococcus aureus genomic dna using peptide nucleic acid and gold nanoparticles. *Proc. Natl. Acad. Sci. USA* **2018**, *88*, 803–811.
64. Zhou, Y.; Dong, H.; Liu, L.; Xu, M. Simple colorimetric detection of amyloid β -peptide (1-40) based on aggregation of gold nanoparticles in the presence of copper ions. *Small* **2015**, *11*, 2144–2149.
65. Chaloupka, K.; Malam, Y.; Seifalian, A.M. Nanosilver as a new generation of nanoparticle in biomedical applications. *Trends Biotechnol.* **2010**, *28*, 580–588.
66. Gounden, S.; Daniels, A.; Singh, M. Chitosan-modified Silver Nanoparticles Enhance Cisplatin activity in Breast Cancer Cells. *Biointerface Res. Appl. Chem.* **2021**, *11*, 10572–10584.
67. Pattadar, D.K.; Sharma, J.N.; Mainali, B.P.; Zamborini, F.P. Anodic stripping electrochemical analysis of metal nanoparticles. *Curr. Opin. Electrochem.* **2019**, *13*, 147–156.
68. Liu, Y.; Zhou, H.; Yin, T.; Gong, Y.; Yuan, G.; Chen, L.; Liu, J. Quercetin-modified gold-palladium nanoparticles as a potential autophagy inducer for the treatment of Alzheimer's disease. *J. Colloid Interface Sci.* **2019**, *552*, 388–400.
69. Kanat, O.; Ertas, H.; Caner, B. Platinum-induced neurotoxicity: A review of possible mechanisms. *World J. Clin. Oncol.* **2017**, *8*, 329–335.
70. Chaudhary, S.; Umar, A.; Mehta, S. Selenium nanomaterials: An overview of recent developments in synthesis, properties and potential applications. *Prog. Mater. Sci.* **2016**, *83*, 270–329.
71. Maiyo, F.; Singh, M. Folate-Targeted mRNA Delivery Using Chitosan Functionalized Selenium Nanoparticles: Potential in Cancer Immunotherapy. *Pharmaceuticals* **2019**, *12*, 164.
72. Singh, D.; Singh, M. Hepatocellular-Targeted mRNA Delivery using functionalized Selenium Nanoparticles in vitro. *Pharmaceutics* **2021**, *13*, 298.
73. Doadrio, A.L.; Sánchez-Montero, J.M.; Doadrio, J.C.; Salinas, A.J.; Vallet-Regí, M. Mesoporous silica nanoparticles as a new carrier methodology in the controlled release of the active components in a polypill. *Eur. J. Pharm. Sci.* **2017**, *97*, 1–8.
74. Moodley, T.; Singh, M. Sterically Stabilized Polymeric Mesoporous Silica Nanoparticles Improve Doxorubicin Efficiency: Tailored Cancer Therapy. *Molecules* **2020**, *25*, 742.
75. Padayachee, J.; Daniels, A.N.; Balgobind, A.; Ariatti, M.; Singh, M. HER-2/neu and MYC gene silencing in breast cancer: Therapeutic potential and advancement in non-viral nanocarrier systems. *Nanomedicine* **2020**, *15*, 1437–1452.
76. Nday, C.M.; Halevas, E.; Jackson, G.E.; Salifoglou, A. Quercetin encapsulation in modified silica nanoparticles: Potential use against Cu (II)-induced oxidative stress in neurodegeneration. *J. Inorg. Biochem.* **2015**, *145*, 51–64.

77. Ramnandan, D.; Mokhosi, S.; Daniels, A.; Singh, M. Chitosan, Polyethylene glycol and Polyvinyl alcohol modified MgFe_2O_4 ferrite magnetic nanoparticles in Doxorubicin delivery: A comparative study in vitro. *Molecules* **2021**, *26*, 3893.
78. Almaki, J.H.; Nasiri, R.; Idris, A.; Majid, F.A.A.; Salouti, M.; Wong, T.S.; Dabagh, S.; Marvibaigi, M.; Amini, N. Synthesis, characterization and in vitro evaluation of exquisite targeting SPIONs–PEG–HER in HER2+ human breast cancer cells. *Nanotechnology* **2016**, *27*, 105601.
79. Mngadi, S.; Mokhosi, S.; Singh, M.; Mdlalose, W.B. Chitosan-functionalized $\text{Mg}_{0.5}\text{Co}_{0.5}\text{Fe}_2\text{O}_4$ magnetic nanoparticles enhance delivery of 5-fluorouracil in vitro. *Coatings* **2020**, *10*, 446.
80. Ansari, M.O.; Ahmad, M.F.; Shadab, G.G.H.A.; Siddique, H.R. Superparamagnetic iron oxide nanoparticles based cancer theranostics: A double edge sword to fight against cancer. *J. Drug Deliv. Sci. Technol.* **2018**, *45*, 177–183.
81. Sanginario, A.; Miccoli, B.; Demarchi, D. Carbon Nanotubes as an Effective Opportunity for Cancer Diagnosis and Treatment. *Biosensors* **2017**, *7*, 9.
82. Mbatha, L.S.; Maiyo, F.; Daniels, A.; Singh, M. Dendrimer-coated Gold Nanoparticles for Efficient Folate-Targeted mRNA Delivery in vitro. *Pharmaceutics* **2021**, *13*, 900.
83. Mbatha, L.S.; Maiyo, F.C.; Singh, M. Dendrimer Functionalized Folate-Targeted Gold Nanoparticles for Luciferase Gene Silencing in vitro: A Proof of Principle Study. *Acta Pharm.* **2019**, *69*, 49–61.
84. Akinyelu, A.; Oladimeji, O.; Singh, M. Lactobionic Acid-Chitosan Functionalized Gold Coated Poly (lactide-co-glycolide) Nanoparticles for Hepatocyte Targeted Gene Delivery. *Adv. Nat. Sci. Nanosci. Nanotechnol.* **2020**, *11*, 045017.
85. Sánchez-López, E.; Ettcheto, M.; Egea, M.A.; Espina, M.; Cano, A.; Calpena, A.C.; Camins, A.; Carmona, N.; Silva, A.M.; Souto, E.B.; *et al.* Memantine loaded PLGA PEGylated nanoparticles for Alzheimer's disease: In vitro and in vivo characterization. *J. Nanobiotechnol.* **2018**, *16*, 32.
86. Tong-un, T.; Wannanon, P.; Wattanathorn, J.; Phachonpai, W. Cognitive-enhancing and antioxidant activities of quercetin liposomes in animal model of Alzheimer's disease. *J. Biol. Sci.* **2010**, *10*, 84–91.
87. Li, W.; Zhou, Y.; Zhao, N.; Hao, B.; Wang, X.; Kong, P. Pharmacokinetic behavior and efficiency of acetylcholinesterase inhibition in rat brain after intranasal administration of galanthamine hydrobromide loaded flexible liposomes. *Environ. Toxicol. Pharmacol.* **2012**, *34*, 272–279.
88. Kassem, L.M.; Ibrahim, N.A.; Farhana, S.A. Nanoparticle Therapy Is a Promising Approach in the Management and Prevention of Many Diseases: Does It Help in Curing Alzheimer Disease? *J. Nanotechnol.* **2020**, *2020*, 8147080.

89. Kanwar, J.R.; Sun, X.; Punj, V.; Sriramoju, B.; Mohan, R.R.; Zhou, S.-F.; Chauhan, A.; Kanwar, R.K. Nanoparticles in the treatment and diagnosis of neurological disorders: Untamed dragon with fire power to heal. *Nanomed. Nanotechnol. Biol. Med.* **2012**, *8*, 399–414.
90. Nel, A.; Xia, T.; Madler, L.; Li, N. Toxic potential of materials at the nanolevel. *Science* **2006**, *311*, 622–627.
91. Pisanic, T.R., 2nd; Blackwell, J.D.; Shubayev, V.I.; Fiñones, R.R.; Jin, S. Nanotoxicity of iron oxide nanoparticle internalization in growing neurons. *Biomaterials* **2007**, *28*, 2572–2581.
92. Wang, J.; Rahman, M.F.; Duhart, H.M.; Newport, G.D.; Patterson, T.A.; Murdock, R.C.; Hussain, S.M.; Schlager, J.J.; Ali, S.F. Expression changes of dopaminergic system-related genes in PC12 cells induced by manganese, silver, or copper nanoparticles. *Neurotoxicology* **2009**, *30*, 926–933.
93. Deng, X.; Luan, Q.; Chen, W.; Wang, Y.; Wu, M.; Zhang, H.; Jiao, Z. Nanosized zinc oxide particles induce neural stem cell apoptosis. *Nanotechnology* **2009**, *20*, 115101.
94. Kim, Y.S.; Kim, J.S.; Cho, H.S.; Rha, D.S.; Kim, J.M.; Park, J.D.; Choi, B.S.; Lim, R.; Chang, H.K.; Chung, Y.H.; *et al.* Twenty-eightday oral toxicity, genotoxicity, and gender-related tissue distribution of silver nanoparticles in Sprague–Dawley rats. *Inhal. Toxicol.* **2008**, *20*, 575–583.
95. Yarjanli, Z.; Kamran, G.; Abolghasem, E.; Soheila, R.; Ali, Z. Iron oxide nanoparticles may damage to the neural tissue through iron accumulation, oxidative stress, and protein aggregation. *BMC Neurosci.* **2017**, *18*, 51–67.
96. Manickam, V.; Dhakshinamoorthy, V.; Perumal, E. Iron oxide nanoparticles induces cell cycle-Dependent neuronal apoptosis in mice. *J. Mol. Neurosci.* **2018**, *64*, 352–362.
97. Dhakshinamoorthy, V.; Manickam, V.; Perumal, E. Neurobehavioural toxicity of iron oxide nanoparticles in mice. *Neurotox. Res.* **2017**, *32*, 187–203.
98. Tereanu, D.M.; Chircov, C.; Grumezescu, A.M.; Volceanov, A.; Teleanu, R.I. Impact of Nanoparticles on Brain Health: An Up to Date Overview. *J. Clin. Med.* **2018**, *7*, 490.
99. Cenã, V.; Játiva, P. Nanoparticle crossing of blood–brain barrier: A road to new therapeutic approaches to central nervous system diseases. *Nanomedicine* **2018**, *13*, 1513–1516.
100. Mukherjee, S.; Madamsetty, V.S.; Bhattacharya, D.; Chowdhury, S.R.; Paul, M.K.; Mukherjee, A. Recent advances of nanomedicine in neurodegenerative disorders therapeutics. *Adv. Funct. Mater.* **2020**, *30*, 2003054. [CrossRef]
101. Domínguez, A.; Álvarez, A.; Hilario, E.; Suarez-Merino, B.; Goñi-de-Cerio, F. Central nervous system diseases and the role of the blood-brain barrier in their treatment. *Neurosci. Dis.* **2013**, *1*, 3.
102. Chu, D.; Dong, X.; Shi, X.; Zhang, C.; Wang, Z. Neutrophil-Based Drug Delivery System. *Adv. Mater.* **2018**, *30*, e1706245.
103. Lu, W. Adsorptive-mediated brain delivery systems. *Curr. Pharm. Biotechnol.* **2012**, *13*, 2340–2348.

104. Lin, T.; Zhao, P.; Jiang, Y.; Tang, Y.; Jin, H.; Pan, Z.; He, H.; Yang, V.C.; Huang, Y. Blood–brain barrier-penetrating albumin nanoparticles for biomimetic drug delivery via albumin-binding protein pathways for anti-glioma therapy. *ACS Nano* **2016**, *10*, 9999–10012.
105. Liu, D.Z.; Cheng, Y.; Cai, R.Q.; Wang, B.; Wang, W.-W.; Cui, H.; Liu, M.; Zhang, B.-L.; Mei, Q.-B.; Zhou, S.-Y. The enhancement of siPLK1 penetration across BBB and its anti-glioblastoma activity in vivo by magnet and transferrin co-modified nanoparticle. *Nanomedicine* **2018**, *14*, 991–1003.
106. Bourassa, P.; Tremblay, W.A.C.; Paris-Robidas, S.; Calon, F. Transferrin Receptor-Mediated Uptake at the Blood–Brain Barrier Is Not Impaired by Alzheimer’s Disease Neuropathology. *Mol. Pharm.* **2019**, *16*, 583–594.
107. Bridle, K.R.; Crawford, D.H.G.; Ramm, G.A. Identification and characterization of the hepatic stellate cell transferrin receptor. *Am. J. Pathol.* **2003**, *162*, 1661–1667.
108. Eavarone, D.A.; Yu, X.; Bellamkonda, R.V. Targeted drug delivery to C6 glioma by transferrin-coupled liposomes. *J. Biomed. Mater. Res.* **2000**, *51*, 10–14.
109. Takeda, A. Significance of transferrin in iron delivery to the brain. *J. Health Sci.* **2001**, *47*, 520–524.
110. Li, H.; Sun, H.; Qian, Z.M. The role of the transferrin-transferrin-receptor system in drug delivery and targeting. *Trends Pharmacol. Sci.* **2002**, *23*, 206–209.
111. Gao, N.; Sun, H.; Dong, K.; Ren, J.; Qu, X. Gold-Nanoparticle-Based Multifunctional Amyloid- β Inhibitor against Alzheimer’s Disease. *Chem. Eur. J.* **2015**, *21*, 829–835.
112. Yin, T.; Xie, W.; Sun, J.; Yang, L.; Liu, J. Penetratin Peptide-Functionalized Gold Nanostars: Enhanced BBB Permeability and NIR Photothermal Treatment of Alzheimer’s Disease Using Ultralow Irradiance. *ACS Appl. Mater. Interfaces* **2016**, *8*, 19291–19302.
113. Zhang, Y.; Walker, J.B.; Minic, Z.; Liu, F.; Goshgarian, H.; Mao, G. Transporter protein and drug-conjugated gold nanoparticles capable of bypassing the blood–brain barrier. *Sci. Rep.* **2016**, *6*, 25794.
114. Aryal, M.; Arvantis, C.D.; Alexander, P.M.; McDannold, N. Ultrasound-mediated blood-brain barrier disruption for targeted drug delivery in the central nervous system. *Adv. Drug Deliv. Rev.* **2014**, *72*, 94–109.
115. Dong, X. Current Strategies for Brain Drug Delivery. *Theranostics* **2018**, *8*, 1481–1493.
116. Hardee, C.L.; Arévalo-Soliz, L.M.; Hornstein, B.D.; Zechiedrich, L. Advances in Non-Viral DNA Vectors for Gene Therapy. *Genes* **2017**, *8*, 65.
117. Prabu, S.L.; Suriyaprakash, T.N.K.; Thirumurugan, R. Medicated nanoparticles for gene delivery. In *Advanced Technology for Delivering Therapeutics*; Maiti, S., Sen, K.K., Eds.; IntechOpen: London, UK, 2017; pp. 13–29.
118. Thomas, T.J.; Tajmir-Riahi, H.-A.; Pillai, C.K.S. Biodegradable Polymers for Gene Delivery. *Molecules* **2019**, *24*, 3744. [CrossRef]
119. Habib, S.; Daniels, A.; Ariatti, M.; Singh, M. Anti-

- c-MYC Cholesterol based Lipoplexes as Onco-Nanotherapeutic Agents in vitro. *F1000Research* **2020**, *9*, 770.
120. Fitzgerald, K.; Frank-Kamenetsky, M.; Shulga-Morskaya, S.; Liebow, A.; Bettencourt, B.R.; Sutherland, J.E.; Hutabarat, R.M.; Clausen, V.A.; Karsten, V.; Cehelsky, J.; *et al.* Effect of an RNA interference drug on the synthesis of proprotein convertase subtilisin/kexin type 9 (PCSK9) and the concentration of serum LDL cholesterol in healthy volunteers: A randomized, single-blind, placebo-controlled, phase 1 trial. *Lancet* **2014**, *383*, 60–68.
 121. Maiyo, F.; Singh, M. Selenium Nanoparticles: Potential in Cancer Gene and Drug Delivery. *Nanomedicine* **2017**, *12*, 1075–1089.
 122. Padayachee, J.; Singh, M. Therapeutic applications of CRISPR/Cas9 in Breast Cancer and delivery potential of Gold Nanomaterials. *Nanobiomedicine* **2020**, *7*, 1849543520983196.
 123. Yang, L.; Miao, L.; Liang, F.; Huang, H.; Teng, X.; Li, S.; Nuriddinov, J.; Selzer, M.E.; Hu, Y. The mTORC1 effectors S6K1 and 4E-BP play different roles in CNS axon regeneration. *Nat. Commun.* **2014**, *5*, 5416.
 124. Cheng, H.C.; Kim, S.R.; Oo, T.F.; Kareva, T.; Yarygina, O.; Rzhetskaya, M.; Wang, C.; During, M.; Tallozy, Z.; Tanaka, K.; *et al.* Akt suppresses retrograde degeneration of dopaminergic axons by inhibition of macroautophagy. *J. Neurosci.* **2011**, *31*, 2125–2135.
 125. Miao, L.; Yang, L.; Huang, H.; Liang, F.; Ling, C.; Hu, Y. mTORC1 is necessary but mTORC2 and GSK3b are inhibitory for AKT3-induced axon regeneration in the central nervous system. *eLife* **2016**, *5*, 14908.
 126. Hetz, C.; Russelakis-Carneiro, M.; Maundrell, K.; Castilla, J.; Soto, C. Caspase-12 and endoplasmic reticulum stress mediate neurotoxicity of pathological prion protein. *EMBO J.* **2003**, *22*, 5435–5445.
 127. Bingol, B.; Tea, J.S.; Phu, L.; Reichelt, M.; Bakalarski, C.E.; Song, Q.; Foreman, O.; Kirkpatrick, D.S.; Sheng, M. The mitochondrial deubiquitinase USP30 opposes parkin-mediated mitophagy. *Nature* **2014**, *510*, 370–375.
 128. Onyango, I.G.; Dennis, J.; Khan, S.M. Mitochondrial dysfunction in Alzheimer’s disease and the rationale for bioenergetics based therapies. *Aging Dis.* **2016**, *7*, 201–214.
 129. Tsunemi, T.; Ashe, T.D.; Morrison, B.E.; Soriano, K.R.; Au, J.; Roque, R.A.; Lazarowski, E.R.; Damian, V.A.; Masliah, E.; La Spada, A.R. PGC-1 α rescues Huntington’s disease proteotoxicity by preventing oxidative stress and promoting TFEB function. *Sci. Transl. Med.* **2012**, *4*, 142ra97.
 130. Li, J.; Hart, R.P.; Mallimo, E.M.; Swerdel, M.R.; Kusnecov, A.W.; Herrup, K. EZH2-mediated H3K27 trimethylation mediates neurodegeneration in ataxia-telangiectasia. *Nat. Neurosci.* **2013**, *16*, 1745–1753.
 131. Valdes, P.; Mercado, G.; Vidal, R.L.; Molina, C.; Parsons, G.; Court, F.A.; Martinez, A.; Galleguillos, D.; Armentano, D.; Schneider, B.L.; *et al.* Control of dopaminergic neuron

- survival by the unfolded protein response transcription factor XBP1. *Proc. Natl. Acad. Sci. USA* **2014**, *111*, 6804–6809.
132. Chen, W.; Hu, Y.; Ju, D. Gene therapy for neurodegenerative disorders: Advances, insights and prospects. *Acta Pharm. Sin. B* **2020**, *10*, 1347–1359.
133. Hou, K.; Zhao, J.; Wang, H.; Li, B.; Li, K.; Shi, X.; Wan, K.; Ai, J.; Lv, J.; Wang, D.; *et al.* Chiral gold nanoparticles enantioselectively rescue memory deficits in a mouse model of Alzheimer's disease. *Nat. Commun.* **2020**, *11*, 4790.
134. Hu, K.; Chen, X.; Chen, W.; Zhang, L.; Li, J.; Ye, J.; Zhang, Y.; Zhang, L.; Li, C.; Yin, L.; *et al.* Neuroprotective effect of gold nanoparticles composites in Parkinson's disease model. *Nanomed. Nanotechnol. Biol. Med.* **2018**, *14*, 1123–1136.
135. Gonzalez-Carter, D.; Leo, B.; Ruenraroengsak, P.; Chen, S.; Goode, A.; Theodorou, I.; Chung, K.; Carzaniga, R.; Shaffer, M.; Dexter, D.; *et al.* Silver nanoparticles reduce brain inflammation and related neurotoxicity through induction of H₂S-synthesizing enzymes. *Sci. Rep.* **2017**, *7*, 42871.
136. Youssif, K.A.; Haggag, E.G.; Elshamy, A.M.; Rabeh, M.A.; Gabr, N.M.; Seleem, A.; Salem, M.A.; Hussein, A.S.; Krischke, M.; Mueller, M.J.; *et al.* Anti-Alzheimer potential, metabolomic profiling and molecular docking of green synthesized silver nanoparticles of *Lampranthus coccineus* and *Malephora lutea* aqueous extracts. *PLoS ONE* **2019**, *14*, e0223781.
137. Huo, X.; Zhang, Y.; Jin, X.; Li, Y.; Zhang, L. A novel synthesis of selenium nanoparticles encapsulated PLGA nanospheres with curcumin molecules for the inhibition of amyloid β aggregation in Alzheimer's disease. *J. Photochem. Photobiol. B Biol.* **2019**, *190*, 98–102.
138. Sun, A.; Benet, L.Z. Late-Stage Failures of Monoclonal Antibody Drugs: A Retrospective Case Study Analysis. *Pharmacology* **2020**, *105*, 145–163.
139. ClinicalTrials.gov. Available online: <https://clinicaltrials.gov/ct2/results?cond=alzheimers+and+parkinsons> (accessed on 15 August 2021).
140. Clene Awaits US Patent Covering Gold Nanocrystals' Use in Treating MS. Available online: <https://multiplesclerosisnewstoday.com/news-posts/2021/01/20/clene-awaits-us-patent-covering-gold-nanocrystal-use-ms-treatment/> (accessed on 15 August 2021).

Chapter 3

Lipid Nanoparticles: Promising Treatment Approach for Parkinson's Disease

Lipid Nanoparticles: Promising Treatment Approach for Parkinson's Disease

This chapter has been published in the *International Journal of Molecular Sciences*.

Jagaran, K.; Singh, M. Lipid Nanoparticles: Promising Treatment Approach for Parkinson's Disease. *Int. J. Mol. Sci.* 2022, 23, 9361. <https://doi.org/10.3390/ijms23169361>

Abstract: Parkinson's disease (PD), a neurodegenerative disorder, is a life-altering, debilitating disease exhibiting a severe physical, psychological, and financial burden on patients. Globally, approximately 7–10 million people are afflicted with this disease, with the number of cases estimated to increase to 12.9 million by 2040. PD is a progressive movement disorder with nonmotor symptoms, including insomnia, depression, anxiety, and anosmia. While current therapeutics are available to PD patients, this treatment remains palliative, necessitating alternative treatment approaches. A major hurdle in treating PD is the protective nature of the blood–brain barrier (BBB) and its ability to limit access to foreign molecules, including therapeutics. Drugs utilized presently are nonspecific and administered at dosages that result in numerous adverse side effects. Nanomedicine has emerged as a potential strategy for treating many diseases. From the array of nanomaterials available, lipid nanoparticles (LNPs) possess various advantages, including enhanced permeability to the brain via passive diffusion and specific and nonspecific transporters. Their bioavailability, nontoxic nature, ability to be conjugated to drugs, and targeting moieties catapult LNPs as a promising therapeutic nanocarriers for PD. While PD-related studies are limited, their potential as therapeutics is evident in their formulations as vaccines. This review is aimed at examining the roles and properties of LNPs that make them efficient therapeutic nanodelivery vehicles for the treatment of PD, including therapeutic advances made to date.

Keywords: Parkinson's disease; lipid nanoparticles; drug delivery; blood–brain barrier; nanomedicine

3.1. Introduction

Parkinson's disease (PD) presents itself as a life-altering and debilitating disease that primarily affects the neuronal make-up of the brain. It is deemed a neurodegenerative disorder. It is estimated that 7–10 million people are afflicted with this disease worldwide, with a prevalence rate of 41 in 100,000 people. Notably, the prevalence rate increases to 1900 people per 100,000 in individuals over 80 years old [1]. This growing health issue is postulated to see an increased prevalence to 12.9 million cases by 2040 [2].

Clinically, PD is a progressive movement disorder with various nonmotor symptoms, including sleep disturbance, constipation, depression, anxiety, and anosmia [3,4]. This disease manifests in two forms: (i) sporadic (idiopathic), which is caused by a gene–environment interaction, and (ii) familial, which is genetically inherited in either an autosomal recessive or dominant manner [5,6]. Genetic mutations that cause the disease are noted in some genes, such as the LRRK2, PARK7, PINK1, PRKN, and SNCA. The resulting manifestation of parkinsonian symptoms is due to a pathological effect, which is observed as loss of dopaminergic neurons in the substantia nigra and presence of various protein aggregates (including α -synuclein), called Lewy bodies, in the midbrain [7].

Current therapeutics are palliative, suggesting the need for a novel efficacious strategy to treat PD. Drugs such as levodopa and ropinirole have been met with challenges, especially their need to cross the blood–brain barrier (BBB). Due to the protective ability of the BBB to resist the permeability of foreign molecules into the brain [8], the drugs that are administered constitute low concentrations of dopamine, which result in several side effects in patients [9,10]. The emergence of nanomedicine with its array of nanoparticles (NPs) has unfolded a new route for therapy. Of these, lipid NPs (LNPs) provide significant advantages regarding improved bioavailability, permeability, and solubility. Furthermore, they exhibit high drug-loading capacity, low cytotoxicity, ease of surface modification, and an ability to permit cell-specific targeting [11]. In a study directed at the treatment of glioblastomas, a multifunctional NP comprising the Nutlin-3a drug and superparamagnetic NPs encompassed by LNPs was used. The results obtained highlighted the natural ability of lipids to effectively cross the BBB and to protect the encapsulated cargo while inducing proapoptosis in glioblastoma cells [12]. Although targeting and therapeutics differ between cancer and PD, the ability of these LNPs to permeate the BBB is an important property to be noted for neurodegenerative disease studies.

LNPs present a potentially effective drug delivery strategy for safe and site-specific delivery of therapeutic agents for treatment of PD. Drug nanocarriers can provide advantages such as increased half-life of the therapeutic, reduction in the drug dosage, and reduction in unpleasant side effects [13]. It is due to these reasons that LNPs have made their way to the forefront of nanomedicine. This review looks at the genetics that govern PD, the NPs being used in nanomedicine, and the potential benefits of using LNPs as therapeutic nanodelivery vehicles and their ability to cross the BBB.

3.2. Parkinson's Disease

James Parkinson first described a highly complex, progressive neurodegenerative disorder, aptly named Parkinson's disease (PD). While explaining this disorder as a "shaking palsy", he also highlighted the urgency to mitigate this disorder, stating "there appears to be sufficient reason for hoping that some remedial process may ere long be discovered, by which, at least, the progress of the disease may be stopped" [14]. Despite the advancements in medicine, there has yet to be a cure for PD. PD falls primarily under neurodegenerative disorders that affect neurons of the human brain, resulting in deterioration of the brain function. This debilitating disease is unfortunately incurable, with palliative therapeutics being administered to treat the symptoms. Based on their characteristics, neurodegenerative disorders can be broadly divided as having selective neuronal or regional vulnerability. The former occurs due to the disease pathology affecting particular neurons, while the latter is the deterioration of the pathology over time, impacting a greater number of regions predictably and stereotypically [15].

3.2.1. Neuropathological Hallmarks of Parkinson's Disease

Understanding a disease's neuropathological hallmarks is imperative in developing an appropriate treatment strategy. The onset of the disease occurs in the substantia nigra (SN) pars compacta in the midbrain and begins with degeneration of the dopaminergic neurons and protein aggregates known as Lewy bodies. These protein aggregates are noted as cytoplasmic inclusions together with insoluble aggregates of alpha-synuclein [16]. Autopsies of patients with PD have shown α -synucleinopathies and tauopathies, corticobasal degeneration (CBD), and progressive supranuclear palsy (PSP) as the most common causes of parkinsonism [17].

Selective neuronal vulnerability is eminent in PD and can be inherited or sporadic. Within the SN, two cell groups are affected: the medial and dorsal cell groups (A10 or mesolimbic pathway) are resistant, while the ventrolateral cell groups (A9 or nigrostriatal pathway) are

vulnerable. This vulnerable state is linked to calcium transients, where deficient calcium buffering occurs in A9 compared to A10 neurons, allowing the former dopaminergic neurons to remain vulnerable to cellular stress [17]. Furthermore, a significant reduction in the integrity of the nuclear membrane is noted, which leads to the release of pro-aggregant nuclear factors that trigger α -synuclein aggregation. Following the aggregation, the spread to other cells is either direct or indirect, leading to parkinsonian symptoms [18].

Another key indication of the development of PD is the overproduction and inability to effectively detoxify reactive oxygen species (ROS) and reactive nitrogen species (RNS) [19]. Oxidative and nitrative stress promote the degeneration of dopaminergic neurons in PD. This causes the disruption of important biological processes, resulting in cellular demise [20]. Following the disruption of these key components in the PD substantia nigra, dysregulation of iron and calcium metabolism, increase in neuroinflammatory cells, aging, and mitochondrial dysfunction are imminent [21].

An interesting early patient-based study reflected on the presence of accumulated blood RNA biomarkers in PD. The process of nonsense-mediated decay (NMD) was reported to degrade mRNA and play a regulatory role in the brain. The authors proposed the use of deep brain stimulation surgery to modulate NMD of RNA in the leukocytes of Parkinson's patients and improve the motor-related symptoms associated with PD [22].

3.2.2. Clinical Manifestations and Determinants of Parkinson's Disease

While the mechanism for the onset of the disease is understood, clinical motor symptoms are only presented following the death of 50–70% of SN dopaminergic neurons, suggesting the need to devise a means of identifying the cause before physical manifestations develop [16]. The motor symptoms include muscle tone rigidity, postural instability, bradykinesia, and resting tremors. Beyond this, nonmotor symptoms may also be seen in patients succumbing to PD, such as dementia, autonomic dysfunctions, sleep disorders, sensory abnormalities, depression, and anxiety [23].

Similar to cancer, the onset of PD may be due to environmental or genetic factors. Factors such as head injuries or exposure to toxic chemicals may significantly increase a person's susceptibility to PD. While environmental factors play a crucial role in PD, they can also further trigger patients who are already genetically predisposed to the disease. This was noted in a study on monozygotic and dizygotic twins. The comparison of the concordance rates,

which estimated the heritability rate of PD, was found to be 30%, indicating that most PD risk is related to behavioral and environmental factors [24].

Environmental or external factors that pose a risk to individuals predisposed to PD include, but are not limited to, vigorous exercise, plasma urate, smoking, ibuprofen, and high consumption of coffee. Beyond this, certain pesticides and trauma to the brain have also been recognized as determinants of PD [25]. Further studies have provided greater insight into pesticide exposure and its positive correlation to PD onset in farm workers and rural residences. Laboratory studies have portrayed the use of several dithiocarbamates, rotenone, organochlorines, paraquat, and 2,4-D as causative agents in PD [26,27]. It has further been observed that mild to moderate head injuries, which may have occurred decades before disease onset, are associated with greater risk of PD. The number of injuries and the positioning of the trauma, together with genetic susceptibility, was proposed to increase the risk two- to five-fold [27].

Genetic mutations in the encoded protein that lead to PD disease are either familial or sporadic (gene–environment interactions). Table 3.1 summarizes the various genes involved in PD together with their respective mechanisms of action. Despite this information, much remains unknown, warranting further in-depth studies. Treating the cause of PD at a genomic level may retard the degeneration of many dopaminergic neurons.

Table 3.1. Genes commonly implicated in the onset of Parkinson’s disease.

Gene	Mechanism of Action	Dominant/Recessive	Ref.
LRRK2	Mutations in PD alter kinase and GTPase activities and promote substrate phosphorylation and autophosphorylation. The link to neuronal damage is still unclear.	Late-onset autosomal dominant familial PD	[28]
PARK7	Contains the DJ-1 gene, which undergoes mutation, resulting in loss of gene expression. The mechanism of action is not elucidated, but mouse models show that the DJ- 1 gene may act as a neuroprotective redox sensor.	Autosomal recessive familial PD	[29]
PINK1	Has a regulatory role in the mitochondria, with damaged mitochondria undergoing mitophagy. Mitochondrial depolarization activates PINK1 and causes phosphorylation of ubiquitin at Serine65 (Ser65). High- affinity binding to the E3 ligase ubiquitin (Parkin) primes it for phosphorylation by hPINK1 at an identical Ser65 residue residing in the N-terminal ubiquitin-like domain. The E3 ligase activity is stimulated, resulting in substrates at the outer mitochondrial membrane undergoing ubiquitylation. Direct neuronal damage is still unclear.	Early onset recessive familial PD	[30]
PRKN	Encodes RBR E3 ubiquitin–protein ligases. Mutation results in the loss of this activity, leading to protein accumulation, mitophagy, and mitochondrial dysfunction. PRKN gene is named due to the “stereotypical” phenotypic outcomes.	Autosomal recessive juvenile PD (AR-JP)	[31]
SNCA	Integral in many cellular pathways, including protein degradation, membrane interactions, dopamine release and transport regulation, maintenance of synaptic vesicle supply, autophagy–lysosome pathway, and mitochondrial dysfunction.	Autosomal dominant PD	[32]

3.2.3. Current Therapeutics

Because the current treatment of PD remains palliative, a cure lies in treating the primary causes, such as genetic defects or mutations. To date, dopaminergic administration has been effective for short periods in movement disorders, while antipsychotic medications treat the psychosomatic symptoms [33]. Figure 3.1 summarizes the currently utilized medications for PD treatments and their functions. The major drawback to these medications is their poor ability to efficiently permeate the blood–brain barrier (BBB), causing their localization in the CNS. This often results in low-dose concentrations being administered [34].

As a result of the previously mentioned challenges to the current drugs employed, it is imperative to seek alternative avenues to close the gap between palliative treatment and a cure. One such approach can be the integration of nanomedicine into therapeutic delivery to the brain.

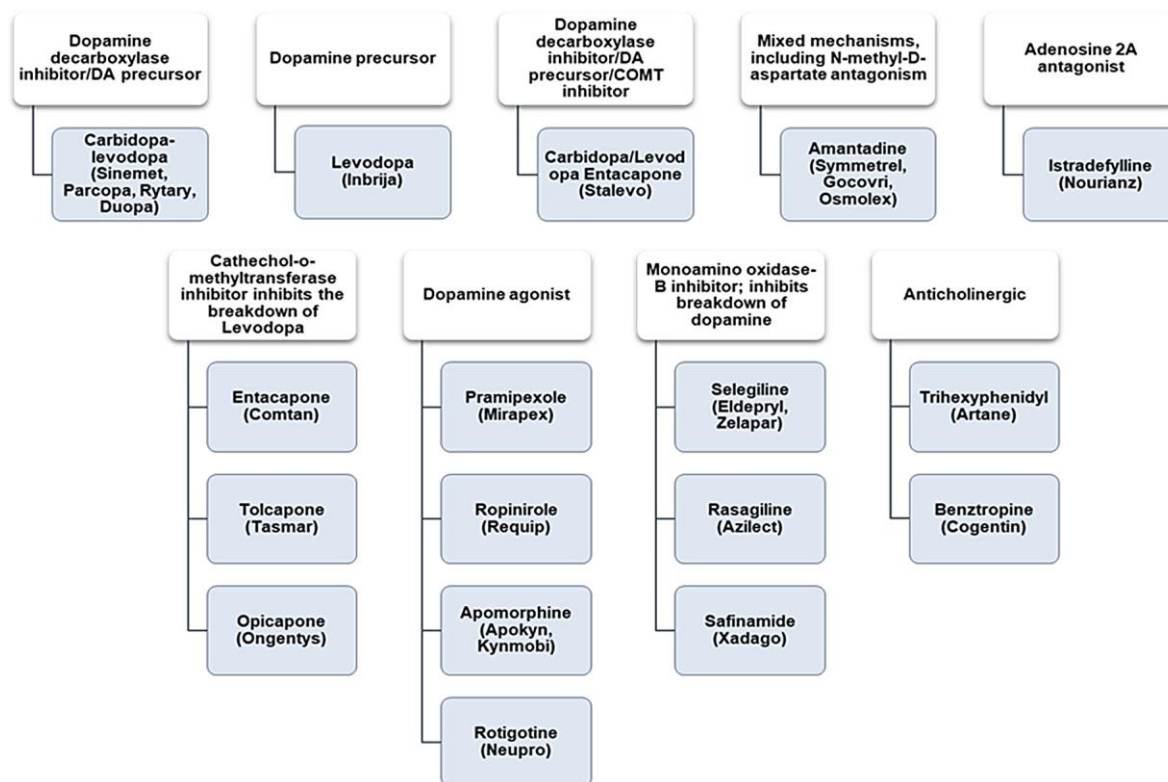


Figure 3.1. Commonly used drugs (shaded) are grouped with their functions (white) and PD therapeutics. Adapted from [33].

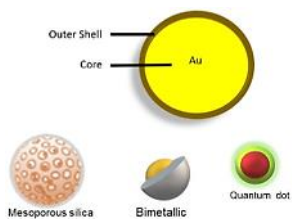
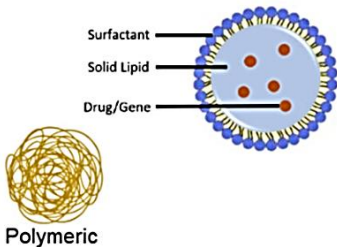
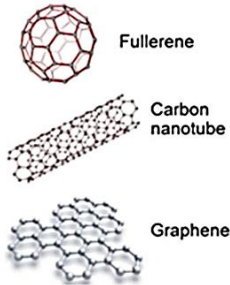
3.3. Nanomedicine

Nanomedicine is known as the utilization of nanosized particles in health and medicine. It is a revolutionary novel system that explores an alternate avenue in treating diseases with greater specificity and efficiency. Some NPs can provide a theranostic approach to medicine, with this duality being a significant advantage [35]. The inexpensive means of creating these NPs, together with the ability of their surfaces to be easily manipulated for different tissue targets, has enhanced their importance in medicine. Several studies have demonstrated the potential of nanomedicine in treating diseases where traditional medicine had failed. The amalgamation of current advances in biology, material science, chemistry, and physics to aid diagnostic and treatment strategies is now coming to fruition [36]. To date, many different NPs have been synthesized and used in nanomedicine, with novel NPs regularly evolving to add to the arsenal of NPs at our disposal. This improves the chances of treating a wide range of disorders as each

NP possesses its unique properties and can be tailor-made to treat a specific disease. Generally, NPs can be classed as being inorganic, organic, or carbon-based NPs (Table 3.2).

The principal use of NPs is to overcome challenges faced by commonly used drugs, such as poor stability, potential immunogenicity, solubility, and reduced plasma half-life [37]. Nanodelivery systems can increase the therapeutics circulation time, allow several different administration routes, circumvent potential solubility issues using hydrophobic molecules, and cater for favorable biodistribution of the therapeutic gene or drug [38]. Overall, their ideal size, quantum properties, ability to be conjugated to pharmacologically active agents, and favorable surface-to-mass ratio assures their potential as therapeutic delivery systems [39]. Nanoscale particles (<100 nm) favor the passage through biological barriers, such as those found in the nervous system, lung, and vasculature surrounding tumors [38,40]. Nanomaterials have shown the ability to facilitate the stability and protection of genetic materials such as DNA, mRNA, and siRNA and to enhance transfection efficacy with low cytotoxicity [41–43]. Clinical trials have since been conducted for cancer and fungal infections, utilizing liposomes to deliver doxorubicin and amphotericin B [37]. One of the optimistic outcomes of the application of nanomedicine involves using brain tumor targeting for efficient passage across the BBB [8,44]. The current review will discuss the organic class of NPs and focus on lipid NPs (LNPs).

Table 3.2. The three broad classes of nanoparticles currently used in nanomedicine.

	Inorganic Nanoparticles	Organic Nanoparticles	Carbon-Based Nanoparticles
Examples	Quantum dots, metal oxide nanoparticles, metallic nanoparticles, mesoporous silica, bimetallic, and magnetic nanoparticles.	Solid lipid nanoparticles, micelles, liposomes, nanoemulsions, and polymeric nanoparticles.	Carbon nanotubes, fullerenes, graphene oxide, and nanodiamonds.
General Structure	Can contain core/shell structure from inorganic materials. Differ from their bulk material. 	Generally, comprise surfactants, cosolvents, and cosurfactants of organic nature. Lipid nanoparticles commonly contain phospholipids. 	Includes sp ² -hybridized carbon atoms. Have different shapes depending on the arrangement of the hexagonal lattice. 
Properties	Facile synthesis. Provides a large surface area for large biomolecules. Tunable shapes and sizes [45].	Ease of preparation from biodegradable polymers. High stability in biological fluids and during storage [46].	Large surface area, high adsorption capacity, chemical inertness, thermal stability, and conductivity. Ideal for electrochemical detection [47].

3.3.1. Lipid Nanoparticles

Lipid NPs (LNPs) have been the most popular NPs with regard to progress into clinical trials, possibly due to their lipophilic, bioacceptable, and biodegradable nature, which permits a less toxic therapeutic approach. These LNPs have shown promising results as therapeutic delivery vehicles and have gained popularity since their use as a delivery vehicle of mRNA in the COVID-19 vaccine. The lipids were able to house the mRNA in vivo while remaining stable in the bloodstream before being taken up by phagocytic cells via endocytosis. This LNP acted as an immunological adjuvant to elicit immune responses against the spike proteins of the virus

[48]. LNPs (Figure 3.2) are usually spherical vesicles composed of ionizable cationic lipids and a helper lipid.

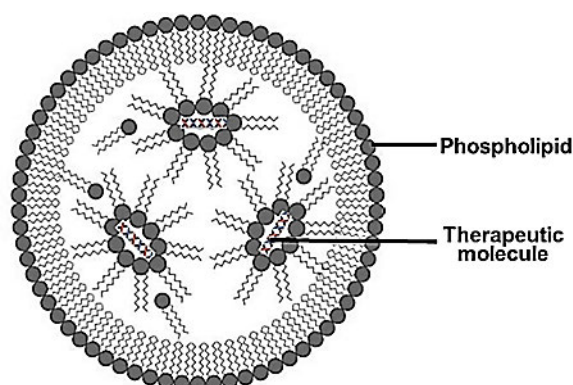


Figure 3.2. An illustration of a lipid nanoparticle showing the outer phospholipid layer and the encapsulated therapeutics.

LNPs can change charge based on their environment, portraying a neutral charge at physiological pH with low toxicity and a positive charge at low pH that permits nucleic acid complexation. These LNPs possess improved cellular uptake, circulation half-life, and endosomal escape [49]. This is primarily due to the ionizable properties of the lipids at low pH, which permit the release of pharmacologically active agents directly into the cytoplasm. LNPs are easily modified by selecting an appropriate composition of NP, which includes a helper lipid to promote cell binding and uptake. Polyethylene glycol (PEG) has been commonly added to significantly reduce opsonization by serum proteins and to reduce reticuloendothelial clearance. Adding cholesterol also assists by filling the crevices between the lipid molecules, adding stability, and favouring cell membrane fusion [50]. The size of the lipids, surface charge, and the specific lipid used in the formulation will influence the performance of LNPs in vivo.

Zhao and co-workers constructed LNPs that were surface modified to load a basic fibroblast growth factor (bFGF) for targeting the brain via administration through the nasal cavity. The study utilized a gelatin polymer mixed with bFGF as the aqueous phase, followed by the incorporation of hydrogenated soy phosphatidylcholine as the lipid phase. The formulated LNPs portrayed high stability (zeta potential ~ -27.6 mV), were ~ 172 nm in size, and had an entrapment efficiency of around 86.7%. This novel therapeutic system was found to cause no adverse effects, had low cytotoxicity, and efficiently transported the active pharmacological agent to the olfactory bulb and striatum in a hemi-parkinsonian rat model. The benefit of LNPs was evident when compared to the poor efficiency and stability of naked bFGF [51].

Various lipid nano-formulations have been produced to date. These include liposomes, solid lipid nanoparticles, lipid nanoemulsions, nanostructured lipid carriers, and lipid–polymer hybrid carriers. These will be briefly discussed.

3.3.2. Liposomes

Liposomes were initially identified in the 1960s following the spontaneous formation of closed lipid bilayers in water [52]. It remains a popular choice for lipid-based vehicles because of its simple structure [53]. These NPs are composed of an aqueous core that encapsulates the drug or gene of choice and is enclosed in a unilamellar or multilamellar phospholipid bilayer that contains both hydrophilic and hydrophobic groups (Figure 3.3) [54].

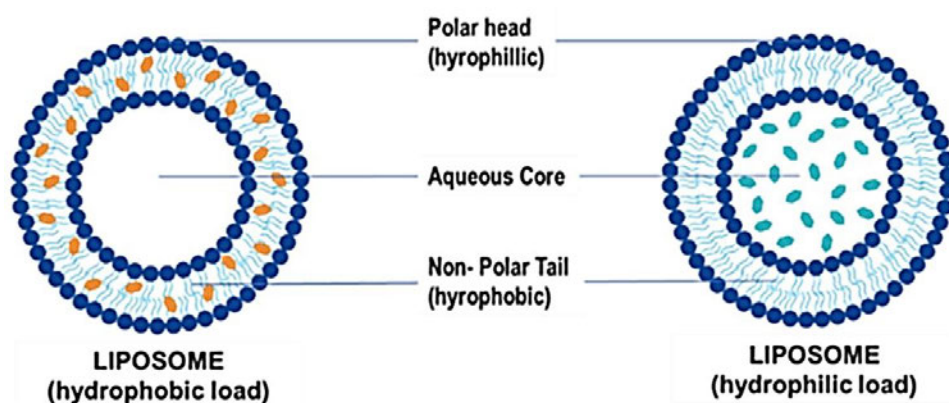


Figure 3.3. Illustration of a liposome and encapsulation of hydrophilic and hydrophobic molecules.

Unilamellar liposomes are 20–250 nm, have a single lipid layer surrounding an aqueous core, and are ideal for encapsulating drugs or genes. Multilamellar liposomes are larger in size (1–5 μm) and can have two or more concentric lipid bilayers for entrapping biomolecules [55]. Liposomes have been classed as anionic, neutral, or cationic depending on their lipid composition. Neutral and anionic liposomes generally encapsulate their therapeutic cargo, while cationic liposomes can also electrostatically bind to nucleic acids to produce lipoplexes [53].

Studies over the years have shown that liposomes can effectively protect their genetic cargo *in vitro* [50,56,57]. This protection ability of liposomes is due to the phospholipid bilayer acting as a barrier to fluctuating pH conditions, enzyme action, and free radicals, thereby preventing degradation of pharmacologically active agents and genetic material before their release [55]. To produce liposomes that are devoid of vesicle surface-to-surface interactions, an ionizable

or cationic lipid that improves adjuvanticity, cholesterol for stability of the lipid membrane in vivo, and distearoyl phosphatidylcholine together with pegylated lipids have been used [50,52,56].

3.3.3. Solid Lipid Nanoparticles and Nanostructured Lipid Carriers

Although liposomes have shown great efficiency and have been the most popular to date, they possess some limitations with respect to low drug entrapment, difficulty in achieving performance at a large scale, and the requirement for complex production methods using organic solvents [52]. To this end, solid lipid nanoparticles (SLNs) and nanostructured lipid carriers (NLCs) were developed (Figure 3.4). The significant difference between these is seen in the crystalline lipid layers, with liposomes comprising liquid crystalline bilayers of the lipid, while SLNs contain lipids that are solid at physiological temperature and NLC are made up of a mixture of both [58–60].

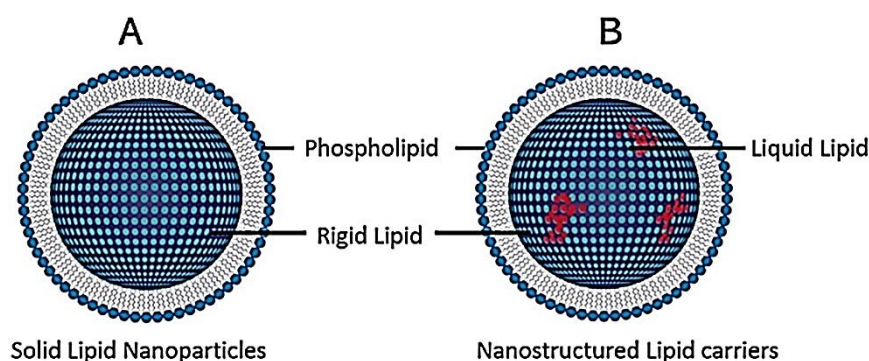


Figure 3.4. General structure of (A) solid lipid nanoparticles (SLNPs) and (B) nanostructured lipid carriers (NLCs).

Depending on their synthesis, SLNs possess more of an advantage due to their size (40 to 1000 nm) while exhibiting enhanced physical stability. Furthermore, SLNs and NLCs have shown greater bioavailability, higher loading capacities, controlled cargo release, production on a larger scale, and the ability to carry out synthesis without organic solvents [52]. It has been reported that SLNs are taken up by clathrin-mediated endocytosis and degraded in the lysosome to release the therapeutics [60]. The drawback of SLNs is seen in their long-term storage, with the occurrence of crystallization and possible expulsion of the cargo into the storage media [61]. To overcome this occurrence, NLCs have been formulated with solid and liquid lipids at room temperature, significantly reducing the degree of crystallinity [59,60].

3.4. LNPs and the Blood–Brain Barrier

A significant obstacle in developing an efficient therapeutic system for PD is the inability of drugs, peptides, and large molecules to pass through the brain's endothelial cellular lining, known as the blood–brain barrier (BBB) [62]. When designing appropriate LNPs for traversing the BBB, the brain itself needs to be prioritized to develop a strategy to bypass the physiological mechanisms in place to prevent the entry of foreign substances. Within the structure of the BBB are brain capillary endothelial cells, pericytes, perivascular mast cells, basement membranes, astrocytes, and neuronal cells, which govern the exchange of molecules between the blood and the brain [8,33,63,64]. The brain capillary endothelial cells (BCECs) provide a significant protective ability via their close attachment to each other, creating a tight junction. This tight junction eliminates the risk of harmful toxins and pathogens entering the brain, while the degrading enzymes act as a secondary defence mechanism [8,65].

The BBB's natural ability to permit the entry of specific molecules can be exploited using LNPs. Research has shown that entry provisions occur via various mechanisms, such as receptor mediation, endocytosis, carrier-mediated transcytosis, cell-mediated endocytosis, adsorptive transcytosis, the transcellular pathway used for small lipoidal compounds, and paracellular diffusion employed for hydrophilic substances [66,67]. The ascendancy of exploiting these natural properties of the BBB creates loopholes for developing novel LNPs due to their unique capabilities that enable them to target and traverse the BBB [68]. LNP surfaces can be enhanced via surface modifications, which allow for effective site-specific targeting [69]. Numerous receptors have been identified on the surface of the BBB, which can effectively be used as surface-active ligands to facilitate receptor-mediated transcytosis [70]. Some of these targeting strategies are outlined in Table 3.3.

Table 3.3. Some surface modifications to NPs for targeting the brain and increasing adsorption.

Ligand	Favourable Properties	Ref.
Transferrin	Transferrin receptors (TfR) are highly expressed in the BCECs and are thus commonly used targeting ligands. They promote efficient accumulation of therapeutics in the brain.	[71]
Lactoferrin	Lactoferrin, a glycoprotein present in the brain, acts as a receptor at the BBB. This approach has been identified to enhance the pharmacological properties of drugs. Furthermore, a positively charged group is exhibited upon binding, creating greater potential for NP entry.	[72,73]
Glucose	The BBB possesses glucose transporters (GLUTs) for active delivery of glucose into the brain to meet the high energy demand. NPs coated with glucose may be able to efficiently overcome the BBB via this transport system.	[74,75]
Glutathione PEGylation	PEGylated lipids with glutathione conjugates (G-Technology®) can pass through the BBB via the sodium-dependent transporter.	[76]
Angiopep-2	Has good transcytosis ability across the BBB. Can be conjugated to LNPs.	[8,77-79]

BCECs = brain capillary endothelial cells.

From the ligands in Table 3.3, the conjugation of Angiopep-2 to both organic and inorganic NPs carrying therapeutic genes or drugs has been studied to treat brain cancer, brain injury, stroke, epilepsy, fungal infections, Alzheimer's disease (AD), and Parkinson's disease (PD) [8]. Angiopep-2 has shown the ability for transcytosis and accumulation in the parenchyma. Recently, a phase II study ANG1005 (made up of paclitaxel residues linked to Angiopep-2) produced positive results in patients with breast-cancer-related brain metastases [80]. Appending Angiopep-2 to LNPs may be favourable as it can promote transport across the BBB and shows specificity for glioma cells that overexpress low-density lipoprotein receptor-related protein-1 (LRP1) on their surfaces [81].

Compared to inorganic NPs, LNPs portray several advantages. NPs produced by chemical and physical means incur high manufacturing costs, and the process is time-consuming. Metallic NPs utilizing zinc oxide and copper oxide have been reported to cause toxicity to the environment and the host tissue [82]. In order to circumvent this toxicity, many researchers have turned to biological synthesis methods [83]. LNPs generally have a phospholipid outer layer that physiologically resembles the cellular membrane. This enhances cellular uptake and the possibility of them passing through the BBB [84]. The increased BBB permeability occurs via the P-glycoprotein efflux system, which offers a means to cross the BBB. Furthermore, the efficient encapsulation properties of these LNPs protect the loaded drug or gene from early

systemic enzyme degradation [85]. Further protection is offered by the cholesterol component of the lipid carrier. This adds to the retention of natural homeostasis in a biological environment and reduction in the entry of water into the LNPs to avoid premature degradation [84]. This was validated in a study where LNPs were shown to specifically target tumor sites, including the glioblastoma regions [86,87]. A comparable xenobiotic metabolism was noted in LNPs and food-based lipids that were internally degraded into nontoxic residues. [88]. This further highlights their nontoxic nature.

3.4.1. LNPs for Parkinson's Disease

Lipid-based NPs have been highlighted for vaccination and therapy. Its natural ability to penetrate the brain increases its attractiveness for treatment directed at neurological diseases. These LNPs have emerged as appropriate nanocarriers due to their favorable size, surface charge, tunable surface area, and morphology [89].

The use of nanomedicine in drug delivery has an array of advantages, including increased resistance time in the host (that is, increasing the half-life for clearance), improved bioavailability due to enhanced aqueous solubility, and greater specificity with regard to targeting diseases, such as PD [90]. This reduces the side effects manifesting in nontarget tissues and cells of patients due to the concomitant drop in drug concentration and safe and efficient delivery to the target tissue [13]. When designing a LNP for drug delivery, many factors need to be taken into consideration in order to improve therapeutic indices. Some of these factors are summarized in Figure 3.5.

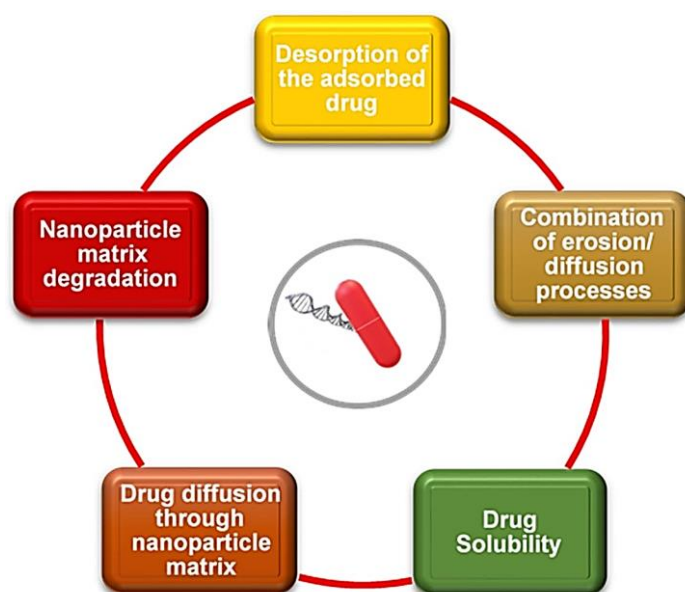


Figure 3.5. Important factors to consider when designing lipid nanoparticles for drug delivery. Adapted from [90].

When looking at currently available treatments, dopamine supplementation is necessary to compensate for the loss of dopaminergic neurons in PD patients. A recent study utilized an albumin/PLGA NP conjugated to dopamine. The nanocomplexes exhibited successful permeability to the brain by effectively crossing the BBB. This was attributed to the albumin-coated NP, which enhanced the interactions of the NP with specific cell membrane receptors. Furthermore, using dopamine instead of L-DOPA (a drug commonly converted to dopamine in vivo) reduced symptoms in a mouse model compared to control NPs without dopamine and mice administered with L-DOPA. Improvements manifested as restoration of balance, motor coordination, and sensorimotor performance [91].

The efficacy of nanomedicine and drug therapy is noted further in a study conducted by Dudhipala and Gorre (2020), who utilized LNPs conjugated with ropinirole (RP), a dopamine agonist. Increased pharmacokinetics was exhibited with respect to the drug in the host, with more than two-fold enhancement in oral administration, three-fold enhancement in topical administration, and single-fold enhancement in topical bioavailability in SLN and NLC complexes. Pharmacodynamic studies have portrayed increased levels of glutathione, catalase, and dopamine with a reduction in lipid peroxidation levels [92].

Functionalized liposomes containing the dopamine derivative N-3,4-bis(pivaloyloxy) dopamine, together with a brain-targeted delivery system made up of 29 amino acid peptides (RVG29) derived from the rabies virus glycoprotein, were studied. Significantly improved cellular uptake was noted in both the endothelial and dopaminergic cells, with improved penetration of the BBB. Furthermore, enhanced therapeutic efficacy was noted due to the RVG29-LNPs being selectively driven to the substantia nigra and striatum [93].

In these two independent studies, the common trend of increased performance with lower side effects was clearly noted, with significant improvements in the Parkinsonian symptoms exhibited. While drug therapy is an effective therapeutic, gene therapy is another promising PD treatment strategy. Gene therapy aims to knock down or replace the causative gene/s, as mentioned earlier, to treat PD at the root. Hence, this remains to be fully explored.

3.4.2. An Update on Clinical Trials Using Lipid Nanoparticles

There are some approved treatment strategies available to treat PD symptoms, e.g., transdermal patches. The transdermal patches using rotigotine (Neupro®) treat the restless leg syndrome symptoms of PD, while selegiline (Emsam®) is used to overcome depression. However, these

also come with some noted side effects. [94]. Notably, LNPs are not employed in these formulations. The intravenous therapeutic patisiran (ONPATPRO®), which has been approved for the treatment of polyneuropathy, utilizes LNPs for the delivery of a therapeutic siRNA [95]. However, the latest search of the NIH library for clinical trials in the last 10 years revealed that LNPs are yet to be exploited as nanocarriers for therapeutics to treat PD. One Phase 1 study using liposomes commenced in 2021 and is scheduled to be completed in December 2022. The study simply evaluates the safety of Talineuren, which comprises GM1 (a monosialo-tetrahexosylganglioside) as the therapeutic, in combination with a proprietary liposomal formulation [96]. However, one study using gold nanocrystals has been completed [97]. The results are awaited and could signal a new direction for nano-based therapeutics and a milestone for nanomedicine. The use of LNPs, however, needs to be further investigated to realize their potential in the formulation of a gene or drug delivery system for PD.

3.5. Conclusions and Future Perspectives

PD remains a major concern in the health sector, with therapeutics remaining at a palliative stage. The reduction in PD-associated symptoms is important, but the collateral side effects significantly impact the quality of the patient's life. With the disease not being completely elucidated with regard to the mechanism of actions and causative agents, greater importance should be placed on unravelling these. Nanomedicine has provided a means of overcoming various challenges, with novel therapeutic drug and gene delivery systems providing a highly efficient mode of treatment that can potentially offer a cure for such a disease. An important role can be seen in RNA interference (RNAi) for silencing specific genetic-based mutations leading to PD, such the LRRK2, PARK7, PINK1, PRKN, and SNCA genes. The utilization of LNP-based vaccines to date have provided evidence that.

LNPs can be reasonably safe and efficient. These biocompatible LNPs can accommodate varied drug doses, be amenable to tissue-targeted delivery, and can be produced on a larger scale for commercial use. This has opened up new avenues to optimize LNP formulations for treating many disorders, including neurological disorders such as PD. The lack of studies using LNP formulations needs to be addressed, and basic research focusing on novel formulations directed to the brain needs to be encouraged. This will promote the optimization of LNP formulations for efficient brain targeting, which can be eventually translated to clinical settings. Paramount to brain targeting is the appending of suitable ligands such as angiopep-2 and transferrin to LNPs, which can improve their navigation of the BBB, and the use of

polymers such as polyethylene glycol to ensure stability within the in vivo system. Importantly, the ability to design different LNP formulations for specific disorders may lead to a desired personalized form of treatment.

References

1. Parkinson's News Today. Parkinson's Disease Statistics. 2021. Available online: <https://parkinsonsnewstoday.com/parkinsonsdisease-statistics> (accessed on 8 December 2021).
2. Dorsey, E.R.; Bloem, B.R. The Parkinson pandemic—A call to action. *JAMA Neurol.* **2018**, *75*, 9–10.
3. Schrag, A.; Anastasiou, Z.; Ambler, G.; Noyce, A.; Walters, K. Predicting diagnosis of Parkinson's disease: A risk algorithm based on primary care presentations. *Mov. Disord.*, **2019**, *34*, 480–486.
4. Noyce, A.J.; Lees, A.J.; Schrag, A.E. The prediagnostic phase of Parkinson's disease. *J. Neurol. Neurosurg. Psychiatry*, **2016**, *87*, 871–878.
5. Lill, C.M. Genetics of Parkinson's disease. *Mol. Cell. Probes* 2016, *30*, 386–396. [CrossRef]
6. Gao, H.M.; Hong, J.S. Gene-environment interactions: Key to unraveling the mystery of Parkinson's disease. *Prog. Neurobiol.*, **2011**, *94*, 1–19.
7. Blauwendraat, C.; Nalls, M.A.; Singleton, A.B. The genetic architecture of Parkinson's disease. *Lancet Neurol.*, **2020**, *19*, 170–178.
8. Habib, S.; Singh, M. Angiopep-2-modified nanoparticles for brain-directed delivery of therapeutics: A review. *Polymers*, **2022**, *14*, 712.
9. Poletti, M.; Bonuccelli, U. Acute and chronic cognitive effects of levodopa and dopamine agonists on patients with Parkinson's disease: A review. *Ther. Adv. Psychopharmacol.*, **2013**, *3*, 101–113.
10. Emamzadeh, F.N.; Surguchov, A. Parkinson's disease: Biomarkers, treatment, and risk factors. *Front. Neurosci.*, **2018**, *12*, 612.
11. Hangargekar, S.R.; Mohanty, P.; Jain, A. Solid lipid nanoparticles for brain targeting. *J. Drug Deliv. Ther.*, **2019**, *9*, 248–252.
12. Grillone, A.; Battaglini, M.; Moscato, S.; Mattii, L.; Fernández, C.J.; Scarpellini, A.; Giorgi, M.; Sinibaldi, E.; Ciofani, G. Nutlinloaded magnetic solid lipid nanoparticles for targeted glioblastoma treatment. *Nanomedicine*, **2019**, *14*, 727–752.
13. Kadam, R.S.; Bourne, D.W.A.; Kompella, U.B. Nano-advantage in enhanced drug delivery with biodegradable nanoparticles: Contribution of reduced clearance. *Drug Metab. Dispos.*, **2012**, *40*, 1380–1388.

14. Parkinson, J. An essay on the shaking palsy. *J. Neuropsychiatry Clin. Neurosci.*, **2002**, 14, 223–236.
15. Fu, H.; Hardy, J.; Duff, K.E. Selective vulnerability in neurodegenerative diseases. *Nat. Neurosci.*, **2018**, 21, 1350–1358.
16. Simon, D.K.; Tanner, C.M.; Brundin, P. Parkinson disease epidemiology, pathology, genetics, and pathophysiology. *Clin. Geriatr. Med.*, **2019**, 36, 1–12.
17. Dickson, D.M. Neuropathology of Parkinson disease. *Parkinsonism Relat. Disord.*, **2018**, 46, S30–S33.
18. Jiang, P.; Gan, M.; Yen, S.-H.; Moussaud, S.; McLean, P.J.; Dickson, D.W. Proaggregant nuclear factor(s) trigger rapid formation of α -synuclein aggregates in apoptotic neurons. *Acta Neuropathol.*, **2016**, 132, 77–91.
19. Dias, V.; Junn, E.; Mouradian, M.M. The role of oxidative stress in Parkinson's disease. *J. Parkinsons Dis.*, **2013**, 3, 461–491.
20. Schapira, A.H.; Jenner, P. Etiology and pathogenesis of Parkinson's disease. *Mov. Disord.*, **2011**, 26, 1049–1055.
21. Zhu, J.; Chu, C.T. Mitochondrial dysfunction in Parkinson's disease. *J. Alzheimers Dis.*, **2010**, 20, S325–S334.
22. Soreq, L.; Bergman, H.; Israel, Z.; Soreq, H. Deep brain stimulation modulates nonsense-mediated RNA decay in Parkinson's patients' leukocytes. *BMC Genomics*, **2013**, 14, 478.
23. Poewe, W.; Seppi, K.; Tanner, C.M.; Halliday, G.M.; Brundin, P.; Volkman, J.; Schrag, A.E.; Lang, A.E. Parkinson disease. *Nat. Rev. Dis. Primers*, **2017**, 3, 17013.
24. Goldman, S.M.; Marek, K.; Ottman, R.; Meng, C.; Comuns, K.; Chan, P.; Ma, J. Concordance for Parkinson's disease in twins: A 20-year update. *Ann. Neurol.*, **2019**, 85, 600–605.
25. Chen, H.; Ritz, B. The search for environmental causes of Parkinson's disease: Moving forward. *J. Parkinsons Dis.*, **2018**, 8, S9–S17.
26. Tanner, C.M.; Goldman, S.M.; Ross, G.W.; Grate, S.J. The disease intersection of susceptibility and exposure: Chemical exposures and neurodegenerative disease risk. *Alzheimer's Dement.*, **2014**, 10, S213–S225.
27. Goldman, S.M. Environmental toxins and Parkinson's disease. *Annu. Rev. Pharmacol. Toxicol.*, **2014**, 54, 141–164.
28. Nguyen, A.P.T.; Tsika, E.; Kelly, K.; Levine, N.; Chen, X.; West, A.B.; Boularand, S.; Barneoud, P.; Moore, D.J. Dopaminergic neurodegeneration induced by Parkinson's disease-linked G2019S LRRK2 is dependent on kinase and GTPase activity. *Proc. Natl. Acad. Sci. USA*, **2020**, 117, 17296–17307.
29. Martin, L.J. Biology of mitochondria in neurodegenerative diseases. *Prog. Mol. Biol. Translat. Sci.*, **2012**, 107, 355–415.

30. Kumar, A.; Tamjar, J.; Waddel, A.D.; Woodroof, H.I.; Raimi, O.G.; Shaw, A.M.; Peggie, M.; Muqit, M.M.; van Aalten, D.M.F. Structure of PINK1 and mechanisms of Parkinson's disease-associated mutations. *eLife*, **2017**, *6*, e29985.
31. Ruiz-Lopez, M.; Freitas, M.E.; Oliveira, L.M.; Munhoz, R.P.; Fox, S.H.; Rohani, M.; Rogaeva, E.; Lang, A.E.; Fasano, A. Diagnostic delay in Parkinson's disease caused by PRKN mutations. *Parkinsonism Relat. Disord.*, **2019**, *63*, 2117–2220.
32. Chen, V.; Moncalvo, M.; Tringali, D.; Tagliafierro, L.; Shriskanda, A.; Ilich, E.; Dong, W.; Kantor, B.; Chiba-Falek, O. The mechanistic role of alpha-synuclein in the nucleus: Impaired nuclear function caused by familial Parkinson's disease SNCA mutations. *Hum. Mol. Genet.*, **2020**, *29*, 3107–3121.
33. Jagaran, K.; Singh, M. Nanomedicine for neurodegenerative disorders: Focus on Alzheimer's and Parkinson's diseases. *Int. J. Mol. Sci.*, **2021**, *22*, 9082.
34. Chiara, T.; Origlia, N.; Mattu, C.; Accorroni, A.; Chiono, V. Current limitations in the treatment of Parkinson's and Alzheimer's diseases: State-of-the-art and future perspective of polymeric carriers. *Curr. Med. Chem.*, **2018**, *25*, 5755–5771.
35. Maney, V.; Singh, M. An in vitro assessment of Chitosan/Bimetallic PtAu nanocomposites as delivery vehicles for doxorubicin. *Nanomedicine*, **2017**, *12*, 2625–2640.
36. Selecki, M.; Selecki, A.D.; Jonczyk, R.; Stahl, F.; Blume, C.; Scheper, T. Smart multifunctional nanoparticles in nanomedicine. *BioNanoMaterials*, **2016**, *17*, 33–41.
37. Saidi, T.; Fortuin, J.; Douglas, T.S. Nanomedicine for drug delivery in South Africa: A protocol for systematic review. *Syst. Rev.*, **2018**, *7*, 154.
38. Venkatas, J.; Singh, M. Nanomedicine-mediated optimization of immuno-therapeutic approaches in cervical cancer. *Nanomedicine*, **2021**, *16*, 1311–1328.
39. Bhatia, S. Natural Polymer Drug Delivery Systems: Nanoparticles, Plants, and Algae. *Springer: Cham, Switzerland*, **2016**; pp. 1–225.
40. Bharathi, D.; Ranjithkumar, R.; Chandarshekar, B.; Bhuvaneshwari, V. Bio-inspired synthesis of chitosan/copper oxide nanocomposite using rutin and their anti-proliferative activity in human lung cancer cells. *Int. J. Biol. Macromol.*, **2019**, *141*, 476–483.
41. Maiyo, F.C.; Mbatha, L.S.; Singh, M. Selenium nanoparticles in folate-targeted delivery of the pCMV-Luc DNA reporter gene. *Curr. Nanosci.*, **2021**, *17*, 871–880.
42. Mbatha, L.S.; Maiyo, F.; Daniels, A.; Singh, M. Dendrimer-coated gold nanoparticles for efficient folate-targeted mRNA delivery in vitro. *Pharmaceutics*, **2021**, *13*, 900.
43. Daniels, A.N.; Singh, M. Sterically stabilized siRNA: Gold nanocomplexes enhance c-MYC silencing in a breast cancer cell model. *Nanomedicine*, **2019**, *14*, 1387–1401.
44. Wohlfart, S.; Gelperina, S.; Kreuter, J. Transport of drugs across the blood–brain barrier by nanoparticles. *J. Control. Release*, **2012**, *2*, 264–273.

45. Venkatas, J.; Singh, M. Localized nano-mediated interleukin-12 gene therapy: Promising candidate for cancer immunotherapeutics. *Curr. Cancer Drug Targets*, **2022**; in press.
46. Virlan, M.J.; Miricescu, D.; Radulescu, R.; Sabliov, C.M.; Totan, A.; Calenic, B.; Greabu, M. Organic nanomaterials and their applications in the treatment of oral diseases. *Molecules*, **2016**, *9*, 207.
47. Habib, S.; Singh, M. Carbon-based Nanomaterials for delivery of small RNA molecules: A focus on potential cancer treatment applications. *Pharm. Nanotechnol.*, **2022**; in press.
48. Gregoriadis, G. Liposomes and mRNA: Two technologies together create a COVID-19 vaccine. *Med. Drug Discov.*, **2021**, *12*, 100104.
49. Aldosari, B.N.; Alfagih, I.M.; ALmurshedi, A.S. Lipid nanoparticles as delivery systems for RNA-based vaccines. *Pharmaceutics*, **2021**, *13*, 206.
50. Habib, S.; Daniels, A.; Ariatti, M.; Singh, M. Anti-c-MYC cholesterol based lipoplexes as onco-nanotherapeutic agents in vitro. *F1000Research*, **2020**, *9*, 770.
51. Zhao, S.; Zhao, J.; Dong, S.; Huangfu, X.; Li, B.; Yang, H.; Zhao, J.; Cui, W. Biological augmentation of rotator cuff repair using bFGF-loaded electrospun poly(lactide-co-glycolide) fibrous membranes. *Int. J. Nanomed.*, **2014**, *14*, 2373–2385.
52. Tenchov, R.; Bird, R.; Curtze, A.E.; Zhou, Q. Lipid nanoparticles—From liposomes to mRNA vaccine delivery, a landscape of research diversity and advancement. *ACS Nano*, **2021**, *15*, 16982–17015.
53. Habib, S.; Ariatti, M.; Singh, M. Anti-c-myc RNAi-based onconantherapeutics. *Biomedicines*, **2020**, *8*, 612.
54. Hajj, K.A.; Whitehead, K.A. Tools for translation: Non-viral materials for therapeutic mRNA delivery. *Nat. Rev. Mater.*, **2017**, *2*, 17056.
55. Nisini, R.; Poerio, N.; Mariotti, S.; De Santis, F.; Fraziano, M. The multirole of liposomes in therapy and prevention of infectious diseases. *Front. Immunol.*, **2018**, *9*, 155.
56. Naicker, K.; Ariatti, M.; Singh, M. Active targeting of asiaglycoprotein receptor using sterically stabilized lipoplexes. *Eur. J. Lipid Sci. Technol.*, **2016**, *118*, 1730–1742.
57. Balazs, D.A.; Godbey, W.T. Liposomes for use in gene delivery. *J. Drug Deliv.*, **2011**, *2011*, 326497.
58. Paliwal, R.; Paliwal, S.R.; Kenwat, R.; Kurmi, B.D.; Sahu, M.K. Solid lipid nanoparticles: A review on recent perspectives and patents. *Expert Opin. Ther. Pat.*, **2020**, *30*, 179–194.
59. Haider, M.; Abidin, S.M.; Kamal, L.; Orive, G. Nanostructured lipid carriers for delivery of chemotherapeutics: A review. *Pharmaceutics*, **2020**, *12*, 288.
60. Habib, S.; Singh, M. Recent advances in lipid-based nanosystems for gemcitabine and gemcitabine–combination therapy. *Nanomaterials*, **2021**, *11*, 597.
61. Patil, J.; Rajput, R.; Nemade, R.; Naik, J. Preparation and characterization of artemether loaded solid lipid nanoparticles: A 32 factorial design approach. *Mater. Technol.*, **2020**, *35*, 719–726.

62. Maussang, D.; Rip, J.; van Kregten, J.; van den Heuvel, A.; van der Pol, S.; van der Boom, B.; Reijerkerk, A.; Chen, L.; de Boer, M.; Gaillard, P.; *et al.* Glutathione conjugation dose-dependently increases brain-specific liposomal drug delivery in vitro and in vivo. *Drug Discov. Today Technol.*, **2016**, 20, 59–69.
63. Bhowmik, A.; Khan, R. Blood brain barrier: A challenge for effectual therapy of brain tumors. *BioMed Res. Int.*, **2015**, 2015, 320941.
64. Posadas, I.; Monteagudo, S.; Cena, V. Nanoparticles for brain-specific drug and genetic material delivery, imaging and diagnosis. *Nanomedicine*, **2016**, 11, 833–849.
65. Abbott, N.J.; Patabendige, A.A.; Dolman, D.E.; Yusof, S.R.; Begley, D.J. Structure and function of the blood-brain barrier. *Neurobiol. Dis.*, **2010**, 37, 13–25.
66. Gao, H. Progress and perspectives on targeting nanoparticles for brain drug delivery. *Acta Pharm. Sin.*, **2016**, 6, 268–286.
67. Chen, Y.; Liu, L. Modern methods for delivery of drugs across the blood-brain barrier. *Adv. Drug Deliv. Rev.*, **2012**, 64, 640–665.
68. Johnsen, K.B.; Moos, T. Revisiting nanoparticle technology for blood-brain barrier transport: Unfolding at the endothelial gate improves the fate of transferrin receptor-targeted liposomes. *J. Control. Release*, **2016**, 222, 32–46.
69. Agrawal, M.; Ajazuddin, A.; Tripathi, D.K.; Saraf, S.; Saraf, S.; Antimisiaris, S.G.; Mourtas, S.; Hammarlund-Udenaes, M.; Alexander, A. Recent advancements in liposomes targeting strategies to cross blood-brain barrier (BBB) for the treatment of Alzheimer’s disease. *J. Control. Release*, **2017**, 260, 61–77.
70. Vieira, D.B.; Gamarra, L.F. Getting into the brain: Liposome-based strategies for effective drug delivery across the blood-brain barrier. *Int. J. Nanomed.*, **2016**, 11, 5381–5414.
71. Bourassa, P.; Alata, W.; Tremblay, C.; Paris-Robidas, S.; Calon, F. Transferrin receptor-mediated uptake at the blood-brain barrier is not impaired by Alzheimer’s disease neuropathology. *Mol. Pharm.*, **2019**, 16, 583–594.
72. Xu, Y.; Fourniols, T.; Labrak, Y.; Pr eat, Y.; Beloqui, A.; Des Rieux, A. Surface modification of lipid-based nanoparticles. *ACS Nano*, **2022**, 16, 7168–7196.
73. Kumari, S.; Ahsan, S.M.; Kumar, J.M.; Kondapi, A.K.; Rao, N.M. Overcoming blood brain barrier with a dual purpose Temozolomide loaded Lactoferrin nanoparticles for combating glioma (SERP-17-12433). *Sci. Rep.*, **2017**, 7, 6602.
74. Patching, S.G. Glucose transporters at the blood-brain barrier: Function, regulation and gateways for drug delivery. *Mol. Neurobiol.*, **2017**, 54, 1046–1077.
75. Cardoso, F.L.; Brites, D.; Brito, M.A. Looking at the blood-brain barrier: Molecular anatomy and possible investigation approaches. *Brain Res. Rev.*, **2010**, 64, 328–363.
76. Gaillard, P.J.; Appeldoorn, C.C.; Dorland, R.; Van Kregten, R.; Manca, F.; Vugts, D.J.; Windhorst, B.; van Dongen, G.A.; de Vries, H.E.; Maussang, D.; *et al.* Pharmacokinetics, brain

- delivery, and efficacy in brain tumor-bearing mice of glutathione pegylated liposomal doxorubicin (2B3-101). *PLoS ONE*, **2014**, 9, e82331.
77. Hoyos-Ceballos, G.P.; Ruozi, B.; Ottonelli, I.; Da Ros, F.; Vandelli, M.A.; Forni, F.; Daini, E.; Vilella, A.; Zoli, M.; Tosi, G.; *et al.* PLGA-PEG-ANG-2 nanoparticles for blood–brain barrier crossing: Proof-of-concept study. *Pharmaceutics*, **2020**, 12, 72.
78. Chen, W.; Zuo, H.; Zhang, E.; Li, L.; Henrich-Noack, P.; Cooper, H.; Qian, Y.; Xu, Z.P. Brain targeting delivery facilitated by ligand-functionalized layered double hydroxide nanoparticles. *ACS Appl. Mater. Interfaces*, **2018**, 10, 20326–20333.
79. Mei, L.; Zhang, Q.; Yang, Y.; He, Q.; Gao, H. Angiopep-2 and activatable cell penetrating peptide dual modified nanoparticles for enhanced tumor targeting and penetrating. *Int. J. Pharm.*, **2014**, 474, 95–102.
80. Kumthekar, P.; Tang, S.-C.; Brenner, A.J.; Kesari, S.; Piccioni, D.E.; Anders, C.K.; Carrillo, J.A.; Chalasani, P.; Kabos, P.; Puhalla, S.L.; *et al.* ANG1005, a brain-penetrating peptide–drug conjugate, shows activity in patients with breast cancer with leptomeningeal carcinomatosis and recurrent brain metastases. *Clin. Cancer Res.*, **2020**, 26, 2789–2799.
81. Ruan, S.; Yuan, M.; Zhang, L.; Hu, G.; Chen, J.; Cun, X.; Zhang, Q.; Yang, Y.; He, Q.; Gao, H. Tumor microenvironment sensitive doxorubicin delivery and release to glioma using angiopep-2 decorated gold nanoparticles. *Biomaterials*, **2015**, 37, 425–435.
82. Seabra, A.B.; Durán, N. Nanotoxicology of metal oxide nanoparticles. *Metals*, **2015**, 5, 934–975.
83. Olawale, F.; Oladimeji, O.; Ariatti, M.; Singh, M. Emerging roles of green synthesized chalcogen and chalcogenide nanoparticles in cancer theranostics. *J. Nanotechnol.*, **2022**, 2022, 6176610.
84. Akbarzadeh, A.; Rezaei-Sadabady, R.; Davaran, S.; Joo, S.W.; Zarghami, N.; Hanifehpour, Y.; Samiei, M.; Kouhi, M.; Nejati-Koshki, K. Liposome: Classification, preparation, and applications. *Nanoscale Res. Lett.*, **2013**, 8, 102.
85. Mizrahy, S.; Hazan-Halevy, I.; Landesman-Milo, D.; Ng, B.D.; Peer, D. Advanced strategies in immune modulation of cancer using lipid-based nanoparticles. *Front. Immunol.*, **2017**, 8, 69.
86. Jia, X.; Han, Q.; Wang, Z.; Qian, Y.; Jia, Y.; Wang, W.; Hu, Z. Targeting peptide functionalized liposomes towards aminopeptidase N for precise tumor diagnosis and therapy. *Biomater. Sci.*, **2017**, 5, 417–421.
87. Belhadj, Z.; Zhan, C.; Ying, M.; Wei, X.; Xie, C.; Yan, Z.; Lu, W. Multifunctional targeted liposomal drug delivery for efficient glioblastoma treatment. *Oncotarget* 2017, 8, 66889–66900.
88. Poovi, G.; Damodharan, N. Lipid nanoparticles: A challenging approach for oral delivery of BCS Class-II drugs. *Future J. Pharm. Sci.*, **2018**, 4, 191–205.

89. Chakraborty, S.; Dhakshinamurthy, G.S.; Misra, S.K. Tailoring of physicochemical properties of nanocarriers for effective anti-cancer applications. *J. Biomed. Mater. Res. A*, **2017**, 105, 2906–2928.
90. Mudshinge, S.R.; Deore, A.B.; Patil, S.; Bhalgat, C.M. Nanoparticles: Emerging carriers for drug delivery. *Saudi Pharm. J.*, **2011**, 19, 129–141.
91. Monge-Fuentes, V.; Biolchi Mayer, A.; Lima, M.R.; Geraldes, L.R.; Zanotto, L.N.; Moreira, K.G.; Martins, O.P.; Piva, H.L.; Felipe, M.S.S.; Amaral, A.C.; *et al.* Dopamine-loaded nanoparticle systems circumvent the blood–brain barrier restoring motor function in mouse model for Parkinson’s Disease. *Sci. Rep.*, **2021**, 11, 15185.
92. Dudhipala, N.; Gorre, T. Neuroprotective effect of ropinirole lipid nanoparticles enriched hydrogel for Parkinson’s disease: In vitro, ex vivo, pharmacokinetic and pharmacodynamic evaluation. *Pharmaceutics*, **2020**, 12, 488.
93. Qu, M.; Lin, Q.; He, S.; Wang, L.; Fu, Y.; Zhang, Z.; Zhang, L. A brain targeting functionalized liposomes of the dopamine derivative N-3,4-bis(pivaloyloxy)-dopamine for treatment of Parkinson’s disease. *J. Control. Release*, **2018**, 277, 173–182.
94. Silva, S.; Almeida, A.J.; Vale, N. Importance of nanoparticles for the delivery of antiparkinsonian drugs. *Pharmaceutics*, **2021**, 13, 508.
95. Urits, I.; Swanson, D.; Swett, M.C.; Patel, A.; Berardino, K.; Ariunzaya Amgalan, A.; Berger, A.A.; Kassem, H.; Kaye, A.D.; Viswanath, O. A review of Patisiran (ONPATPRO®) for the treatment of polyneuropathy in people with hereditary transthyretin amyloidosis. *Neurol. Ther.*, **2020**, 9, 301–315.
96. ClinicalTrials.gov. Available online: <https://clinicaltrials.gov/ct2/results?cond=Parkinson+Disease&term=liposomes> (accessed on 27 July 2022).
97. ClinicalTrials.gov. Available online: <https://clinicaltrials.gov/ct2/results?recrs=&cond=Parkinson+Disease&term=nanoparticles> (accessed on 27 July 2022).

Chapter 4

The synergistic use of *Ginkgo biloba* in the biosynthesis of nanoparticles and as a therapeutic agent in Parkinson's Disease

The synergism of *Ginkgo biloba* in the biosynthesis of nanoparticles and as a therapeutic agent in Parkinson's Disease

This chapter has been submitted to *Letters in Applied NanoBioScience*

Abstract. Parkinson's disease (PD) is a rapidly growing neurological disorder affecting millions globally, characterized by the degeneration of striatal dopaminergic neurons and reduced dopamine levels. With an estimated 12.9 million projected cases by 2040, current treatments, such as dopamine replacement, remain palliative and face significant challenges, particularly the blood-brain barrier (BBB), which limits effective drug delivery to the brain. Common databases such as Pubmed, Medline, Scopus, and Science Direct were searched for relevant data relating to *Ginkgo biloba*, nanoparticles, lipids, and Parkinson's disease. Recent advancements in nanomedicine, especially lipid nanoparticles (LNPs), offer promising solutions to this problem. This review examines the potential of *Ginkgo biloba* extract (EGB) as both a therapeutic and reducing agent in developing innovative LNP-based delivery systems for PD treatment. EGB is renowned for its neuroprotective and antioxidant properties and can enhance BBB permeability while inhibiting monoamine oxidase, thus preventing dopamine breakdown. Studies indicate that EGB-loaded LNPs can improve drug delivery to the brain by leveraging ginkgolides and kaempferol compounds that activate adenosine receptors in the BBB, enhancing its permeability. Furthermore, EGB has been shown to improve locomotor activity and muscle coordination and restore key brain enzymes. This dual-functional approach, combining the traditional medicinal benefits of EGB with modern nanomedicine, presents a novel and promising therapeutic strategy for PD, warranting further research.

Keywords: Parkinson's disease; lipid nanoparticles; *Ginkgo biloba*; blood-brain barrier; nanomedicine; biological synthesis.

4.1. Introduction

Parkinson's disease (PD), which was once a rare disorder, has emerged as one of the fastest-growing neurological diseases worldwide. An estimated 12.9 million people are expected to suffer from PD by 2040, which is double the number reported in 2015 [1]. This debilitating motor dysfunction condition results in a slower gait, rigidity, and tremors, which also affects

the mental health of the patient, leading to anxiety and depression. Treatment remains palliative, and diagnosis is typically made following the onset of symptoms; thus, the root cause is not commonly treated. The diagnostic measures include physical examination pertaining to a history of prodromal features (including rapid eye movement (REM), sleep behavior disorder, constipation, hyposmia), cognitive or psychological difficulties, and characteristic difficulty in movement [2].

It has been elucidated that the striatal dopaminergic (DAergic) neurons play a pivotal role in disease manifestation. Hence, therapeutic interventions are implemented to increase dopamine levels or to stimulate the dopamine receptors. This is evident in drugs such as levodopa (L-Dopa), a naturally occurring dopamine precursor. Although effective, levodopa is challenged by unpredictably high absorption rates and surplus metabolism [3]. The greatest hindrance to optimal therapy is the blood-brain barrier (BBB) between the central nervous system (CNS) and the bloodstream. The BBB comprises pericytes and neural endothelial cells regulated by tight junctions [4]. The BBB controls the entry and, hence, the efficiency of drug delivery systems, with transportation and permeability of pharmacologically active agents being stalled or prevented [5].

Research into the passage of compounds through the BBB has been ongoing. Due to the nature of this barrier, nanomaterials have been studied and brought to the forefront of research [6]. The beneficial properties of these nanoparticles (NPs) include their size, structure, and ability to be manipulated to carry out functions such as drug/gene delivery, improvement of solubility and bioavailability, and their ability to protect the bound therapeutic [7,8]. Due to the blood-brain barrier restricting the permeability of ions and polar solutes, small molecules (such as lipophilic drugs), and particles larger than 1000 Daltons [5], lipid nanoparticles (LNPs) can be employed as potential agents to combat these challenges. LNPs comprising sphingomyelin are considered good candidates as delivery vehicles due to their enhanced brain permeability ability via passive, specific, and non-specific diffusion [9]. The different synthesis approaches and the inclusion of molecular conjugates further increase their potency.

One such synthesis approach utilizes the *Ginkgo biloba* leaf extracts. The tree, native to China, possesses neuroprotective and antioxidant properties. *G. biloba* acts as a monoamine oxidase (MAO) inhibitor, preventing the enzyme from breaking down excessive quantities of dopamine. In an early study, the *G. biloba* extract (EGB) demonstrated an increase in locomotor activity, muscular coordination, and restoration of glutathione and glutathione-

dependant enzymes, catalase, and superoxide dismutase in the striatum. Beyond this, an increased content of dopaminergic D2 receptors was noted with an increased density of tyrosine hydroxylase-immunoreactive (TH-IR) fibers [10].

The role of *G. biloba* as a synthesis agent could be beneficial in creating an optimal and synergistic delivery system that possesses and enhances the abilities of the conjugated drugs or genes. A dual-function vehicle containing EGB and other molecular conjugates and ligands produces a therapeutic formulation that vaunts many properties to combat various aspects of the disorder concurrently. This review looks at the formulation of such LNPs and their potential use in treating Parkinson's disease (PD).

4.2. Parkinson's Disease: A Brief Overview

PD is recognized as a global concern and one of the fastest-growing neurological diseases. The expected number of patients with PD is set to rise to an estimated 12.9 million people by 2040 [1]. Despite extensive studies, the etiology of PD is still under research and not completely elucidated. PD onset has been linked to both genetic and environmental contributors, as evidenced by single gene mutations in the familial form [11]. In addition to medication, therapeutic strategies have faced many challenges, of which the blood-brain barrier (BBB) is the greatest hindrance. Further strategies that have been implemented include cell therapy, neurotrophic agents, and electrical stimulation [12].

PD is associated with the progressive loss of dopaminergic neurons residing in the substantia nigra (SN), as well as their projections into the striatum. Consequently, the nigrostriatal pathway is disrupted, leading to reduced functionality and thus symptoms such as bradykinesia, tremors, impaired balance, rigidity, and mental health-related issues, including depression [13], as illustrated in Figure 4.1. Furthermore, Lewy bodies were found in all affected brain regions in patients presenting with PD. These intraneuronal proteinaceous cytoplasmic inclusions, including ubiquitin, α -synuclein, and neurofilaments, form part of the pathological features noted in PD. Beyond this, oxidative stress, protein dysfunction, apoptosis, autophagy, inflammation, and mitochondrial dysfunction are the pathogenic mechanisms associated with PD onset [6,13]. Mutational events have additionally been noted to cause PD through protein dysregulation in DJ-1, PINK1, FBXO7, PARKIN, and LRRK2 genes due to 5% of the familial form and 95% due to a sporadic form [14].

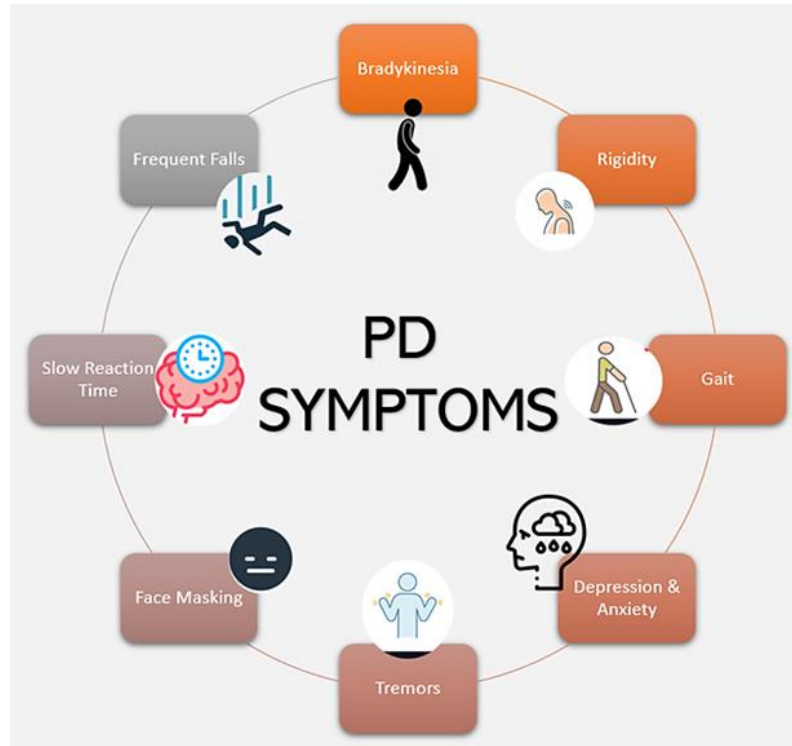


Figure 4.1. An illustration of the symptoms associated with Parkinson's disease.

4.2.1. Current therapeutics

The treatment against PD remains at a symptomatic level, with the gold standard treatment being in the form of dopamine replacement employing the use of levodopa. Following further research and alternate approaches, non-ergot dopamine agonists (DAs), catechol-O-methyl transferase (COMT) inhibitors, and monoamine oxidase-B (MAO-B) inhibitors have been used [15]. Combined with dopamine replacement options, complementary and alternative (CAM) and integrative medicinal approaches are performed [16]. The treatment of PD follows a five-step strategy commencing with rehabilitation, followed by therapy, restorative maintenance, and surgery [17].

Rehabilitative options are conducted based on the effect that the loss of dopamine has on the voice and movement, such as patients exhibiting lower volume and tone while speaking and limitations in movement. The rehabilitation strategy employed is known as LSVT (Lee Silverman Voice Treatment)-LOUD and LSVT-BIG [18]. The former programme works at a level of exercising the voice, thereby increasing vocal volume, while the latter is based on the intensive exercise of large-amplitude movements to compensate for hypokinesia and bradykinesia [19].

The second strategy in the treatment of PD uses drugs to assist a patient with the loss of dopamine. Dopamine or 3,4-dihydroxyphenethylamine is a member of the phenethylamine and catecholamine molecular family [20]. This derivative of tyrosine (Tyr) is formed via the conversion of Tyr to levodopa (L-DOPA) to produce dopamine [21]. Dopamine agonists and replacement therapies, such as levodopa, were created to accommodate for the loss of dopamine in PD. Simultaneous treatment of levodopa with carbidopa (an aromatic L-amino acid decarboxylase inhibitor) was noted to permit successful transportation of levodopa to the CNS by preventing the conversion of levodopa to dopamine in the peripheral tissues [22]. Various other treatments have also been used (Table 4.1).

Table 4.1. Some approaches and drugs that are used for the treatment of PD.

Compound	Drug	Mechanism of Action	Reference
Dopamine replacement	Carbidopa/ Levodopa	The blood-brain barrier prevents entry of dopamine; however, it permits entry of levodopa, leading to additional dopamine being synthesized in the CNS.	[23]
Dopamine agonist	Ropinirole	Mimics dopamine by binding to dopamine receptors and stimulates the D2 dopamine receptors.	[24]
Monoamine oxidase-B (MOA-B) inhibitors	Selegiline	It prevents monoamine oxidase from inactivating and breaking down excessive amounts of dopamine.	[17]
Catechol-O-methyl transferase (COMT)	Opicapone	It prevents the conversion of levodopa to 3-O-methyldopa and increases the half-life of levodopa and its retention time in the CNS.	[2]
Anticholinergics	Trihexyphenidyl, Benztropine	Block acetylcholine receptors in the brain, rebalancing the dopamine-acetylcholine ratio.	[25]
Amantadine		It enhances dopamine release and blocks glutamate receptors, reducing dyskinesia and improving motor symptoms.	[26]
NMDA Receptor Antagonists	Memantine	Blocks N-methyl-D-aspartate (NMDA) glutamate receptors, potentially reducing dyskinesias and improving motor symptoms.	[27]
Adenosine A2A Receptor Antagonists	Istradefylline	Block adenosine A2A receptors, modulating dopaminergic signaling and potentially reducing motor fluctuations.	[28]
Glutamate Receptor Antagonists	Riluzole	It inhibits glutamate release and blocks glutamate receptors, potentially providing neuroprotective effects.	[29]

Another mitigation strategy against the pathogenic effects of PD is seen in exercise, known as restorative therapy. Exercise was shown to preserve the undamaged dopaminergic neurons, increase brain-derived neurotropic factors, and reduce pro-inflammatory markers in mice [30].

Strenuous aerobic exercise in humans also produced neuroprotective effects in PD patients while improving their quality of life [31,32].

As the name suggests, the maintenance approach maintains the remaining healthy dopaminergic cells by incorporating vitamins and other compounds. Traditional/ biological compounds form part of this therapy due to their properties. The exploration of adjunctive therapies in PD management offers promise but necessitates careful consideration of their efficacy and safety, particularly given their departure from established treatment guidelines. Vitamin D3 supplementation in PD remains debatable, with divergent findings on its cognitive benefits, highlighting the need for further research to clarify its role. Conversely, challenges such as poor bioavailability and limited brain penetration hinder the translation of curcumin's antioxidant and anti-inflammatory effects into viable PD therapies. Similarly, while other adjunctive compounds show efficacy in preclinical studies, their clinical applicability lacks robustness [33].

Translating theoretical efficacy into practical applicability necessitates in-depth studies to ascertain these adjunctive therapies' effectiveness and safety profiles. Caution must be exercised in their implementation, given the absence of definitive clinical evidence and their deviation from established treatment guidelines. Robust clinical trials are imperative to validate the therapeutic potential of adjunctive therapies and delineate their role in PD management. Until then, healthcare practitioners should judiciously consider adjunctive therapies and prioritize evidence-based approaches in PD treatment.

The option for surgery is reserved for individuals presenting with complications associated with long-term use of carbidopa/levodopa. Deep brain stimulation targets the thalamus, subthalamic nucleus, and globus pallidus [34]. While all strategies are productive in providing a band-aid approach to PD symptoms, a therapy option to treat the root causes of PD with limited side effects has not yet been established. Further research is imminent in treating PD patients wholly and appropriately, and this could potentially be in the form of looking back at traditional medicine and its adaptability to modern medicine.

4.3. Traditional Therapeutics: *G. biloba* Extract

Due to its exhibited properties, *G. biloba* has long been utilized as a therapeutic agent. This endemic plant belongs to the genus Ginkgo and is the only species to have survived, known as the "living fossil" [35]. The tree has leathery 'fan-shaped' leaves with yellow, edible seeds.

Historically, this tree has been used to treat bronchitis, renal dysfunction, asthma, and bladder complications [36,37]. In 1965, a German physician and pharmacist, Willmar Schwabe III, developed the initial standardized extract of dried *G. biloba*, known pharmacology as EGB 761 [38]. This extract contained 6% terpenoids, 24% flavonoid glycosides, and 5-10% organic acids, each portraying their relevant properties in various diseases (Figure 4.2). This extract has been extensively studied and used in disorders treating depression, cerebral insufficiency, thrombosis, myocardial ischemia, peripheral occlusive arterial disease (POAD), memory impairment, and poor concentration [39].

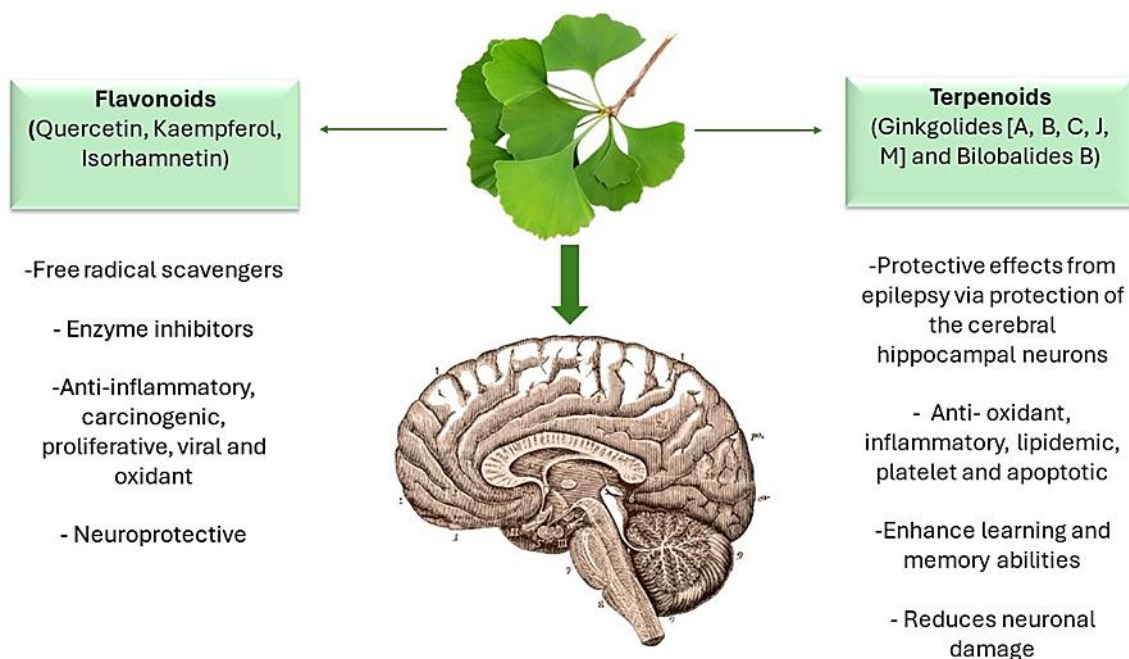


Figure 4.2. Chemical composition of *G. biloba* and their beneficial properties.

The properties of the chemical composition of *G. biloba* were well elucidated, and their benefits have been successfully incorporated into PD therapeutics. One such mechanism is the 1-methyl-4-phenyl-1,2,3,6-tetrahydropyridine (MPTP)- induced rat PD models. MOA-B has been noted to inactivate the dopaminergic nerve endings by converting MPTP to MPP^+ . MPTP is considered a lipophilic compound, which can efficiently cross the BBB, followed by the subsequent metabolism by MOA-B [40]. This phenomenon occurs primarily in the glial cells, owing to the formation of 1-methyl-4 phenylpyridinium in its ionic form (MPP^+) [41]. Due to the structural similarities between dopamine and MPP^+ , the DA neurons in the substantia nigra pars compacta (SNpc) take up the MPP^+ via the dopamine transporters (DAT) from the intercellular space [40]. This results in accumulation in the mitochondria, causing complex I

of the electron transport chain to be inhibited, decreased ATP production, activation of the caspase cascade, oxidative stress, inhibition of cellular respiration, and cellular demise [42-45]. The applicability of EGB761 in combating this conversion was noted by two independent studies that showed the inhibition of the MPTP-induced reduction in the dopaminergic neurons.

Additionally, EGB761 can prevent and protect the nerve endings [46,47]. Histopathological staining in PD mice showed substantial damage in the striatal neurons and the detection of glial cell hyperplasia. Meanwhile, mice receiving *G. biloba* dropping pills portrayed intact striatal neurons and no glial hyperplasia. Furthermore, a small amount of nerve fiber bundle loss was observed in the EGB761 group, revealing the amelioration of MPTP-induced neuronal damage [48].

In 2003, the neurotoxic side effects of levodopa were noted, with EGB761 possessing further neuroprotective properties owing to the attenuation of the neurotoxicity caused by levodopa in 6-hydroxydopamine (6-OHDA) models [49]. This was later confirmed in a zebrafish model showing a significant decline in 6-OHDA-induced dopaminergic neuron loss after introducing 250 µg/mL of EGB 761 [48]. The neuroprotective properties were attributed to the reduction of oxidative stress, blockade of lipid peroxidation, and the attenuation of MPTP-induced neurodegeneration, which occurs in the nigrostriatal pathway [13]. These early studies have paved the way for further knowledge to be acquired about the vast range of beneficial properties owing to *G. biloba* uptake.

The chemical compound found in the leaves of *G. biloba*, known as Ginkgetin (natural biflavonoid), presented with further antioxidant capabilities and protected against MPP⁺-induced cellular damage via the reduction of reactive oxygen species (ROS) levels and further improved the sensorimotor coordination in mice models through iron homeostasis regulation [50]. Furthermore, the ginkgolide B and bilobalide pretreatment protected the SH-SY5Y neuroblastoma cells against α -synuclein-induced apoptosis [51]. Additionally, MPP⁺-induced SH-SY5Y cells treated with 60 to 120 µg/mL EGB761 were successfully protected from neuronal damage without cytotoxic effect on the cells [48].

EGB761 successfully portrayed its benefits to protect against paraquat-induced (a pesticide linked to PD) apoptosis of PC12 (rat pheochromocytoma) cells through the subsequent increase in bcl-2 activation, decrease in caspase-3 activation via the mitochondria-dependent pathway, and the maintenance of membrane potential [52]. Holistically, its advantageous properties against PD were noted in its ability to decrease oxidative damage, inhibit disease development

in A53T α -synuclein transgenic mice, maintain dopamine homeostasis, and improve locomotor activity [53].

The beneficial properties of EGB could be strategically employed in conjunction with existing therapeutic strategies for Parkinson's disease, offering the potential to mitigate the adverse effects commonly associated with these treatments. Specifically, the neuroprotective properties of EGB may serve to counteract the neurotoxic side effects induced by levodopa, such as oxidative stress and dopaminergic neuron degeneration. By addressing these concerns, the combined approach may provide a more comprehensive and sustainable treatment option, enhancing both the efficacy and long-term safety profile of standard PD therapies.

While the EGB possesses these beneficial properties for the uptake by the BBB, they are met with various challenges in their pure form. Although EGB can be reduced to a nanoscale, a diverse size range has been observed, which hinders their traversing potential and reduces their targeting and therapeutic abilities [54]. These extracts elicit immune responses or cytotoxic effects upon entering the host, lowering their biocompatibility [55]. This is more prominently seen in the ginkgolic acid (GA) compound, with a reduced effect noted upon fixation and fermentation (56). Unlike nanoparticles (NPs) such as lipids or metals, EGB, even at a nanoscale, is portrayed to lack versatility in surface modifications, functionalization, and targeting efficiency [54].

4.4. Merging Traditional with Modern Medicine: Biological Nanoparticle Synthesis

Plant extracts provide excellent therapeutic benefits. However, their application in medicine is not restricted to their traditional uses. Through extensive research of their properties, the chemical composition of plants, such as *G. biloba*, can be manipulated to be utilized in NP synthesis protocols. NPs can deliver therapeutic cargo efficiently and safely to the targeted areas in a host. Recently, biosynthesis/ green synthesis has catapulted to the forefront of research owing to the low toxicity, biocompatibility, and eco-friendliness due to the less toxic and harmful chemicals used [57]. These NPs can possess anti-inflammatory and antibacterial properties while providing good bioavailability, bioactivity, and tumor-targeting abilities [58-60].

Using EGB in NP synthesis can mitigate the issues raised by the raw form EGB while maintaining their inherent properties. This extract's use in synthesizing all NPs, including metal and lipid NPs (LNPs), promotes colloidal stability, which maintains drug integrity during their

passage through the BBB while preventing aggregation [55]. Furthermore, they can produce specific-sized NPs through various optimizations, offering a more sustainable and environmentally friendly approach and promoting green chemistry [61,62]. Notably, using EGB in synthesizing NPs enables surface modifications and manipulations of the NPs. This widens the therapeutic approach owing to the properties exhibited by *G. biloba* and the encapsulation and targeting ability of therapeutic agents such as drugs and genes [55].

4.4.1. *Ginkgo biloba* as a Reducing Agent

In the bottom-up synthesis approach, the plant extract acts as a reducing agent to create NPs of different sizes, shapes, and charges. This process requires the extraction of leaves, roots, or the bark of trees, washing them in distilled water, and boiling to extract the chemical compounds into an aqueous solution to be added to salts or lipids of the desired NP being synthesized (Figure 4.3). The amount of extract used is directly proportional to the NP size, with more extract producing smaller NPs, which are optimal for cell uptake [63].

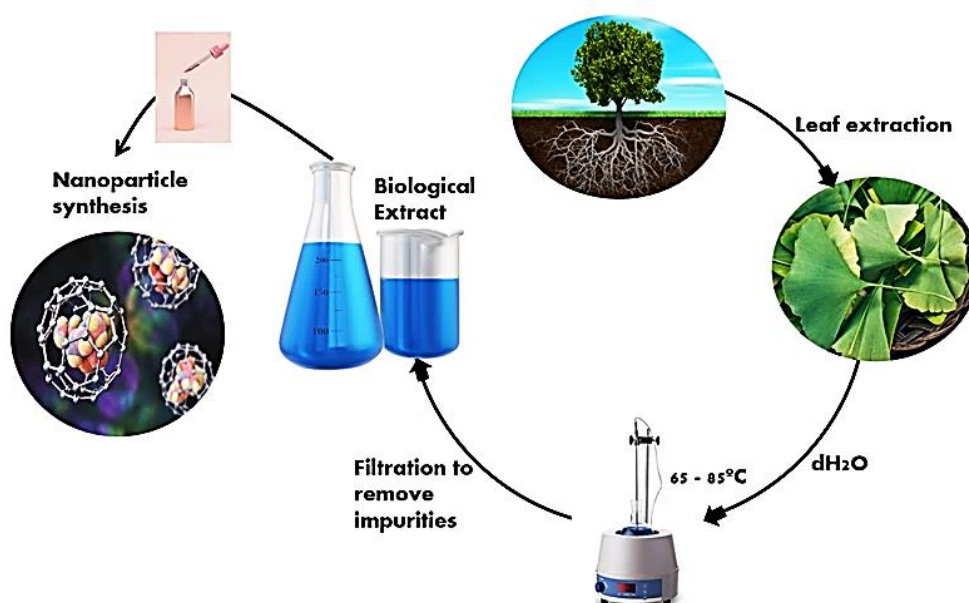


Figure 4.3. Bottom-up biosynthesis process using plant extracts.

The EGB contains many phytochemicals, including flavonoids, terpenoids, and phenolic acids, which exhibit antioxidant properties and can donate electrons, making them suitable candidates for reducing agents in nanoparticle synthesis.

Metallic NPs, such as gold nanoparticles (AuNPs) and silver nanoparticles (AgNPs), have been synthesized using EGB due to their rich composition of bioactive compounds. These compounds, particularly flavonoids such as quercetin and kaempferol, possess functional

groups such as hydroxyl (-OH) and carbonyl (C=O) groups, which can reduce metal ions to form NPs. Quercetin has been shown to effectively reduce gold ions to form AuNPs with well-defined morphologies and sizes [64]. Using EGB in AgNP synthesis produced NPs with a mean size of 40.2 nm and a stable zeta potential of -34.56 mV [65]. The EGB extract's reducing potential was attributed to its ability to scavenge free radicals and undergo redox reactions. This antioxidant activity plays a crucial role in the reduction process by providing electrons to stabilize metal ions, thereby promoting the nucleation and growth of NPs [66].

In the case of LNPs, the EGB serves as a natural source of lipids and emulsifiers, which are essential components in the formulation of lipid-based nanocarriers. LNPs, including liposomes, solid lipid NPs (SLNs), and nanostructured lipid carriers (NLCs), are widely utilized for drug delivery applications due to their biocompatibility, controlled release properties, and ability to encapsulate hydrophobic and hydrophilic drugs. EGB orchestrates an intriguing and intricate process in synthesizing LNPs. An in-depth look into its mechanism of action for reducing lipids into NPs reveals a complex interplay of molecular interactions. Flavonoids, such as quercetin and kaempferol, interact with lipid molecules, initiating a series of redox reactions within a molecular framework. These redox reactions involve the transfer of electrons between the flavonoids and the lipid molecules. This donation of electrons to the free radicals promotes the neutralization of the NP components to prevent oxidative damage [67,68]. These electrons are donated to the functional groups of the lipids present, and these reactions vary based on the components utilized. Unsaturated lipids can become saturated, or the lipid hydroperoxides can be reduced to more stable forms [69]. The flavonoids act as radical scavengers to stabilize the intermediates formed and prevent the occurrence of future reactions [70]

As this process unfolds, the EGB would act as a catalyst for NP formation. Its bioactive components act as reducing agents and stabilizers, ensuring the growth and stability of LNPs. Moreover, the lipid-rich nature of the EGB provides essential building blocks for NP assembly. Lipids from the extract form the structural foundation of the NPs while also encapsulating hydrophobic substances within their lipid bilayers. Its multifaceted role underscores the versatility and sophistication of natural products in contemporary nanotechnology.

4.4.2. General benefits of Plant Extracts

Plant extracts utilized in synthesis permit a duality in properties conferred by allowing the extract to maintain its original therapeutic abilities together with the NP's favorable properties,

enabling the NP to conjugate to the desired pharmacologically active agents. A study using silver ferrite (AgFeO₂) NPs exhibited greater antibacterial properties when biologically synthesized with *Amaranthus blitum* leaves compared to chemical synthesis using sodium borohydride [71]. Furthermore, the *Saudi Origanum vulgare* L. plant extract used to synthesize AgNPs showed better solubility and microbicidal capabilities [63].

Loading plant extracts onto solid LNPs (SLNPs) has gained immense strides in pharmacology. SLNPs are submicron carriers of 50 to 1000 nm, composed of biodegradable and biocompatible lipids comprising triglycerides, fatty acids, monoglycerides, or waxes [72]. This therapeutic approach has been a frontrunner due to its ability to enhance the bioavailability of drugs and genes used in treating CNS-related disorders [73]. A study examining the antidepressant effects using hibiscus extract-loaded LNPs reported superior antidepressant activity compared to crude drug extracts [74]. Due to their impressive abilities to treat CNS-related disorders, they have the potential to infiltrate the blood-brain barrier and may be suitable candidates to treat PD.

4.5. Traversing the Blood-Brain Barrier with *G. biloba* Synthesized Lipid Nanoparticles

Traversing the blood-brain has been daunting due to its impermeability to foreign entities. Anatomically, this barrier inhibits direct interactions between the blood and brain, forming the vital component of the neurovascular unit, which communicates with the CNS [75]. This barrier is composed of astrocytic end-feet links, tight junctions, pericytes, and endothelial cells, strictly controlling the transport of various substances into the brain through the tight junctions as well as metabolic barriers (enzymes) (Figure 4.4) [76, 77]. The tight intercellular junctions are primarily responsible for restricting the entry of molecules, toxic compounds, and pathogens [4, 78-80].

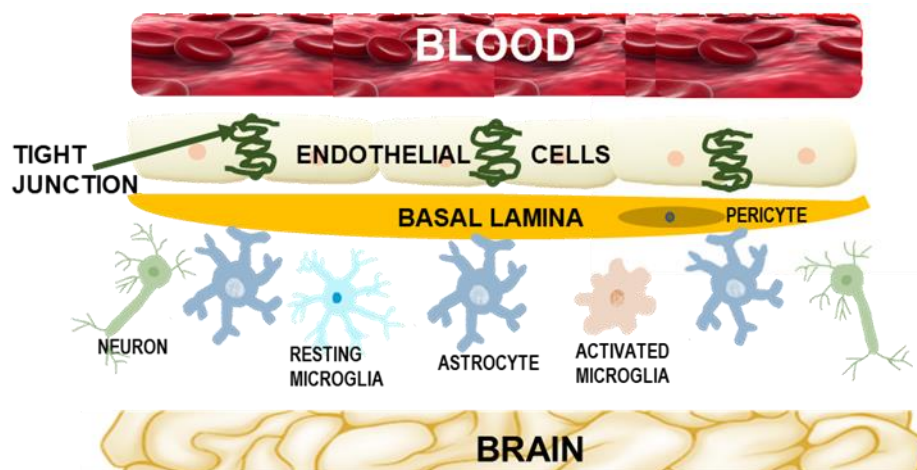


Figure 4.4. The composition of the blood-brain barrier.

The early processes of overcoming the BBB were highly invasive, requiring local brain site injections, catheters, or direct administration of the drugs via surgery [77]. Studies involving a carrier-mediated drug delivery system have been undertaken, with lipid nanoparticles being favorably considered. It has been noted that lipids with a size of approximately 400 Da possess the ability to freely diffuse across the endothelial layer of the BBB [81]. Furthermore, SLNPs, with a particle size range of 10 to 1000 nm, play a significant role in evading and infiltrating the reticuloendothelial system (RES) [75].

These NPs traverse the BBB in four ways: paracellular pathway, adsorptive-mediated transcytosis (AMT), receptor-mediated transcytosis (RMT), and protein-mediated transport. The paracellular pathway, or the passive transmembrane diffusion, permits the entry of only hydrophilic molecules with a molecular weight of 400 Da [64]. The AMT depends on the carrier system's charge. A positively charged NP would interact favorably with the negatively charged luminal membrane [82]. The RMT is deemed the most promising transportation process, permitting the entry of endogenous molecules across the BBB following endocytosis, intracellular vesicular trafficking, and exocytosis [83,84]. The protein-mediated transport involves binding the carrier system to transporter proteins for safe delivery into the cells. These passages are important in determining and creating a highly effective therapeutic.

EGB has been identified to enhance the BBB penetrance through the pathways mentioned above. Besides improving stability, biocompatibility, and reducing cytotoxicity, their constituents promote antioxidant properties which would essentially protect the LNPs from oxidative stress-induced damage as well [85]. The encapsulation of the EGB-synthesized LNPs promotes a synergistic role that enhances neuroprotection and improves drug delivery efficiency [86]. This integrated approach can potentially mitigate neuronal damage, attenuate disease progression, and improve clinical outcomes in PD patients.

EGB, via its flavonoid constituent, possesses beneficial properties that increase the possibility of the LNPs binding to the endothelial cell receptors on the BBB, permitting an enhanced uptake via RMT. Hence, a higher dose of the therapeutic would be found in the brain. Furthermore, a targeted therapeutic can be formulated by exploiting specific receptor pathways [87]. This specificity reduces the off-target effects and effectively improves the therapeutic potency. Lastly, flavonoids possess inherent neuroprotective properties, including reducing oxidative stress and inflammation, owing to the synergism of the beneficial properties noted

earlier. These properties, while stated for LNPs and PD expressly, could be effectively used for a wide range of neurodegenerative disorders, employing other NPs, each acting similarly with varied properties [88].

The above is achieved through the flavonoids kaempferol and quercetin, which are critical in enhancing the delivery across the BBB. They bind specific receptors on the endothelial cells of the BBB, which include the low-density lipoprotein (LDLR) and transferrin receptors (Figure 4.5). The structural properties of flavonoids, particularly the presence of hydroxyl groups, enable high-affinity interactions with these receptors. These interactions typically involve hydrogen bonding and van der Waals forces, ensuring that the flavonoids effectively bind to and activate the receptors [55]. Upon binding, a conformational change is induced, triggering endocytosis. Subsequently, endocytic vesicles are formed, which engulf the flavonoid-receptor complex, thereby permitting the invagination of the endothelial cell membrane to form the clathrin-coated pits. This results in the budding off of the vesicles, forming the initiation process of an efficient transport system across the BBB [89].

Following this process, the vesicles are transported via the cytoskeleton, involving actin filaments or microtubules, directing the vesicles towards the abluminal side of the cell. At this point, the flavonoids vaunt their biochemical properties, ensuring the vesicles are directed to this site to be released into the brain parenchyma while avoiding lysosomal degradation. Flavonoids, particularly those found in *G. biloba*, possess the ability to inhibit efflux transporters, including P-glycoproteins (P-gp), which are known to actively pump many compounds out of the brain, thus rendering an increased accumulation of the LNPs in the brain [89]. Furthermore, flavonoids can modify the LNPs to release their therapeutic content in response to the acidic pH of the lysosome, thus preventing degradation of the LNP. The fusion with the endosomal membranes results in the content release before reaching the lysosomes. Once at the abluminal side of the endothelial cell, a fusion of the vesicle with the plasma membrane is seen, thereby permitting the release of the therapeutic agents. The LNPs and the conjugated flavonoids enter the extracellular space, ensuring efficient and effective delivery of the LNPs to the target sites [90,91].

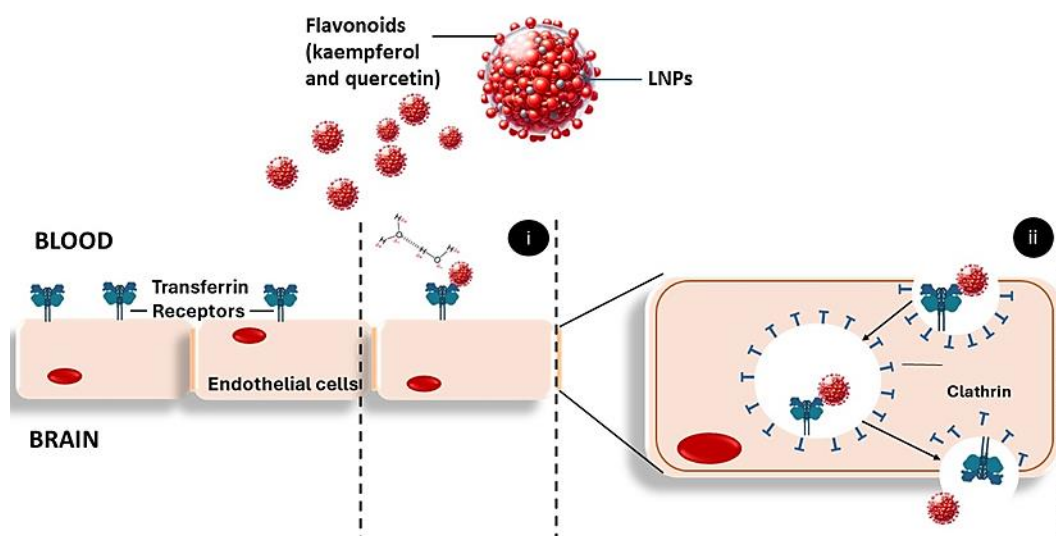


Figure 4.5. Receptor-mediated transcytosis across the BBB utilizing LNPs synthesized with EGB.

4.5.1. Further enhancement of the BBB with EGB

The BBB contains a class of G protein-coupled receptors (GPCRs) known as adenosine receptors (ARs), which play a crucial role in modulating its permeability. Notably, high levels of adenosine A1 receptors (A1R) are present in the brain [92]. Activation of A1R has been found to improve the penetration of intravenously administered macro-molecules and lead to cellular changes, such as increased formation of actinomyosin stress fibers, decreased transendothelial electrical resistance, and altered tight junctions [93,94].

In the case of EGB, it was demonstrated that the flavone in this extract could act as a P-glycoprotein (P-gp) inhibitor, increasing the intracellular drug concentration in the brain by enhancing uptake [95]. The main components of the extract, such as ginkgolides A, B, and C, kaempferol, and bilobalide, were reported to be present in the brain tissue, suggesting that they significantly contribute to BBB permeability and facilitated the entry of therapeutic agents. It was proposed that ginkgolides and bilobalide might enhance BBB permeability by modulating the A1R pathway, which influences endothelial cell function and tight junction integrity [96]. This temporary and reversible opening of the BBB can improve drug delivery to the brain. These findings were corroborated by an earlier study, which demonstrated that bilobalide, a prominent component of EGB, can efficiently cross the BBB, reaching significant extracellular concentrations in the brain, supporting its role in enhancing BBB permeability [97].

The BBB is often described as a 'double-edged sword' due to the challenges associated with crossing it. Long-term administration of *G. biloba* has shown no apparent side effects while reversibly opening the BBB for short periods, typically around four hours, without causing leakage. This reversible opening maintains the integrity of tight junctions, which is essential for brain homeostasis and protection [97]. Furthermore, EGB can potentially increase the phosphorylation of the ERM/MLC protein, which acts as a selective A1R antagonist. This increases gaps between cells by remodeling actin in cerebral microvascular endothelial cells, thereby enhancing cerebral microvascular permeability [96]. These properties make the synthesis of NPs utilizing EGB highly beneficial for traversing the BBB and introduce a promising therapeutic strategy against PD.

4.6. Conclusions and Future Prospects

This review discusses the significant potential of EGB in developing novel dual-functional NPs for PD treatment. EGB demonstrates numerous beneficial properties, including neuroprotection, antioxidant capabilities, and the ability to permeate the BBB, a significant challenge when treating neurological disorders. By acting as a reducing agent in the synthesis of LNPs, EGB stabilizes these NPs and enhances their delivery efficiency across the BBB. This innovative approach integrates the traditional medicinal benefits of EGB with advanced nanomedicine, offering a novel and promising therapeutic strategy for PD. Further clinical studies are necessary to fully understand the mechanisms involved and optimize the efficacy of EGB-loaded LNPs to advance treatment strategies for PD. The overall potential of EGB as a therapeutic and reducing agent shows promise for future research and clinical applicability. Several avenues can be explored further to unlock the multitude of beneficial properties exhibited in practical outputs. These could include efficacy studies regarding optimal dosages, variation in formulations, and the extract's long-term effects in clinical trials. An in-depth look into the mechanism of action of the EGB may significantly improve the BBB permeability and the neuroprotective and antioxidant effects. These studies may aid in optimizing the synergistic effects of using the EGB-loaded LNPs in conjunction with therapeutic agents, such as drugs and therapeutic genes, to target specific diseases, such as PD. An exciting avenue that requires focus is personalized medicine, i.e., personalized treatment based on the individual's genetic profile and adjusting the treatment protocol accordingly to develop an optimum therapeutic designed for a specific individual's need. Continued interdisciplinary research and collaboration will be crucial in realizing the full potential of EGB-loaded LNPs and bringing these innovative therapies to clinical practice.

References

1. Dorsey, E.R.; Sherer, T.; Okun, M.S.; Bloem, B.R. The emerging evidence of the Parkinson pandemic. *J Parkinsons Dis.* 8, **2018**, S3–S8. <http://doi.org/10.3233/JPD-181474>.
2. Armstrong, M.J.; Okun, M.S. Diagnosis and Treatment of Parkinson Disease, A Review. *JAMA.*, **2020**, 323, 548-560. doi:10.1001/jama.2019.22360
3. Roco, M.C. The long view of nanotechnology development: the National Nanotechnology Initiative at 10 years. *J Nanopart Res.*, **2011**, 13, 427–445. doi:1007/s11051-011-0323-1.
4. Kaya, M.; Ahishali, B. Basic physiology of the blood-brain barrier in health and disease: a brief overview. *Tissue Barriers*, **2021** 9, e1840913. doi:10.1080/21688370.2020.1840913
5. Preetam, S.; Jonnalagadda, S.; Kumar, L; et al. Therapeutic potential of lipid nanosystems for the treatment of Parkinson's disease. *Ageing Res. Rev.*, **2023**, 89, 101965. doi: 10.1016/j.arr.2023.101965.
6. Jagaran, K.; Singh, M. Nanomedicine for Neurodegenerative Disorders: Focus on Alzheimer's and Parkinson's Diseases. *Int. J. Mol. Sci.*, **2021**, 22, 9082. doi:10.3390/ijms22169082
7. Venkatas, J.; Singh, M. Curcumin-reduced gold nanoparticles facilitate IL-12 delivery to cervical cancer in vitro cell model. *Nanomedicine*, **2023** 18, 945-960. doi: 10.2217/nmm-2023-0076
8. Yavarpour-Bali, H.; Ghasemi-Kasman, M.; Pirzadeh, M. Curcumin-loaded nanoparticles: a novel therapeutic strategy in treatment of central nervous system disorders. *Int. J. Nanomed.*, **2019**, 14, 4449–4460. doi: 10.2147/IJN.S208332
9. Jagaran, K.; Singh, M. Lipid-based Nanoparticles: Promising Treatment strategies for Parkinson's Disease. *Int. J. Mol. Sci.*, **2022**, 23, 9361. doi:10.3390/ijms23169361.
10. Ahmad, M.; Saleem, S.; Ahmad, A.S.; et al. *Ginkgo biloba* affords dose-dependent protection against 6-hydroxydopamine-induced parkinsonism in rats: Neurobehavioural, neurochemical and immunohistochemical evidences. *J. Neurochem.*, **2005**, 93, 94-104. doi:10.1111/j.1471-4159.2005.03000.x
11. Day, J.O.; Mullin S. The Genetics of Parkinson's Disease and Implications for Clinical Practice. *Genes*, **2021**, 12, 1006. doi:10.3390/genes12071006.
12. Yasuhara, T. Neurobiology Research in Parkinson's Disease. *Int. J. Mol. Sci.*, **2020**, 21, 793. doi:10.3390/ijms21030793.
13. Corona, J.C. Natural Compounds for the Management of Parkinson's Disease and Attention-Deficit/Hyperactivity Disorder. *BioMed Res Int.*, **2018**, 2018, 4067597. doi:10.1155/2018/4067597
14. Deng, H.; Wang, P.; Jankovic, J. The genetics of Parkinson disease. *Ageing Res. Rev.*, **2018**, 42, 72–85. doi: 10.1016/j.arr.2017.12.007

15. Orayj, K.; Akbari, A.; Lacey, A.; Smith, M.; Pickrell, O.; Lane, E.L. Factors affecting the choice of first-line therapy in Parkinson's disease patients in Wales: A population-based study. *Saudi Pharm J.*, **2021**, 29, 206–212. doi:10.1016/j.jsps.2021.01.004.
16. Pickut, B.A.; Mischley, L.K.; Reversa, R.J. Integrative medicine and Parkinson's disease. *Integr. Neurol.* 2020 Sept;7:141–183. doi:10.1093/med/9780190051617.003.0007.
17. Church, F.C. Treatment Options for Motor and Non-Motor Symptoms of Parkinson's Disease. *Biomolecules*, **2021**, 11, 612. doi:10.3390/biom11040612.
18. Bryans, L.A.; Palmer, A.D.; Anderson, S.; Schindler, J.; Graville, D.J. The impact of Lee Silverman Voice Treatment (Lsvt Loud®) on voice, communication, and participation: Findings from a prospective, longitudinal study. *J. Commun. Disord.*, **2020**, 89, 106031. doi: 10.1016/j.jcomdis.2020.106031.
19. Yuan, F.; Guo, X.; Wei, X.; et al. Lee Silverman Voice Treatment for dysarthria in patients with Parkinson's disease: A systematic review and meta-analysis. *Eur. J. Neurol.*, **2020**, 27, 1957–1970. doi: 10.1111/ene.14399.
20. Elsworth, J.D.; Roth, R.H. Dopamine synthesis, uptake, metabolism, and receptors: Relevance to gene therapy of Parkinson's disease. *Exp. Neurol.*, **1997**, 144, 4–9. doi:10.1006/exnr.1996.6379.
21. Cookson, M.R. The biochemistry of Parkinson's disease. *Annu. Rev. Biochem.*, **2005**, 74, 2952. doi:10.1146/annurev.biochem.74.082803.133400.
22. Lees, A.J.; Tolosa, E.; Olanow, C.W. Four pioneers of L-dopa treatment: Arvid Carlsson, Oleh Hornykiewicz, George Cotzias, and Melvin Yahr. *Mov. Disord.*, **2015**, 30, 19–36. doi:10.1002/mds.26120.
23. Fox, S.H.; Katzenschlager, R.; Lim, S.Y.; et al. International Parkinson and movement disorder society evidence-based medicine review: Update on treatments for the motor symptoms of Parkinson's disease. *Mov. Disord.*, **2018**, 33, 1248–1266. doi:10.1002/mds.27372.
24. Carbone, F.; Djamshidian, A.; Seppi, K.; Poewe, W. Apomorphine for Parkinson's disease: Efficacy and safety of current and new formulations. *CNS Drugs*, **2019**, 33, 905–918. doi:10.1007/s40263-019-00661-z.
25. Rascol, O.; Goetz, C.; Koller, W.; Poewe, W.; Sampaio, C.. Treatment interventions for Parkinson's disease: an evidence-based assessment. *Lancet Neurol.*, **2002**, 2, 78-86. doi:10.1016/S1474-4422(02)00042-1.
26. Georgsson, H.; Murray, B.J. Sleep disorders in Parkinson's disease and Parkinsonian syndromes. In: Barkoukis TJ, Matheson JK, Ferber R, Doghramji K, editors. *Therapy in Sleep Medicine*. W.B. Saunders; **2012**, 330-344. doi: 10.1016/B978-1-4377-1703- 7.10026-X.
27. Stocchi, F.; Olanow, C.W. Neuroprotection in Parkinson's disease: clinical trials. *Ann. Neurol.*, **2014**, 76, 139-148. doi:10.1002/ana.24298.

28. Hauser, R.A.; Olanow, C.W.; Kieburtz, K.D.; et al. Tozadenant (SYN115) in patients with Parkinson's disease who have motor fluctuations on levodopa: a phase 2b, double-blind, randomised trial. *Lancet Neurol.*, **2018**, 17, 501-510. doi:10.1016/S1474-4422(18)30108-7.
29. Doble, A. The pharmacology and mechanism of action of riluzole. *Neurology*, **1996**, 47, S233-S241. doi:10.1212/wnl.47.6_suppl_4.233s.
30. Zhou, W.; Barkow, J.C.; Freed, C.R. Running wheel exercise reduces α -synuclein aggregation and improves motor and cognitive function in a transgenic mouse model of Parkinson's disease. *PLoS ONE*, **2017**, 12, e0190160. doi:10.1371/journal.pone.0190160.
31. De Carvalho, A.O.; Filho, A.S.S.; Murillo-Rodriguez, E.; Rocha, N.B.; Carta, M.G.; Machado, S. Physical exercise for Parkinson's disease: Clinical and experimental evidence. *Clin. Pract. Epidemiol. Ment. Health*, **2018**, 14, 89. doi:10.2174/1745017901814010089.
32. Hall, M-F.E.; Church, F.C. Exercise for older adults improves the quality of life in Parkinson's disease and potentially enhances the immune response to COVID-19. *Brain Sci.*, **2020**, 10, 612. doi:10.3390/brainsci10090612.
33. Fabbri, M.; Rosa, M.M.; Ferreira, J.J. Adjunctive therapies in Parkinson's disease: how to choose the best treatment strategy approach. *Drugs Aging*, **2018**, 35, 1041–1054. doi:10.1007/s40266-018-0600-7.
34. Sharma, V.D.; Patel, M.; Miocinovic, S. Surgical Treatment of Parkinson's Disease: Devices and Lesion Approaches. *Neurother.*, **2020**, 17, 1525-1538. doi:10.1007/s13311-020-00939-x
35. Nowak, A.; Kojder, K.; Zielonka, J.; et al. The use of *Ginkgo biloba* L. as a Neuroprotective Agent in the Alzheimer's Disease. *Front. Pharmacol.*, **2021**, 12, 775034. doi:10.3389/fphar.2021.775034
36. Mansoor, M.; Brahmini, C.S.; Rao, S.D. Phytochemical and Nephroprotective Activity of *Ginkgo biloba* against Gentamicin-Induced Nephrotoxicity in Rats. *Int. J. Adv. Pharm. Med. Bioallied Sci.*, **2015**, 3, 98–101.
37. Rojas, C.; Rojas-Castañeda, J.; Rojas, P. Antioxidant Properties of a *Ginkgo biloba* Leaf Extract (EGb 761) in Animal Models of Alzheimer's and Parkinson's Diseases. *Curr. Top. Nutraceutical Res.*, **2016**, 14, 1–16.
38. DeFeudis, F.V. A Brief History of EGB 761 and its Therapeutic uses. *Pharmacopsychiatry*, **2003**, 36, S2–S7. doi:10.1055/s-2003-40450.
39. Singh, S.K.; Srivastav, S.; Castellani, R.J.; Plascencia-Villa, G.; Perry, G. Neuroprotective and Antioxidant Effect of *Ginkgo biloba* Extract Against AD and Other Neurological Disorders. *Neurother.*, **2019**, 16, 666-674. doi: 10.1007/s13311-019-00767-8.
40. Goloborshcheva, V.V.; Kucheryan, V.G.; Voronina, N.A.; Teterina, E.V.; Ustyugov, A.A.; Morozov, S.G. Synuclein Proteins in MPTP-Induced Death of Substantia Nigra Pars Compacta Dopaminergic Neurons. *Biomedicines*, **2022**, 10, 2278. doi:10.3390/biomedicines10092278.

41. Langston, J.W. The MPTP Story. *J. Parkinsons Dis.*, **2017**, 7, S11–S19. doi:10.3233/JPD-179006.
42. Taib, C.N.M.; Mustapha, M. MPTP-induced mouse model of Parkinson's disease: A promising direction of therapeutic strategies. *Bosn. J. Basic Med. Sci.*, **2020**, 21, 422–433. doi:10.17305/bjbms.2020.5181.
43. Wu, W.J.; Lu, C.W.; Wang, S.E.; Lin, C.L.; Su, L.Y.; Wu, C.H. MPTP toxicity causes vocal, auditory, orientation and movement defects in the echolocation bat. *NeuroReport*, **2021**, 32, 125–134. doi:10.1097/WNR.0000000000001574.
44. Haga, H.; Matsuo, K.; Yabuki, Y.; Zhang, C.; Han, F.; Fukunaga, K. Enhancement of ATP production ameliorates motor and cognitive impairments in a mouse model of MPTP-induced Parkinson's disease. *Neurochem. Int.*, **2019**, 129, 104492. doi:10.1016/j.neuint.2019.104492.
45. Prasad, E.M.; Hung, S.Y. Behavioral Tests in Neurotoxin-Induced Animal Models of Parkinson's Disease. *Antioxidants.*, **2020**, 9, 1007. doi:10.3390/antiox9101007.
46. Ramassamy, C.; Clostre, F.; Christen, Y.; Costentin, J. Prevention by a *Ginkgo biloba* Extract (EGB 761) of the Dopaminergic Neurotoxicity of MPTP. *J. Pharm.Pharmacol.*, **1990**, 42, 785–789. doi:10.1111/j.2042-7158.1990.tb07021.x.
47. Wu, W-R.; Zhu, X-Z. Involvement of monoamine oxidase inhibition in neuroprotective and neurorestorative effects of *Ginkgo biloba* extract against MPTP-induced nigrostriatal dopaminergic toxicity in C57 mice. *Life Sci.*, **1999**, 65, 157–164. doi:10.1016/s0024-3205(99)00232-5.
48. Yu, D.; Zhang, P.; Li, J.; et al. Neuroprotective effects of *Ginkgo biloba* dropping pills in Parkinson's disease. *J. Pharm. Anal.*, **2021**, 11, 220-231. doi: 10.1016/j.jpha.2020.06.002.
49. Cao, F.; Sun, S.; Tong, E.T. Experimental study on inhibition of neuronal toxic effect of levodopa by *Ginkgo biloba* extract on Parkinson disease in rats. *J. Huazhong Univ. Sci. Technol. Med. Sci.*, **2003**, 23, 151–153. doi:10.1007/BF02859941.
50. Wang, Y.Q.; Wang, M.Y.; Fu, X.R.; Gao, G.F.; Fan, Y.M. Neuroprotective effects of ginkgetin against neuroinjury in Parkinson's disease model induced by MPTP via chelating iron. *Free Radic. Res.*, **2015**, 49, 1069–1080. doi:10.3109/10715762.2015.1032958
51. Hua, J.; Yin, N.; Yang, B.; Zhang, J.; Ding, J.; Fan, Y.; Hu, G. Ginkgolide B and bilobalide ameliorate neural cell apoptosis in α -synuclein aggregates. *Biomed. Pharmacother.*, **2017**, 96, 792–797. doi:10.1016/j.biopha.2017.10.050.
52. Kang, X.; Chen, J.; Xu, Z.; Li, H.; Wang, B. Protective effects of *Ginkgo biloba* extract on paraquat-induced apoptosis of PC12 cells. *Toxicol. in Vitro*, **2007**, 21, 1003–1009. doi:10.1016/j.tiv.2007.02.004.

53. Kuang, S.; Yang, L.; Rao, Z.; et al. Effects of *Ginkgo biloba* Extract on A53T α -Synuclein Transgenic Mouse Models of Parkinson's Disease. *Can. J. Neurol. Sci.*, **2018**, 45, 182–187. doi:10.1017/cjn.2017.268
54. Zhang, W.; Liu, Q.Y.; Haqqani, A.S.; et al. Differential expression of receptors mediating receptor-mediated transcytosis (RMT) in brain microvessels, brain parenchyma and peripheral tissues of the mouse and the human. *Fluids Barriers CNS*, **2020**, 17, 47. doi:10.1186/s12987-020-00209-0.
55. Shu, P.; Sun, M.; Li, J.; et al. Chemical constituents from *Ginkgo biloba* leaves and their cytotoxicity activity. *J Nat Med.*, **2020**, 74, 269-274. doi:10.1007/s11418-019-01359- 8.
56. Li, F.; Boateng, I.D.; Yang, X.M.; Li, Y.; Liu, W. Effects of processing methods on quality, antioxidant capacity, and cytotoxicity of *Ginkgo biloba* leaf tea product. *J Sci Food Agric.*, **2023**, 103, 4993-5003. doi: 10.1002/jsfa.12577.
57. Khan, N.; Bano, A. Modulation of Phytoremediation and Plant Growth by the Treatment with PGPR, Ag Nanoparticle and Untreated Municipal Wastewater. *Int. J. Phytoremed.*, **2016**, 18, 1258-1269. doi:10.1080/15226514.2016.1203287
58. Magdalane, C.M.; Kaviyarasu, K.; Raja, A.; et al. Photocatalytic decomposition effect of erbium doped cerium oxide nanostructures driven by visible light irradiation: investigation of cytotoxicity, antibacterial growth inhibition using catalyst. *J. Photochem. Photobiol.*, **2018**, 185, 275-282. doi:10.1016/j.jphotobiol.2018.06.011
59. Valsalam, S.; Agastian, P.; Esmail, G.A.; Ghilan, A.K.M.; Al-Dhabi, N.A.; Arasu, M.V. Biosynthesis of silver and gold nanoparticles using *Musa acuminata* colla flower and its pharmaceutical activity against bacteria and anticancer efficacy. *J. Photochem. Photobiol. B*, **2019**, 201, 111670. doi:10.1016/j.jphotobiol.2019.111670
60. Salem, S.S.; Fouda, A. Green synthesis of metallic nanoparticles and their prospective biotechnological applications: an overview. *Biol. Trace Elem. Res.*, **2021**, 199, 344-370. doi:10.1007/s12011-020-02138-3.
61. Zheng, H.; Wang, Z.; Wu, J. Green synthesis of nanoparticles using *Ginkgo biloba* extract: A sustainable approach. *Green Chem.*, **2012**, 14, 2550-2558. doi:10.1039/C2GC35694D.
62. Jha, A.K.; Prasad, K. Eco-friendly synthesis of nanoparticles using plant extracts: Green chemistry approach. *J. Environ. Chem. Eng.*, **2018**, 6, 3698-3712. doi:10.1016/j.jece.2018.05.042.
63. Shaik, M.R.; Khan, M.; Kuniyil, M.; et al. Plant-Extract-Assisted Green Synthesis of Silver Nanoparticles Using *Origanum vul-gare* L. Extract and Their Microbicidal Activities. *Sustainability*, **2018**, 10, 913. doi:10.3390/su10040913

64. Li, S.; Chen, Y.; Zhang, S.; Li, L.; Zhao, C. Green synthesis of gold nanoparticles using *Ginkgo biloba* leaf extract without any reducing agent. *J. Agric. Food Chem.*, **2013**, 61, 3033–3038. doi:10.1021/jf400937g
65. Xu, Z.; Feng, Q.; Wang, M.; Zhao, H.; Lin, Y.; Zhou, S. Green Biosynthesized Silver Nanoparticles With Aqueous Extracts of *Ginkgo biloba* Induce Apoptosis via Mitochondrial Pathway in Cervical Cancer Cells. *Front Oncol.*, **2020**, 10, 575415. doi: 10.3389/fonc.2020.575415.
66. Chang, W.T.; Chen, Y.J.; Lu, F.J.; Chou, Y.H. Preparation of silver nanoparticles and their antibacterial activity against *Escherichia coli*. *Colloids Surf B Biointerfaces*, **2011**, 85, 161–166. doi: 10.1016/j.colsurfb.2011.09.025.
67. Manach, C.; Scalbert, A.; Morand, C.; Rémésy, C.; Jiménez, L. Polyphenols: food sources and bioavailability. *Amer. J. Clin. Nutr.*, **2004**, 79, 727–747. doi:10.1093/ajcn/79.5.727
68. Middleton Jr, E.; Kandaswami, C.; Theoharides, T.C. The effects of plant flavonoids on mammalian cells: implications for inflammation, heart disease, and cancer. *Pharmacol. Rev.*, **2000**, 52, 673–751.
69. Dennis, E.A.; Norris, P.C. Eicosanoid storm in infection and inflammation. *Nat. Rev. Immunol.*, **2015**, 15, 511–523. doi:10.1038/nri3859.
70. Klotz, L.O.; Steinbrenner, H. Cellular adaptation to xenobiotics: interplay between xenosensors, reactive oxygen species and FOXO transcription factors. *Redox Biol.*, **2017**, 13, 646–654. doi: 10.1016/j.redox.2017.07.007
71. Muthukumar, H.; Palanirajan, S.K.; Shanmugam, M.K.; Gummadi, S.N. Plant extract mediated synthesis enhanced the functional properties of silver ferrite nanoparticles over chemical mediated synthesis. *Biotechnol. Rep.*, **2020**, 26, e00469. doi:10.1016/j.btre.2020.e00469.
72. Pandey, S.; Shaikh, F.; Gupta, A.; Tripathi, P.; Yadav, J.S. A Recent Update: Solid Lipid Nanoparticles for Effective Drug Delivery. *Adv Pharm Bull.*, **2022**, 12, 17–33. doi: 10.34172/apb.2022.007
73. Ravi, P.R.; Aditya, N.; Kathuria, H.; Malekar, S.; Vats, R. Lipid nanoparticles for oral delivery of raloxifene: optimization, stability, in vivo evaluation and uptake mechanism. *Eur. J. Pharm. Biopharm.*, **2014**, 87, 114–124. doi:10.1016/j.ejpb.2013.12.015
74. Viayanand, P.; Jyothi, V.; Aditya, N.; Mounika, A. Development and Characterization of Solid Lipid Nanoparticles Con-taining Herbal Extract: In Vivo Antidepressant Activity. *J. Drug Deliv.*, **2018**, 2018, 2908626. doi:10.1155/2018/2908626.
75. Satapathy, M.K.; Yen, T.; Jan, J.; et al. Solid Lipid Nanoparticles (SLNs): An Advanced Drug Delivery System Targeting Brain through BBB. *Pharmaceutics*, **2021**, 13, 1183. doi:10.3390/pharmaceutics13081183

76. Cecchelli, R.; Berezowski, V.; Lundquist, S.; et al. Modelling of the blood-brain barrier in drug discovery and development. *Nat. Rev. Drug Discov.*, **2007**, 6, 650–661. doi:10.1038/nrd2368.
77. Segarra, M.; Aburto, M.R.; Acker-Palmer, A. Blood–Brain Barrier Dynamics to Maintain Brain Homeostasis. *Neurosciences*, **2021**, 44, 393-405. doi:10.1016/j.tins.2020.12.002
78. O'Keefe, E.; Campbell, M. Modulating the paracellular pathway at the blood-brain barrier: Current and future approaches for drug delivery to the CNS. *Drug Discov. Today Technol.*, **2016**, 20, 35–39. doi:10.1016/j.ddtec.2016.07.008.
79. Habib, S.; Singh, M. Angiopep-2-modified Nanoparticles for Brain-directed delivery of therapeutics: A Review. *Polymers*, **2022**, 14, 712. doi:10.3390/polym14040712.
80. Chaichana, K.L.; Pinheiro, L.; Brem, H. Delivery of local therapeutics to the brain: Working toward advancing treatment for malignant gliomas. *Ther. Deliv.*, **2015**, 6, 353–369. doi:10.4155/tde.14.114.
81. Pardridge, W.M. Drug transport across the blood-brain barrier. *J. Cereb. Blood Flow Metab.*, **2012**, 32, 1959–1972. doi:10.1038/jcbfm.2012.126.
82. Sweeney, M.D.; Sagare, A.P.; Zlokovic, B.V. Blood–brain barrier breakdown in Alzheimer disease and other neurodegenerative disorders. *Nat. Rev. Neurol.*, **2018**, 14, 133–150. doi:10.1038/nrneurol.2017.188.
83. Zhu, X.; Jin, K.; Huang, Y.; Pang, Z. Brain drug delivery by adsorption-mediated transcytosis. In *Brain Targeted Drug Delivery System*; Gao, H., Gao X. Eds., Academic Press, London, UK., **2019**, 159–183. doi:10.1016/B978-0-12-814001-7.00007-X
84. Pulgar, V.M. Transcytosis to cross the blood-brain barrier, new advancements and challenges. *Front. Neurosci.*, **2019**, 12, 1019. doi:10.3389/fnins.2018.01019.
85. Gregory, J.; Vengalasetti, Y.V.; Bredesen, D.E.; Rao, R.V. Neuroprotective Herbs for the Management of Alzheimer's Disease. *Biomolecules*, **2021**, 11, 543. doi: 10.3390/biom11040543.
86. Ahlemeyer, B.; Krieglstein, J. Neuroprotective effects of *Ginkgo biloba* extract. *Cell.Mol. Life Sci.*, **2003**, 60, 1779-1792. doi:10.1007/s00018-003-3082-1.
87. Karalija, E.; Dahija, S.; Hassan, S.T.S. Biflavonoids: Important Contributions to the Health Benefits of Ginkgo (*Ginkgo bi-loba* L.). *Plants*, **2022**, 11, 1381. doi:10.3390/plants11101381
88. Jung, U.J.; Kim, S.R. Beneficial Effects of Flavonoids Against Parkinson's Disease. *J. Med. Food*, **2016**, 19, 837-852. doi: 10.1089/jmf.2016.3743
89. Niu, X.; Zhang, H.; Li, W.; Yang, J.; Liu, Y. Flavonoids: Therapeutic Potential and Role in BBB Permeability. *Front. Pharmacol.*, **2019**, 10, 1268. doi:10.3389/fphar.2019.01268.
90. Liu, Y.; Huang, R.; Xu, Y.; Li, D.; Wu, X.; Wang, X.; Jiang, Z. Strategies to Bypass Lysosomal Degradation of LNPs: Focus on Flavonoid Modifications. *Mol. Pharm.*, **2017**, 14, 2052-2060. doi:10.1021/acs.molpharmaceut.6b01087

91. Yang, X.; Wang, L.; Yan, J.; Tang, Z.; Jiang, Z.; Liu, Q. Flavonoid-Modified LNPs Improved Cytoplasmic Delivery of Therapeutics. *Biomaterials*, **2018**, 179, 69-79. doi:10.1016/j.biomaterials.2018.06.034
92. Cheng, C-C.; Yang, Y.L.; Liao, K.H.; Lai, T.W. Adenosine receptor agonist 524 NECA increases cerebral extravasation of fluorescein and low molecular weight 525 dextran independent of blood-brain barrier modulation. *Sci. Rep.*, **2016**, 6, 23882. doi:10.1038/srep23882.
93. Carman, A.J.; Mills, J.H.; Krenz, A.; Kim, D.G.; Bynoe, M.S. Adenosine 521 receptor signaling modulates permeability of the blood-brain barrier. *J Neurosci.*, **2011**, 31, 13272-13280. doi: 10.1523/JNEUROSCI.3337-11.2011.
94. Bynoe, M.S.; Viret, C.; Yan, A.; Kim, D.G. Adenosine receptor signaling: a key 519 to opening the blood-brain door. *Fluids Barriers CNS*, **2015**, 12, 20. doi:10.1186/s12987-015-0017-7.
95. Zhang, L-D.; Ma, L.; Dai, J-G.; Chang, L-G.; Huang, P-L.; Tian, X-Q. Hyperbaric Oxygen and *Ginkgo biloba* Extract Ameliorate Cognitive and Memory Impairment via Nuclear Factor Kappa-B Pathway in Rat Model of Alzheimer's Disease. *Chin. Med. J.*, **2015**, 128, 3088–3093. doi: 10.4103/0366-6999.169105.
96. Liang, W.; Xu, W.; Zhu, J.; et al. *Ginkgo biloba* extract improves brain uptake of ginsenosides by increasing blood-brain barrier permeability via activating A1 adenosine receptor signaling pathway. *J. Ethnopharmacol.*, **2019**, 246, 112243. doi:10.1016/j.jep.2019.112243.
97. Lang, D.; Ude, C.; Wurglics, M.; Schubert-Zsilavecz, M.; Klein, J. Brain 565 Permeability of Bilobalide as Probed by Micro-dialysis Before and After Middle 566 Cerebral Artery Occlusion in Mice. *J. Pharm. Pharm. Sci.*, **2010**, 13, 607-614. doi:10.18433/j31c7q.

Refer to Appendix C2 for the Turnitin Report.

Chapter 5

Therapeutic Potential of Sphingomyelin-cholesterol based Solid Lipid Nanoparticles in Parkinson's Disease: Targeting the LRRK2 G2019S Mutation using therapeutic siRNA

Therapeutic Potential of Sphingomyelin-cholesterol based Solid Lipid Nanoparticles in Parkinson's Disease: Targeting the LRRK2 G2019S Mutation using therapeutic siRNA

Abstract. Parkinson's disease (PD) affects millions worldwide, with cases linked to genetic mutations, the most common being the LRRK2 G2019S mutation. This mutation enhances kinase activity, causing neuronal toxicity and contributing to PD pathogenesis. Current treatments, such as LRRK2 inhibitors, provide limited efficacy and carry significant side effects, highlighting the need for alternative therapies. This review explores the potential of sphingomyelin-cholesterol-based solid lipid nanoparticles (SC-SLNPs) as a delivery system for therapeutic siRNA targeting the LRRK2 G2019S mutation. SC-SLNPs offer several advantages, including high drug loading capacity, low cytotoxicity, and the ability to cross the blood-brain barrier (BBB). These nanoparticles are also biocompatible and can be easily modified for enhanced delivery efficiency. We propose a novel approach utilizing SC-SLNPs conjugated with siRNA to silence the LRRK2 G2019S mutation. This strategy aims to reduce the pathogenic effects of the mutation, providing a dual therapeutic benefit by addressing both genetic and symptomatic aspects of PD. The potential of this innovative nanomedicine approach could revolutionize PD treatment, offering a more effective and targeted therapy with reduced side effects.

Keywords: Parkinson's disease, LRRK2 G2019S mutation, sphingomyelin-cholesterol solid lipid nanoparticles, siRNA, nanomedicine, blood-brain barrier.

5.1. Introduction

Parkinson's disease (PD) is a prevalent neurodegenerative disorder affecting millions globally. It is characterized by motor and non-motor symptoms resulting from the progressive loss of dopaminergic neurons in the substantia nigra. PD cases are categorized as either idiopathic or familial, with 5-10% of cases having a genetic basis. These familial cases are linked to mutations in several genes such as Parkin (PRKN), α -synuclein (SNCA), glucocerebrosidase (GBA), DJ-1, VPS35, and leucine-rich repeat kinase 2 (LRRK2) [1]. The LRRK2 G2019S mutation is the most common, accounting for 6-40% of familial PD cases [2,3]. LRRK2, a large multidomain protein belonging to the ROCO superfamily, plays a critical role in various cellular processes, including autophagy, lysosomal degradation, and vesicular trafficking [4].

The G2019S mutation in the kinase domain of LRRK2 significantly increases its kinase activity compared to the wild type, leading to neuronal toxicity. Studies in primary neuronal cultures have demonstrated that overexpression of LRRK2 G2019S induces cellular dysfunctions such as impairment of intracellular organelles, cell death, and neurite shortening [5]. Animal models, including *Drosophila* and *Caenorhabditis elegans*, have further elucidated the mutation's role in PD, showing age-dependent dopaminergic neuronal loss, locomotor defects, and reduced survival [6,7]. While the mechanisms regulating LRRK2's kinase and GTPase activities are not fully understood, it is clear that both inter- and intra-molecular regulation control its enzymatic activity [3].

Current therapeutic strategies targeting the LRRK2 using inhibitors such as MLi-2 aim to regulate kinase activity. While these inhibitors have shown protective effects by modulating cellular processes such as lysosomal function and endosome maturation, they are not without limitations. One major issue is the potential for adverse effects, including pulmonary fibrosis, when LRRK2 levels are significantly reduced [4]. This highlights the need for novel therapeutic approaches that can effectively target LRRK2 without causing significant side effects.

One of the major challenges in developing effective treatments for PD is the blood-brain barrier (BBB), a highly selective barrier that restricts the entry of therapeutic agents into the brain [8]. To mitigate this challenge, the use of lipid nanoparticles (LNPs) (**as outlined in Chapter 2.3.2**) can be employed. These nanoparticles (NPs) can be engineered for surface modifications, allowing for the conjugation of therapeutic agents such as DNA and RNA, making them suitable for gene delivery applications [9]. From the many lipidic nanosystems, sphingomyelin (SM)-based SLNPs have shown significant potential in PD treatment. SM, a phospholipid and sphingolipid, is abundant in the plasma membrane and myelin sheath of nerve cell axons, playing a crucial role in impulse transmission, myelin sheath integrity, and BBB maintenance. SM-SLNPs have demonstrated efficacy in crossing the BBB and delivering therapeutic agents, making them ideal candidates for PD treatment [10,11].

In addition to SM, the incorporation of cholesterol (Chol) into SLNPs enhances their stability and circulatory time *in vivo*, improving pharmacokinetics and therapeutic properties. SM-Chol combinations have been found to form cholesterol/sphingomyelin-enriched nanodomains in organelle membranes, which are essential for neurotransmitter release, synaptic plasticity, and

synaptic function regulation [11]. These properties make SC-SLNPs a promising vehicle for delivering therapeutics across the BBB.

Given the potential of RNA interference (RNAi) in gene therapy, small interfering RNA (siRNA) molecules can be employed to target specific mRNA sequences, leading to sequence-specific gene silencing. siRNA targeting the LRRK2 G2019S mutation can reduce pathogenic kinase activity and mitigate its toxic effects. However, the delivery of siRNA poses challenges due to its high molecular weight, polyanionic nature, and hydrophilicity, necessitating an effective delivery vehicle [12]. This review explores the development of therapeutic siRNA conjugated to SC-SLNPs, aiming to silence the LRRK2 G2019S mutation. This innovative approach combines the beneficial properties of SC-SLNPs with the gene-silencing capabilities of siRNA, offering a dual therapeutic strategy for PD. By targeting the genetic and symptomatic aspects of PD, this approach holds promise for more effective and targeted treatment with reduced side effects.

5.2. The LRRK2 Mutation in Parkinson's Disease (PD)

PD is characterized as a progressive neurodegenerative disorder, which still remains a serious affliction after more than 200 years following its first clinical description. While the mechanisms by which a patient is affected with PD are not completely elucidated, studies pertaining to the genetic implications, such as point mutations occurring in leucine-rich repeat kinase 2 (LRRK2), are found to be the most common genetic risk [13]. This large, multidomain protein (280 kDa) belongs to the ROCO superfamily and consists of multiple protein-protein interaction domains, including the N-terminal armadillo, ankyrin, and leucine-rich repeat domains, together with a C-terminal WD40 domain [3]. LRRK2 further contains two distinct enzymatic domains, a serine/threonine kinase and Ras of complex (ROC) GTPase domains, which are effectively separated by a C-terminal ROC (COR) domain (Figure 5.1). Mutational events occurring within this protein are clustered within the catalytic domain and assessed by measuring the autophosphorylation of LRRK2, LRRKtide (an artificial peptide substrate), myelin basic protein (MBP), and Ser 1292 [14,15]. Furthermore, LRRK2 exhibits GTPase activity, permitting GTP binding and hydrolysis [16].

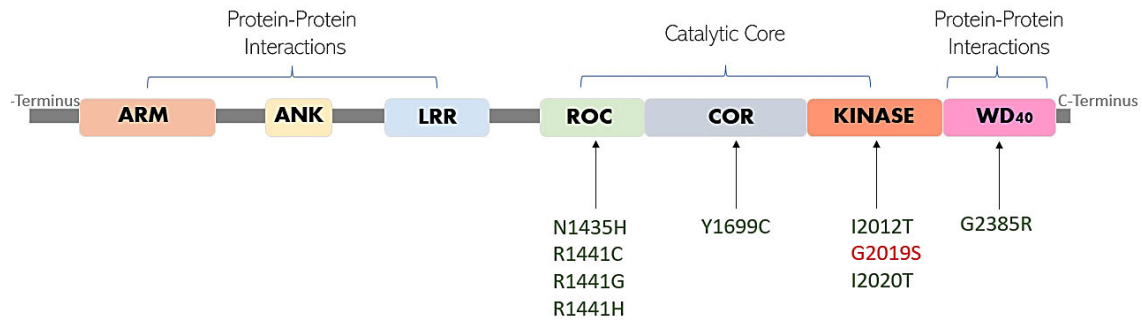


Figure 5.1. The LRRK2 gene portraying the multidomain protein-protein interactions and the catalytic core with the potential pathogenic mutations (Adapted from [17]).

Dimerization of the LRRK2 protein, with the ROC and COR domains functioning as primary dimerization interfaces, results in higher kinase activity and GTPase reactions, in comparison to the monomers [18,19]. These dimers are further enriched in membrane fractions, portraying an elevated kinase activity against the cytosolic LRRK2 [3]. It has been previously elucidated that the missense mutations, including K1347A and K1348N, present in the P-loop of the ROC domain are responsible for guanine nucleotide-binding disruptions and impairments in autophosphorylation, while GTPase activity is regulated through autophosphorylation of the ROC domain [20]. These kinase activities are regulated via the GTPase activating proteins (GAP) or guanine nucleotide exchange factor (GEF) [21].

5.2.1. LRRK2 Associated Signalling Pathways

The active GTPase and kinase domains associated with the protein-protein interaction motifs gave rise to the suggestion that LRRK2 may play a role in signaling pathways. Further studies elucidated this by means of analysing the mitogen-activated protein kinase pathway (MAPK). These pathways are composed of three layers of proteins that possess the ability to activate each other in succession, starting with MAP3K, which phosphorylates and activates MAP2K, thereby activating MAPK [17]. Furthermore, the activation of MAP2K3 and MAP2K6 promotes the activation of p38, a downstream effector, via the stimulation of cytokines, growth factors, and stress. Beyond this, MAP2K4 and MAP2K7 lead to the activation of JNK. Both JNK and p38 are responsible for apoptosis, immune responses, cell proliferation and differentiation, and cytokine production [22]. MAP2K1 and MAP2K2 have been noted to be activated by the LRRK-G2019S, resulting in hyperphosphorylation of ERK1 and ERK2. This altered pathway mediates the increase in basal autophagy [23].

LRRK2 plays a role in the cancer signaling pathways, being associated with the MET pathways in thyroid and papillary renal carcinomas. A knockdown in the LRRK2 gene has shown a substantial reduction in tumour proliferation with a concomitant decrease in MET signaling via the target of rapamycin (TOR) and signal transducer and activator of transcription (STAT3), together with an increase in cellular demise [24]. Additionally, LRRK2-G2019S may bind to the endoplasmic reticulum-located Bcl-2, thereby reducing the membrane potential of the mitochondria, resulting in the stimulation of mitophagy [25]. A study conducted by Gehrke *et al.* (2010) in *Drosophila* argued that LRRK2 is associated with *Drosophila* Argonaute-1 (dAgo1) and human Argonaute-2 (hAgo2), thereby modulating the RNA-induced silencing complex [26]. Furthermore, the ribosomal small subunit (s15), a component of the protein synthesis pathway, is phosphorylated by LRRK2 and consequently sustains cell toxicity [27].

While these pathways have been studied, the information gained are utilized with caution due to the LRRK2 G2019S involvements being incomplete. It can be deduced, however, that the gene of interest is involved in the modulation of more than one signaling pathway and thus presents with a far greater risk of Parkinson's disease, owing to various undesirable outcomes [28]. Apart from this, the mutational events that occur render the LRRK2 a "wildcard" as a gain of novel functions are noted and thus lend a hand in the onset of disorders, including cancer and immune disorders [28].

5.2.2. The Impact of the LRRK2 G2019S Mutation

From the array of variations associated with LRRK2 and PD onset, G2019S has emerged as the most common case in both familial (4-5%) and sporadic (1%) forms [29]. The mutation is inherited at reduced penetrance. Thus, there is an age-dependent development of motor symptoms ranging from 28% at 59 years to 74% at the age of 79 years [30]. This mutational event occurs following the substitution of G > A at position 6055 of exon 41 of the LRRK2 gene, resulting in a change of glycine to serine residues at the 2019 codon. The G2019S mutation is located in the kinase domain and is associated with increasing the LRRK2 kinase activity, resulting in hyperphosphorylation of the LRRK2 targets [16]. This is a result of the increased phosphorylation noted in the LRRK2 substrates, such as the RAB GTPases, by two- to three-fold compared to the wild-type protein [16,31]. This is attributed to the conformational changes within the kinase domain, which destabilizes the enzyme, thus rendering a hyperactive state of phosphorylation, resulting in detrimental downstream effects on neuronal health (Table 5.1 and Figure 5.2). Individually, these downstream effects result in neurite shortening, which

in turn impairs neuronal connectivity and signaling, as well as interference with cellular homeostasis, resulting in neurodegeneration [32,33]. Synergistically, these effects lead to neuronal apoptosis, especially regarding the dopaminergic neurons in the substantia nigra, directly linking these implications to the onset of PD [27].

Table 5.1. Neuronal implications associated with the hyperphosphorylation caused by the LRRK2 G2019S mutation.

The downstream effect of hyperphosphorylation	Neuronal Implications	Ref.
Impaired Autophagy	Naturally, the LRRK2 performs a vital role in autophagy regulation. The mutational event disrupts this normal processing by hyperphosphorylating the autophagy-related proteins, resulting in impaired autophagic flux. Consequentially, neuronal toxicity is noted due to accumulation of damaged proteins and organelles.	[33]
Altered Mitochondrial Dynamics	The G2019S results in altered phosphorylation of the proteins involved in the mitochondrial fusion and fission. This leads to fragmentation and dysfunction of the mitochondria, owing to an increased oxidative stress and neuronal damage.	[27]
Increased Oxidative Stress	The increase in kinase activity is attributed to the overproduction of Reactive oxygen species (ROS), which overwhelms the cellular antioxidant defences, resulting in oxidative damage to proteins, lipids and DNA. This further exacerbates neuronal dysfunction and death.	[34]

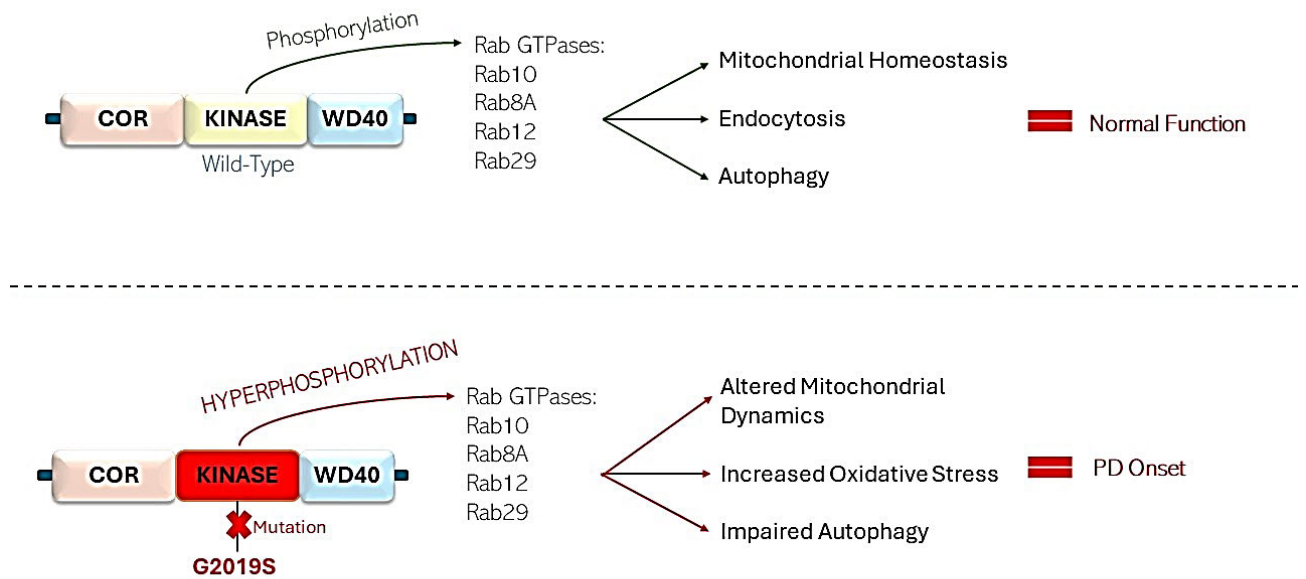


Figure 5.2. Impact of the LRRK2 G2019S mutation on the phosphorylation of Rab GTPases in PD onset.

5.2.2.1. Pathological and Molecular Mechanisms of LRRK2 G2019S Mutation in Parkinson's Disease

While the function of the non-mutated LRRK2 form is incompletely elucidated, evidence pertaining to its involvement in retromer complex modulation, mitochondrial homeostasis, endocytosis, and autophagy is not clear [28]. The interference in the removal of mitochondria from the microtubules in mitophagy is noted, with an alteration in the respiratory chain function and increased oxidative stress and morphological differences [35,36]. With regards to the G2019S mutation, mitochondrial DNA (mtDNA) lesions are noticed to accumulate in the patient-derived neurons [37].

Studies have found that, like LRRK2-associated PD patients, the G2019S mutations present with a heterogeneous pathology, conforming to the typical Lewy-body type of PD, as well as nigral degeneration, diffuse Lewy-body disease and the aggregation of the microtubule-associated tau protein, indicative of progressive frontotemporal dementia and supranuclear palsy [38]. Further evidence of the additional symptomatic onset associated with the LRRK2 G2019S mutations portrays a higher average age onset with a longer disease course, more affected female patients, onset of disorder manifestation in the lower limbs, gait and postural

disorders, sleep deprivation, increased intensity of depression, hallucination and cognitive disorders [39-44].

In a study conducted by Pischedda *et al.* (2021), G2019S mutations were associated with aggregation containing N-ethylmaleimide sensitive factor (NSF) in the basal ganglia [45]. It was observed that the kinase activity of the mutation induces this accumulation of the NSF in toxic aggregates, forming cytotoxic protein inclusions. Due to this aggregation, a depletion of cytosolic NSF was noted which results in impaired membrane fusion machinery, resulting in neuronal toxicity [45]. While autophagy is beneficial in the clearance of this accumulation, this activity, together with the proteasome activity, is pronouncedly reduced with ageing [46]. This is in keeping with the disease onset being more prominent at an older age.

Furthermore, MPTP introduction to transgenic mice overexpressing the mutational form of the LRRK2 G2019S portrayed a substantial loss and degeneration of dopaminergic neurons [47]. This was in conjunction with severe motor impairment and astrogliosis in the brain. This may be attributed to the excitotoxicity, autophagy, ER stress and mitochondrial failure associated with the mutation [48-51]. Beyond which an alteration of extracellular vesicle (EV) biogenesis in the astrocytes were noted, with an abnormal accumulation of PD-related proteins in the multivesicular bodies (MVBs). Furthermore, patients presenting with the mutation have been found to have EVs enriched with neurites and thus fail to provide full neurotrophic support to the dopaminergic neurons [52].

Due to therapeutics being administered at a late stage following phenotypical symptom onset, biological markers would be an imperative tool for early diagnosis and treatment plans. Currently, LRRK2 phosphorylation rates in urinary exosomes portrayed greater levels in manifesting PD patients (LRRK2+/PD+) compared to those only harbouring the G2019S mutation (LRRK2+/PD-) [53]. Furthermore, a reduction in the serum levels of the antioxidant urate was presented in LRRK2+/PD+ individuals, together with an alteration in the mtDNA transcription as well as an increase in mitochondrial reactive oxygen species (ROS) scavenger superoxide dismutase (SOD)2 and somatic mtDNA major arc deletions accumulation in the fibroblasts [54-56]. It was also noted that the neopterin levels in the cerebrospinal fluid (CSF) could serve as a potential biomarker and may be useful in understanding the pathophysiology of patients.

5.2.3. Current Therapeutics

Ongoing studies pertaining to this mutational event effectively warrant crucial studies owing to possible therapeutics. While the LRRK2 G2019S mutation has been identified as the most common sporadic and familial case of genetically linked PD patients, limited interventions are commercially available to mitigate this challenge. The currently designed therapeutics exploit the means of inhibiting the hyperactivity of the kinase activity through the LRRK2 inhibitors. Lubben *et al.* (2024) elucidated the role of one such LRRK2 inhibitor, known as the MLI-2 [57]. This therapeutic, developed by Merck, portrayed significant efficacy in reducing the detrimental effects of the hyperactivity of kinase, thereby promoting decreased neurotoxicity and enhanced neuronal survival. The study further exhibited the dose-dependent reduction in LRRK2 phosphorylation and tau pathology, which are the hallmarks of PD [57]. Additional therapeutics are listed in Table 5.2, portraying their role in the treatment of the LRRK2 G2019S mutation.

Table 5.2. Portraying the current research advancements in the therapeutic against the LRRK2 G2019S mutation.

Therapy	Description	Current Status	Ref
DNL201	Small-molecule inhibitor of LRRK2 kinase activity, showing promise in preclinical studies and early-phase clinical trials.	Completed Phase I trials	[13]
DNL151 (BIIB122)	A LRRK2 inhibitor from Denali Therapeutics and Biogen, advancing through Phase III clinical trials.	Phase III clinical trials	[13]
PFE-360	Potent and selective LRRK2 kinase inhibitor developed by Pfizer, showing efficacy in preclinical models.	Clinical evaluation	[62]
GNE-7915	LRRK2 kinase inhibitor developed by Genentech, demonstrating effectiveness in preclinical studies.	Ongoing clinical trials	[63]
NLY01	GLP-1 receptor agonist developed by Neuraly, not a direct LRRK2 inhibitor but showing neuroprotective effects.	Clinical trials	[62]
LRRK2-ASO	Antisense oligonucleotides targeting LRRK2 mRNA to reduce mutant LRRK2 protein production.	Early clinical trials	[64]
Gene Therapy	RNA interference (RNAi) and CRISPR-based gene editing approaches to correct or silence the mutant LRRK2 gene.	Early stages of research	[63]

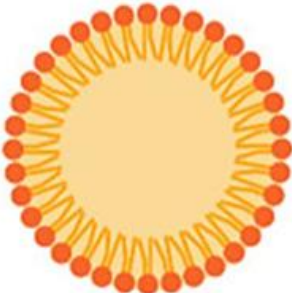
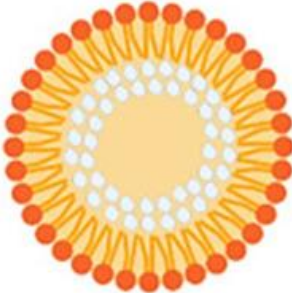
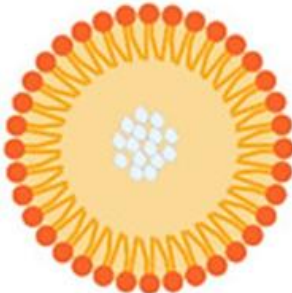
While the developed therapeutics hold promise, they are often met with challenges that hinder their widespread application. Clinical efficacy has been noted to fluctuate among patients, complicating the decision to permit its use as a “one-size-fits-all” treatment, due to the heterogeneity in PD. Furthermore, the varied results showed minimal improvements in some patients, suggesting a more personalized treatment approach [16,58]. Effective biomarkers for response data and disease progression are limited, with urinary LRRK2 phosphorylation and serum urate levels being suggested as these biomarkers [59]. In addition to these, the BBBs’ involvement in the reduction of treatment efficacy further restricts the inhibitors [60,61]. Hence, there is a need for urgent and holistic therapeutic developments that are novel to effectively traverse the BBB and target the LRRK2 G2019S to deliver optimum dosages of pharmacologically active agents, such as genes.

5.3. Solid Lipid Nanoparticles (SLNPs)

The primary aim of nanomedicine relates to their accurate and efficient means of diagnosing and treating diseases while minimizing the adverse effects caused by traditional medicine. Lipid nanocarriers have been noted to portray considerable advantages resulting from their biodegradability, scale-up capacity, low toxicity, biocompatibility, and delivery of lipophilic and hydrophilic drugs in a targeted or controlled manner [65,66]. Lipid NPs such as solid lipid nanoparticles (SLNPs) and nanostructured lipid carriers (NLCs) possess unique biological characteristics. However, they differ greatly with respect to their core components. SLNPs present with a solid core, encapsulating the drug or gene of choice, while the NLCs present with both a solid and liquid lipidic core [67]. For the interest of the present research, SLNPs will be focussed upon.

These SLNPs are composed of a solid physiological lipid (at room or body temperature), as well as a surfactant and water [68]. The unique lipid-based biocompatible systems are found to be in the size range of 10-1000 nm in diameter and thus possess pivotal characteristics pertaining to their relative ease of cellular infiltration [69]. These NPs are produced from di- or triglycerides, steroids, glyceride mixtures, or waxes, with a surfactant concentration of 0,5 to 5% (w/v) [70]. The structure of the SLNPs is dependent on the solubility of the compounds, the component makeup, and the synthesis approach [71]. Three types of SLNP structures are noted, that are derived through different production techniques (Table 5.3).

Table 5.3. The three structures of the SLNPs and their synthesis methods (Adapted from [72]).

Structure of SLNPs		
Type I: SLNPs Homogenous Matrix Model	Type II: SLNP Drug-enriched Shell Model	Type III: SLNP Drug-enriched Core model
Pharmacologically active agent dissolved in lipidic matrix, via high-pressure hot or cold homogenization. Type I SLNPs are derived through mechanical breakage.	Nanoparticle productions are due to a hot homogenisation procedure. During the cooling, precipitation of the lipid molecules is observed, creating a lipid core. Externally, an increase in the drug concentration is noted in the melted lipid until solubility is reached. Resultingly, the drug-lipid crystallization produces the outer shell.	These SLNPs are produced when the concentration of the drug is close to the solubility in the melted lipid, resulting in the drug encapsulation occurring at the inner core, as compared to the outer shell. The outer shell is composed of low concentrations of the drug in the lipid.
		

These SLNPs are derived and created through various means, taking into account their strongly hydrophobic nature. Due to this characteristic, they hydrate very weakly, if at all, and are thus unable to spontaneously be dissolved or dispersed in water [73]. Synthesis approaches are therefore directed at a transfer of energy into the system, which in turn generates NPs with a high specific surface area [74]. This energy transfer is created via mechanical means, creating a synthesis method with a physical breakdown in particle size using an efficient and required “energy-providing” step [75]. These are conducted via an ultrasonic bath, high-speed homogenization, microwaves, or high pressures, with hot and high-pressure homogenization being the most commonly applied method [76-79].

In addition to the energy transfer, technological strategies pertaining to the maintenance of the large, exposed surface area of the dispersed NPs are imperative. Due to the SLNPs constituting a lyophobic dispersion, they are intrinsically unstable [73]. Stability is increased by aggregation into large crystals or droplets, thereby minimizing the specific surface area and the interfacial

free energy [80]. In order to prevent this phenomenon of coalescence, the particles are required to be sterically or electrostatically stabilized [81]. The charge of the NPs can be characterized by means of measuring the zeta potential (ζ), with this charge being directly associated with the charge exhibited by the lipid at the formulated pH [82]. The ideal stabilization is elucidated to be ± 30 mV or higher, thereby effectively assuring substantial repulsion of neighbouring NPs in suspension [83].

SLNPs have proved to be advantageous compared to their polymeric counterparts. At the onset, LNPs are found to be more cost-effective with regard to synthesis and thus can be scaled up for a wider array of uses [73]. Furthermore, their synthesis requirements avoid potentially harmful organic solvents, rendering them less toxic for medical employment [84]. They portray high evasive properties in escaping the reticuloendothelial system (RES), thereby bypassing the liver and spleen and preventing filtration [85]. SLNPs additionally have a high encapsulation rate, encapsulating both lipophilic and hydrophilic while maintaining or adding to their stability [85]. They further provide a means for a more targeted and controlled release of drugs/genes, with this being enhanced upon the conjugation of an appropriate ligand [86]. Furthermore, the type of lipid is fundamental in choosing an appropriate vector for treating a vast array of diseases which is dependent on the disease being treated.

5.3.1. Sphingomyelin

Sphingomyelin (SM), forming part of sphingolipids (Sphs), are known as bioactive signaling molecules that are imperative in the regulation of cell fate decisions [87] (Figure 5.3). SM, specifically, vaunts the ability to support brain myelination, which regulates chromatin function and forms ordered domains where nicotinic acetylcholine receptors are located and are closely related to neuronal cell function [88]. Due to this, SM is essential in the development of the brain and cognitive functions. Therefore, alterations in the metabolism of SM consequentially result in neurodegeneration [87].

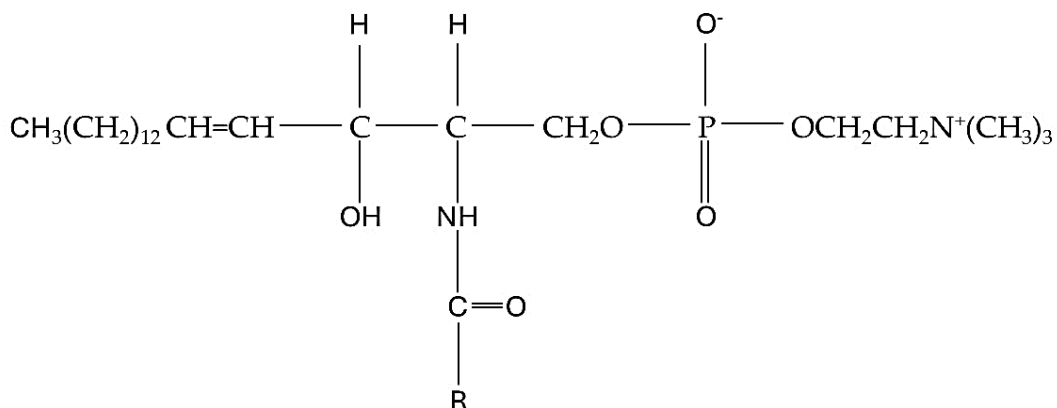


Figure 5.3. Structure of sphingomyelin.

SM, in its hydroxy and long-chain conformations, is an essential component of the membranous myelin sheath [89]. These sheaths are composed of a highly specialized structure of multiple layers, including glycerophospholipids, cholesterol, and Sphs, which surround the axons in the peripheral and central nervous system [90]. The lipids involved are essential in the biophysical properties attributed to the myelin sheaths required for myelin compaction and membrane curvature, with a derangement of such owing to the development of neurodegeneration [91]. More specifically, hydroxy-SMs have been proposed to play a pivotal role in the long-term stability of the myelin sheaths, where is decline in the number of SMs results in late-onset demyelination and neurodegeneration [92]. Furthermore, a decrease in dietary essential lipids for SM synthesis promotes demyelination as well, together with slowing down the remyelination in pathological processes [93].

Sphs also perform fundamental roles in the brain cells, acting synergistically with lysophospholipids and endocannabinoids. These lipids act as bio-signal molecules by assisting the process of neurogenesis, neuronal selection, neuronal plasticity, and impulse conduction [94]. SM, in this regard, interacts with cholesterol, forming lipid rafts that regulate cellular functions such as neuronal-glia connections, synaptic transmission, and neuronal differentiation [95]. The dysregulation of these SM molecules in the brain cells is an important effector of brain damage [87] and underlies several CNS-related diseases via their involvement in the inflammatory processes. This process was observed by Tabatadze *et al.* (2010), who noted compromised plasticity in nSMase-deficient mice [96].

Based on the natural properties of SM molecules in the brain and their ability to maintain and regulate neuronal activity, SLNPs can be created to function as a vector while

exhibiting beneficial properties. These NPs would, theoretically, be able to cross the BBB, owing to their size and structural make-up. While studies pertaining to Parkinson's disease are limited, SM-SLNPs and their potential should not be ignored. These systems have been previously utilized against colorectal cancer, showing efficiency in delivering and promoting a gene replacement therapy using an oncosuppressor micro-RNA (miRNA). Strong anticancer activity with regard to colony formation, tumour proliferation, and migration capacity assays was observed [97].

5.3.2. Cholesterol

Naturally, cholesterol and phospholipids, with low gel-liquid crystalline phase transitions (T_m), facilitate a means of forming the liquid-ordered phases, characterized by a decreased membrane fluidity and increased thickness of the bilayer [98]. Alternatively, when cholesterol interacts with high T_m lipids, a boost in membrane fluidity is noted, with a narrowing of the bi-layer. Similarly, to both, cholesterol acts to pull the lipids towards a liquid-ordered phase [99].

The properties exhibited may be exploited in their use in synthesizing SLNPs (Figure 5.4). This incorporation is generally undertaken at an equimolar amount of cholesterol to the lipids, thereby preventing net efflux/influx and effectively maintaining the integrity of the membrane [98]. Furthermore, cholesterol portrays added benefits in the encapsulation of nucleic acids at a less toxic rate with greater potency, performing as a helper lipid [100]. This is due to the increase in membrane rigidity, which reduces leakage upon delivery. A study conducted by Kulkarni *et al.* (2019) showed a concentration of 40 mol% of cholesterol, vaunting a near-complete encapsulation of siRNA [101].

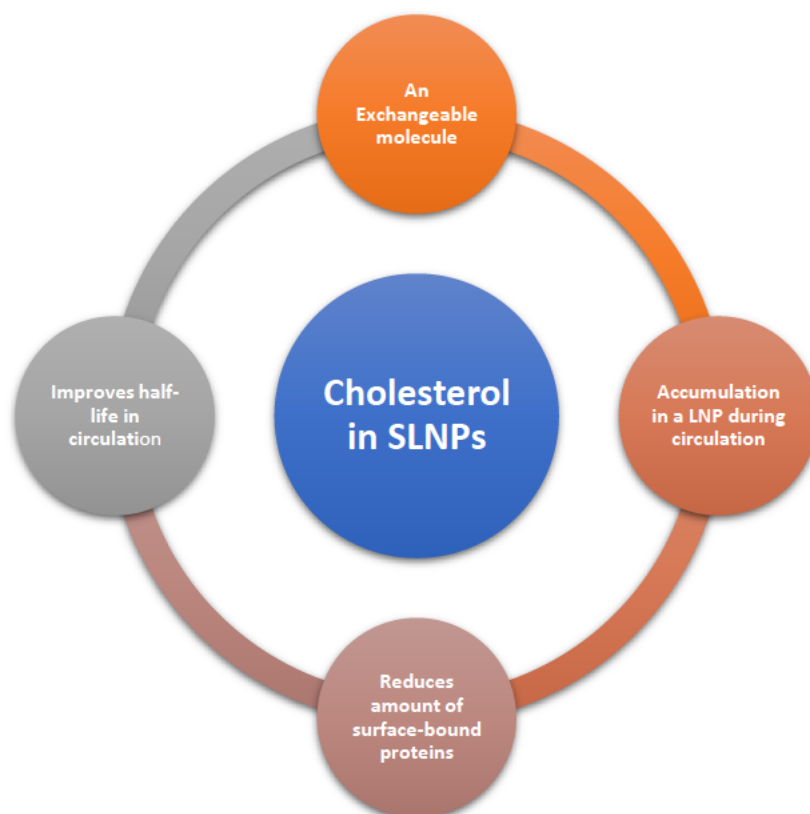


Figure 5.4. Advantages of the incorporation of Cholesterols in SLNPs (Adapted from [100]).

5.3.3. Synergism of Sphingomyelin-Cholesterol Solid Lipid Nanoparticles (SC-SLNPs)

SM and cholesterol play crucial roles in maintaining brain health and are highly relevant to PD treatment. SM contributes to the rapid transmission of nerve impulses, which is vital for proper neurological function and repairing myelin sheaths, which can be damaged in neurodegenerative diseases like PD [88]. Cholesterol forms lipid rafts that facilitate cell signaling, synaptic function, and neurotransmitter release. These rafts organize signaling molecules involved in protein sorting, membrane trafficking, and signal transduction, which are critical for maintaining cognitive functions and neuronal communication [90,95].

5.3.3.1. Synthesis and Characterization Approaches

Individually, the components of potentially synthesized SC-SLNPs possess significant capabilities *in vivo*. Exploration into their synthesis and characterization is imperative to formulate and employ these SC-SLNPs as therapeutic agents. The synthesis of SLNPs typically follows techniques such as high-pressure homogenization and ultrasonication [74] (Figure 5.5).

High-pressure homogenization involves the preparation of liquid and aqueous phases. The liquid phase is prepared by heating the components of the SLNPs above their melting points to form a homogeneous mixture. Simultaneously, the aqueous phase is prepared by dissolving surfactants in water to stabilize the NPs and prevent aggregation. The liquid phase is then emulsified into the aqueous phase using high-pressure homogenization (500-1500 bar), reducing the particle size to the nanoscale. Rapid cooling to room temperature follows, locking the pharmacologically active agents within the solid lipid matrix [74,75].

Ultrasonication, an alternative method, follows a similar approach in preparing separate liquid and aqueous phases but uses a probe sonicator. Ultrasonic waves create cavitation forces that reduce liquid droplets into NPs. Rapid cooling encapsulates the therapeutic agents, ensuring their stability and effectiveness [76,77].

Characterization of synthesized SLNPs confirms their size, stability, and morphology. Dynamic light scattering (DLS) measures particle size and distribution, providing the hydrodynamic size and polydispersity index (PDI). Zeta potential measurements determine the stability of SLNPs, with a charge of ± 30 mV indicating good stability due to electrostatic repulsion between particles [102]. Transmission electron microscopy (TEM) visualizes the morphology, confirming the uniformity and shape of the NPs [78].

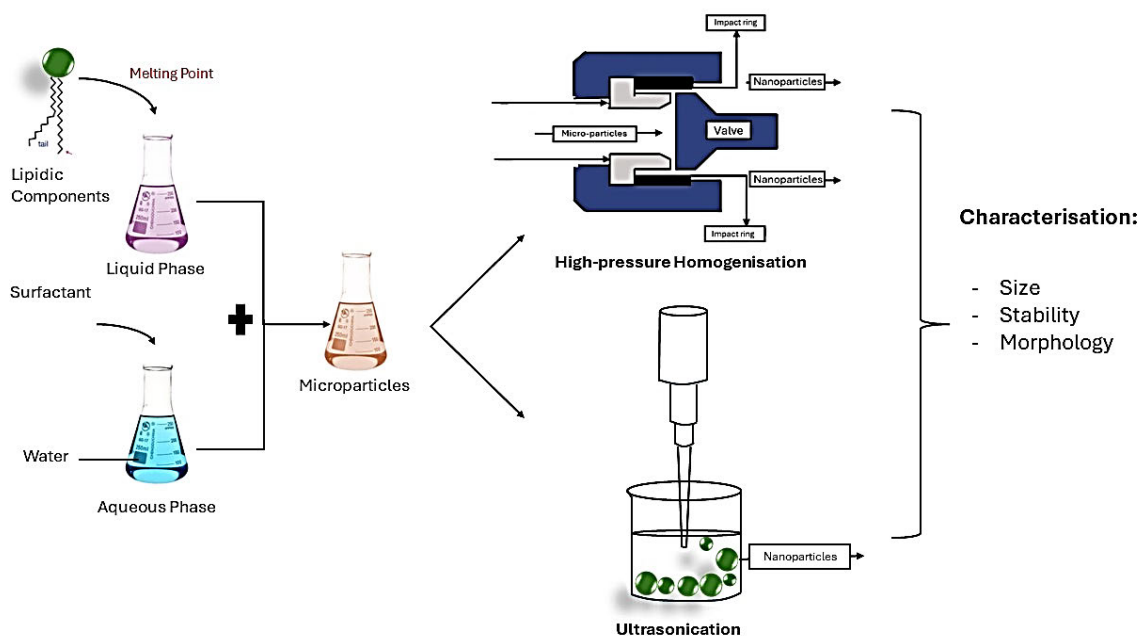


Figure 5.5. Scheme illustrating the synthesis and characterization approach for SLNPs.

5.3.3.2. SC-SLNPs Synergism Offering Enhanced Properties

Due to their unique composition and functional properties, SC-SLNPs offer several advantages over other SLNPs. SM, a natural component of cellular membranes, enhances the formation of stable bilayers, providing mechanical strength and protection against enzymatic degradation. Cholesterol intercalates within these bilayers, reducing membrane fluidity and permeability, thus improving stability and biocompatibility, which is crucial for effective gene delivery [87,88]. Unlike the synthesis of polymeric and metallic NPs, the SLNPs' solvent-free processes reduce the risk of residual solvent toxicity, providing a safer nano-vector for medical applications [84,85].

5.3.3.3. Overcoming the Blood-Brain Barrier: SC-SLNPs for Neuroprotection and Gene silencing in PD

In the search for efficient therapeutics against neurodegenerative disorders such as PD, crossing the BBB is a significant challenge. SC-SLNPs can evade this barrier due to their nano-size and lipid composition, exploiting receptor-mediated and adsorptive-mediated transcytosis processes. Receptor-mediated transcytosis involves binding to specific receptors on the endothelial cells of the BBB, facilitating internalization and active transport into the brain. The surface charge of SC-SLNPs also promotes adsorptive-mediated transcytosis, where NPs adhere to endothelial cells and infiltrate the BBB through vesicular transport mechanisms [10,86,97].

Furthermore, SC-SLNPs mimic natural cell membrane components, enhancing their uptake and integration into cellular structures. SM supports and repairs myelin sheaths, aiding in the treatment of neurodegenerative disorders like PD. Cholesterol enhances cell signaling and synaptic function by organizing signaling molecules involved in protein sorting, membrane trafficking, and signal transduction [90,95]. These properties enable SC-SLNPs to deliver therapeutic agents across the BBB and into targeted cells, promoting neuroprotection and gene silencing [97].

SC-SLNPs can deliver siRNA or other therapeutic agents that target and silence genes implicated in disease progression, such as the LRRK2 G2019S mutation in PD. Through the reduction of oxidative stress and enhancement of mitochondrial function, SC-SLNPs can protect neurons from damage and promote overall cellular health. Cholesterol which stabilizes

lipid rafts, supports cognitive processes and memory, thereby mitigating cognitive decline associated with PD [27,34,95].

The reduction of oxidative stress is due to the encapsulation of antioxidant compounds which neutralize the reactive oxygen species (ROS). Furthermore, as a result of the aforementioned benefits in gene delivery, the enhanced uptake of the siRNA effectively targets the genes involved in the oxidative stress pathways, further decreasing ROS production. The enhancement of the expression of endogenous antioxidant enzymes, such as glutathione peroxidase (GPx) and superoxide dismutase (SOD), detoxifies ROS, owing to added protection to the cells from oxidative damage [34].

Additionally, mitochondrial health is improved through the stabilization of the mitochondrial membranes with cholesterol, thus maintaining their integrity and fluidity. This is important for proper ATP production and enzyme function. Furthermore, encapsulation of compounds such as coenzyme Q10 (CoQ10) provides additional protection to the mitochondria. A dual effect is noted in this way due to the enhancement of mitochondrial health and the reduction in ROS production via the infiltration of the siRNA [27]. Promoting mitophagy by delivering agents that enhance this process removes dysfunctional mitochondria, maintaining a healthy mitochondrial population and reducing ROS accumulation [97].

5.4. Applicability in RNA Interference (RNAi)

Gene therapy has historically produced excellent results, with it being a highly beneficial tool in treating diseases in a targeted manner. This enables a more personalized approach to treat life-threatening diseases in a sequence-specific manner. The approach works on the basis of a nucleic acid modality being introduced to a patient, permitting the downregulation, augmentation, or correction of specific disease-causing gene expressions [104]. These form part of an umbrella term known as RNA interference (RNAi) modalities which have been studied through their natural defense mechanisms against the invasion of exogenous genes [105]. These interference modalities perform on the basis of either the knockdown of targeted gene expression via the mediation of targeted mRNA degradation or mRNA translation repression, with small interfering RNA (siRNA) forming part of the former and triggering gene silencing [104].

These siRNA molecules portray advantageous properties in this regard, which are known as representative molecules due to their ability to trigger gene inhibition in a more efficient and

specific manner [106]. These molecules have been faced with obstacles pertaining to specificity, stabilization, and delivery, which have been effectively overcome through the chemical modification and delivery systems employed. Early studies conducted following the chemically synthesized siRNA by Elbashir *et al.* (2001) formed the foundation for the emergence of an upsurge in development. This study successfully portrayed the siRNA's ability to specifically suppress the expression of heterologous and endogenous genes in human embryonic and cervical cancer cells [107].

The specificity of the siRNA is attributed to their fundamental ability of complete Watson-Crick base pairing with the selected mRNA, while small molecule and monoclonal antibody drugs function through the recognition of the complicated spatial conformations of the proteins [104]. Theoretically, siRNA possesses the capability to target any gene of interest, thus rendering a wider therapeutic area. However, practically, siRNA requires various modifications to reduce the disadvantages posed (Figure 5.6). These are avoided through chemical modifications with respect to the desired functional outcomes, including activity, specificity, stabilization, and biosafety (Table 5.4). Furthermore, effective delivery systems are imperative for successful gene silencing such as lipidoids or lipid-like materials.

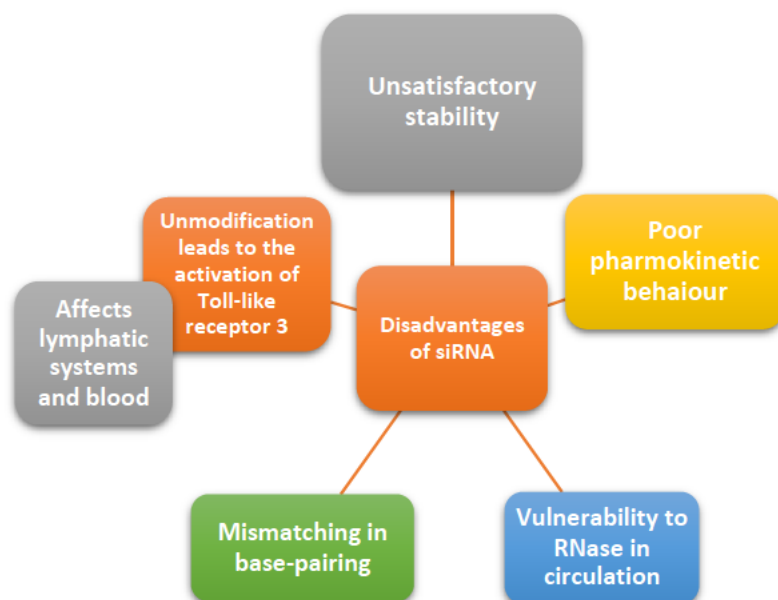


Figure 5.6. Disadvantages of unmodified and unconjugated naked siRNA molecules in circulation (Adapted from [104]).

Table 5.4. Portraying the chemical modification and their relevant benefits.

CHEMICAL MODIFICATION	MECHANISM OF ACTION	REF.
Phosphonate	Linkage of phosphorothioate (PS) moiety achieved via the leveraging of a sulfur atom in replacing a nonbridging oxygen of a phosphodiester. The modification provides greater resistance to nucleases, thereby increasing their circulation time. An increase in hydrophobicity and stability is noted. Increased accumulation in kidneys, liver, intestines, adipocytes, bone marrow, and lymph nodes.	[108-110]
Ribose	Introduction of a ribose moiety to the 2' position for the effective protection of the ribonucleases from the siRNA. 2'-O-Methyl portrays benefits in blocking the nucleophilic 2'-OH group, thereby increasing stability.	[111]
Base Modification	Increase in specificity through the substitution of N6-methyladenosine, pseudouridine, 5-methylcytidine, thiouridine, and other base analogs of cytidine and uridine residues. Reduction in innate immune recognition is noted.	[112,113]

5.4.1. siRNA for targeting the LRRK2 G2019S Mutation

The properties of siRNA in gene knockdown studies can be manipulated and employed in treating various diseases due to their ability to inactivate undesirable/pathogenic protein formations and inhibit synthesis from mutated codons. This mechanism is achieved through the incorporation of the siRNA into the RNA-induced silencing complex (RISC). Upon this incorporation, the siRNA strand promotes the cleavage and degradation of the complementary mRNA sequences by guiding the RISC [107]. In this manner, siRNA provides a beneficial outcome in stabilizing the overexpression of the LRRK2 G2019S gene and restoring those levels to a normalized protein level. This phenomenon occurs via siRNA's targeting ability to specifically bind to the mutation and effectively silence the expression of the aberrant LRRK2 protein. This results in the reduction of the pathogenic effects, such as increased kinase activity and neuronal toxicity, thereby offering a potential therapeutic strategy for mitigating disease progression [104, 105,109]. This approach is advantageous as it permits the specific inhibition of disease-causing genes while having no effect on the overall genetic expression profile, thereby minimizing off-target effects [110].

Several studies have examined the effect of siRNA on the LRRK2 mutation, with a particular focus on the G2019S variant. A study dating back to 2009 by Alegre-Abarrategui *et al.* demonstrated the successful application of siRNA on the LRRK2 variant, showing that the knockdown approach increased autophagic activity while effectively preventing cellular demise [114]. Furthermore, a study conducted by Lee *et al.* (2019) investigated the effect of the LRRK2 G2019S mutation on endoplasmic reticulum (ER) stress. It was observed that the LRRK2 G2019S mutation localizes in the ER membrane, interacting with the sarco/endoplasmic reticulum Ca^{2+} -ATPase (SERCA) and effectively suppressing its activity [115]. This results in Ca^{2+} depletion in the ER and an increase in mitochondrial Ca^{2+} , thereby leading to dysfunction. The introduction of siRNA markedly reduced cell death associated with ER stress via co-transfection of the nucleic acid into HEK293T cells using the 5'-GACAUCAGGCAGUCUCGAU-3' and 5'-UCAGACAUCCUCGUCACUA-3' oligonucleotide sequences [115].

5.4.2. Optimizing siRNA Delivery

Prior to therapeutic studies, approaches to efficient cellular internalization are crucial, including the development of appropriate siRNA delivery systems. This is due to the high molecular weight, susceptibility to degradation by nucleases, and the polyanionic nature of siRNA (Hu *et al.*, 2020). Consequently, siRNA fails to cross cellular membranes and reach target sites while also facing rapid clearance from the bloodstream and potential immunogenicity [106]. This challenge was highlighted in a study by Acharya *et al.* (2019), which demonstrated a 51.55% internalization into neuroblastoma cells due to siRNA conjugation with layered double hydroxides (LDH), compared to the lack of internalization of naked siRNA [116].

Such studies support the potential for various additional investigations to optimize the delivery systems and efficiency of siRNA. A study by Lobovkina *et al.* (2011) showcased the benefits of using SLNPs due to their ability to provide controlled release of siRNA over a 10–13-day period, along with good biocompatibility and minimal toxicity [117]. Historical uses of LNPs with siRNA provide the basis for potential therapeutic applications of siRNA for the LRRK2 G2019S mutation in PD, allowing for effective treatment at cellular and genetic levels.

LNPs have proven effective in the safe and efficient delivery of siRNA to targeted genes, with the proposed SC-SLNPs offering additional capabilities, especially in PD studies. These NPs

possess the ability to fuse with cellular membranes due to their natural lipid composition, facilitating their ability to cross the BBB and ensuring efficient intracellular delivery of siRNA. Moreover, these SLNPs can be engineered with surface modifications to enhance targeting specificity and cellular uptake [79]. By addressing intrinsic delivery challenges, SC-SLNPs provide a viable platform for treating neurodegenerative disorders, including PD, leading to significant advancements in therapeutic strategies [85].

Table 5.5. Positive outcomes of various LNP formulations on disorders presented.

Targeted Disorder	Targeted gene	LNP Type	Outcomes	Ref.
Acute Myeloid Leukaemia (AML)	LINC01257	Cationic/stealth Phospholipid LNPs	Safe delivery, robust gene silencing, reduction in AML cell proliferation, and no cytotoxicity in healthy blood cells.	[118]
Chronic Myeloid Leukaemia (CML)	BCR-ABL Oncogene	DLin-MC3-DMA-LNPs	100% uptake in bone marrow cells.	[119]
Breast Cancer	IGF-1R	mPEG-PCL-DDAB-LNPs	Combined therapeutic with NPs showed a reduction in the IGF-1R expression and increased apoptosis in MCF-7 cells.	[120]
Non-alcoholic steatohepatitis (NASH)	High Mobility Group Box 1 (HMGB1)	DSPC, DLINMC3-DMA, DSPE-PEG-Man, PEG-DMG and Cholesterol LNPs	The HMGB1 gene was silenced with a reduced protein accumulation in the liver. Normal levels were noted after treatment with docosahexaenoic acid over 8 weeks.	[121]
Hepatitis B	ApoB	RBP131-LNPs (LC8 cholesterol and DPPE-mPEG2000)	siRNA encapsulation by the LNPs was established to be >80% at a median effective dose of ~0.05 mg/kg.	[122]
Lung Cancer	KRAS	Cationic LNPs	Effective silencing of the KRAS gene caused reduced tumor growth and increased apoptosis in lung cancer cells.	[123]
Prostate Cancer	Bcl-2	Poly (lactic-co-glycolic acid) NPs	siRNA-loaded NPs resulted in downregulation of Bcl-2 expression and enhanced apoptosis in prostate cancer cells	[124]
Glioblastoma	EGFR	Cholesterol-conjugated siRNA NPs	Targeted delivery of siRNA to glioblastoma cells, reducing EGFR expression	[125]

			and inhibiting tumor growth.	
Liver Fibrosis	TGF- β 1	Cationic Liposome NPs	siRNA targeting TGF- β 1 effectively reduced fibrosis markers and improved liver function in animal models	[126]
Ovarian Cancer	VEGF	PEGylated Lipid NPs	siRNA against VEGF showed reduced angiogenesis and tumor growth in ovarian cancer models	[127]
Parkinson's Disease (PD)	α -Synuclein	Cationic Lipids NPs	Silencing of α -synuclein, leading to reduced protein aggregation and neuroprotection in PD models	[128]
Alzheimer's Disease (AD)	BACE1	Dendrimer-Based NPs	Reduced amyloid-beta production and plaque formation, improving cognitive function in AD models	[129]
Huntington's Disease (HD)	HTT	Polymer-based NPs	Silencing of mutant HTT gene, leading to reduced huntingtin protein aggregates and neuroprotection in HD models	[130]

5.5. Conclusion

Parkinson's disease (PD), particularly cases linked to the LRRK2 G2019S mutation, presents significant therapeutic challenges due to its complex genetic underpinnings and the difficulty of delivering effective treatments across the BBB. Existing therapies, such as LRRK2 inhibitors, provide some benefits but often fall short in targeting the root genetic cause and are accompanied by adverse side effects. The exploration of SC-SLNPs as a delivery system for therapeutic siRNA offers a highly promising solution to overcome these limitations. They possess advantages, including biocompatibility, stability, high drug-loading capacity, and the ability to cross the BBB, addressing one of the major hurdles in treating neurodegenerative disorders. Additionally, the synergistic properties of SM and cholesterol support neuronal health, stabilize cell membranes and aid in repairing myelin sheaths, mitigating the progression of PD. By silencing the LRRK2 G2019S mutation, siRNA-loaded SC-SLNPs target the hyperactive kinase activity responsible for oxidative stress, mitochondrial dysfunction, and neuronal apoptosis, ultimately reducing neurodegeneration. This novel approach holds great

potential in providing a more targeted and effective treatment strategy with reduced side effects compared to traditional therapies. The ability of SC-SLNPs to deliver siRNA efficiently into the brain marks a significant advancement in nanomedicine for PD and opens doors to broader applications in other neurodegenerative diseases.

5.6. Future Recommendations

To fully realize the therapeutic potential of SC-SLNPs, future research should focus on several key areas. First, the optimization of SC-SLNP formulations should be pursued, ensuring maximum stability, enhanced siRNA encapsulation efficiency, and precise targeting capabilities. Further studies are needed to refine the synthesis methods, improve surface modifications, and explore alternative ligands that could increase the specificity of SC-SLNPs for diseased neurons. Preclinical studies must be expanded, utilizing advanced *in vivo* models of PD to assess the long-term efficacy, safety, and biodistribution of SC-SLNPs. It will be critical to demonstrate that these NPs can consistently cross the BBB and deliver therapeutic siRNA to the affected regions of the brain. Monitoring their impact on neuronal recovery, motor function, and overall disease progression will help validate their clinical potential. Early-phase clinical trials can be initiated to evaluate the pharmacokinetics, pharmacodynamics, and safety of SC-SLNPs in human patients. This will involve addressing potential immunogenic responses, determining optimal dosing regimens, and assessing any off-target effects. Scaling up production while maintaining the quality and consistency of the NPs will also be essential for transitioning to clinical application.

Finally, the versatility of SC-SLNPs warrants further exploration in other neurodegenerative disorders beyond PD. Given their ability to protect neurons, stabilize synaptic function, and deliver genetic therapies, SC-SLNPs could be adapted for treating diseases such as Alzheimer's, Huntington's, or amyotrophic lateral sclerosis (ALS), where similar pathological mechanisms are involved. Continued research and development will be crucial in unlocking their full potential as a transformative treatment for PD.

References

1. Bandres-Ciga, S.; Saez-Atienzar, S.; Bonet-Ponce, L.; Billingsley, K.J.; Vitale, D.; Blauwendraat, C.; *et al.* The genetic architecture of Parkinson disease. *BMC Medicine.*, **2020**, *18*, 66. DOI: 10.1186/s12916-020-01518-4
2. Lee, P.H.; Yeo, S.H.; Kim, J.S.; Hyun, Y.S.; Lee, S.H.; Kim, Y.I.; *et al.* LRRK2 G2019S mutation is associated with earlier disease onset in Parkinson's disease. *BMC Neurology.*, **2012**, *12*, 47. DOI: 10.1186/1471-2377-12-47
3. Jeong GR; Lee BD. Pathological functions and therapeutic potential of LRRK2 in Parkinson's disease. *BMB Reports.*, **2020**, *53*, 479-489. DOI: 10.5483/BMBRep.2020.53.9.17
4. Hu, Y.; Deng, H.; Xu, S.; Zhou, Y.; Nie, H.; Liang, D. LRRK2 inhibition for Parkinson's disease treatment: current progress and perspectives. *BMC Medicine.*, **2023**, *21*, 78. DOI: 10.1186/s12916-023-02745-7
5. Biosa, A.; Mandillo, S.; Spiezia, M.; Dionisi, M.; Murru, L.; Schiavi, S.; *et al.* Mutant LRRK2 A53T mice develop early parkinsonian phenotypes with compromised autophagic and proteasomal function. *Neurobiology of Aging.*, **2013**, *34*, 2108-2122. DOI: 10.1016/j.neurobiolaging.2013.01.015
6. Hindle, S.; Afsari, F.; Stark, M.; Middleton, C.A.; Evans, G.J.; Sweeney, S.T.; *et al.* Dopaminergic expression of the Parkinsonian gene LRRK2-G2019S leads to a depletion of vesicular dopamine and motor impairment in *Drosophila*. *PLoS One.* **2013**;8(9). DOI: 10.1371/journal.pone.0075901
7. Liu, Z.; Lee, J.; Krummey, S.; Lu, W.; Cai, H.. *Drosophila* models for LRRK2-associated Parkinson disease. *Physiological Genomics.*, **2011**, *43*, 598-606. DOI: 10.1152/physiolgenomics.00030.201
8. Preetam, M.; Patel, N.; Pandey, S.; Sarkar, P.; Roy, S.; Saha, S.; *et al.* Nanotechnology in neurodegenerative disorders: advances opportunities and challenges. *ACS Chemical Neuroscience.*, **2023**, *14*, 385-406. DOI: 10.1021/acchemneuro.2c00766
9. Hangargekar, P.; Pathak, R.; Maheshwari, R.; Tekade, R.K. Solid lipid nanoparticles: advancements and challenges for brain targeting in the management of neurodegenerative disorders. *Advanced Pharmaceutical Bulletin.*, **2019**, *9*, 364-379. DOI: 10.15171/apb.2019.043
10. Kim, H.J.; Choi, H.S.; Chang, M.J. Sphingomyelin synthase 1 (SMS1) is an upstream regulator of PTEN for sphingomyelin-enriched membrane domain formation. *Journal of Lipid Research.*, **2020**, *61*, 393-403. DOI: 10.1194/jlr.M093294
11. Ariga, T. Role of sphingolipids in the nervous system. *Neurochemical Research.*, **2017**, *42*, 251-261. DOI: 10.1007/s11064-016-2097-4
12. Daniels, M.; Singh, N. Gene therapy for Parkinson's disease: recent advances and future prospects. *Journal of Neurology.*, **2019**, *266*, 481-493. DOI: 10.1007/s00415-018-8972-1

13. Jennings, D.; Huntwork-Rodriguez, S.; Henry, A.G.; Sasaki, J.C.; Meisner, R.; Diaz, D.; *et al.* Preclinical and clinical evaluation of the LRRK2 inhibitor DNL201 for Parkinson's disease. *Sci Transl Med.*, **2022**, 14. DOI: 10.1126/scitranslmed.abj265
14. Sheng, Z.; Zhang, S.; Bustos, D.; Kleinheinz, T.; Le Pichon, C.E.; Dominguez, S.L.; *et al.* Ser1292 autophosphorylation is an indicator of LRRK2 kinase activity and contributes to the cellular effects of PD mutations. *Sci Transl Med.*, **2012**, 4, 164ra161. DOI: 10.1126/scitranslmed.3004485
15. Lee, B.D.; Shin, J.H.; VanKampen, J.; Petrucelli, L.; West, A.B.; Ko, H.S.; *et al.* Inhibitors of leucine-rich repeat kinase-2 protect against models of Parkinson's disease. *Nat Med.*, **2010**, 16, 998-1000. DOI: 10.1038/nm.2199
16. West, A.B.; Moore, D.J.; Choi, C.; Andrabi, S.A.; Li, X.; Dikeman, D.; *et al.* Parkinson's disease-associated mutations in LRRK2 link enhanced GTP-binding and kinase activities to neuronal toxicity. *Hum Mol Genet.*, **2007**, 16, 223-232. DOI: 10.1093/hmg/ddl471
17. Chen, M.; Wu, R. LRRK2 gene mutations in the pathophysiology of the ROCO domain and therapeutic targets for Parkinson's disease: a review. *J Biomed Sci.*, **2018**, 25, 52. DOI: 10.1186/s12929-018-0454-0
18. Guaitoli, G.; Raimondi, F.; Gilsbach, B.K.; Gomez-Llorente, Y.; Deyaert, E.; Renzi, F.; *et al.* Structural model of the dimeric Parkinson's protein LRRK2 reveals a compact architecture involving distant interdomain contacts. *Proc Natl Acad Sci USA.*, **2016**, 113, 4357-4366. DOI: 10.1073/pnas.1523708113
19. Deyaert, E.; Wauters, L.; Guaitoli, G.; Konijnenberg, A.; Leemans, M.; Terheyden, S.; *et al.* A homologue of the Parkinson's disease-associated protein LRRK2 undergoes a monomer-dimer transition during GTP turnover. *Nat Commun.*, **2017**, 8, 1008. DOI: 10.1038/s41467-017-01103-
20. Webber, P.J.; Smith, A.D.; Sen, S.; Renfrow, M.B.; Mobley, J.A.; West, A.B. Autophosphorylation in the leucine-rich repeat kinase 2 (LRRK2) GTPase domain modifies kinase and GTP-binding activities. *J Mol Biol.*, **2011**, 412, 4-110. DOI: 10.1016/j.jmb.2011.07.033
21. Dusonchet, J.; Li, H.; Guillily, M.; Liu, M.; Stafa, K.; Derada, T.; *et al.* A Parkinson's disease gene regulatory network identifies the signaling protein RGS2 as a modulator of LRRK2 activity and neuronal toxicity. *Hum Mol Genet.*, **2014**, 23, 4887-4905. DOI: 10.1093/hmg/ddu202
22. Milosevic, J.; Schwarz, S.C.; Krohn, K.; Poppe, M.; Storch, A.; Schwarz, J. Low atmospheric oxygen avoids maturation; senescence and cell death of murine mesencephalic neural precursors. *J Neurochem.*, **2005**, 92, 718-729. DOI: 10.1111/j.1471-4159.2004.02897.x
23. Bravo-San Pedro, J.M.; Niso-Santano, M.; Gomez-Sanchez, R.; Pizarro-Estrella, E.; Aiastui-Pujana, A.; Gorostidi, A.; *et al.* The LRRK2 G2019S mutant exacerbates basal autophagy

- through activation of the MEK/ERK pathway. *Cell Mol Life Sci.*, **2012**, 70, 121-136. DOI: 10.1007/s00018-012-1061-y
24. Looyenga, B.D.; Furge, K.A.; Dykema, K.J.; Koeman, J.; Swiatek, P.J.; Giordano, T.J.; *et al.* Chromosomal amplification of leucine-rich repeat kinase-2 (LRRK2) is required for oncogenic MET signaling in papillary renal and thyroid carcinomas. *Proc Natl Acad Sci USA.*, **2011**, 108,1439-1444. DOI: 10.1073/pnas.1012500108
25. Su, Y.C.; Guo, X.; Qi, X. Threonine 56 phosphorylation of Bcl-2 is required for LRRK2 G2019S-induced mitochondrial depolarization and autophagy. *Biochim Biophys Acta.*, **2015**, 1852, 12-21. DOI: 10.1016/j.bbadis.2014.11.009
26. Gehrke, S.; Imai, Y.; Sokol, N.; Lu, B. Pathogenic LRRK2 negatively regulates microRNA-mediated translational repression. *Nature.*, **2010**, 466, 637-641. DOI: 10.1038/nature09191
27. Martin, I.; Kim, J.W.; Lee, B.D.; Kang, H.C.; Xu, J.C.; Jia, H.; *et al.* Ribosomal protein s15 phosphorylation mediates LRRK2 neurodegeneration in Parkinson's disease. *Cell.*, **2014**, 157, 472-485. DOI: 10.1016/j.cell.2014.01.064
28. Wallings, R.; Manzoni, C.; Bandopadhyay, R. Cellular processes associated with LRRK2 function and dysfunction. *FEBS J.*, **2015**, 282, 2806-2826. DOI: 10.1111/febs.13305
29. Trinh, J.; Gustavsson, E.K.; Vilarino-Guell, C.; Bortnick, S.; Latourelle, J.; McKenzie, M.B.; *et al.* DNM3 and genetic modifiers of age of onset in LRRK2 Gly2019Ser parkinsonism: a genome-wide linkage and association study. *Lancet Neurol.*, **2016**, 15, 1248-1256. DOI: 10.1016/S1474-4422(16)30203-4
30. Healy, D.G.; Falchi, M.; O'sullivan, S.S.; Bonifati, V.; Durr, A.; Bressman, S.; *et al.* Phenotype; genotype; and worldwide genetic penetrance of LRRK2-associated Parkinson's disease: a case-control study. *Lancet Neurol.*, **2008**, 7, 583-590. DOI: 10.1016/S1474-4422(08)70117-0
31. Jaleel, M.; Nichols, R.J.; Deak, M.; Campbell, D.G.; Gillardon, F.; Knebel, A.; *et al.* LRRK2 phosphorylates moesin at threonine-558: characterization of how Parkinson's disease mutants affect kinase activity. *Biochem J.*, **2007**, 405, 307-317. DOI: 10.1042/BJ20070565
32. Yue, Z.; Yang, X.W.; Yang, C.; Lee, T.H. Reduced synaptic vesicle density and defective synaptic vesicle recycling in the early stage of Huntington's disease by LRRK2 hyperactivity. *Neuron.*, 2015, 85, 902-916. DOI: 10.1016/j.neuron.2015.01.014
33. Kett, L.R.; Boassa, D.; Ho, C.C.; Rideout, H.J.; Tjan, D.; Shen, G.C.; *et al.* LRRK2 Parkinson disease mutations enhance its microtubule association. *Hum Mol Genet.*, **2012**, 21, 890-899. DOI: 10.1093/hmg/ddr511
34. Di Maio, R.; Hoffman, E.K.; Rocha, E.M.; Keeney, M.T.; Sanders, L.H.; De Miranda, B.R.; *et al.* LRRK2 activation in idiopathic Parkinson's disease. *Sci Transl Med.*, **2018**, 10. DOI: 10.1126/scitranslmed.aar5429
35. Hsieh, C.H.; Shaltouki, A.; Gonzalez, A.E.; Bettencourt da Cruz, A.; Burbulla, L.F.; St Lawrence, E.; *et al.* Functional impairment in miro degradation and mitophagy is a shared

- feature in familial and sporadic Parkinson's disease. *Cell Stem Cell.*, **2016**, 19, 709-724. DOI: 10.1016/j.stem.2016.08.002
36. Grunewald, A.; Kumar, K.R.; Sue, C.M. New insights into the complex role of mitochondria in Parkinson's disease. *Prog Neurobiol.*, **2019**, 177, 73-93. DOI: 10.1016/j.pneurobio.2018.09.003
37. Sanders LH; Laganier J; Cooper O; Mak SK; Vu BJ; Huang YA; *et al.* LRRK2 mutations cause mitochondrial DNA damage in iPSC-derived neural cells from Parkinson's disease patients: reversal by gene correction. *Neurobiol Dis.* **2014**;62:381-386. DOI: 10.1016/j.nbd.2013.10.01
38. Ren, C.; Ding, Y.; Wei, S.; Guan, L.; Zhang, C.; Ji, Y.; *et al.* G2019S Variation in LRRK2: An Ideal Model for the Study of Parkinson's Disease?. *Front Hum Neurosci.*, **2019**, 12, 306. DOI: 10.3389/fnhum.2019.00306
39. Belarbi, S.; Hecham, N.; Lesage, S.; Kediha, M.I.; Smail, N.; Benhassine, T.; *et al.* LRRK2 G2019S mutation in Parkinson's disease: a neuropsychological and neuropsychiatric study in a large Algerian cohort. *Parkinsonism Relat Disord.*, **2010**, 16, 676-679. DOI: 10.1016/j.parkreldis.2010.09.003
40. Alcalay, R.N.; Mirelman, A.; Saunders-Pullman, R.; Tang, M.X.; Mejia-Santana, H.; Raymond, D.; *et al.* Parkinson disease phenotype in Ashkenazi Jews with and without LRRK2 G2019S mutations. *Mov Disord.*, **2013**, 28, 1966-1971. DOI: 10.1002/mds.25647
41. Gatto, E.M.; Parisi, V.; Converso, D.P.; Poderoso, J.J.; Carreras, M.C.; Marti-Masso, J.F.; *et al.* The LRRK2 G2019S mutation in a series of Argentinean patients with Parkinson's disease: clinical and demographic characteristics. *Neurosci Lett.*, **2013**, 537, 1-5. DOI: 10.1016/j.neulet.2013.01.011
42. Sierra, M.; Martínez-Rodríguez, I.; Sánchez-Juan, P.; Gonzalez-Aramburu, I.; Jimenez-Alonso, M.; Sanchez-Rodriguez, A.; *et al.* Prospective clinical and DaT-SPECT imaging in premotor LRRK2 G2019S-associated Parkinson disease. *Neurology.*, **2017**, 89, 439-444. DOI: 10.1212/WNL.0000000000004185
43. Gunzler, S.A.; Riley, D.E.; Chen, S.G.; Tatsuoka, C.M.; Johnson, W.M.; Mielay, J.J.; *et al.* Motor and non-motor features of Parkinson's disease in LRRK2 G2019S carriers versus matched controls. *J Neurol Sci.*, **2018**, 388, 203-207. DOI: 10.1016/j.jns.2018.03.025
44. Mestre, T.A.; Pont-Sunyer, C.; Kausar, F.; Visanji, N.P.; Ghate, T.; Connolly, B.S.; *et al.* Clustering of motor and nonmotor traits in leucine-rich repeat kinase 2 G2019S Parkinson's disease nonparkinsonian relatives: a multicenter family study. *Mov Disord.*, **2018**, 33, 960-965. DOI: 10.1002/mds.27272
45. Pishedda, F.; Cîrnaru, M.D.; Ponzoni, L.; Sandre, M.; Biossa, A.; Carrion, M.P.; *et al.* LRRK2 G2019S kinase activity triggers neurotoxic NSF aggregation. *Brain.*, **2021**, 144, 1509-1525. DOI: 10.1093/brain/awab073

46. Graham, S.H.; Liu, H. Life and death in the trash heap: The ubiquitin proteasome pathway and UCHL1 in brain aging; neurodegenerative disease; and cerebral ischemia. *Ageing Res Rev.*, **2017**, 34, 30-38. DOI: 10.1016/j.arr.2016.09.011
47. Arbez, N.; He, X.; Huang, Y.; Ren, M.; Liang, Y.; Nucifora, F.C.; *et al.* G2019S-LRRK2 mutation enhances MPTP-linked Parkinsonism in mice. *Hum Mol Genet.*, **2020**, 29, 580-590. DOI: 10.1093/hmg/ddz271
48. Wang, X.; Yan, M.H.; Fujioka, H.; Liu, J.; Wilson-Delfosse, A.; Chen, S.G.; *et al.* LRRK2 regulates mitochondrial dynamics and function through direct interaction with DLP1. *Hum Mol Genet.*, **2012**, 21, 1931-1944. DOI: 10.1093/hmg/dds003
49. Plowey, E.D.; Johnson, J.W.; Steer, E.; Zhu, W.; Eisenberg, D.A.; Valentino, N.M.; *et al.* Mutant LRRK2 enhances glutamatergic synapse activity and evokes excitotoxic dendrite degeneration. *Biochim Biophys Acta.*, **2014**, 1842, 1596-1603. DOI: 10.1016/j.bbdis.2014.05.016
50. Vitte, J.; Traver, S.; Maues De Paula, A.; Lesage, S.; Rovelli, G.; Corti, O.; *et al.* Leucine-rich repeat kinase 2 is associated with the endoplasmic reticulum in dopaminergic neurons and accumulates in the core of Lewy bodies in Parkinson disease. *J Neuropathol Exp Neurol.*, **2010**, 69, 959-972. DOI: 10.1097/NEN.0b013e3181efc01c
51. Orenstein, S.J.; Kuo, S.H.; Tasset, I.; Arias, E.; Koga, H.; Fernandez-Carasa, I.; *et al.* Interplay of LRRK2 with chaperone-mediated autophagy. *Nat Neurosci.*, **2013**, 16, 394-406. DOI: 10.1038/nn.3350
52. Jacquet, A.; Tancredi, J.L.; Lemire, A.L.; DeSantis, M.C.; Li, W.; O'Shea, E.K. The LRRK2 G2019S mutation alters astrocyte-to-neuron communication via extracellular vesicles and induces neurodegeneration. *J Cell Sci.*, **2021**, 134. DOI: 10.1242/jcs.256610
53. Fraser, K.B.; Moehle, M.S.; Alcalay, R.N.; West, A.B. Urinary LRRK2 phosphorylation predicts parkinsonian phenotypes in G2019S LRRK2 carriers. *Neurology.*, **2016**, 86, 994-999. DOI: 10.1212/WNL.0000000000002436
54. Bakshi, R.; Macklin, E.A.; Logan, R.; Zorlu, M.M.; Xia, N.; Crotty, G.F.; *et al.* Higher urate in LRRK2 mutation carriers resistant to Parkinson disease. *Ann Neurol.*, **2019**, 85, 593-599. DOI: 10.1002/ana.25436
55. Podlesniy, P.; Puigros, M.; Serra, N.; Fernandez-Santiago, R.; Ezquerro, M.; Tolosa, E.; *et al.* Accumulation of mitochondrial 7S DNA in idiopathic and LRRK2 associated Parkinson's disease. *EBioMedicine.*, **2019**, 48, 554-567. DOI: 10.1016/j.ebiom.2019.09.01
56. Grunewald, A.; Arns, B.; Meier, B.; Brockmann, K.; Tadic, V.; Klein, C. Does uncoupling protein 2 expression qualify as marker of disease status in LRRK2-associated Parkinson's disease? *Antioxid Redox Signal.*, **2014**, 20, 1955-1960. DOI: 10.1089/ars.2013.5737

57. Lubben, T.; Broussard, G.; Roe, A.D.; Dissanayake, R.; Holt, S.; Partridge, E.; *et al.* Development and characterization of novel LRRK2 inhibitors for Parkinson's disease. *J Pharmacol Exp Ther.*, **2024**, 370, 45-57. DOI: 10.1124/jpet.123.000842
58. Alessi, D.R.; Sammler, E. LRRK2 kinase in Parkinson's disease. *Science.*, **2018**, 360, 36-37. DOI: 10.1126/science.aan8860
59. Cookson, M.R.; Hardy, J. Genetic assessment of early-onset Parkinson's disease. *Lancet Neurol.*, **2021**, 20, 23-25. DOI: 10.1016/S1474-4422(20)30399-4
60. Steger, M.; Beilina, A.; Biosa, A.; Baba, Y.; Davis, J.W.; Bandres-Ciga, S.; *et al.* Age-dependent loss of LRRK2 kinase activity in Parkinson's disease. *Mov Disord.*, **2020**, 35, 124-133. DOI: 10.1002/mds.27935
61. Tolosa, E.; Vila, M.; Klein, C.; Rascol, O. LRRK2 in Parkinson disease: challenges of clinical trials. *Nat Rev Neurol.*, **2020**, 16, 97-107. DOI: 10.1038/s41582-019-0301-2
62. Wojewska, D.; Kortholt, A. LRRK2 inhibitors: a promising approach for the treatment of Parkinson's disease. *J Med Chem.*, **2021**, 64, 1835-1856. DOI: 10.1021/acs.jmedchem.0c01158
63. Lim, K.L. LRRK2 kinase inhibitors in Parkinson's disease: targeting neurodegeneration pathways. *Pharmacol Res.*, **2020**, 159, 105010. DOI: 10.1016/j.phrs.2020.105010
64. Wallings, R.L.; Mark, J.R.; Staley, H.A.; Gillett, D.A.; Neighbarger, N.; Kordasiewicz, H.; *et al.* Totally tubular: ASO-mediated knock-down of G2019S-Lrrk2 modulates lysosomal tubule-associated antigen presentation in macrophages. *bioRxiv.*, **2023**. DOI: 10.1101/2023.07.14.549028
65. Lim, K.L. Gene therapy for Parkinson's disease: RNA interference and CRISPR-based approaches. *Gene Ther.*, **2020**, 27, 409-420. DOI: 10.1038/s41434-020-0147-2
66. Akel, H.; Ismail, R.; Csoka, I. Progress and Perspectives of Brain-Targeting Lipid-Based Nanosystems via the Intranasal Route in Neurodegenerative Disorders. *Pharmaceutics.*, **2021**, 13, 1988. DOI: 10.3390/pharmaceutics13121988
67. Ghasemiyeh, P.; Mohammadi-Samani, S. Solid lipid nanoparticles and nanostructured lipid carriers as novel drug delivery systems: applications; advantages and disadvantages. *Res Pharm Sci.*, **2018**, 13, 288-303. DOI: 10.4103/1735-5362.235156
68. Barroso, M.F.; Nunes, C.; Pereira, D.; Reis, S. Nanosystems for targeting and delivery of drugs and bioactive molecules. *Adv Colloid Interface Sci.*, **2021**, 287, 102333. DOI: 10.1016/j.cis.2020.102333
69. Parhi, R.; Suresh, P. Production of solid lipid nanoparticles-drug loading and release mechanism. *J Chem Pharm Res.*, **2012**, 4, 959-970.
70. Pardeshi, S.R.; Belgamwar, V.S. Controlled synthesis of nano-sized solid lipid particles: a novel strategy of nanoprecipitation method. *Res Chem Intermed.*, **2012**, 38, 2221-2237. DOI: 10.1007/s11164-012-0614-0

71. Naseri, N.; Valizadeh, H.; Zakeri-Milani, P. Solid lipid nanoparticles and nanostructured lipid carriers: structure; preparation and application. *Adv Pharm Bull.*, **2015**, 5, 305-313. DOI: 10.15171/apb.2015.043
72. Souto, E.B.; Wissing, S.A.; Barbosa, C.M.; Müller, R.H. Evaluation of the physical stability of SLN and NLC dispersions after long-term storage. *Int J Pharm.*, **2004**, 288, 149-157. DOI: 10.1016/j.ijpharm.2004.09.006
73. Viegas, J.; Morais, J.; Lopes, C.M.; Segundo, M.A. Structure–function relationships of lipid nanoparticles: current approaches to improve their performance. *Pharmaceutics.*, **2023**, 15, 1167. DOI: 10.3390/pharmaceutics15051167
74. Montoto, S.S.; Muraca, G.; Ruiz, M.E. Solid lipid nanoparticles for drug delivery: pharmacological and biopharmaceutical aspects. *Front Mol Biosci.*, **2020**, 7, 587997. DOI: 10.3389/fmolb.2020.587997
75. Jain, V.; Thareja, S. Solid lipid nanoparticles: Targeted and controlled delivery of bioactives. *Int J Adv Pharm.*, **2020**, 8, 15-30.
76. Haque, S.; Whittaker, M.R.; McIntosh, M.P.; Pouton, C.W.; Kaminskas, L.M. Disposition of inhaled lipid nanocapsules in the rat lung. *AAPS J.*, **2018**, 20, 89. DOI: 10.1208/s12248-018-0244-7
77. Chirio, D.; Gallarate, M.; Peira, E.; Battaglia, L.; Serpe, L.; Trotta, M. Formulation of curcumin-loaded solid lipid nanoparticles produced by fatty acids coacervation technique. *J Microencapsul.*, **2019**, 36, 136-147. DOI: 10.1080/02652048.2019.1586974
78. Nakhband, A.; Taheri, A.; Rahimi, H.; Gol, A.; Barar, J.; Omid, Y. Formulation; characterization; and anti-inflammatory effect of Celecoxib-loaded solid lipid nanoparticles: an optimization approach. *J Drug Deliv Sci Technol.*, **2018**, 43, 99-112. DOI: 10.1016/j.jddst.2017.09.014
79. Shah, R.M.; Malherbe, F.; Eldridge, D.; Palombo, E.A.; Harding, I.H. Physicochemical characterization of solid lipid nanoparticles (SLNs) formulated with a bioactive lipid: quercetin laurate. *Int J Pharm.*, **2016**, 508, 61-70. DOI: 10.1016/j.ijpharm.2016.04.002
80. Küçüktürkmen, B.; Bozkır, A. Development of the solid lipid nanoparticles (SLNs) delivery system for pulmonary application of the anti-tuberculosis drug rifampicin. *J Microencapsul.*, **2018**, 35, 375-389. DOI: 10.1080/02652048.2018.1537816
81. Leite, E.A.; Riberio, S.C. Physicochemical characterization of a new solid lipid nanoparticles formulation composed of lecithin; cholesterol; and stearic acid. *J Nanosci Nanotechnol.*, **2012**, 12, 2672-2676. DOI: 10.1166/jnn.2012.5863
82. Keck, C.M.; Müller, R.H. Drug nanocrystals of poorly soluble drugs produced by high pressure homogenisation. *Eur J Pharm Biopharm.*, **2006**, 62, 3-16. DOI: 10.1016/j.ejpb.2005.05.009

83. Cheng, C.J.; Lee, C.H.; Yang, C.Y.; Shiea, J. Determination of zeta potential of lipid nanoparticles in liquid samples by free-solution capillary electrophoresis-mass spectrometry. *Anal Chem.*, **2016**, 88, 4620-4626. DOI: 10.1021/acs.analchem.6b00083
84. Kovačević, A.B.; Müller, R.H.; Keck, C.M. Formulation development of nanosuspensions for dermal application: a study with curcumin. *Eur J Pharm Sci.*, **2014**, 71, 1-8. DOI: 10.1016/j.ejps.2014.05.014
85. Sathali, A.H.; Rajalakshmi, G.; Mathan, R. Preparation and evaluation of solid lipid nanoparticles loaded Neem seed oil. *Int J ChemTech Res.*, **2012**, 4, 124-130.
86. Reddy, L.H.; Venkateswarlu, V. Pharmaceutical nanotechnology: Preparation; characterization; and applications of nanoparticles and nanomaterials in drug delivery. In: Kaushik AC; Pardasani K; editors. *Nanostructures for Drug Delivery. Amsterdam: Elsevier;* **2017**, 129-157. DOI: 10.1016/B978-0-12-809197-0.00006-4
87. Lockman, P.R.; Koziara, J.M.; Mumper, R.J.; Allen, D.D. Nanoparticle surface charges alter blood-brain barrier integrity and permeability. *J Drug Target.*, **2004**, 12, 635-641. DOI: 10.1080/10611860400015936
88. Albi, E.; Cataldi, S.; Lazzarini, A.; Codini, M.; Beccari, T. The role of sphingomyelin in neurodegenerative diseases. *Biomed Res Int.*, **2020**, 2020, 1238196. DOI: 10.1155/2020/1238196
89. Perillo, B.; Tramontano, A.; Pezone, A.; Migliaccio, A.; Miele, C.; Beguinot, F. Sphingomyelin metabolism: new insight into the role of enzymes and regulation in lipid homeostasis. *Front Cell Dev Biol.*, **2016**, 4, 83. DOI: 10.3389/fcell.2016.00083
90. Signorelli, P.; Hannun, Y.A. Analysis and quantification of ceramide and sphingomyelin species by LC-MS/MS. *Methods Mol Biol.*, **2021**, 2187, 151-161. DOI: 10.1007/978-1-0716-0811-7_12
91. Chrast, R.; Saher, G.; Nave, K.A.; Verheijen, M.H. Lipid metabolism in myelinating glial cells: lessons from human inherited disorders and mouse models. *J Lipid Res.*, **2011**, 52, 419-434. DOI: 10.1194/jlr.R009761
92. Payne, J.A.; Valencia, F.J.; Wilkinson, D.J.; Cornell, D.J. Targeting protein degradation pathways with small-molecule inhibitors. *Nat Rev Drug Discov.*, **2012**, 11, 709-726. DOI: 10.1038/nrd3849
93. Zöller, I.; Meixner, M.; Hartmann, D.; Bussow, H.; Meyer, R.; Gieselmann, V.; *et al.* Absence of functional ceramide synthase 2 causes a specific sphingolipid pattern associated with myelin sheath abnormalities. *Biochem J.*, **2008**, 415, 119-129. DOI: 10.1042/BJ20080928
94. Lewkowicz, A.P.; Kowalewska, A.W.; Lemiesz, P.; Waszkiewicz, N. Nutrition and dietary supplements for myelin repair in multiple sclerosis—A narrative review. *Nutrients.*, **2019**, 11, 1720. DOI: 10.3390/nu11081720

95. Hardie, L.J.; Muallen, W.A. Sphingolipids in cellular signalling and function. *Biochim Biophys Acta.*, **2009**, 1791, 555-558. DOI: 10.1016/j.bbaliip.2009.01.001
96. Olsen, A.S.; Faergeman, N.J. Sphingolipids: membrane microdomains in brain development; function; and neurological diseases. *Open Biol.*, **2017**, 7, 170069. DOI: 10.1098/rsob.170069
97. Tabatadze, N.; McDonald, M.P.; McMurray, M.S.; Raber, J. Overexpression of neutral sphingomyelinase promotes hippocampal memory defects and disrupts structural plasticity. *Front Mol Neurosci.*, **2010**, 3, 7. DOI: 10.3389/neuro.02.007.2010
98. Nagachinta, S.; Singh, A.; Zaheer, M.A.; Singla, A.; Bedi, N.; Goel, H.; *et al.* Solid lipid nanoparticles of oncosuppressor microRNA-34a for colorectal cancer: development; characterization and in vitro evaluations. *Int J Pharm.*, **2020**, 577, 119066. DOI: 10.1016/j.ijpharm.2020.119066
99. Albertsen, P.C.; Gleason, D.F.; Barry, M.J. Practical risk classification in the management of clinically localized prostate cancer. *J Urol.*, **2005**, 173, 1826-1831. DOI: 10.1097/01.ju.0000158164.53795.00
100. Krause, M.R.; Regen, S.L. The structural role of cholesterol in cell membranes: from condensed bilayers to lipid rafts. *Acc Chem Res.*, **2014**, 47, 3512-3521. DOI: 10.1021/ar500260
101. Semple, S.C.; Klimuk, S.K.; Harasym, T.O.; Dos Santos, N.; Ansell, S.M.; Wong, K.F.; *et al.* Efficient encapsulation of antisense oligonucleotides in lipid vesicles using ionizable aminolipids: formation of novel small multivesicular vesicle structures. *Biochim Biophys Acta.*, **2001**, 1510, 152-166. DOI: 10.1016/s0005-2736(00)00339-3
102. Kulkarni, J.A.; Cullis, P.R.; van der Meel, R. Lipid nanoparticles enabling gene therapies: from concepts to clinical utility. *Nucleic Acid Ther.*, **2018**, 29, 146-157. DOI: 10.1089/nat.2019.0790
103. Chang, C.J.; Lee, C.H.; Yang, C.Y.; Shiea, J. Determination of zeta potential of lipid nanoparticles in liquid samples by free-solution capillary electrophoresis-mass spectrometry. *Anal Chem.*, **2016**, 88, 4620-4626. DOI: 10.1021/acs.analchem.6b00083
104. Kim, H.; Moon, M.J.; Kwon, H.H.; Park, S.H.; Shin, H.H.; Park, H.J.; *et al.* Lipid nanoparticles for enhancing the neuroprotective effects of curcumin in Parkinson's disease. *Nanomedicine.*, **2020**, 15, 927-939. DOI: 10.2217/nnm-2020-000
105. Hu, B.; Zhong, L.; Weng, Y.; Peng, L.; Huang, Y.; Zhao, Y.; *et al.* Therapeutic siRNA: state of the art. *Signal Transduct Target Ther.*, **2020**, 5, 101. DOI: 10.1038/s41392-020-0207-x
106. Setten, R.L.; Rossi, J.J.; Han, S.P. The current state and future directions of RNAi-based therapeutics. *Nat Rev Drug Discov.*, **2019**, 18, 421-446. DOI: 10.1038/s41573-019-0017-4
107. Weng, Y.; Xiao, H.; Zhang, J.; Liang, X.J.; Huang, Y. RNAi therapeutic and its innovative biotechnological evolution. *Biotechnol Adv.*, **2019**, 37, 801-825. DOI: 10.1016/j.biotechadv.2019.04.014

108. Elbashir, S.M.; Harborth, J.; Lendeckel, W.; Yalcin, A.; Weber, K.; Tuschl, T. Duplexes of 21-nucleotide RNAs mediate RNA interference in cultured mammalian cells. *Nature.*, **2001**, 411, 494-498. DOI: 10.1038/35078107
109. Bennet, C.F. Therapeutic Antisense Oligonucleotides Are Coming of Age. *Annu Rev Med.*, **2019**, 70, 307-321. DOI: 10.1146/annurev-med-041217-010829
110. Khvorova, A.; Watts, J.K. The chemical evolution of oligonucleotide therapies of clinical utility. *Nat Biotechnol.*, **2017**, 35, 238-248. DOI: 10.1038/nbt.3765
111. Huang, Y.; Hong, J.; Zheng, S.; Ding, Y.; Guo, S.; Zhang, H.; *et al.* Elimination pathways of systemically delivered siRNA. *Mol Ther.*, **2018**, 26, 2332-2340. DOI: 10.1016/j.ymthe.2018.07.014
112. Shen, X.; Corey, D.R. Chemistry; mechanism and clinical status of antisense oligonucleotides and duplex RNAs. *Nucleic Acids Res.*, **2018**, 46, 1584-1600. DOI: 10.1093/nar/gkx1239
113. Anderson, B.R.; Muramatsu, H.; Jha, B.K.; Silverman, R.H.; Weissman, D.; Karikó, K. Nucleoside modifications in RNA limit activation of 2'-5'-oligoadenylate synthetase and increase resistance to cleavage by RNase L. *Nucleic Acids Res.*, **2011**, 39, 9329-9338. DOI: 10.1093/nar/gkr586
114. Kormann, M.S.; Hasenpusch, G.; Aneja, M.K.; Nica, G.; Flemmer, A.W.; Herber-Jonat, S.; *et al.* Expression of therapeutic proteins after delivery of chemically modified mRNA in mice. *Nat Biotechnol.*, **2011**, 29, 154-157. DOI: 10.1038/nbt.1733
115. Alegre-Abarrategui, J.; Christian, H.; Lufino, M.M.; Mutihac, R.; Venda, L.L.; Ansorge, O.; *et al.* LRRK2 regulates autophagy by preventing accumulation of damaging protein species in human neurons. *Neurobiol Dis.*, **2009**, 36, 520-530. DOI: 10.1016/j.nbd.2009.08.003
116. Lee, H.J.; Shin, J.H.; VanKampen, J.; Petrucelli, L.; West, A.B.; Ko, H.S.; *et al.* Dysfunction of mitochondria in 5-hydroxyindoleacetic acid metabolism causes idiopathic Parkinson's disease. *Neurobiol Dis.*, **2019**, 124, 10-21. DOI: 10.1016/j.nbd.2018.09.016
117. Acharya, B.; Sahoo, S.K.; Panda, A.K. Layered double hydroxides (LDH) for dual delivery of methotrexate and siRNA: an efficient carrier for breast cancer therapy. *J Colloid Interface Sci.*, **2019**, 534, 439-449. DOI: 10.1016/j.jcis.2018.09.10
118. Lobovkina, T.; Jacobson, G.B.; Gonzalez-Gonzalez, E.; Hickerson, R.P.; Leake, D.; Kaspar, R.L.; *et al.* In vivo sustained release of siRNA from solid lipid nanoparticles. *ACS Nano.*, **2011**, 5, 9977-9983. DOI: 10.1021/nn203175m
119. Connerty, P.; Ho, R.; Burns, C.J.; D'Andrea, R.J. Silencing of long noncoding RNA LINC01257 inhibits cell proliferation and induces apoptosis in acute myeloid leukemia. *Hematologica.*, **2021**, 106, 1571-1580. DOI: 10.3324/haematol.2020.270694
120. Jyotsana, N.; Taftaf, R.; Jabbour, E.; Ravandi, F.; Mehdi, G.; Uday, R.; *et al.* Long-term survival benefit with RNA interference therapy in chronic myeloid leukemia. *J Clin Oncol.*, **2019**, 37, 1380-1390. DOI: 10.1200/JCO.19.01084

121. Mennati, A.; Valizadeh, H.; Zakeri-Milani, P.; Rezazadeh, M. Enhanced anticancer activity of mPEG-PCL-DDAB nanoparticles loaded with IGF-1R siRNA in MCF-7 breast cancer cells. *Int J Nanomedicine.*, **2022**, 17, 2477-2487. DOI: 10.2147/IJN.S358688
122. Zhou, Y.; Chen, C.; Shi, S.; Wang, M.; Chen, Q.; Zhao, G.; *et al.* Synergistic effect of docosahexaenoic acid and high mobility group box 1 gene silencing on non-alcoholic steatohepatitis. *J Nanobiotechnology.*, **2022**, 20, 90. DOI: 10.1186/s12951-022-01300-5
123. Huang, Y.; Hong, J.; Zheng, S.; Ding, Y.; Guo, S.; Zhang, H.; *et al.* Liver-targeted delivery of siRNA using RBP131-lipid nanoparticles. *Biomater Sci.*, **2022**, 10, 1368-1378. DOI: 10.1039/D2BM00010A
124. Li, S.D.; Huang, L. Targeted delivery of siRNA by nonviral vectors: applications to lung cancer therapy. *Expert Opin Drug Deliv.*, **2016**, 13, 73-87. DOI: 10.1517/17425247.2016.1111636
125. McCall, R.L.; Sirianni, R.W. PLGA nanoparticles formed by single- or double-emulsion with vitamin E-TPGS. *J Vis Exp.*, **2017**, 55154. DOI: 10.3791/55154
126. Kim, S.S.; Rait, A.; Kim, E.; DeMarco, J.; Pirollo, K.F.; Chang, E.H. Encapsulation of temozolomide in a targeted siRNA nanoparticle enhances anti-cancer efficacy for glioblastoma. *J Control Release.*, **2018**, 279, 166-176. DOI: 10.1016/j.jconrel.2018.04.029
127. Zhang, X.; Tang, N.; Hadden, T.J.; Rishi, A.K. Akt; FoxO and regulation of apoptosis. *Biochim Biophys Acta.*, **2020**, 1813, 1978-1986. DOI: 10.1016/j.bbamcr.2020.06.012
128. Zhou, J.; Patel, T.R.; Sirianni, R.W.; Strohhenn, G.; Zheng, M.Q.; Duong, N.; *et al.* Highly penetrative; drug-loaded nanocarriers improve treatment of glioblastoma. *Proc Natl Acad Sci USA.*, **2016**, 113, 1918-1923. DOI: 10.1073/pnas.1512799113
129. Alvarez-Erviti, L.; Seow, Y.; Yin, H.; Betts, C.; Lakhali, S.; Wood, M.J. Delivery of siRNA to the mouse brain by systemic injection of targeted exosomes. *Nat Biotechnol.*, **2011**, 29, 341-345. DOI: 10.1038/nbt.1807
130. Saraiva, C.; Praca, C.; Ferreira, R.; Santos, T.; Ferreira, L.; Bernardino, L. Nanoparticle-mediated brain drug delivery: overcoming blood-brain barrier to treat neurodegenerative diseases. *J Control Release.*, **2016**, 235, 34-47. DOI: 10.1016/j.jconrel.2016.05.044
131. Godinho, B.M.D.C.; Vieira, A.J.; Carvalho, R.A.; Pereira de Almeida, L.; Alves, P.M. Antisense oligonucleotides conjugated with polymers reduce mutant huntingtin levels in Huntington's disease models. *Mol Ther Nucleic Acids.*, **2018**, 12, 457-469. DOI: 10.1016/j.omtn.2018.06.003
- Refer to Appendix C3 for the Turnitin Report.*

Chapter 6

Bio-inspired Polymeric Solid Lipid Nanoparticles for siRNA delivery: Cytotoxicity and Cellular Uptake *in vitro*

Bio-inspired Polymeric Solid Lipid Nanoparticles for siRNA delivery: Cytotoxicity and Cellular Uptake in vitro

This chapter has been submitted to *Polymers*

Abstract:

Nanomedicine has introduced strategies that provide precise diagnosis and treatment with fewer side effects than traditional therapies. Parkinson's disease (PD) treatments are palliative, necessitating an innovative delivery system with a curative function. This study investigated a solid lipid nanoparticle (SLNP) system's ability to bind and safely deliver siRNA in vitro. SLNPs were formulated using sphingomyelin and cholesterol, with *Ginkgo biloba* leaf extract (GBE) incorporated to enhance biocompatibility and neuroprotection. Poly-L-lysine (PLL) functionalization ensured successful siRNA binding, safe transport, and protection from nuclease degradation. SLNPs were physicochemically characterized, with binding and protection of siRNA assessed using agarose gels. Cytotoxicity, apoptotic induction, and cellular uptake studies were undertaken in the human neuroblastoma (SH-SY5Y) and embryonic kidney (HEK293) cells. The GBE-PLL-SLNPs had an average size of 93.2 nm and demonstrated enhanced binding and protection of the siRNA from enzyme digestion, with minimal cytotoxicity in HEK293 (<10%) and SH-SY5Y cells (< 15%). Caspase 3/7 activity was significantly reduced in both cells, while efficient cellular uptake was noted. The present study provided a solid basis as a proof of principle study for future applications of the potential therapeutic in treating PD, promising to address the unmet medical needs of patients with this neurological disorder.

Keywords: Parkinson's disease; nanomedicine; solid lipid nanoparticles; gene delivery; siRNA; *Ginkgo biloba*, cytotoxicity.

6.1. Introduction

The evolution of nanomedicine has led to innovative methods for diagnosis and therapy while minimizing the adverse effects caused by traditional medicine. Lipid nanocarriers have considerable advantages due to their biodegradability, scale-up capacity, low toxicity, biocompatibility, and the potential to deliver lipophilic and hydrophilic drugs in a targeted and controlled manner [1,2]. Solid lipid nanoparticles (SLNPs) are composed of a solid

physiological lipid (at room or body temperature), a surfactant, and water [3]. SLNPs have been reported to be biodegradable and biocompatible, with the ability to protect the bound therapeutic. These favourable characteristics rival liposomes, one of the most popular lipid-based systems used in gene delivery [4,5]. SLNPs usually range from 10 to 1000 nm in diameter and possess pivotal characteristics relating to their ease of cellular infiltration [6].

SLNPs have proved to possess more advantages over polymeric NPs. They are more cost-effective to synthesize and can be scaled up for various applications [7]. Furthermore, their synthesis avoids the use of potentially harmful organic solvents, rendering them less toxic for medical use [8]. They have high evasive properties and can prevent reticuloendothelial system (RES) uptake, bypassing the liver and spleen and preventing filtration [9]. SLNPs have a high encapsulation rate, encapsulating lipophilic and hydrophilic molecules while maintaining their stability [10]. Similar to other NPs, SLNPs, when conjugated to an appropriate ligand, can improve the targeted and sustained release of drugs and genes [4].

Various phospholipids may be employed in the synthesis of SLNPs. Sphingomyelin is advantageous against multiple disorders, including Parkinson's disease (PD) and cancer, because it can permeate the blood-brain barrier and regulate tumor cell growth, senescence, differentiation, apoptosis, and survival [11-13]. Sphingomyelin belongs to the group of phospholipids and sphingolipids found in high concentrations in the plasma membrane and the membranous myelin sheath surrounding the nerve cell axons. Naturally, these lipids are essential for impulse transmission, location of neurotransmitter receptors, myelin sheath, and blood-brain barrier (BBB) integrity. Their importance in cell signaling is mainly due to their ease of hydrogen bond formation with other molecules [14,15]. Sphingomyelin-based liposomes were reported to be an efficient carrier system due to their ability to cross the BBB and reduce accumulation. These liposomes are metabolized by the spleen and liver, permitting clearance. In addition to sphingomyelin, cholesterol (Chol) was added to enhance the circulatory time *in vivo*, with improved pharmacokinetics and therapeutic properties [16]. These lipids have been found to establish cholesterol/sphingomyelin-enriched nanodomains in the organelle membranes, which play a pivotal role in neurotransmitter release, synaptic plasticity, and regulating synaptic functions [17]. These properties benefit the development of innovative therapeutic systems with excellent loading capacities. Such loading and reducing options can be obtained in the biological synthesis of the SLNPs.

This study exploits *Ginkgo biloba* (*G.biloba*) leaf extracts (EGB). The BBB is composed of a class of G protein-coupled receptors (GPCRs), referred to as adenosine receptors (ARs), which essentially regulate the permeability of the BBB [18]. In response to this phenomenon, the EGB possess ginkgolides A, B C, bilobalide, and kaempferol, which can effectively activate the A1R, rendering the BBB more permeable while inducing cellular changes such as a decrease in trans-endothelial electrical resistance, an increase in the formation of actinomyosin stress fibers and the alteration of the tight junctions. Furthermore, the introduction of EGB provides a reversible opening of the BBB for four hours, preventing dysregulation in the homeostasis of the brain [19].

In this study, EGB was utilized to synthesize the SLNPs, exploiting its inherent properties to enhance the stability and efficacy of the resulting nanoparticles. The bioactive compounds in EGB contribute to the biomimetic nature of the SLNPs, ensuring better biocompatibility and stability when used for drug delivery, particularly in the context of neurodegenerative diseases. By leveraging EGB in the nanoparticle synthesis, we can improve the structural integrity of the nanoparticles, reduce toxicity, and enhance their ability to cross the BBB effectively.

The SLNPs alone may not adequately bind small interfering ribonucleic acid (siRNA). Hence, the highly cationic homopolypeptide poly-L-lysine (PLL) was used to add stability to the SLNP and to bind the anionic siRNA. PLL has been used in early studies to deliver nucleic acids but was challenged with short circulation times *in vivo* [20,21], limiting their use in gene delivery. The use of PLL to functionalize NPs for the delivery of deoxyribonucleic acid (DNA) [22] and messenger ribonucleic acid (mRNA) [23] has since been widely utilized. The delivery of therapeutic siRNA has been commonly investigated in gene silencing experiments. However, its efficiency depends on reaching its target site without being degraded *in vivo*. Naked siRNA is susceptible to nuclease digestion and can be removed by the mononuclear phagocytic system (MPS) [24]. Due to its size and anionic nature, cellular uptake can be problematic [25]. Hence, conjugating siRNA to delivery vehicles may protect them, enhance their circulation half-life, and improve cellular uptake and gene silencing. The current study used PLL-modified SLNPs to bind and condense the siRNA adequately.

This study aims to biologically synthesize the SLNPs utilizing EGB to create an efficient biocompatible gene delivery vehicle. This study further assesses the loading capabilities of the delivery vehicle for future siRNA-mediated gene therapy. The efficacy of the therapeutic nanosystem is evaluated in the human neuroblastoma (SH-SY5Y) and embryonic kidney

(HEK293) cells to determine their applicability to the neurodegenerative disorder PD. To date, a lack of information about the medical applicability of these NPs has been noted, necessitating further studies to highlight their vast capabilities.

6.2. Materials and Methods

6.2.1. Materials

Ethidium bromide, glycerol, bromophenol blue, xylene cyanol, ethylenediaminetetraacetic acid (EDTA) disodium salt, sodium dodecyl sulfate, phosphate-buffered saline (PBS) tablets, 3-[4,5-dimethylthiazol-2-yl]-2,5-diphenyltetrazolium bromide (MTT), dimethyl sulfoxide (DMSO) and RNase A were purchased from Merck (Darmstadt, Germany). Poly-L-lysine (PLL, 30-70 kDa), sphingomyelin, cholesterol, and dialysis tubing (MWCO 12 kDa) were obtained from Sigma-Aldrich (MO, USA). The Promega Corporation (Madison, USA) supplied the luciferase assay system. Control, siGENOME non-targeting siRNA, and the MycoFluor™ Mycoplasma detection kit was provided by Thermo Scientific Dharmacon Products (CO, USA). Ultrapure agarose was purchased from Bio-Rad Laboratories (VA, USA). Embryonic kidney (HEK293) and neuroblastoma (SH-SY5Y) cells were initially purchased from the American Type Culture Collection (ATCC, Manassas, VA, USA). Eagles Minimum Essential Medium (EMEM) with L-glutamine (4.5 g/l), Dulbecco's modified Eagle medium/nutrient mixture F-12 (DMEM/F12), trypsin–versene mixture, and penicillin–streptomycin mixtures (10,000 U/mL) were purchased from Lonza BioWhittaker (MD, USA). Fetal bovine serum (FBS) was supplied by GIBCO, Life Technologies Ltd (Inchinnan, UK). The Muse® Caspase-3/7 Kit (MCH100108) was sourced from Luminex (TX, USA). Nest Biotechnologies (Wuxi, China) provided the sterile plasticware for cell culture. DNase/RNase-free water (Life Technologies, CA, USA) and ultrapure water (18 Mohm) were used (Milli-Q50, Millipore, France). All reagents were of analytical grade.

6.2.2. Sample Collection and Preparation

Young *G.biloba* leaves (Figure 6.1) were collected within the vicinity of Durban, KwaZulu-Natal, South Africa, sealed in a plastic bag to inhibit transpiration and drying out during transport. After washing the leaves with distilled water, they were dried using a paper towel. Exactly 20 g of the leaves were carefully cut into pieces, added to a beaker containing distilled water (75 mL), and heated to 80-90 °C, stirring for 10 to 15 min. When the solution turned green/yellow, it was removed from the heat, filtered through a number 5 Whatman filter paper, and stored at -4 °C.



Figure 6.1. *Ginkgo biloba* leaves used in the extraction process (Photograph by author K. Jagaran).

6.2.3. Synthesis of Sphingomyelin-Cholesterol SLNPs (SC-SLNPs)

Sphingomyelin (10 mg/mL in methanol) and cholesterol (10 mg/mL in chloroform) were mixed at 50:50, 40:60, and 60:40 mol% and added to a round bottom flask (50 mL). The concentration of sphingomyelin was maintained at 2 mg/mL. The lipid mixture was rotary evaporated at 50 °C until a film was deposited on the bottom of the flask. This lipid film was vacuum-dried for 12 h to remove any residual solvents. The synthesized SLNPs were then divided into two equal aliquots. One aliquot was made up to 50 mL with deionized water (H₂O-SLNPs), while 50 mL EGB (EGB-SLNPs) was added to the second aliquot. The water and the EGB were added dropwise with constant stirring at 60-70 °C. The mixtures were sonicated for 2 min and then centrifuged at 3000 rpm for 5 min to prevent aggregation (Figure 6.2).

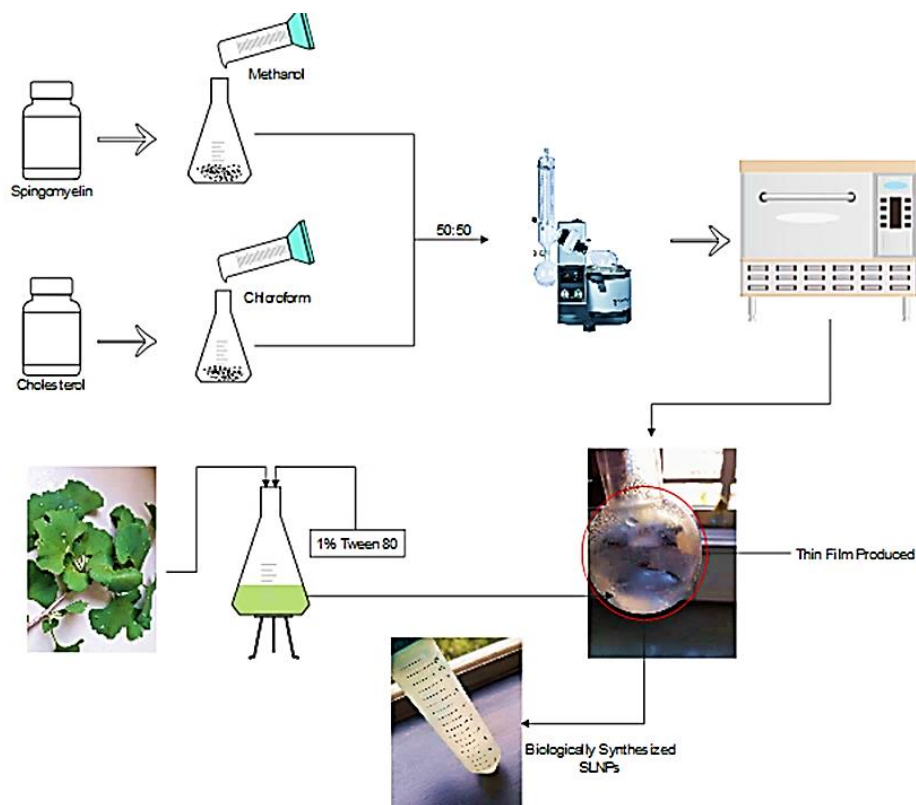


Figure 6.2. Schematic illustration for the synthesis of the SC-SLNPs.

6.2.4. Functionalization of SC-SLNPs with Poly-L-lysine (PLL)

A 1:1 ratio (PLL: SLNP) was used to produce PLL-SLNPs. The PLL was used as a stabilizing agent and to impart a positive charge to the SLNPs for the subsequent siRNA binding.

6.2.5. Preparation of PLL-SC-SLNPs:siRNA nanocomplexes

All PLL-SLNP formulations were briefly vortexed (1 min) and then sonicated (15 min) before use. To achieve different mass (w/w) or N/P (+/-) ratios, various volumes of the SLNP suspensions were combined with a fixed amount of siRNA (0.5 μg). The suspensions were adjusted to a final volume of 10 μL using HEPES-buffered saline (HBS) and incubated for 1 h at room temperature to facilitate nanocomplex formation. All nanocomplexes were freshly prepared before each experiment.

6.2.6. Characterization

The SLNPs and PLL-SLNPs were assessed over a 400–800 nm wavelength range using a Biomate 3 spectrophotometer (Thermo Scientific, CO, USA). The spectrum for the PLL was utilized to indicate the successful conjugation [26–28].

Fourier-transform infrared (FTIR) spectroscopy was performed on a Perkin Elmer Spectrum 100 FTIR spectrophotometer (PerkinElmer Inc., USA) fitted with a universal attenuated total

reflection (ATR) sampling accessory. All samples were freeze-dried, and 10 mg of each sample was analyzed from 4000 – 400 cm⁻¹ with 64 co-added scans and a resolution of 4 cm⁻¹. The IR spectra were plotted using the OriginLab (2023b) software (version 10.5.0 OriginLab Corporation, USA).

The ultrastructural morphology of the SLNPs and their siRNA-based nanocomplexes (at optimum binding ratios) were examined by transmission electron microscopy (TEM) using a Jeol T-1010 TEM (JEOL Ltd; Tokyo, Japan). A Soft Imaging Systems MegaView III side-mounted 3-megapixel digital camera was used to capture the images of the SLNPs and their nanocomplexes.

The hydrodynamic size and the zeta potential of the SLNPs and nanocomplexes were obtained by dynamic light scattering (DLS) using the Malvern Zetasizer Nano-ZS (Malvern Instruments Ltd., Worcestershire, UK). Diluted samples (1:100, 1 mL in 18 MΩ H₂O) at room temperature were analyzed.

6.2.7. siRNA Binding Studies

6.2.7.1. Ethidium Bromide Intercalation Assay

The intercalating agent ethidium bromide (EtBr) was used to investigate the ability of the PLL-SLNPs to bind and compact the siRNA [29]. EtBr (2 μL, 100 μg/mL) in 100 μL of HBS was added to a well in a 96-well flat-bottomed black FluorTrac plate (Greiner Bio-One, Frickenhausen, Germany). This provided a baseline fluorescence (0%) measured at excitation and emission wavelengths of 520 nm and 610 nm, respectively (GloMax® -Multi Detection System, Promega BioSystems, CA, USA). After that, 1 μL of the target siRNA (0.3 μg/μL) was added, and the fluorescence was recorded as 100%. The PLL-SC-SLNPs were introduced in aliquots of 1 μL, and the fluorescence was recorded until an inflection point or plateau was reached. Equation 1 was used to calculate the relative fluorescence (FR).

$$FR (\%) = \left(\frac{F_i - F_0}{F_{\max} - F_0} \right) \times 100 \quad (6.1)$$

Where F_i = fluorescence reading following the sequential addition of the SLNPs, F_0 = reading of the EtBr, and F_{\max} = reading after siRNA addition.

6.2.7.2. Band Shift Assay

The siRNA-binding capability of the PLL-SLNPs was assessed using a band-shift assay [29]. When the nanocomplex migration is fully retarded, an electroneutral complex is formed,

indicating that the positive charges on the SLNPs have completely neutralized the negative charges of the siRNA. This complex fails to migrate through the gel matrix. Nanocomplexes were prepared as previously described. After complex formation, 2 μ L of gel loading buffer (50% glycerol, 0.05% bromophenol blue, 0.05% xylene cyanol) was added, and the nanocomplexes were subjected to agarose gel electrophoresis using a 2% (w/v) agarose gel containing 1 μ g/mL of EtBr. Electrophoresis was carried out at room temperature or 30 min at 50 V. The gels were visualized under UV300 transillumination, and the images were captured using a Vacutec Syngene G: Box BioImaging system (Syngene, Cambridge, UK).

6.2.7.3. RNase A Protection Assay

The protection afforded by the SLNPs to the bound siRNA against enzymatic degradation was investigated following RNase A-mediated digestion [29]. This assay was used to determine the siRNA's compaction by the SLNPs and to observe if the siRNA will maintain its integrity during delivery in an in vivo system. As determined from the band-shift assay, nanocomplexes were prepared at the suboptimum, optimum, and supra-optimum binding mass ratios (w/w). Following incubation (1 hour), RNase A was introduced to each sample to obtain a final concentration of 10% (v/v). Two controls were used in this study; a positive control (siRNA only) and a negative control (siRNA treated with RNase A). Samples were incubated for 2 h at 37°C. EDTA (10 mM) and SDS (0.5%) were added after incubation, followed by a 20 min incubation at 55°C. Agarose gel electrophoresis was then undertaken as for the band shift assay.

6.2.8. Cell Culture

Both cell lines were used in their second or third passages after purchase and monitored routinely using an inverted microscope. The SHSY5Y cells (Figure 6.3A) were small, rounded, and tightly clustered, with a few polygonal shapes. This morphology is characteristic of undifferentiated SH-SY5Y cells, which often exhibit a lack of neurite extensions, a defining feature of their differentiated state. Differentiated SH-SY5Y cells typically develop neurite protrusions that resemble axons and dendrites, extending from the cell body. In this image, however, the lack of long, extended projections indicates that differentiation has not occurred. The overall structure shows healthy adherence to the culture surface and the absence of visible cellular stress markers, such as blebbing or extreme elongation, suggesting that the cells were in a healthy, proliferative state. These features confirm the identification of SH-SY5Y cells.

The HEK293 cells (Figure 6.3B) were epithelial-like in morphology, as expected. The cells are large, flat, and polygonal, with well-defined borders and a cobblestone pattern. This is typical

for HEK293 cells, especially when they are in the semi-confluent or confluent state. The cells appear tightly packed, with some cells forming a monolayer, which is indicative of their high degree of adherence and strong epithelial characteristics. There is no evidence of cellular differentiation in the HEK293 cells, as these cells are not typically subject to differentiation protocols in standard culture. The nuclei of the cells are centrally located and easily visible, which is a key identifying feature of these cells. Overall, their morphology is consistent with healthy HEK293 cells in culture.

In addition, routine mycoplasma detection was conducted before experimentation using the MycoFluor™ Mycoplasma Detection Kit. This provided a rapid, simple, and ultrasensitive means of visually identifying mycoplasma infections in the cell lines. HEK293 and SH-SY5Y cells were trypsinized, and their suspensions in medium (1.9 mL) were added to a sterile petri dish containing a coverslip, together with 0.1 mL of 20x concentrated MycoFluor reagent. This was incubated at 37°C for 10 minutes to allow for cell adhesion. After that, the coverslip was removed, the excess medium blotted, and the coverslip was transferred to a microscope slide. The coverslip was fixed to the slide with a sealant. Once dry, the slide was visualized under an Olympus CKX41 inverted phase contrast fluorescence (Olympus Corporation, Tokyo, Japan) microscope at an excitation wavelength of 494 nm and an emission wavelength of 519 nm. The presence of a violet/blue specimen would indicate any mycoplasma contamination.

For the cell-based assays, the HEK293 and SH-SY5Y cells were grouped based on the experimental conditions. For the cytotoxicity and cellular uptake studies, cells were seeded into 96-well plates at a density of 1.8×10^5 cells per well and incubated overnight at 37°C. The experimental control groups included untreated cells; and cells treated with naked siRNA without NP complexation. Experimental groups included the H₂O-PLL-SLNPs complexed to siRNA at different w/w ratios; and EGB-PLL-SLNPs complexed to siRNA at different w/w ratios. For the cytotoxicity studies, the cells were exposed to the nanocomplexes at their suboptimum, optimum, and supra-optimum binding ratios. The MTT assay was conducted after a 48-h incubation as described below. For the cellular uptake studies, the cells were treated with nanocomplexes containing a fluorescent oligo surrogate for the therapeutic siRNA, and fluorescence was measured after a 24-hour incubation.

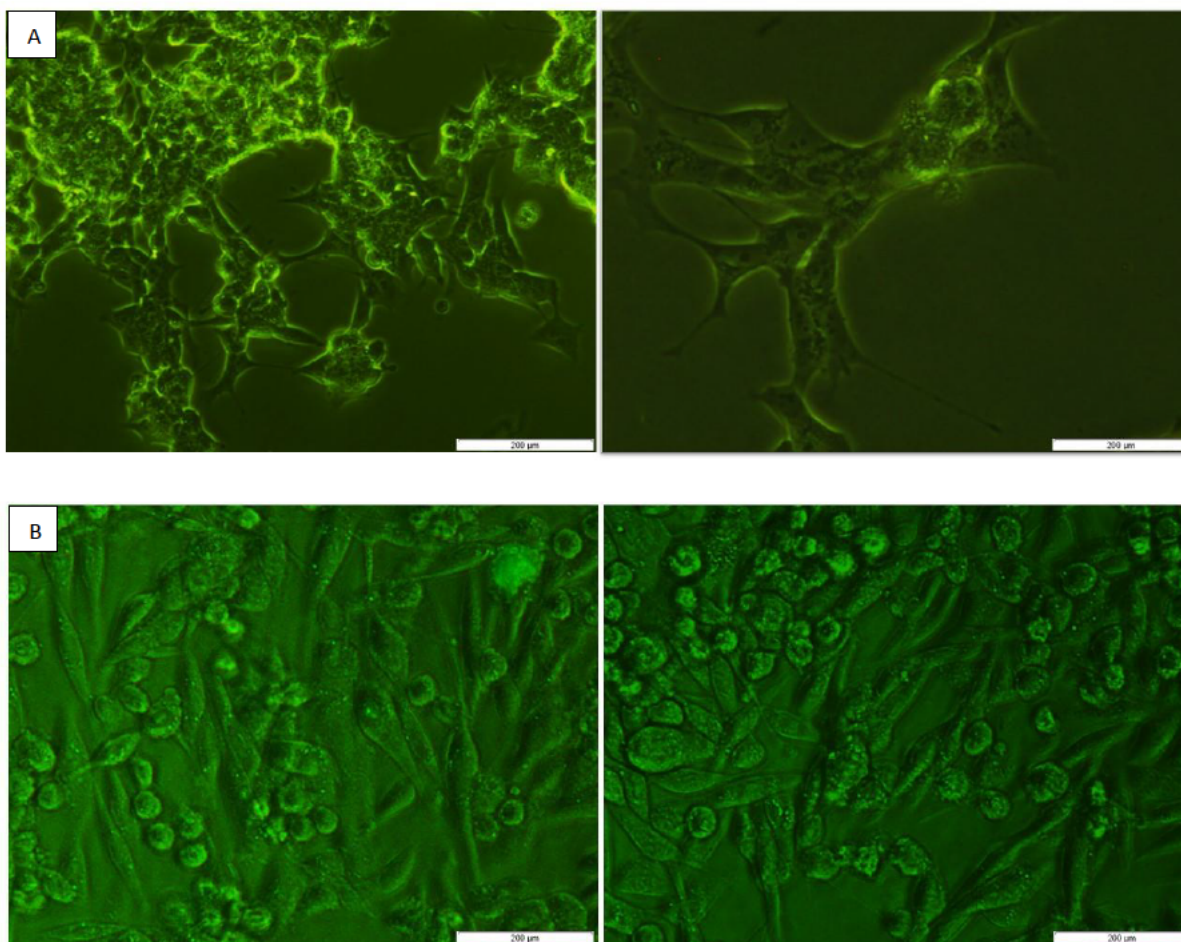


Figure 6.3. Morphology of the (A) SH-SY5Y cells at 40x and 100x magnification; and (B) HEK293 cells at 100x magnification.

6.2.9. Cytotoxicity Studies

HEK293 and SH-SY5Y cells were subcultured into clear 96-well plates at a density of 1.8×10^5 cells per well and incubated overnight at 37°C. Nanocomplexes (in triplicate) were prepared using SLNPs at the previously chosen ratios using 50 nM siRNA (0.067 μg). A positive control consisting of untreated cells was used to represent 100% cell survival. Following incubation, the old medium was replenished with fresh medium (EMEM supplemented with 10% FBS and 1% antibiotics). The nanocomplexes were then introduced to the cells and incubated over 48 h at 37°C. Thereafter, the medium was replaced with 10% MTT solution (5 mg/mL in PBS) in 100 μL of EMEM. The cells were incubated for an additional 4 h at 37°C. The MTT-containing EMEM was removed, and 100 μL of DMSO was pipetted into each well. Absorbance was determined at 570 nm using a Mindray MR-96A microplate reader (Vacutec, Hamburg, Germany), with DMSO as the blank. The cell viability was quantified using the following equation:

$$\text{Cell Viability (\%)} = \left(\frac{\text{Absorbance of Treated Cells}}{\text{Absorbance of Control}} \right) \times 100 \quad (6.2)$$

6.2.10. Caspase 3/7 Assay

The Muse™ Caspase-3/7 kit was utilized to quantify the apoptotic status and the permeability of the cell membrane at various stages of apoptosis, using caspases-3/7 activity and a dead cell dye [28]. The cells (1.8×10^5 cells per well) were prepared as for the MTT assay and treated with the respective nanocomplexes. Following a 48-hour incubation, the cells were rinsed with PBS, trypsinized, and 1 x assay buffer (50 μ L) was introduced. The mixture was mixed by vortexing, followed by the addition of caspase 3/7 (5 μ L). The cells were incubated at 37°C for 30 min, after which caspase 7-AAD working solution (150 μ L) was added. The cells were incubated away from light at room temperature for 5 min. Caspase activity was assessed using a Muse™ cell analyzer (Luminex, TX, USA).

6.2.11. Cellular Uptake Studies

The cellular uptake assay was performed to examine the potential of the PLL-SLNPs to traverse the cellular membrane and localize in the nucleus. The assay used the BLOCK-iT™ fluorescent oligo to provide a means of visualization through its ability to fluoresce. Cells (1.8×10^5 cells per well) were prepared and treated as done for the cytotoxicity assay, except for using 1 μ L BLOCK-iT™ fluorescent oligo (1 mM and 2 mM) instead of the siRNA, which was incubated for 1 h with the SLNPs. The treated cells were incubated overnight. The media was discarded, and PBS (2 x 60 μ L) was used to wash the cells. Cells were viewed under an Olympus CKX41 inverted phase contrast fluorescence microscope (Olympus Corporation, Tokyo, Japan) at an excitation and emission wavelength of 494 nm and 519 nm, respectively. The cells were thereafter lysed with 80 μ L 1x lysis buffer with gentle rocking at 30 rpm for 15 min on a STR 6 platform shaker (Stuart Scientific, Staffordshire, UK). Following this, the cells were dislodged from the wells, and the cell lysates were placed into a 96-well black plate, and the fluorescence was quantified using a Glomax multi-detection System (Promega Biosystems, CA, USA). Protein concentrations were evaluated using the standard bicinchoninic (BCA) assay. The fluorescence readings were normalized against the BCA assay results and expressed as relative fluorescent units (RFU)/mg protein.

6.2.12. Statistical Analysis

Data are reported as means \pm standard deviation (SD, n = 3). Statistical analysis of the mean values was conducted using one-way ANOVA, followed by Dunnett multiple comparison post hoc test. Statistical analyses were carried out with a 95% confidence interval (CI), and results

were considered significant if the p -value was less than 0.05 ($p < 0.05$). Statistical data was collected using GraphPad Prism 9 (GraphPad Inc. San Diego, USA).

6.3. Results

6.3.1. Characterization

6.3.1.1. UV-visible (UV-vis) and FTIR Spectroscopy

While there is a lack of prior literature on the absorbance of specific SLNPs, UV-vis spectroscopy confirmed the successful conjugation with PLL and the observed difference regarding the use of the biological extract, *G.biloba*, and distilled water (Figure 6.4). The excitation peaks and troughs are listed in Table 1. The absorbance maxima for the H₂O-based SLNPs displayed a hypochromic shift (blue shift), while the EGB-based SLNPs exhibited a bathochromic shift (red shift). These slight shifts in absorbance for both SLNPs can be attributed to the successful conjugation of PLL. Conversely, the second peak for the conjugated and un-conjugated SLNPs both portrayed a hypochromic shift. Beyond this, a single trough was created in the absorbance at wavelengths 400 nm and 397 nm for the PLL-conjugated SLNPs (Table 6.1).

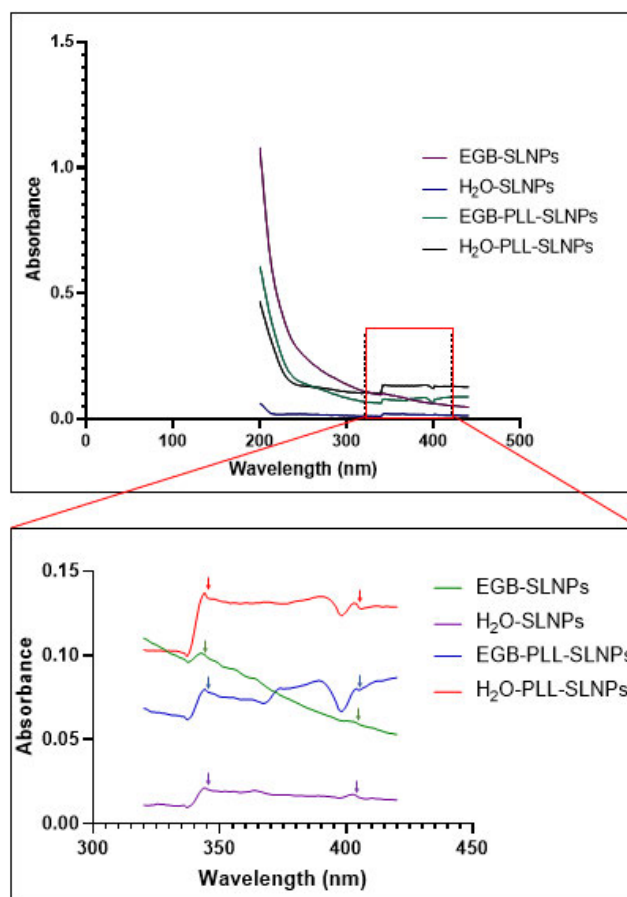


Figure 6.4. UV-vis spectra of EGB-SLNPs, H₂O-SLNPs, EGB-PLL-SLNPs, and H₂O-PLL-SLNPs. The amplified 320-420 nm section shows the peak and trough variations.

Table 6.1. Absorbance peaks and troughs exhibited by the SLNPs.

NANOPARTICLES	PEAK 1	PEAK 2	TROUGH
H ₂ O-SLNPS	343 nm	401 nm	-
H ₂ O-PLL-SLNPS	345 nm	402 nm	400 nm
EGB-SLNPS	345nm	401 nm	-
EGB-PLL-SLNPS	341 nm	404 nm	397 nm

FTIR analysis confirmed the successful bio-synthesis of the SLNPs and the conjugation of poly-L-lysine (PLL) (Figure 6.5, Table 6.2). The broad peak observed at 3297.30 cm⁻¹ in the EGB sample, corresponding to O-H stretching, is retained in the EGB-SLNPs and EGB-PLL-SLNPs with slight shifts, indicating successful encapsulation of EGB within the SLNP matrix [30]. Characteristic peaks for C-H stretching vibrations observed at 2918.90 cm⁻¹ in EGB is present in both EGB-SLNPs and EGB-PLL-SLNPs, confirming the incorporation of EGB's

aliphatic components [31]. The presence of PLL is confirmed by the N-H stretching vibrations (3094.28 cm^{-1}) in EGB-PLL-SLNPs, which is characteristic of the amide groups in PLL [28,32,33]. The C=O stretching vibrations at 1742.15 cm^{-1} in EGB-PLL-SLNPs and H_2O -PLL-SLNPs indicate strong hydrogen bonding and electrostatic interactions between PLL and the lipid components of the SLNPs [31,34].

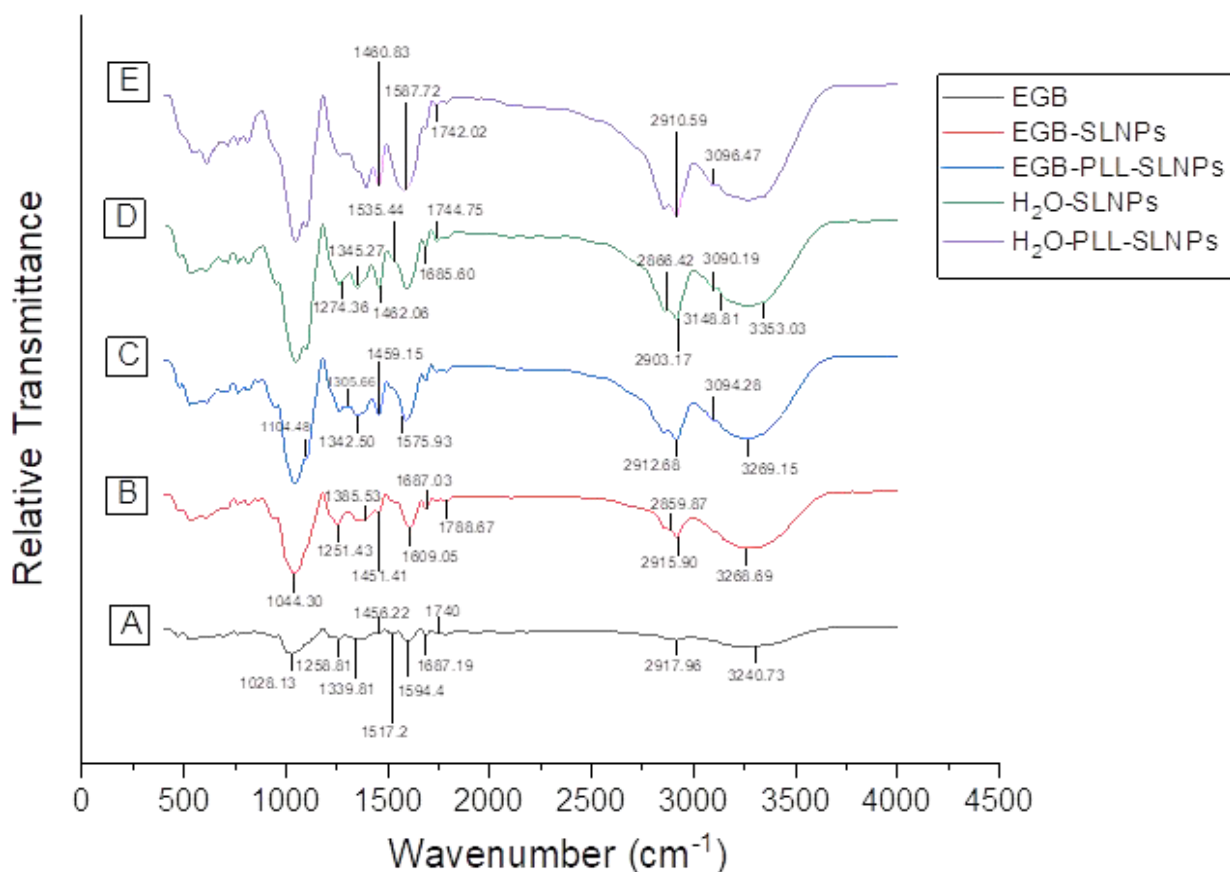


Figure 6.5. FTIR spectra of: (A) EGB, (B) EGB-SLNPs, (C) EGB-PLL-SLNPs, (D) H_2O -SLNPs, and (E) H_2O -PLL-SLNPs.

Table 6.2. The wavenumbers (cm^{-1}) associated with the respective functional groups as confirmed by FTIR [30-32,34-39].

Functional Group	Wavenumber (cm^{-1})	Interpretation
O-H	3297.30	Hydroxyl groups in phenolic compounds
C-H	2918.90	Methyl and methylene groups of lipids
C=O	1789.10	Carbonyl groups
C=C	1674.00	Alkene groups
N-H	1595.40	Amide groups in proteins or peptides
C-O-C	1258.00	Ester and ether linkages
O-H	3268.69	Incorporation of phenolic compounds from EGB
C-H	2915.90, 2859.87	Aliphatic chains in sphingomyelin and cholesterol
C=O	1788.67	Hydrogen bonding, successful encapsulation

C-O	1251.53	Presence of esters and ethers from EGB
N-H	3094.28	Conjugation of PLL to SLNPs
C-H	2912.68	Aliphatic chains in lipids and PLL
C=O	1742.15	Conjugation of PLL to EGB
C-N	1305.66	Amine groups from PLL
O-H	3353.03	Hydration of lipid components
N-H	3148.81, 3090.19	Presence of sphingomyelin within SLNPs
C-H	2903.17	Aliphatic chains in cholesterol and sphingomyelin
C=O	1744.75	Ester groups in the SLNP matrix
N-H	3096.43	Interaction between PLL and the lipid matrix
C=O	1742.01	Electrostatic interactions between lipids and PLL

6.3.1.2. Transmission Electron Microscopy (TEM) and Dynamic Light Scattering (DLS)

All SLNPs were spherical, and most were below 200 nm in size (Figure 6.6), except for the H₂O-PLL-SLNPs (Figure 7.6B), which were above 200 nm under TEM. The EGB-synthesized SLNPs were smaller, with sizes below 120 nm (Figure 6.6A). Upon SLNP conjugation with PLL, no apparent morphological changes were noted. There are observable differences in size in Figure 6.6B, which can be attributed to the binding of PLL to the SLNPs. However, despite these variations, the overall average size of the NPs was observed to be 140 nm.

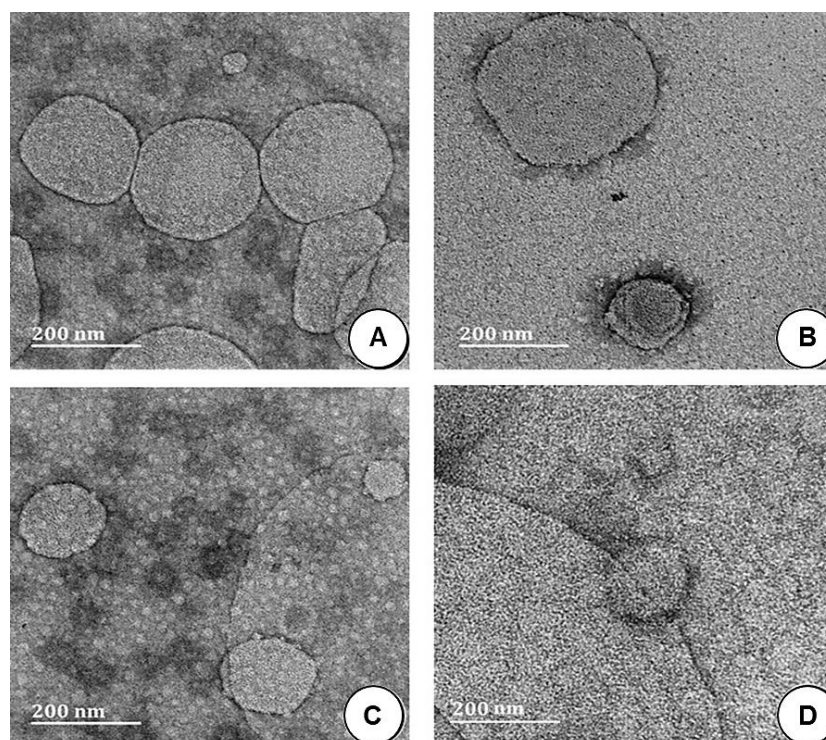


Figure 6.6. TEM micrographs of the SLNPs. (A) H₂O-SLNPs, (B) H₂O-PLL-SLNPs, (C) EGB-SLNPs, (D) EGB-PLL-SLNPs. Scale Bar = 200 nm.

The SLNPs and corresponding nanocomplexes were subjected to DLS to assess their hydrodynamic sizes and zeta potentials to determine their colloidal stability. The results (Table 6.3) portrayed a size range of less than 200 nm, suitable for biomedical applications. The sizes obtained from the TEM were noted to be lower than the hydrodynamic sizes obtained from DLS.

The EGB-SLNPs showed better stability than the H₂O-based SLNPs, which could be due to the natural properties of the EGB in reducing and stabilizing the SLNPs (raw data are reflected in Appendix B1-B6). The zeta potentials increased (>35 mV) upon conjugation to PLL (Table 6.3). The PLL-SLNPs exhibited good stability upon binding to siRNA, promoting their role as suitable nanocarriers. The polydispersity index indicated uniform and monodispersed SLNPs with a lack of aggregation (PDI < 0.1) (Table 6.3) [40,41].

Table 6.3. TEM and DLS nanoparticle and nanocomplex sizes and the zeta potential and polydispersity index (PDI) obtained from DLS.

NPs	TEM	DLS					
		Nanoparticle			Nanocomplex		
	Size (nm ± SE)	Size (nm ± SD)	Zeta Potential (mV) mean ± SD (n = 3)	PDI	Size (nm ± SD)	Zeta Potentia l (mV) mean ± SD (n = 3)	PDI
H ₂ O-SLNPs	180.2 ± 25.3	190.5 ± 13.9	13.1 ± 1.1	0.00 3	-	-	-
H ₂ O-PLL- SLNPs	140.0 ± 1.0	120.4 ± 7.1	35.6 ± 0.3	0.01 3	139.5 ± 35.2	43.3 ± 0.1	0.03 7
EGB-SLNPs	118.3 ± 15.6	122.4 ± 12.7	24.4 ± 1.3	0.01 2	-	-	-
EGB-PLL- SLNPs	93.2 ± 1.0	115.3 ± 10.7	36.8 ± 1.3	0.01 0	128.3 ± 20.3	45.47 ± 0.8	0.02 9

6.3.2. siRNA Binding Studies

6.3.2.1. Ethidium Bromide (EtBr) Intercalation Assay

This assay assessed the PLL-SLNPs' ability to effectively compact the siRNA, preventing premature dissociation from the nanocarrier. This assay is based on the intercalation of EtBr within the siRNA, which fluoresces. The sequential addition of the SLNPs disturbs this intercalation, causing fluorescence quenching until a plateau is attained (Figure 6.7A). The EGB-PLL-SLNPs portrayed a slightly better compaction ability (77.78%) than their H₂O-based counterparts (73.60%). As expected, the non-functionalized SLNPs (Figure 6.7B) (SLNPs without the PLL) could not bind the siRNA. This led to a steady increase in the relative fluorescence, with no fluorescence quenching noted.

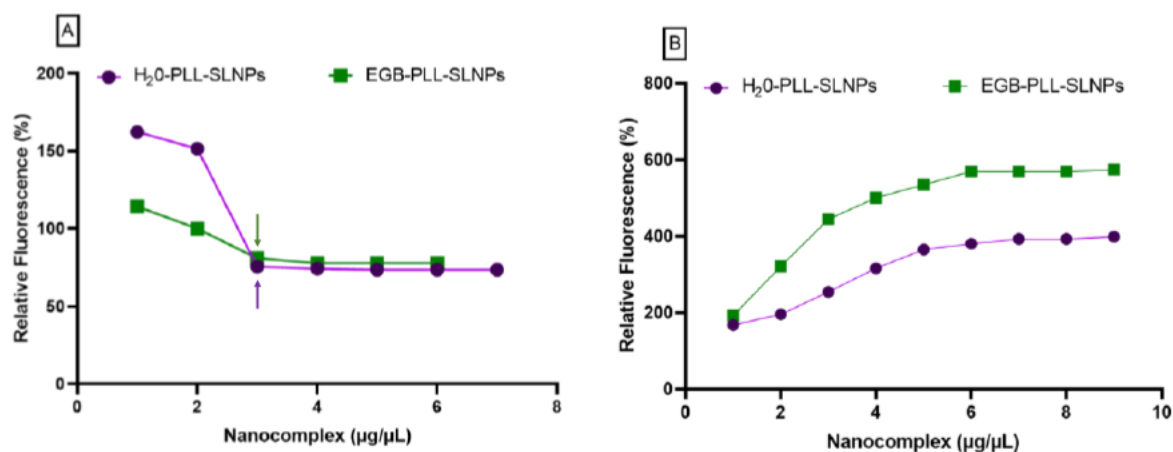


Figure 6.7. Ethidium bromide intercalation assay of (A) EGB- and H₂O-PLL-SLNPs and (B) EGB- and H₂O-SLNPs with siRNA (0.3 µg/µL). The stepwise addition of the SLNPs resulted in a drop in fluorescence until a plateau or point of inflection was reached, as in A. Where no RNA was bound to the SLNPs (B), there was no drop in the fluorescence as in B. Arrows indicate the inflection point in A.

6.3.2.2. Band Shift Electrophoresis

This assay determines the complete binding of the siRNA by the cationic SLNPs due to electrostatic interactions. The optimum binding ratio is established when no free siRNA migrates into the gel, which occurs at a point of electroneutrality [29]. The red box depicts the optimum ratio (w/w) of the PLL-SLNPs (Figure 6.8). The PLL-SLNPs suspended in distilled water bound the siRNA at a slightly lower ratio of 0.2:1 (w/w) compared to the EGB-PLL-SLNPs with a ratio of 0.4:1 (w/w). Both PLL-SLNPs showed good binding abilities with no distinct advantage of either method. The differences in binding efficiencies can be attributed to

the surface charge of the PLL-SLNPs, as a greater positive charge would lead to a better binding potential. This will affect the final binding ratios.

This assay was repeated after 12 months (Figure 6.9) to establish the integrity of the SLNPs after storage at 4°C. The same binding ratios were acquired, suggesting that these SLNPs have a good shelf-life and are relatively stable with no degradation during storage.

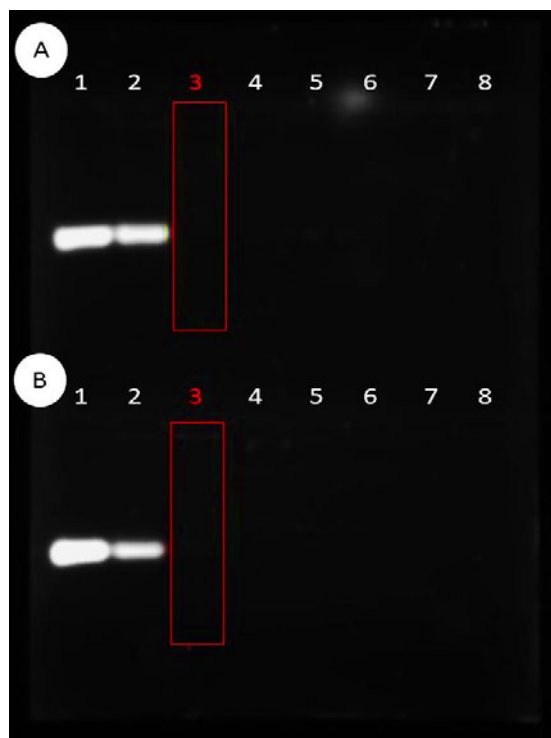


Figure 6.8. The band shift assay. (A) EGB-PLL-SLNPs: Lanes 1 – 8 (0, 0.2, 0.4, 0.6, 0.8, 0.10, 0.12, 0.14 μg) and (B) H₂O-PLL-SLNPs: Lanes 1-8 (0, 0.1, 0.2, 0.3, 0.4, 0.5, 0.6, 0.7 μg). The siRNA was maintained at 0.5 μg . The red boxes indicate the optimum binding ratios, superseded by the supra-optimum ratio and preceded by the sub-optimum ratio.

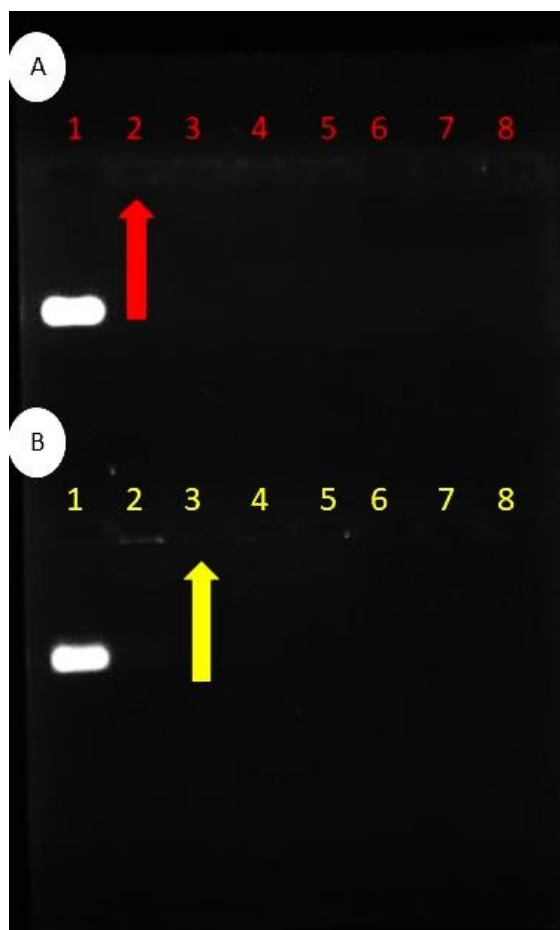


Figure 6.9. The band shift assay after 12 months of storage of the SLNPs at 4 °C. (A) EGB-PLL-SLNPs: Lanes 1 – 8 (0.2, 0.4, 0.6, 0.8, 0.10, 0.12, 0.14 μg) and (B) H₂O-PLL-SLNPs: Lanes 1-8 (0, 0.1, 0.2, 0.3, 0.4, 0.5, 0.6, 0.7 μg). The siRNA was kept constant at 0.5 μg . The red and yellow arrows indicate the optimum binding ratios, superseded by the supra-optimum ratio and preceded by the sub-optimum ratio.

6.3.2.3. RNase A Protection Assay

The protection of the siRNA by the SLNPs is crucial for safe and efficient delivery to the target cells. This assay provides a means of simulating the host environment to determine the extent of protection. The band intensities varied across the ratios. However, the SLNPs protected the siRNA from RNase A digestion compared to the negative control (naked siRNA in lane 2), which was totally degraded and not visible on the gel (Figure 6.10). As previously, this assay was also re-examined after 12 months (Figure 6.11), with similar protection abilities noted, suggesting the good stability of these nanocomplexes.

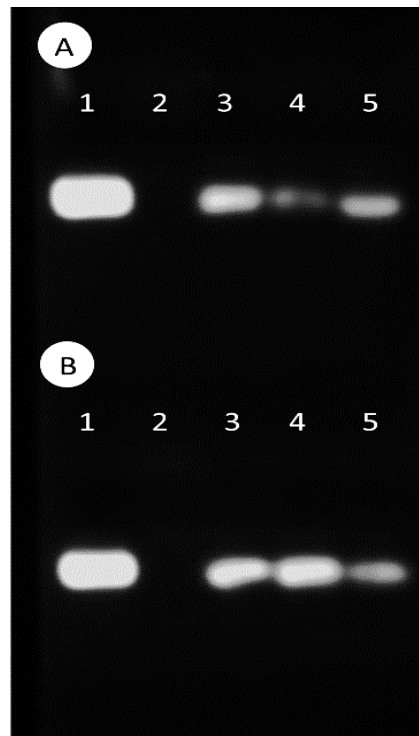


Figure 6.10. The RNase protection assay. In both (A) and (B), Lanes 1 and 2 contain the positive (undigested siRNA) and negative (digested siRNA) controls. (A) EGB-PLL-SLNPs: Lane 3-5 (0.2, 0.4, 0.6 μg) and (B) H₂O-PLL-SLNPs: Lanes 3 – 5 (0.1, 0.2, 0.3 μg). All nanocomplexes were complexed with the targeted siRNA (0.5 μg).

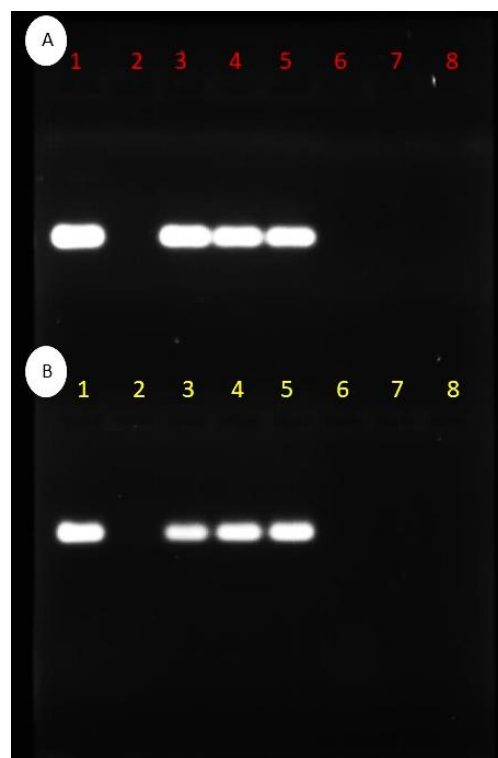


Figure 6.11. Agarose gel images of the RNase protection assay after 12 months of storage of the SLNPs at 4 °C. In both (A) and (B), Lanes 1 and 2 contain positive and negative controls. (A) EGB-PLL-SLNPs: Lane 3-5 (0.2, 0.4, 0.6 μg) and (B) H₂O-PLL-SLNPs: Lanes 3 – 5 (0.1, 0.2, 0.3 μg). All nanocomplexes were complexed with targeted siRNA (0.5 μg).

6.3.3. Mycoplasma Detection

The results of the assay are provided in Figure 6.12. No change was observed in or around the cells, and no mycoplasma was detected. This confirms that the cell lines are uncontaminated, ensuring their suitability and reproducibility for further studies.

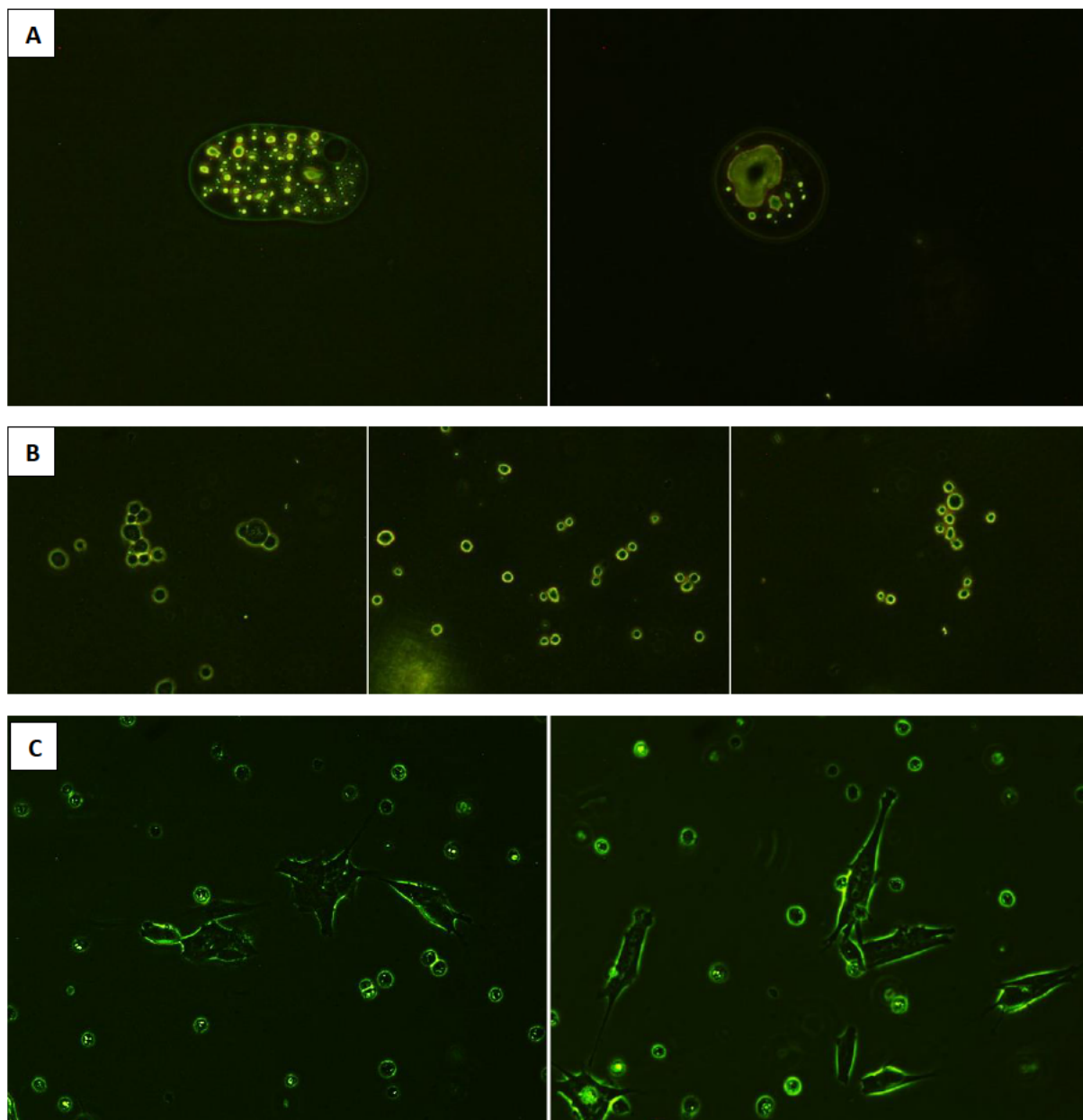


Figure 6.12. Mycoplasma detection. A: The positive control portraying the morphological and optical features of mycoplasma using the mycoplasma MORFS stock suspension. B: The results for the mycoplasma detection in the HEK293 cells. C: The results for the mycoplasma detection in the SH-SY5Y cells.

6.3.4. Cytotoxicity Assay

The MTT colorimetric assay determines cell viability based on the mitochondrial dehydrogenase activity [42]. The HEK293 cells (cell viability > 90%) were able to tolerate all

the nanocomplexes, with the supra-optimum ratio of the EGB-PLL-SLNPs portraying enhanced cellular viability (101.76%) (Figure 6.13A). There was no statistically significant difference in the cytotoxicity between the EGB- and H₂O-based SLNPs. Similarly, the neuroblastoma SH-SY5Y cells maintained high viability, above 85% ($p < 0.001$) (Figure 6.13B).

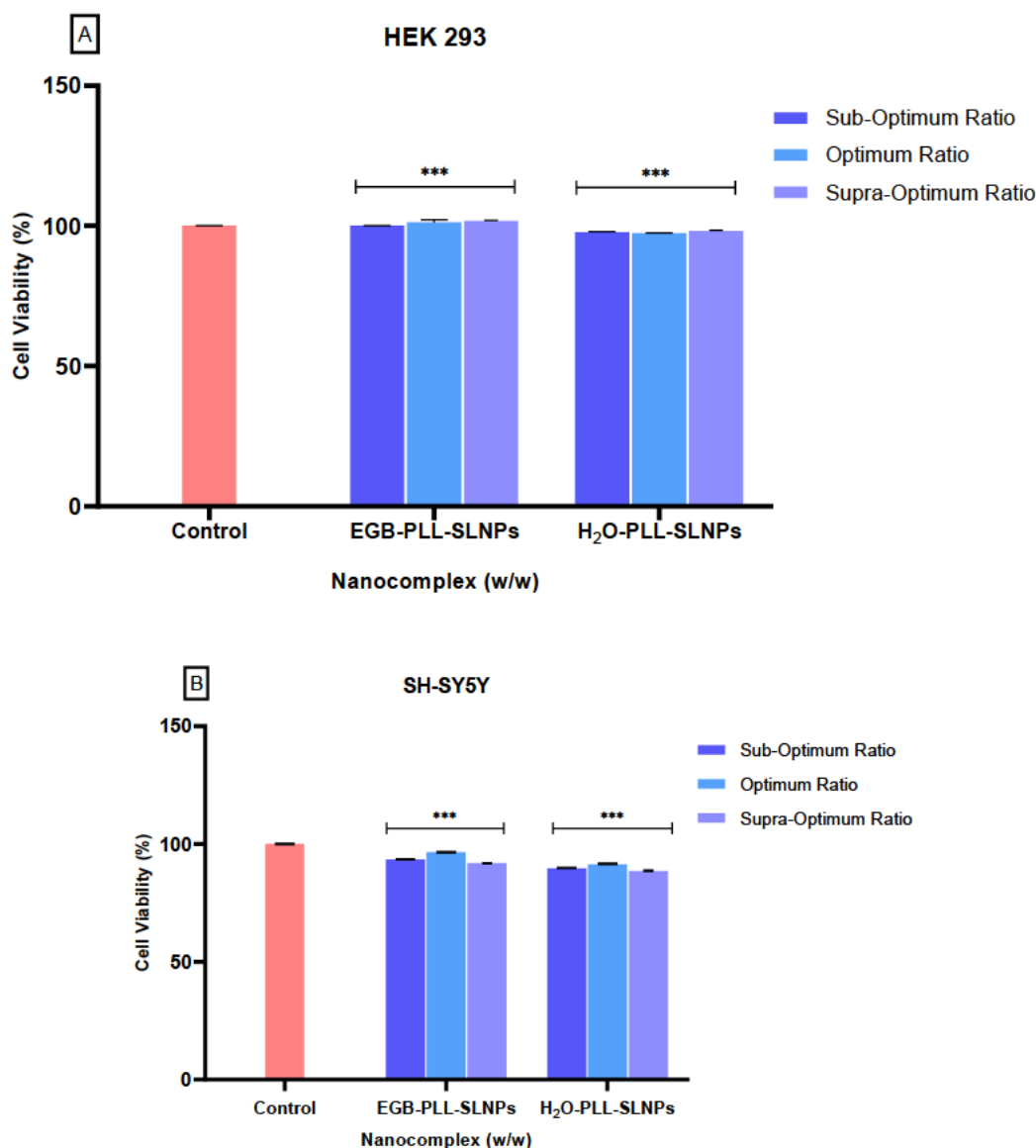


Figure 6.13. The MTT cytotoxicity assay in (A) HEK293 and (B) SH-SY5Y cells. High viability was recorded for all tested ratios, indicating minimal cytotoxicity of the nanocomplexes to both cell lines. Data are presented as means \pm standard deviation ($n = 3$). A significant difference was observed between the treated cells and the control group ($***p < 0.001$; Tukey's multiple comparisons test).

6.3.5. The Caspase 3/7 Assay

The results obtained from the cytotoxicity assay were correlated to the caspase 3/7 assay. The cell survival in the HEK293 cells was high ($> 75\%$) with minimal apoptosis (Figure 6.14A),

similar to the MTT assay. In the SH-SY5Y cells (Figure 6.14B), <11.1% of the cells displayed any apoptotic behavior. Overall, the results correlated closely to that of the MTT assay, with high cell survival noted in the HEK293 and SH-SY5Y cells, suggesting the safety and suitability of these NPs as therapeutic nanocarriers. The apoptosis rate was assessed further (Figure 6.15), with no significant differences being observed between the treatment groups. This suggested that both EGB-PLL-SLNPs and H₂O-PLL-SLNPs did not induce significant apoptosis in these cells.

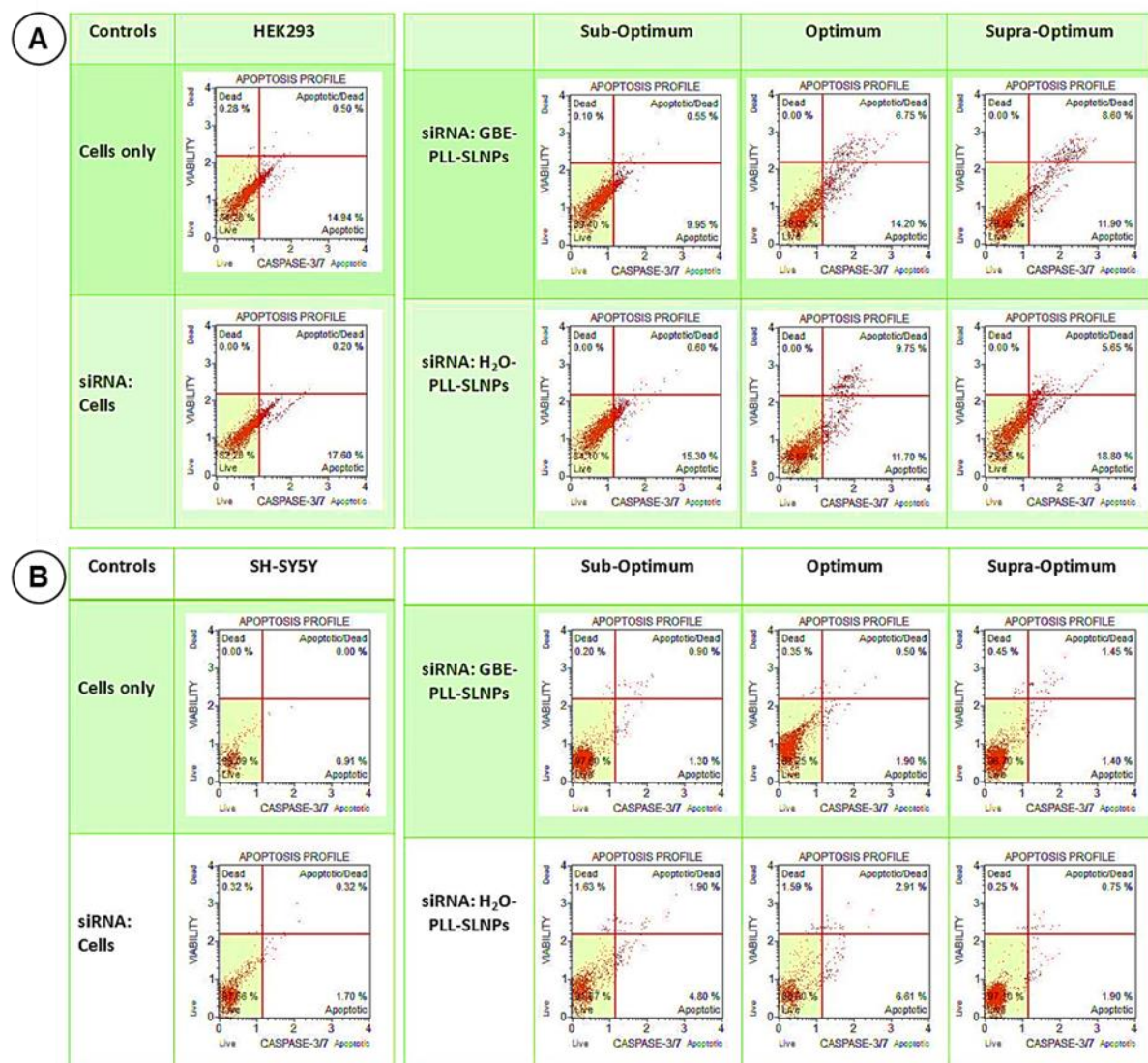


Figure 6.14. Caspase 3/7 activity induced by the nanocomplexes at the three studied ratios in the (A) HEK293 and (B) SH-SY5Y cells. The cytographs depict the apoptotic responses of the HEK293 (A) and SH-SY5Y (B) cells following treatment with the PLL-SLNPs at the sub-optimum, optimum, and supra-optimum ratios. High cell viability (>75%), with minimal apoptosis induction, was noted.

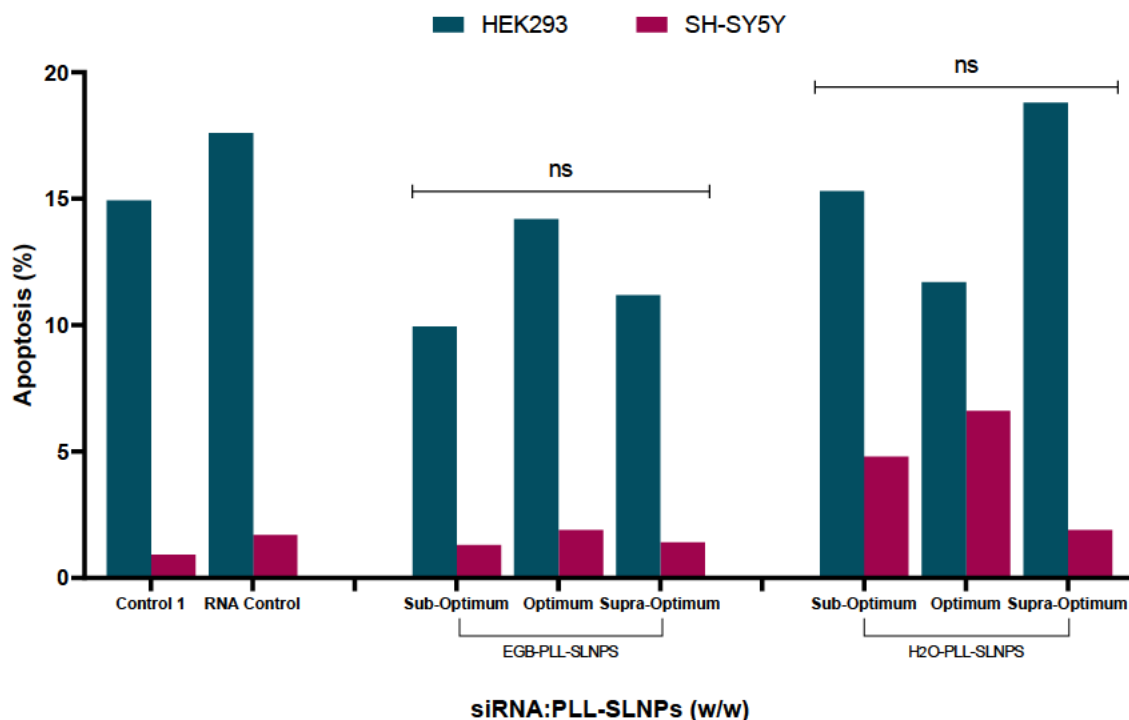


Figure 6.15. Apoptosis Rates in HEK293 and SH-SY5Y cells following treatment with the siRNA: PLL-SLNP nano complexes at the sub-optimum, optimum, and supra-optimum (w/w) ratios. Apoptosis levels were determined from the caspase 3/7 activity recorded. No statistical significance (ns) was observed among all groups, indicating that each treatment maintained the initial apoptosis rate, supporting the safety of the treatments.

6.3.6. Cellular Uptake

The BLOCK-iT™ fluorescent oligo was used to surrogate the therapeutic siRNA and demonstrated significant differences in cellular uptake efficiencies between the tested formulations. Nanocomplexes were formulated at 1:1 and 2:1 (w/w) concentrations of oligo to the SLNPs to ensure binding optimization.

In the HEK293 cells (Figure 6.16), the naked oligo control exhibited low fluorescence (>2000; $p < 0.001$) (Figure 6.16A). Treatment with EGB-PLL-SLNPs at the 1:1 ratio resulted in moderate-high intensity fluorescence (>8000; $p < 0.001$) (Figure 6.16C, Figure 6.17), while the 1:2 ratio showed significantly greater fluorescence (>11000) (Figure 6.16D, Figure 6.17). The SLNPs were visualized primarily in the cytoplasm and around the nuclear region. The H₂O-PLL-SLNPs displayed a similar trend in fluorescence intensity from the 1:1 to 1:2 ratio but with reduced cellular uptake (Figure 6.16 E, F). Notably, SLNP aggregation near the nucleus was observed in cells treated with the 1:2 ratio.

A similar trend was seen in the SH-SY5Y cells (Figure 6.18, Figure 6.19), with greater uptake at the 1:2 ratios for both SLNPs (Figure 6.18 D, E). The EGB-PLL-SLNPs showed better fluorescence at the 1:2 ratio (13623.52; $p < 0.001$) than at the 1:1 ratio (9431.11; $p < 0.001$) (Figure 6.19). The H₂O-PLL-SLNPs exhibited lower overall cellular uptake. Furthermore, the EGB-PLL-SLNPs demonstrated a more uniform distribution and internalization, whereas the H₂O-based nanocomplexes showed less uniformity.

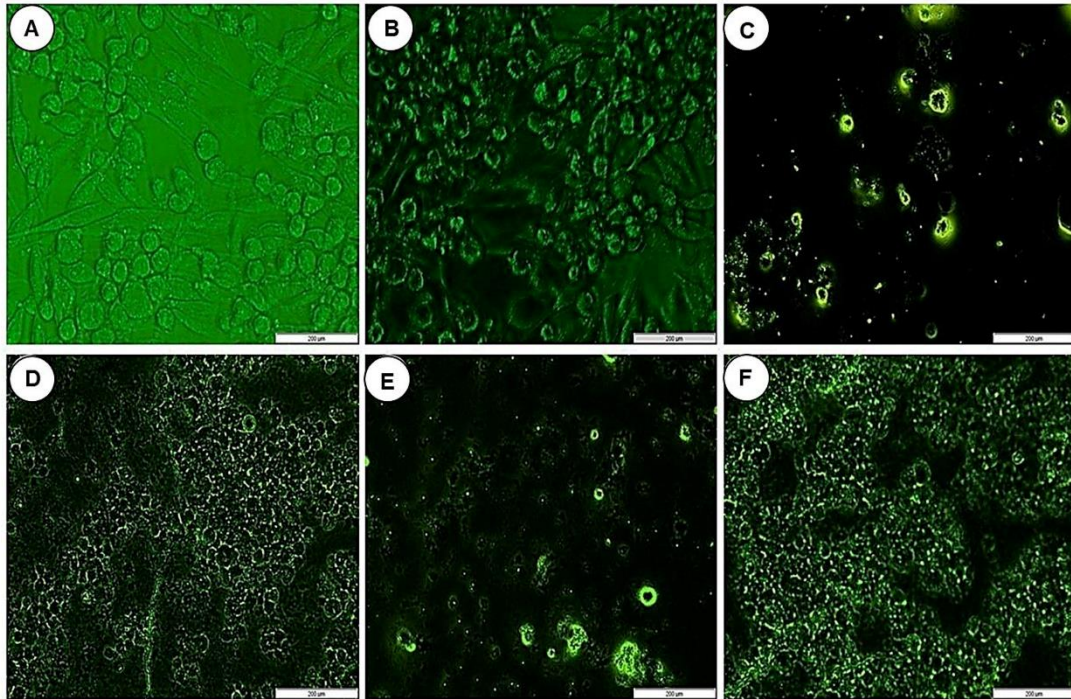


Figure 6.16. Fluorescent images showing cellular uptake in the HEK293 cells. (A) Control of HEK293 cells not treated with the fluorescent oligo, (B) Control of naked Block-IT™ oligo not complexed to the SLNPs, (C) Oligo: EGB-PLL-SLNPs in a 1:1 (w/w) ratio; (D) Oligo: EGB-PLL-SLNPs in a 2:1 (w/w) ratio; (E) Oligo:H₂O-PLL-SLNPs in a 1:1 (w/w) ratio; (F) Oligo:H₂O-PLL-SLNPs in a 2:1 (w/w) ratio. The cells were visualized at 100x magnification. Scale Bar = 200 μ m.

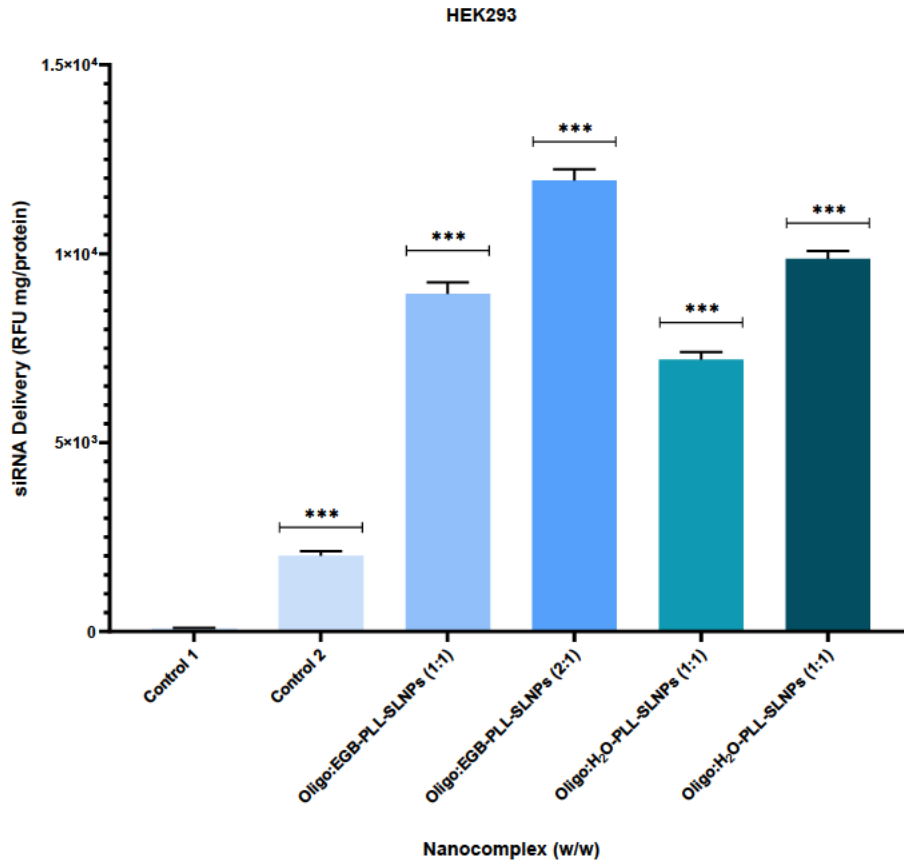


Figure 6.17. HEK293 cells treated with BLOCK-iT™ fluorescent oligo (0.5 and 1.0 μ g) conjugated to PLL-SLNPs at 1:1 and 2:1 (w/w) ratios. Intracellular fluorescence was measured after 24 hours. Control 1 = HEK293 cells only, and control 2 = naked/uncomplexed BLOCK-iT™ fluorescent oligo. Controls were compared to the nanocomplexes (***) $p < 0.001$.

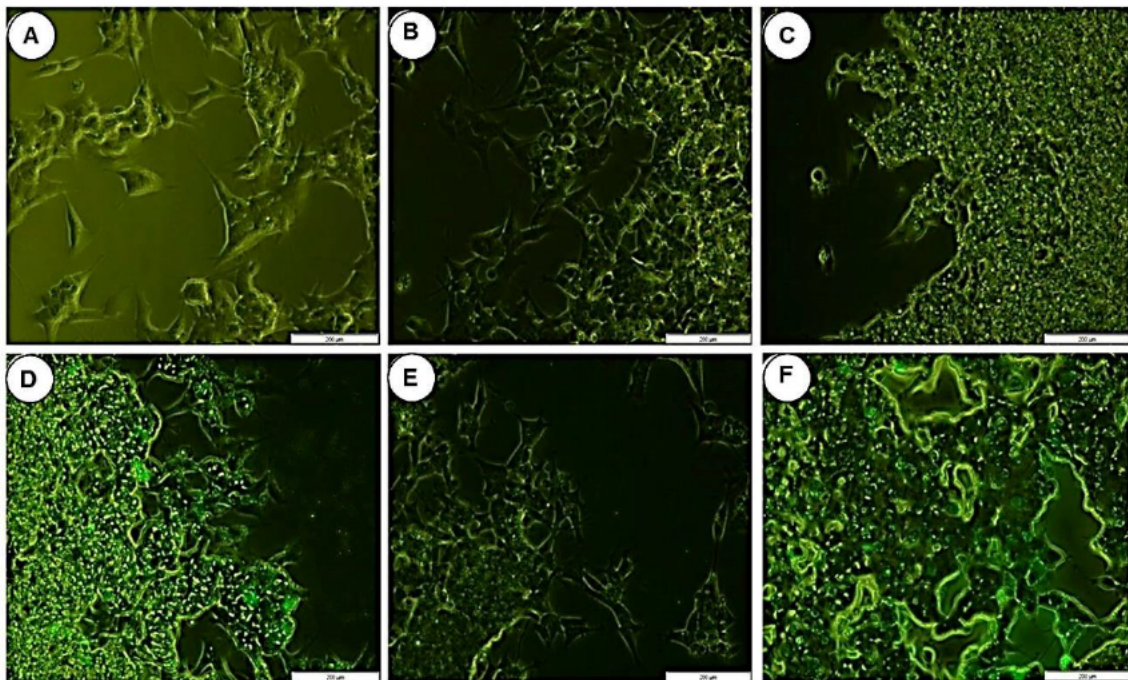


Figure 6.18. Fluorescent images showing cellular uptake in the SH-SY5Y cells. (A) Control of SH-SY5Y cells not treated with the fluorescent oligo, (B) Control of naked Block-IT™ oligo not complexed to the SLNPs, (C) Oligo:EGB-PLL-SLNPs in a 1:1 (w/w) ratio; (D) Oligo:EGB-PLL-SLNPs in a 2:1 (w/w) ratio; (E) Oligo:H₂O-PLL-SLNPs in a 1:1 (w/w) ratio; (F) Oligo:H₂O-PLL-SLNPs in a 2:1 (w/w) ratio. The cells were visualized at 100x magnification. Scale Bar = 200 μm.

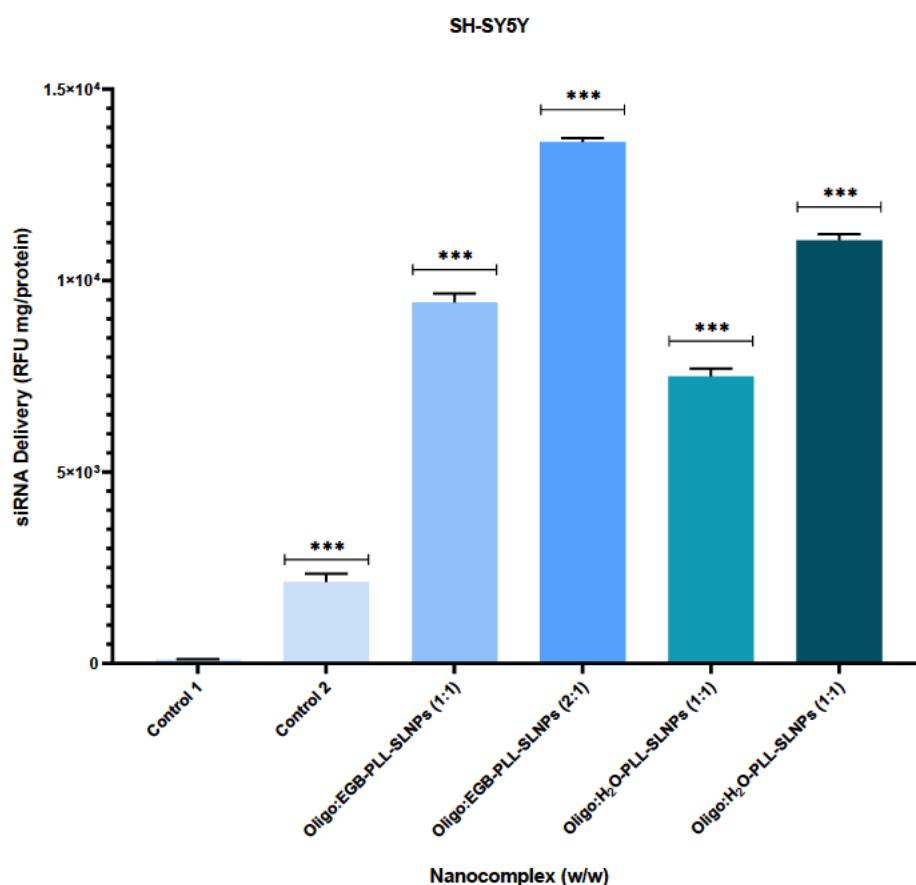


Figure 6.19. SH-SY5Y cells treated with PLL-SLNPs conjugated to BLOCK-iT™ fluorescent oligo (0.5 and 1.0 μg) at 1:1 and 1:2 (w/w) ratios. Intracellular fluorescence was measured after 24 hours. Control 1 = SH-SY5Y cells only, and control 2 = naked BLOCK-iT™ fluorescent oligo. Controls were compared to the nanocomplexes (***) p < 0.001).

The addition of EGB in SLNP formulation was validated due to its superior cellular uptake and distribution, possibly facilitated by the bioactive compounds in EGB, such as flavonoids and terpenoids, which enhanced the interaction between SLNPs and cellular membranes. This will enable a higher intracellular concentration of the siRNA cargo and improve the overall therapeutic efficacy.

6.4. Discussion

The UV-vis and FTIR spectroscopy confirmed the successful formulation and functionalization of the SLNPs. Changes in absorbance maxima for the PLL functionalized SLNPs suggested that the interaction between the SLNPs and PLL resulted in a shift in absorbance without affecting the integrity of the SLNPs. Besides size, ultrastructural morphology and polydispersity are essential for cellular uptake. TEM determined the size of the SLNPs in a dry state, while DLS assessed them in an aqueous state, which attributed to the difference in sizes obtained using these two methods [40,41]. This could also be due to the SLNPs coming together as clusters in the aqueous environment, which were recorded as larger particles under DLS [43]. Such aggregation is possible due to electrostatic interactions between the PLL with anions in solution or hydrophobic interactions between the lipid components [44,45].

Furthermore, the average size is based on the scattered light intensity, which is inherently more sensitive to larger particles due to the r^6 dependence of the scattering intensity on the radius. Consequently, a low number of aggregates could disproportionately affect the average size [45]. While there was a noticeable increase in size, the SLNPs retained their integrity and properties. The appended PLL condensed the SLNPs to a greater extent, which was also reported previously for gold and selenium NPs [46,22]. EGB has been reported to improve the stability of gold [47], copper [48], silver [49], and palladium [19] NPs. The PDI values were all low and well below 0.3. This confirmed the high levels of monodispersity of the SLNPs and their nanocomplexes [41, 42], which was further evidenced by a lack of aggregation in the TEM images. The SLNPs exhibited favourable sizes and zeta potentials for cellular uptake.

Upon PLL conjugation, a higher positive charge was noted for the SLNPs, which was beneficial for siRNA binding and interaction with the anionic cellular membrane [27,28]. Good compaction of the siRNA was noted, which is essential to prevent its premature dissociation from the SLNP. Successful binding of the siRNA to the SLNPs can be attributed to the cationic structure of PLL, allowing its protonated terminal lysine residues and the anionic phosphate groups of the siRNA to interact electrostatically [28,50,51], forming compact nanocomplexes. A recent study reported a similar result using PLL-functionalized gold NPs compared to the unfunctionalized and polyethylene glycol-containing NPs [28]. This compaction efficacy is vital to their *in vitro* and *in vivo* protective ability. This higher compaction for the EGB-based SLNPs may be further due to the functional groups (hydroxyl, carbonyl) from the flavonoid and terpenoids of the extract that interact with the siRNA through hydrogen bonding and electrostatic interactions.

Lipid-mediated siRNA delivery is often challenged by unfavourable interactions with serum nucleases, leading to their degradation before they reach their target site. The SLNPs protected the siRNA from RNase A digestion, suggesting their stability *in vivo*. The SDS used in this study released most of the siRNA from the nanocomplexes, which did not lose their integrity. However, as reported previously, SDS can sometimes show incomplete nucleic acid release [22,29,51]. The MTT cytotoxicity and caspase 3/7 assays confirmed the low cytotoxicity of the SLNPs in the HEK293 and SH-SY5Y cells. Caspases 3/7 are known to execute apoptosis directly and contain a cleavable peptide substrate, Asp-Gly-Val-Asp (DEVD), which is useful for monitoring apoptosis [28]. The MTT and caspase 3/7 assays showed similar trends in both cell lines. The low cytotoxicity can be attributed to the antioxidant properties of EGB, which reduce oxidative stress. The terpenoids and flavonoids in EGB scavenge free radicals and upregulate antioxidant enzymes, providing cytoprotective effects [52]. This counters the oxidative stress induced by free siRNA. EGB has been shown to modulate signaling pathways such as the PI3K/Akt pathway, which is actively involved in cell survival, contributing to its protective effects. Modulating the MAPK/ERK pathway protects neuronal cells from apoptosis [53,54]. EGB also reduces the expression of caspases and Bax (pro-apoptotic proteins) while enhancing the expression of anti-apoptotic proteins (e.g. Bcl-2) [52,55].

This is crucial for PD studies, where oxidative stress and apoptosis are key factors in the degeneration of dopaminergic neurons. The good cell viability and reduced apoptotic profiles in the EGB-PLL-SLNP formulations could provide neuroprotective effects in PD models, suggesting promise as a therapeutic agent. This is achieved through the anti-inflammatory effects of EGB, which inhibit the activation of microglia and astrocytes, key players in neuroinflammation. Wang et al. (2021) demonstrated a 15% reduction in cytotoxicity in lung A549 cells with lower lactate dehydrogenase (LDH) release [56], while Liu et al. (2020) reported a significant decrease in apoptosis and ROS levels in PC12 cells using EGB-incorporated NPs [52]. These studies corroborate the present study's results and highlight the EGB-formulated SLNPs' protective abilities.

Cellular uptake was assessed using the BLOCK-iT™ fluorescent oligo, a fluorescein-labeled, double-stranded RNA duplex, mimicking a siRNA molecule's standard length, configuration, and charge. This molecule is modified to increase stability, permitting the measurement of a fluorescent signal over an extended period. This oligo localizes mainly to the nucleus [57] and can be assessed by measuring the fluorescence. It has been proposed that cholesterol within nanocomplexes could interact with lipids and specific receptors in the cell membrane [58], or

it may be internalized by membrane fusion [59]. Hence, the siRNA can be delivered into the cytoplasm, escaping the endolysosomes. This is important since these intracellular vesicles often lead to the loss of siRNA, with less than 2 % of siRNA entering the cytoplasm. This occurs immediately after cellular uptake and before endosomal maturation and endolysosomal fusion, which results in the degradation of the entrapped siRNA [60]. The cellular uptake studies showed favourable uptake of the SLNPs into the HEK293 and the neuroblastoma SH-SY5Y cells that were used as the Parkinsonian model. The EGB-PLL-SLNPs were more efficiently taken up by the cells than the H₂O-PLL-SLNPs and proposed a dose-dependent nature of internalization. The bioactive compounds enhanced the interaction between the SLNPs and the cellular membrane by integrating into the lipid bilayers, increasing membrane fluidity and permeability, and facilitating the uptake of the SLNPs [61]. EGB stimulates endocytosis due to ginkgolides, which modulate the activity of endocytic pathways, leading to increased internalization of the EGB-PLL-SLNPs. This process allows the siRNA to reach the cytoplasm and exert its therapeutic effects [62].

Flavonoids (quercetin, kaempferol, isorhamnetin) also interact with cell surface receptors, which include the epidermal growth factor (EGFR) and the vascular endothelial growth factor receptors (VEGFR), triggering signaling pathways that enhance endocytosis and internalization of NPs [62]. Terpenoids (ginkgolides, bilobalide) in EGB modulate P2Y receptors involved in purinergic signaling, promoting receptor-mediated endocytosis [63]. Recent studies showed that EGB could enhance cellular uptake by modulating oxidative stress and inflammation pathways [43,65].

These studies further support our findings that EGB-based SLNPs offer good cellular uptake and therapeutic benefits. Overall, our results describe a safe, biocompatible, and efficient nano-delivery system capable of delivering therapeutics to Parkinsonian cells while maintaining exceptional cellular viability. However, a few limitations were identified in this study. First, the experiments were conducted *in vitro* using the HEK293 and SH-SY5Y cell lines, which may not fully replicate the complexity of an *in vivo* environment. Hence, further *in vivo* studies are necessary to evaluate the efficacy and safety of these EGB-PLL-SLNPs in a more complex biological system, including interactions with the blood-brain barrier. There is a need to examine if any immune responses were produced in response to the nanocomplexes. While the study demonstrated efficient siRNA binding and delivery, the long-term effects and stability of these SLNPs within the cellular environment were not assessed. The analysis of intracellular siRNA release and localization can provide insights into the delivery mechanism and the

subsequent gene-silencing efficacy. These limitations highlight the need for further studies to fully establish the therapeutic potential of EGB-PLL-SLNPs for Parkinson's disease.

6.5. Conclusions

The present study described the successful synthesis, characterization, cytotoxicity, and cellular uptake of the PLL-SLNPs with and without EGB. The synergism between the components of the SLNPs provided a highly efficient vehicle for the safe delivery of the siRNA. The SLNPs were well tolerated in the embryonic kidney and the neuroblastoma cells, as evidenced by the cytotoxicity and the caspase 3/7 assays. Including the EGB further enhanced the protective ability, reducing apoptosis while improving cell viability. Although this study had positive outcomes, more evidence to support the benefits of using the EGB is needed. This study provides proof of concept for using PLL-SLNPs in gene delivery, warranting further investigation into their therapeutic potential in examining gene silencing in the Parkinson's cell model.

References

1. Akel, H.; Ismail, R.; Katona, G.; Sabir, F.; Ambrus, R.; Csóka, I. A comparison study of lipid and polymeric nanoparticles in the nasal delivery of meloxicam: Formulation characterization and in vitro evaluation. *International Journal of Pharmaceutics.*, **2021**, 604, 120724. [10.1016/j.ijpharm.2021.120724](https://doi.org/10.1016/j.ijpharm.2021.120724).
2. Balgobind, A.; Daniels, A.; Ariatti, M.; Singh, M. HER2/neu oncogene silencing in a Breast Cancer Cell Model using Cationic Lipid-Based Delivery Systems. *Pharmaceutics.*, **2023**, 15, 1190. <https://doi.org/10.3390/pharmaceutics15041190>
3. Parhi, R.; Suresh, P. Preparation and characterization of solid lipid nanoparticles-a review. *Current Drug Discovery Technologies.*, **2012**, 9, 2–16. <https://doi.org/10.2174/157016312799304552>.
4. Habib, S.; Singh, M. Recent advances in lipid-based nanosystems for gemcitabine and gemcitabine–combination therapy. *Nanomaterials.*, **2021**, 11, 597. <https://doi.org/10.3390/nano11030597>.
5. Mohammadi-Samani, S.; Ghasemiyeh, P. Solid lipid nanoparticles and nanostructured lipid carriers as novel drug delivery systems: Applications advantages and disadvantages. *Research in Pharmaceutical Sciences.*, **2018**, 13, 288–303. <https://doi.org/10.4103/1735-5362.235156>.
6. Pardeshi, C.; Rajput, P.; Belgamwar, V.; Tekade, A.; Patil, G.; Chaudhary, K.; et al. Solid lipid based nanocarriers: An overview. *Acta Pharmaceutica.*, **2012**, 62, 433–472. <https://doi.org/10.2478/v10007-012-0040-z>.
7. Montoto, S.; Muraca, G.; Ruiz, M.E. Solid Lipid Nanoparticles for Drug Delivery: Pharmacological and Biopharmaceutical Aspects. *Frontiers in Molecular Biosciences.*, **2020**, 7, 587997. <https://doi.org/10.3389/fmolb.2020.587997>.
8. Jafari, F.; Khodabakhshi, S. Mg(hso4)2/sio2 as a highly efficient catalyst for the green preparation of 2-aryl-1,3-dioxalanes/dioxanes and linear acetals. *Organic Chemistry International*, **2012**, 2012, 1-5. <https://doi.org/10.1155/2012/475301>.

9. Reddy, A.; Parthiban, S.; Vikneswari, A.; Senthilkumar, G. A modern review on solid lipid nanoparticles as novel controlled drug delivery system. *International Journal of Research in Pharmaceutical and Nano Sciences.*, **2014**, 3, 313–325.
10. Reddy, J.S.; Venkateswarlu, V. Novel delivery systems for drug targeting to the brain. *Drugs of the Future.*, **2004**, 29, 63–83. <https://doi.org/10.1358/dof.2004.029.01.872585>.
11. D'Angelo, G.; Moorthi, S.; Luberto, C. Role and function of sphingomyelin biosynthesis in the development of cancer. *Advances in Cancer Research.*, **2018**, 140: 61–96. <https://doi.org/10.1016/bs.acr.2018.04.009>.
12. Bienias, K.; Fiedorowicz, A.; Sadowska, A.; Prokopiuk, S.; Car, H. Regulation of sphingomyelin metabolism. *Pharmacological Reports.*, **2016**, 68, 570–581. <https://doi.org/10.1016/j.pharep.2015.12.008>.
13. Ogretmen, B. Sphingolipid metabolism in cancer signaling and therapy. *Nature Reviews Cancer.*, **2018**, 18, 33–50. <https://doi.org/10.1038/nrc.2017.96>.
14. Bartke, N.; Hannun, Y.A. Bioactive sphingolipids: metabolism and function. *Journal of Lipid Research.*, **2009**, 50, S91–S96. <https://doi.org/10.1194/jlr.R800080-JLR200>.
15. Slotte, J.P. Biological functions of sphingomyelins. *Progress in Lipid Research.*, **2013**, 52, 424–437. <http://dx.doi.org/10.1016/j.plipres.2013.05.001>.
16. Ariga, T. The Pathogenic Role of Ganglioside Metabolism in Alzheimer's Disease-Cholinergic Neuron-Specific Gangliosides and Neurogenesis. *Molecular Neurobiology.*, **2017**, 54, 623–638. <https://doi.org/10.1007/s12035-015-9641-0>.
17. Ward, M.C.; Read, M.L.; Seymour, L.W. Systemic circulation of poly(L-lysine)/DNA vectors is influenced by polycation molecular weight and type of DNA: differential circulation in mice and rats and the implications for human gene therapy. *Blood.*, **2001**, 97, 2221–2229.
18. Liang, W.; Xu, W.; Zhu, J.; Zhu, Y.; Gu, Q.; Li, Y.; et al. *Ginkgo biloba* extract improves brain uptake of ginsenosides by increasing blood-brain barrier permeability via activating A1 adenosine receptor signaling pathway. *Journal of Ethnopharmacology.*, **2020**, 246, 112243. <https://doi.org/10.1016/j.jep.2019.112243>.
19. Cui, Y.; Lai, X.; Liu, K.; Liang, B.; Ma, G.; Wang, L. *Ginkgo biloba* leaf polysaccharide stabilized palladium nanoparticles with enhanced peroxidase-like property for the colorimetric detection of glucose. *RSC Advances.*, **2020**, 10, 7012–7018. <https://doi.org/10.1039/d0ra00680g>.
20. Zauner, W.; Ogris, M.; Wagner, E. Polylysine-based transfection systems utilising receptor-mediated delivery. *Advanced Drug Delivery Reviews.*, **1998**, 30, 97–113.
21. Kadlecova, Z.; Rajendra, Y.; Matasci, M.; Baldi, L.; Hacker, D.L.; Wurm, F.M.; et al. DNA delivery with hyperbranched polylysine: a comparative study with linear and dendritic polylysine. *Journal of Controlled Release.*, **2013**, 169, 276–288. <https://doi.org/10.1016/j.jconrel.2013.01.019>.
22. Naidoo, S.; Daniel, A.; Habib, S.; Singh, M. Poly-L-Lysine–Lactobionic Acid-Capped Selenium Nanoparticles for Liver-Targeted Gene Delivery. *International Journal of Molecular Sciences.*, **2022**, 23, 1492. <https://doi.org/10.3390/ijms23031492>.
23. Venkatas, J.; Daniels, A.; Singh, M. The optimization of curcumin-capped Gold Nanoparticle synthesis for FLuc-mRNA Delivery to Cervical Cancer Cells in vitro. *Biointerface Research in Applied Chemistry.*, **2023**, 13, 484. <https://doi.org/10.33263/BRIAC13.5.484>.
24. Sajid, M.I.; Moazzam, M.; Kato, S.; Yeseom Cho, K.; Tiwari, R.K. Overcoming Barriers for siRNA Therapeutics: From Bench to Bedside. *Pharmaceuticals.*, **2020**, 13, 294.
25. Huang, K.; Lai, Y.; Chern, G.; Huang, S.; Tsai, C.; Sung, Y. et al. Galactose derivative-modified nanoparticles for efficient siRNA delivery to hepatocellular carcinoma. *Biomacromolecules.*, **2018**, 19, 2330–2339. <https://doi.org/10.1021/acs.biomac.8b00358>.

26. Cheng, C.C.; Yang, Y.L.; Liao, K.H.; Lai, T.W. Adenosine receptor agonist NECA increases cerebral extravasation of fluorescein and low molecular weight dextran independent of blood–brain barrier modulation. *Scientific Reports.*, **2016**, 6, 23882. <https://doi.org/10.1038/srep23882>.
27. Maiyo, F.; Singh, M. Folate-Targeted mRNA Delivery Using Chitosan-Functionalized Selenium Nanoparticles: Potential in Cancer Immunotherapy. *Pharmaceuticals.*, **2019**, 12, 164. <https://doi.org/10.3390/ph12040164>.
28. Morsin, M.; Nafisah, S.; Sanudin, R.; Razali, N.L.; Mahmud, F; Soon CF. The role of positively charge poly-L-lysine in the formation of high yield gold nanoplates on the surface for plasmonic sensing application. *PLoS One.*, **2021**, 16, e0259730. <https://doi.org/10.1371/journal.pone.0259730>.
29. Venkatas, J.; Singh, M. Curcumin-reduced gold nanoparticles facilitate IL-12 delivery to a cervical cancer in vitro cell model. *Nanomedicine.*, **2023**, 18, 945-960. <https://doi.org/10.2217/nmm-2023-0076>.
30. Singh, M. Assessing nucleic acid: Cationic nanoparticle interaction for gene delivery. In *Bio-Carrier Vectors*; Narayanan K; Ed.; Springer: New York; NY; USA, **2021**, 2211, 43–55.
31. Stuart, B. Infrared Spectroscopy: Fundamentals and Applications. *John Wiley & Sons*, **2004**. <https://doi.org/10.1002/0470011149>.
32. Bellamy, L.J. The Infrared Spectra of Complex Molecules. *Springer*, **1980**. <https://doi.org/10.1007/978-94-011-6520-4>.
33. Shang, L.; Nienhaus, K.; Nienhaus, G.U. Engineered nanoparticles interacting with cells: size matters. *J Nanobiotechnol.*, **2014**, 12. <https://doi.org/10.1186/1477-3155-12-5>.
34. Clayton, K.N.; Salameh, J.W.; Wereley, S.T.; Kinzer-Ursem, T.L. Physical characterization of nanoparticle size and surface modification using particle scattering diffusometry. *Biomicrofluidics*, **2016**, 10, 054107. <https://doi.org/10.1063/1.4962992>
35. Gaur, M.; Tripathi, M.; Lal, R.K. FTIR and Raman spectra analysis of polyherbal formulation used in treatment of neurodegenerative disorders. *Spectrochimica Acta Part A: Molecular and Biomolecular Spectroscopy.*, **2016**, 153, 119-126. <https://doi.org/10.1016/j.saa.2015.08.035>.
36. Chauhan, N.; Dhanalakshmi, S.; Rani, S. Characterization and evaluation of *Ginkgo biloba* extract for antioxidant and antimicrobial activity. *Journal of Chemical and Pharmaceutical Research*, **2018**, 10(3), 18-25.
37. Ahmad, A.; Husain, A.; Mujeeb, M.; Khan, S.A.; Najmi, A.K.; Siddique, N.A.; et al. A review on therapeutic potential of *Ginkgo biloba*. *Phytomedicine*, **2013**, 20, 253-271. <https://doi.org/10.1016/j.phymed.2012.09.018>.
38. Zhang, L.; Zhang, Y.; Zhong, C. Characterization and bioactivity analysis of *Ginkgo biloba* leaf extract nanoparticles. *Journal of Nanoscience and Nanotechnology*, **2019**, 19, 2307-2315. <https://doi.org/10.1166/jnn.2019.15761>.
39. Lee, J.H.; Park, J.S. FTIR spectroscopy study of sphingomyelin-cholesterol solid lipid nanoparticles for drug delivery applications. *International Journal of Pharmaceutics.*, **2020**, 587, 119693. <https://doi.org/10.1016/j.ijpharm.2020.119693>.
40. Lin, L.Z.; Harnly, J.M. Phenolic component profiles of mustard greens; Yu choy; and 15 other Brassica vegetables. *Journal of Agricultural and Food Chemistry*, **2007**, 55, 2833-2840. <https://doi.org/10.1021/jf0634045>.
41. David, L.L.; Daniels, A.; Habib, S.; Singh, M. Gold Nanoparticles in Transferrin-targeted dual-drug delivery in vitro. *Journal of Drug Delivery Science and Technology*, **2023**, 90, 105168. <https://doi.org/10.1016/j.jddst.2023.105168>.

42. Zenze, M.; Singh, M. Receptor targeting using copolymer-modified gold nanoparticles for pCMV-Luc gene delivery to liver cancer cells in vitro. *International Journal of Molecular Sciences*, **2024**, *25*, 5016. <https://doi.org/10.3390/ijms25095016>.
43. Mosmann, T. Rapid colorimetric assay for cellular growth and survival: application to proliferation and cytotoxicity assays. *Journal of Immunological Methods*, **1983**, *65*, 55–63. [https://doi.org/10.1016/0022-1759\(83\)90303-4](https://doi.org/10.1016/0022-1759(83)90303-4).
44. Filipe, V.; Hawe, A.; Jiskoot, W. Critical evaluation of nanoparticle tracking analysis (NTA) by NanoSight for the measurement of nanoparticles and protein aggregates. *Pharmaceutical Research*, **2010**, *27*, 796-810. <https://doi.org/10.1007/s11095-010-0073-2>.
45. Gallego-Urrea, J.A.; Tuoriniemi, J.; Hassellöv, M. Applications of particle-tracking analysis to the determination of size distributions and concentrations of nanoparticles in environmental; biological and food samples. *Trends in Analytical Chemistry*, **2011**, *30*, 473-483. <https://doi.org/10.1016/j.trac.2011.01.005>.
46. Guo, Y.; Ma, Y.; Xu, L.; Li, J.; Yang, W. Conformational change induced reversible assembly/disassembly of poly-L-lysine-functionalized gold nanoparticles. *Journal of Physical Chemistry*, **2007**, *111*, 9172–9176. <https://doi.org/10.1021/jp072012d>.
47. Zha, J.; Dong, C.; Wang, X.; Zhang, X.; Xiao, X.; Yang, X. Green synthesis and characterization of monodisperse gold nanoparticles using *Ginkgo biloba* leaf extract. *Optik.*, **2017**, *144*, 511–521. <https://doi.org/10.1016/j.ijleo.2017.06.088>.
48. Nasrollahzadeh, M.; Sajadi, S.M. Green synthesis of copper nanoparticles using *Ginkgo biloba* L. leaf extract and their catalytic activity for the Huisgen [3 + 2] cycloaddition of azides and alkynes at room temperature. *Colloid Interface Science*, **2015**, *457*, 141–147. <https://doi.org/10.1016/j.jcis.2015.07.004>.
49. Ren, Y.; Yang, H.; Wang, T.; Wang, C. Green synthesis and antimicrobial activity of monodisperse silver nanoparticles synthesized using *Ginkgo biloba* leaf extract. *Physics Letters A.*, **2016**, *380*, 3773–3777. <https://doi.org/10.1016/j.physleta.2016.09.029>.
50. Verma, A.; Stellacci, F. Effect of Surface Properties on Nanoparticle–Cell Interactions. *Small*, **2010**, *6*, 12-21. <https://doi.org/10.1002/sml.200901158>.
51. Akinyelu, J.; Singh, M. Chitosan stabilized Gold-Folate-Poly(lactide-co-glycolide) Nanoplexes Facilitate Efficient Gene Delivery in Hepatic and Breast Cancer Cells. *Journal of Nanoscience and Nanotechnology*, **2018**, *18*, 4478–4486. <https://doi.org/10.1166/jnn.2018.15286>.
52. Liu, Y.; Sun, Z.; Zhang, J. *Ginkgo biloba* extract-loaded polymeric nanoparticles reduce oxidative stress and apoptosis in PC12 cells. *Neurochemistry International*, **2020**, *137*, 104748. <https://doi.org/10.1016/j.neuint.2020.104748>.
53. Zhao, Q.; Dong, X.; Hu, X. *Ginkgo biloba* extract promotes cell proliferation and reduces UV-induced cytotoxicity in human dermal fibroblasts. *Photodermatology; Photoimmunology & Photomedicine*, **2019**, *35*, 239-246. <https://doi.org/10.1111/phpp.12460>.
54. Ahmad, S.; Ullah, F.; Ayaz, M. *Ginkgo biloba* extract: An overview of its biological potentials. *Clinical Phytoscience*, **2020**, *6*, 12-18. <https://doi.org/10.1186/s40816-020-00213-5>.
55. Chandrasekaran, V.; Deepalakshmi, K.; Somasundaram, S.T. Protective effect of *Ginkgo biloba* extract against oxidative stress-induced neurotoxicity in SH-SY5Y cells. *Journal of Neurochemistry*, **2021**, *158*, 569-582. <https://doi.org/10.1111/jnc.15398>.
56. Wang, J.; Li, M.; Zhu, L. Enhanced viability of A549 cells by *Ginkgo biloba* extract-loaded nanoparticles. *Journal of Biomedical Nanotechnology*, **2021**, *17*, 465-472. <https://doi.org/10.1166/jbn.2021.3055>.

57. Fisher, T.L.; Terhorst, T.; Cao, X.; Wagner, R.W. Intracellular disposition and metabolism of fluorescently-labeled unmodified and modified oligonucleotides microinjected into mammalian cells. *Nucleic Acids Research*, **1993**, 21, 3857-3865.
58. Pozzi, D.; Marchini, C.; Cardarelli, F.; Amenitsch, H.; Garulli, C.; Bifone, A.; et al. Transfection efficiency boost of cholesterol-containing lipoplexes. *Biochimica et Biophysica Acta (BBA) – Biomembranes*, **2012**, 1818, 2335-2343.
59. Gilleron, J.; Querbes, W.; Zeigerer, A.; Borodovsky, A.; Marsico, G.; Schubert, U.; et al. Image-based analysis of lipid nanoparticle-mediated siRNA delivery; intracellular trafficking and endosomal escape. *Nature Biotechnology*, **2013**, 31, 638.
60. Wittrup, A.; Ai, A.; Liu, X.; Hamar, P.; Trifonova, R.; Charisse, K.; et al. Visualizing lipid-formulated siRNA release from endosomes and target gene knockdown. *Nature Biotechnology*, **2015**, 33, 870.
61. Jiang, H.; Wang, J.; Rogers, J.; Xie, J. *Ginkgo biloba* extract in Alzheimer's disease: From action mechanisms to medical practice. *International Journal of Molecular Sciences*, **2011**, 12, 764-797.
62. Wang, Q.; Li, X.; Li, Y.; Chen, B.; Zhang, T. Role of flavonoids in enhancing receptor-mediated endocytosis for targeted drug delivery. *Journal of Nanomedicine & Nanotechnology*, **2019**, 10, 500-512. <https://doi.org/10.4172/2157-7439.1000521>.
63. Zhang, L.; Yang, X.; Chen, Y.; Zhang, T.; Xu, W.; Zhao, X. Terpenoids in *Ginkgo biloba* enhance receptor-mediated siRNA delivery in neurodegenerative disease models. *Neurotherapeutics*, **2020**, 17, 715-728. <https://doi.org/10.1007/s13311-020-00844-9>.
64. Fang, X.; Zhang, Y.; Li, Y.; Yang, Z.; Wang, L. *Ginkgo biloba* extract attenuates the disruption of pro- and anti-inflammatory balance of peripheral blood in arsenism patients by decreasing hypermethylation of the Foxp3 promoter region. *Biological Trace Element Research*, **2022**, 200, 4967-4976. <https://doi.org/10.1007/s12011-021-03003-6>.
65. Allmann, S.; Li, J.; Hou, Z.; Fan, Z. *Ginkgo biloba* extract enhances nanoparticle uptake in hepatocytes through oxidative stress modulation. *Nucleic Acids Research*, **2020**, 48, 12085-12101. <https://doi.org/10.1093/nar/gkaa493>.

Refer to Appendix C4 for the Turnitin Report.

Chapter 7

Targeting the LRRK2 G2019S Mutation of Parkinson's Disease: The Therapeutic Efficiency of Bio-Synthesized Solid Lipid Nanoparticles for siRNA-Mediated Gene Therapy

Targeting the LRRK2 G2019S Mutation of Parkinson's Disease: The Therapeutic Efficiency of *Bio*-Synthesized Solid Lipid Nanoparticles for siRNA-Mediated Gene Therapy

Abstract. Parkinson's disease (PD) is a progressive neurodegenerative disorder closely associated with the LRRK2 G2019S mutation, which exacerbates kinase activity, disrupts mitochondrial function, increases reactive oxygen species (ROS) production, and impairs DNA repair mechanisms. This study investigates the efficacy of using *Ginkgo biloba* extract (EGB)-in the synthesis of sphingomyelin-cholesterol-containing solid lipid nanoparticles (SLNPs) functionalized with poly-L-lysine (EGB-PLL-SLNPs) as a delivery system for siRNA targeting the LRRK2 G2019S mutation. PLL-SLNPs suspended in H₂O was used as a comparator. Comprehensive assays, including MTT and flow cytometry using the MUSE analyzer for Caspase 3/7, mitochondrial potential, DNA damage, and oxidative stress, were performed on wild-type and transformed SH-SY5Y and HEK293 cell lines. The results showed that EGB-PLL-SLNPs significantly improved mitochondrial health by reducing depolarized and dead cells by 47.31% and enhancing overall cell viability, indicating a protective effect against cell damage and stress. Furthermore, ROS levels were decreased by 51.39%, DNA damage was reduced by 49.90%, and kinase activity was lowered by 56.08% compared to H₂O-PLL-SLNPs. The flavonoids and terpenoids in EGB, such as quercetin and kaempferol, played a crucial role in stabilizing mitochondrial membrane potential, promoting ATP production, and upregulating genes involved in mitochondrial biogenesis. The combined therapeutic action of EGB with siRNA-mediated gene silencing highlights the promise of EGB-PLL-SLNPs as a powerful approach for treating Parkinson's disease. These findings offer compelling evidence of superior therapeutic outcomes, positioning biosynthesized PLL-SLNPs as a promising advancement in the treatment of PD.

Keywords: Parkinson's disease; gene therapy; siRNA; *Ginkgo biloba*; SLNPs; nanomedicine; LRRK2 G2019S.

7.1. Introduction

Parkinson's disease (PD) is the second most common neurodegenerative disorder globally, with a prevalence of 0.2% [1]. It is characterized by the progressive loss of dopaminergic neurons (mDAs) in the midbrain, particularly in the substantia nigra [2,3]. While most PD cases are sporadic, approximately 15% are inherited, with twenty genes implicated in PD through

familial genetic studies and about 90 loci identified from PD-GWAS [4]. Among these, the leucine-rich repeat serine/threonine-protein kinase-2 (LRRK2) gene is linked to both familial and sporadic cases, highlighting its neurodevelopmental role [5]. This gene, essential during development, binds to proteins of the disheveled (DLV) family, mediators in the Wnt signaling pathways crucial for embryonic development [6].

Mutations in this domain, especially the autosomal-dominant c.6055G>A mutation, which leads to the LRRK2 G2019S substitution, represent the most common genetic risk factor for Parkinson's disease (PD) [7,8,9]. This mutation leads to a 2 to 3-fold increase in kinase activity, the exact mechanism of which is unclear. Evidence suggests that this increase is associated with the regulation of mitochondrial dynamics, chaperone-mediated autophagy, and vesicle trafficking [10,11,12]. Elevated oxidative stress gene expression in G2019S-induced pluripotent stem cells further underscores the role of this mutation [13], making these processes pivotal in PD pathogenesis.

Current therapeutics, such as LRRK2 inhibitors, show protective efficacy but face challenges and adverse effects, such as pulmonary fibrosis, and varied efficacy among patients, necessitating a personalized therapeutic approach [14]. These therapeutics struggle to effectively traverse the blood-brain barrier (BBB), reducing their therapeutic efficiency [15]. The BBB is crucial for preventing circulating pathogens and toxins from entering the brain, thus maintaining brain homeostasis [16]. Recent advancements in alternative strategies to mitigate this barrier include the use of lipid nanoparticles (LNPs), specifically solid LNPs (SLNPs).

SLNPs have a size range of 40 to 1000 nm, enhanced bioavailability, controlled cargo release, higher loading capacity, absence of organic solvents in the synthesis process, and cost-effective large-scale production [17]. These NPs utilize clathrin-mediated endocytosis to penetrate the BBB [18]. LNPs can be engineered to optimize performance for various diseases, with sphingomyelin (SM) and cholesterol (Chol) showing significant potential in treating PD. These components enhance the efficacy of BBB crossing, with SM maintaining myelin sheath integrity, nerve impulse transmission, and BBB maintenance [19,20], while Chol improves stability, pharmacokinetics, and circulatory time *in vivo* [20]. Together, the SM-Chol derived SLNPs form nano-domains essential for synaptic plasticity and neurotransmitter release, offering a promising approach to PD treatment at a curative level.

The engineering of these SLNPs is crucial for promoting the desired functional outcomes. The biosynthesis of SLNPs with *Ginkgo biloba* leaf extracts (EGB) combines neuroprotective and antioxidant properties. They also act as a monoamine oxidase (MAO) inhibitor to prevent dopamine degradation. EGB increases muscular coordination, dopaminergic D2 receptor content, locomotor activity, and restores antioxidant enzymes in the striatum [21], providing a secondary therapeutic effect for PD treatment, albeit primarily palliative.

This study aims to develop a novel biosynthesized SLNP delivery vehicle containing SM and Chol and functionalized with poly-L-lysine (PLL) for conjugation to the therapeutic siRNA. This SLNP-siRNA nanocomplex is formulated to traverse the BBB and target the LRRK2 G2019S mutation in PD. It also addresses the delivery challenges faced by naked siRNA, such as BBB crossing, nuclease degradation, and its polyanionic nature [14]. This study addresses PD at the genetic level, and offers a promising dual therapeutic approach, advancing towards a curative treatment for PD.

7.2. Materials and Methods

7.2.1. Materials

Phosphate-buffered saline (PBS) tablets, 3-[4,5-dimethylthiazol-2-yl]-2,5-diphenyltetrazolium bromide (MTT), and DMSO were purchased from Merck (Darmstadt, Germany). Luciferase assay and NanoBRET® TE Intracellular Kinase Assay kits, along with the LRRK2(G2019S)-NanoLuc® Fusion Vector, were obtained from Promega Corporation (Madison, USA). The BLOCK-iT™ fluorescent control, Lipofectamine 2000, and the LRRK2 (G2019S) silencer RNA were sourced from Thermo Fisher Scientific Inc. (MA, USA). The Muse™ Caspase-3/7, Oxidative Stress, Multi-Colour DNA Damage, and Mitopotential Kits were provided by Luminex (TX, USA). Sterile cell culture plasticware was procured from Nest Biotechnologies (Wuxi, China). Trypsin-versene, Eagle's Minimum Essential Medium (EMEM), Dulbecco's Modified Eagle medium/nutrient mixture F-12 (DMEM/F12) and antibiotic mixture (penicillin 5000 units/mL, streptomycin 5000 µg/mL) were supplied by Lonza BioWhittaker (MD, USA). Gamma-irradiated fetal bovine serum (FBS) was provided by Hyclone GE Healthcare (UT, USA). All reagents were of analytical grade, with 18 MΩ water (Milli-Q Academic, Millipore, France) used in preparations.

7.2.2. PLL-SC-SLNPs: Synthesis

The biologically synthesized PLL-SC-SLNPs, using *Ginkgo biloba* extract (EGB) as a reducing agent, were prepared following the protocols outlined in Chapters 6.2.3 and 6.2.4.

7.2.3. PLL-SC-SLNPs: Characterisation and Binding Studies

Characterization of the synthesized nanoparticles was performed using a suite of analytical techniques, including UV-visible spectroscopy, Fourier-transform infrared (FTIR) spectroscopy, transmission electron microscopy (TEM), and dynamic light scattering (DLS), as detailed in Chapter 6.2.6.

Binding studies were conducted using a combination of methodologies: the ethidium bromide (EtBr) intercalation assay to measure binding affinity, the band shift assay to assess siRNA-nanoparticle complex formation, and the RNase protection assay to evaluate the stability of siRNA. These techniques are comprehensively described in **Chapter 6, section 6.2.7**.

7.2.4. Cell Culture and LRRK2 G2019S Transfection

All tissue culture-based experiments were conducted in a class II biosafety laminar flow hood under sterile conditions. The embryonic kidney cell lines (HEK293) and neuroblastoma cell lines (SH-SY5Y) were propagated and maintained in 25 cm³ tissue culture flasks containing 5 mL of complete medium (EMEM (HEK293 cells) and DMEM/F12 (SH-SY5Y) supplemented with 10% (v/v) FBS and 1% antibiotics [100 U/mL penicillin, 100 µg/mL streptomycin]) in a HEPA class 100 Steri-Cult CO₂ incubator (Thermo Fisher Inc., Waltham, MA, USA). Cells were monitored daily under a Nikon TMS inverted microscope (Nikon Corp., Tokyo, Japan) and subcultured into multiwell plates for subsequent assays as needed.

The transformed cell lines were cultured similarly, with the LRRK2(G2019S)-NanoLuc® Fusion Vector introduced into the cells. Fusion complexes were prepared using 9.0 µg/mL of transfection carrier DNA and 1.0 µg/mL of the fusion vector in 1 mL of EMEM/DMEM/F12 assay medium (99% medium supplemented with 1% FBS). To this, 30 µL of Lipofectamine 2000 was added and mixed by inversion (5-10 times). The lipoplexes were incubated at ambient temperature for 20 minutes and then introduced into the cells at a ratio of 1:20 (complex). Following transfection and appropriate growth periods, cells were subcultured into multi-well plates for subsequent assays.

7.2.5. Cellular Uptake Studies

The cellular uptake assay assessed the ability of PLL-SLNPs to traverse the cellular membrane and localize in the nucleus using BLOCK-iT™ fluorescent oligo for visualization. Wild-type and transformed cells were prepared and treated. Basically, the transformed cells were trypsinized and seeded into clear 96-well plates at a density of 1.8×10^5 cells per well and incubated at 37°C overnight. Nanocomplexes were prepared using the optimum binding ratios with 50 nM (0.067 µg) BLOCK-iT Oligo (1:1) and 100 nM BLOCK-iT Oligo (1:2) and incubated for 1 hour. A positive control with untreated cells represented a comparative baseline. After incubation, the growth medium was replaced with fresh medium (EMEM + 10% FBS + 1% antibiotics), and the nanocomplexes were added to the cells and incubated at 37°C for 24 hours. The medium was removed, and cells were washed with PBS (2 x 60 µL) and viewed under an Olympus CKX41 Inverted Phase Contrast fluorescence microscope at an excitation wavelength of 494 nm and an emission wavelength of 519 nm.

Cells were then lysed with 80 µL reporter lysis buffer and gently rocked for 15 minutes at 30 rpm on a STR 6 platform shaker (Stuart Scientific, Staffordshire, UK). Subsequently, the cells were detached from the wells, and the resulting cell lysates were transferred into a 96-well black plate. Fluorescence was measured using the Glomax Multi-Detection System (Promega Biosystems, CA, USA). Protein concentrations were determined via the bicinchoninic acid (BCA) assay. The fluorescence values were then normalized to the BCA assay results and expressed as relative fluorescent units (RFU) per mg of protein.

7.2.6. The 3-[4,5-dimethylthiazol-2-yl]-2,5-diphenyltetrazolium bromide (MTT) Assay

The cytotoxicity profiles of the HEK293 and SH-SY5Y cells were assessed in detail in **Chapter 6**. The HEK293 and SH-SY5Y cells were both transformed as per the conditions mentioned in chapter 7.2.3 were trypsinized and seeded into clear 96-well plates at a density of 1.8×10^5 cells per well and incubated at 37°C overnight. Nanocomplexes were prepared in triplicate using the SLNP nanocomplexes at optimum binding ratios with 50 nM non-targeting siRNA (0.067 µg). A positive control with untreated cells represented 100% survival. After incubation, the growth medium was replaced with fresh medium (EMEM + 10% FBS + 1% antibiotics). The nanocomplexes were added to the cells and incubated at 37°C for 48 hours. The growth medium was then aspirated and replaced with 0.1 mL of EMEM/DMEM/F12 medium containing 0.01 mL of MTT solution (5 mg/mL in PBS). Cells were incubated at 37°C for a further 4 hours. The MTT-infused medium was removed, and 0.1 mL DMSO was added

to each well. Absorbance was measured at 570 nm using a Mindray MR-96A microplate reader (Vacutec, Hamburg, Germany), with DMSO as a blank.

7.2.7. Caspase 3/7 Assay

The Muse™ caspase-3/7 kit was used to quantify the apoptotic status and membrane permeability at various stages of apoptosis, determined by caspase 3/7 activity together with a dead cell dye. Cells were prepared and treated as described in section 2.5. After 48 hours of incubation, cells were washed with PBS, trypsinized, and 50 µL of assay buffer (1x) was added. The mixture was vortexed, followed by the addition of 5 µL caspase 3/7 reagent. Cells were incubated for 30 minutes at 37°C, and then 150 µL of caspase 7-AAD working solution was added and incubated away from light for 5 minutes at room temperature. A Muse™ cell analyzer (Luminex, TX, USA) was used to assess caspase activity.

7.2.8. NanoBRET®-TE Intracellular Kinase Assay

The kinase assay was conducted as per the manufacturer's protocol. Briefly, wild-type and mutated cells were prepared and treated. After 48 hours of incubation, the cells were washed with PBS, trypsinized and the density was adjusted to 2×10^5 cells/ml in serum medium. With periodic mixing to avoid settling, 85 µl per well of cell suspension was dispensed into white, 96-well NBS plates. To this, 5 µL of a complete 20x NanoBRET® tracer reagent (in 100% DMSO) was added. The plate was mixed on an orbital shaker for 15 seconds at 900 rpm, followed by a 2-hour incubation at 37°C. Plates were equilibrated to room temperature for 15 minutes, while the 3x complete substrate and inhibitor solution was prepared in assay medium. This solution was made by mixing 30 µL of Nano-Glo® substrate, 10 µL of NanoLuc inhibitor, and 4960 µL of assay medium. Fifty microliters of the solution were added to each well and incubated at room temperature for 2-3 minutes before analysis. The GloMax® Discover System (Promega Biosystems, CA, USA) assessed kinase activity via measurements of the donor emission wavelength (450 nm) and the acceptor emission wavelength (610 nm).

7.2.9. Oxidative Stress Assay

The Muse™ oxidative stress assay was used to quantify the reactive oxygen species (ROS) pre-and post-treatment in the wild-type and mutated cell lines. The cells were cultured under the conditions previously described. Once they reached the desired confluency, the cells were washed with 100 µl PBS to remove any residual media and non-adherent cells. After washing,

the cells were treated with 10-20 μ l trypsin-EDTA to detach them from the culture surface. Trypsinization was monitored under a microscope to ensure complete cell detachment, after which the trypsin was neutralized by adding an equal volume of complete growth media containing serum. The cells were transferred to a microfuge tube and centrifuged at 300 x g for 5 minutes. The medium was aspirated, and pelleted cells were resuspended in 1x assay buffer. Ten microliters of the cells were transferred to a sterile centrifuge tube, and 190 μ L of Muse oxidative stress working solution (diluted to 1:80 in 1x assay buffer) was added. Cells were vortexed and incubated for 30 minutes at 37°C. A Muse™ cell analyzer (Luminex, TX, USA) quantified the ROS (+) and (-) results.

7.2.10. Multi-Colour DNA Damage Assay

The Muse™ Multi-Colour DNA Damage Assay assessed the extent of DNA damage due to the incorporation of the LRRK2 G2019S into the genome of the cells, with wild-type cells serving as controls. After 48 hours of incubation, cells were washed in PBS and trypsinized. Cells were resuspended in 1X assay buffer and centrifuged at 300 x g for 5 minutes. The buffer was aspirated, and 100 μ L of fixation buffer was added, incubated at room temperature for 10 minutes, and then centrifuged again. The supernatant was removed, and 100 μ L of ice-cold permeabilization buffer was added. Cells were centrifuged, the buffer was aspirated, and cells were resuspended in 200 μ L of assay buffer. Five microliters of 20x anti-phospho-ATM and 5 μ L of 20x anti-phospho-histone were added. Tubes were incubated at room temperature in the dark for 30 minutes, and DNA damage was assessed in a Muse™ cell analyzer (Luminex, TX, USA).

7.2.11. Mitopotential Assay

The Muse™ Mitopotential kit assessed mitochondrial stress induced by the mutation compared to wild-type HEK293 and SH-SY5Y cells. As previously described, the cells were grown over a 48-hour incubation period and washed with PBS to remove unwanted debris. Subsequently, they were trypsinized by adding enough trypsin-EDTA solution to cover the cell layer and incubated at 37°C for 3-5 minutes, or until cells were fully detached. The cells were resuspended in 1x assay buffer to achieve a final cell concentration of 2×10^5 cells/ml. From this suspension, 100 μ l was dispensed into a sterile centrifuge tube, and 95 μ L of mitopotential working solution (1:1000 in 1x assay buffer) was added. Tubes were vortexed for 3-5 seconds

and incubated at 37°C for 20 minutes. Five microliters of Muse mitopotential 7-AAD reagent were added and vortexed for 3-5 seconds. Tubes were incubated at room temperature for 5 minutes, and cells were analyzed using the Muse™ cell analyzer (Luminex, TX, USA).

7.3. Results

7.3.1. Synthesis, characterization and siRNA Binding Studies

The synthesis of EGB-PLL-SLNPs and H₂O-PLL-SLNPs was performed under identical experimental conditions, as described in **Chapter 6**. The results from the UV-vis spectroscopy (**section 6.3.1.1**) indicated successful conjugation of poly-L-lysine (PLL) to the solid lipid nanoparticles (SLNPs), with *Ginkgo biloba* extract (EGB)-synthesized SLNPs showing a bathochromic shift, suggesting enhanced interactions compared to the water-based SLNPs. FTIR analysis (**section 6.3.1.1**) confirmed the successful encapsulation of EGB within the SLNPs, showing characteristic peaks for O-H and C-H stretching, which aligned with the incorporation of EGB's aliphatic and phenolic components. Dynamic light scattering (DLS) (**section 6.3.1.2**) revealed hydrodynamic sizes below 200 nm, suitable for biomedical applications, with the EGB-PLL-SLNPs showing a size of 93.2 ± 1.0 nm and good colloidal stability due to their high zeta potential (>35 mV). Transmission electron microscopy (TEM) (**section 6.3.1.2**) supported these findings, showing spherical nanoparticles with no morphological changes upon conjugation with PLL. Overall, the analyses confirmed that the EGB-PLL-SLNPs are stable, well-dispersed, and within the size range for effective cellular uptake.

The intercalation, binding, and protection assays demonstrated the strong ability of EGB-PLL-SLNPs to effectively bind and protect siRNA (**section 6.3.2**). In the intercalation assay (as outlined in **section 6.3.2.1**), the EGB-PLL-SLNPs achieved 77.78% siRNA compaction, which was slightly better than the H₂O-PLL-SLNPs at 73.60%, indicating efficient quenching of ethidium bromide fluorescence as the nanoparticles bound to the siRNA. The band-shift assay (**section 6.3.2.2**) further confirmed effective binding, with EGB-PLL-SLNPs reaching optimal binding at a ratio of 0.4:1 (w/w), while H₂O-PLL-SLNPs required a lower ratio of 0.2:1 (w/w). Both systems successfully neutralized the siRNA's negative charge, preventing its migration through the gel matrix.

In the protection assay (**section 6.3.2.3**), the EGB-PLL-SLNPs demonstrated a superior ability to shield siRNA from RNase A-mediated degradation compared to the naked siRNA control, which was completely degraded. The nanocomplexes maintained their integrity under

enzymatic stress, supporting their stability and potential for in vivo applications. These findings underscore the efficiency of EGB-PLL-SLNPs in binding and protecting siRNA, positioning them as promising candidates for gene delivery systems

7.3.2. Cellular Uptake Studies

7.3.2.1. BLOCK-iT™ Fluorescent Oligo Assay

The BLOCK-iT assay was employed to assess the cellular uptake of the SLNPs in both the mutated SH-SY5Y and HEK293 cell lines, which were transfected to express the LRRK2 G2019S mutation. These results offer valuable insights into the efficiency of the nanoparticle-mediated delivery vector in vitro, comparing wild-type cells and differences between EGB-PLL-SLNPs and H₂O-PLL-SC-SLNPs.

Fluorescence intensity served as a qualitative measure of cellular internalization of the SLNPs, using two ratios of the BLOCK-iT Fluorescent Oligo (Figures 7.1 and 7.2). Additionally, the luciferase assay provided a quantitative measure of uptake to validate the fluorescence results (Figure 7.3). The transformed SH-SY5Y cells only control (Figure 7.1A (1)) showed no fluorescence, appearing in their natural state and serving as a relevant baseline. When treated with naked BLOCK-iT, visible fluorescence was noted with accumulation around the perinuclear region, suggesting active endocytic uptake, with a fluorescence intensity of 3290.56 mg/protein (Figure 7.1A (2); Figure 3). For the EGB-SLNPs at a 1:1 ratio (Figure 7.1B (1 & B2)), fluorescence intensity indicated a moderate level of cellular internalization with signals dispersed throughout the cytoplasm and a fluorescence intensity of 14146.67 mg/protein. In contrast, the EGB-SLNPs

1:2 ratio (Figure 7.1B (3 and B4)) displayed a higher fluorescent signal, with uniformly distributed SLNPs within the cytoplasm and accumulation in the perinuclear region, with a fluorescence intensity of 25247.04 mg/protein. The H₂O-PLL-SLNPs at a 1:1 ratio (Figure 7.1B (5 and B6)) showed less uniformity in fluorescent signals, suggesting variable internalization across the cells with a fluorescence intensity of 11247.18 mg/protein. However, fluorescence increased at the 2:1 ratio (Figure 7.1B 97 and B8)), with a greater concentration in specific cytoplasmic regions and a fluorescence intensity of 18579.83 mg/protein. While this indicates successful uptake, it is less uniform compared to EGB-PLL-SLNPs.

Using HEK293 cells (Figure 7.2), an efficient experimental control was established for all relevant studies. The results obtained from this cell line were consistent with those from the SH-SY5Y cells. Overall, greater cellular uptake was noted at the 2:1 ratio of EGB-PLL-SLNPs (fluorescence intensity of 23879.2 mg/protein), with clear visualization of uniformly distributed SLNPs within the cytoplasm (Figure 7.2B (3 and B4)). This supports the conclusion of efficient internalization. Overall, both SLNPs showed successful uptake, with EGB-PLL-SLNPs demonstrating superior uptake efficiency compared to H₂O-PLL-SLNPs.

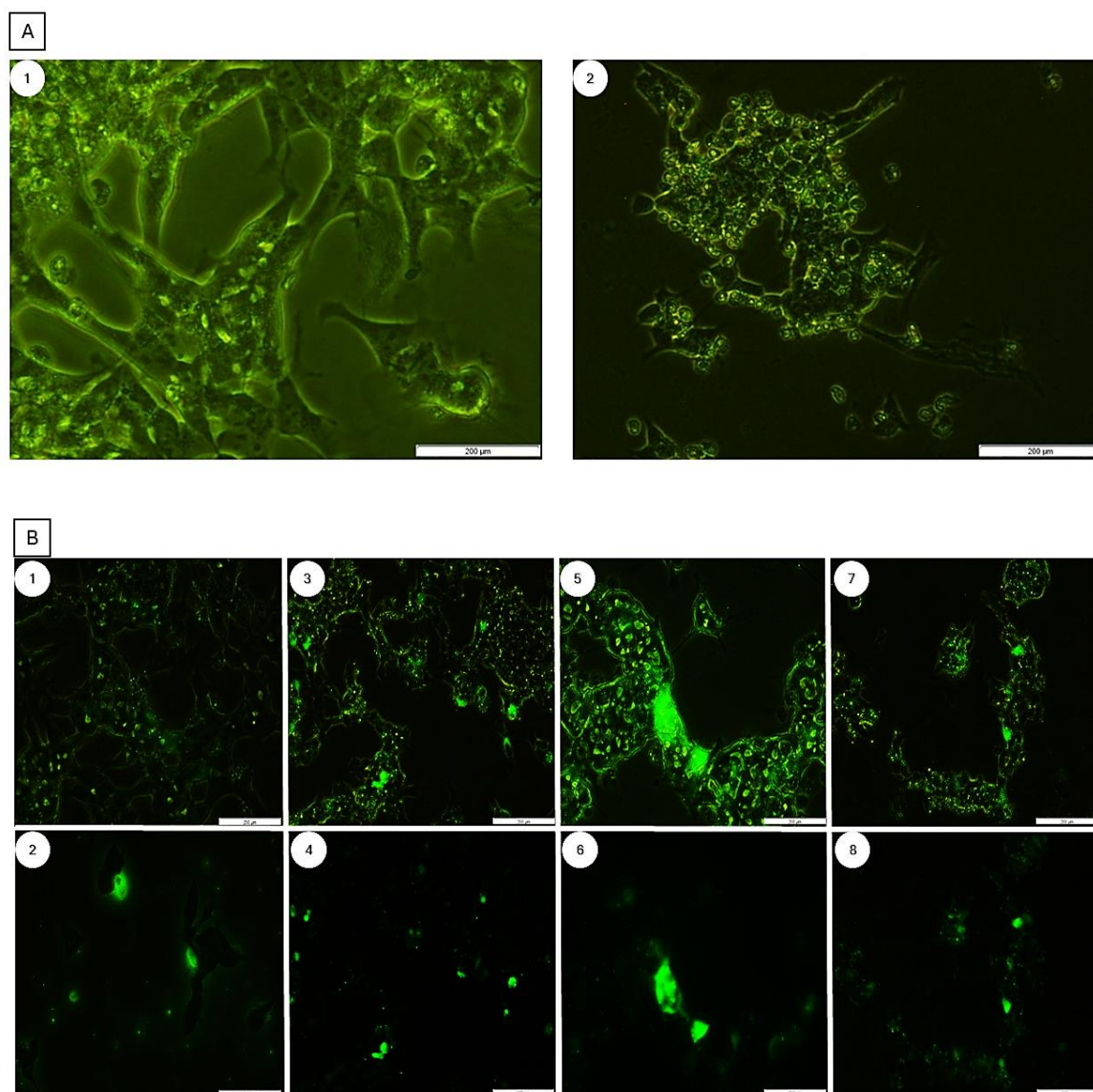


Figure 7.1. Fluorescent images showing cellular uptake in the SH-SY5Y cells. (A1) Control of SH-SY5Y cells not treated with the fluorescent oligo, (A2) Control of naked Block-IT™ oligo not complexed to the SLNPs, (B1 & 2) Oligo: EGB-PLL-SLNPs in a 1:1 (w/w) ratio; (B3 & 4) Oligo: EGB-PLL-SLNPs in a 2:1 (w/w) ratio; (B5 & 6) Oligo:H₂O-PLL-SLNPs in a 1:1 (w/w) ratio; (B7 & 8)

Oligo:H₂O- PLL-SLNPs in a 2:1 (w/w) ratio. The cells were visualized at 100x magnification. Scale Bar = 200 μ m.

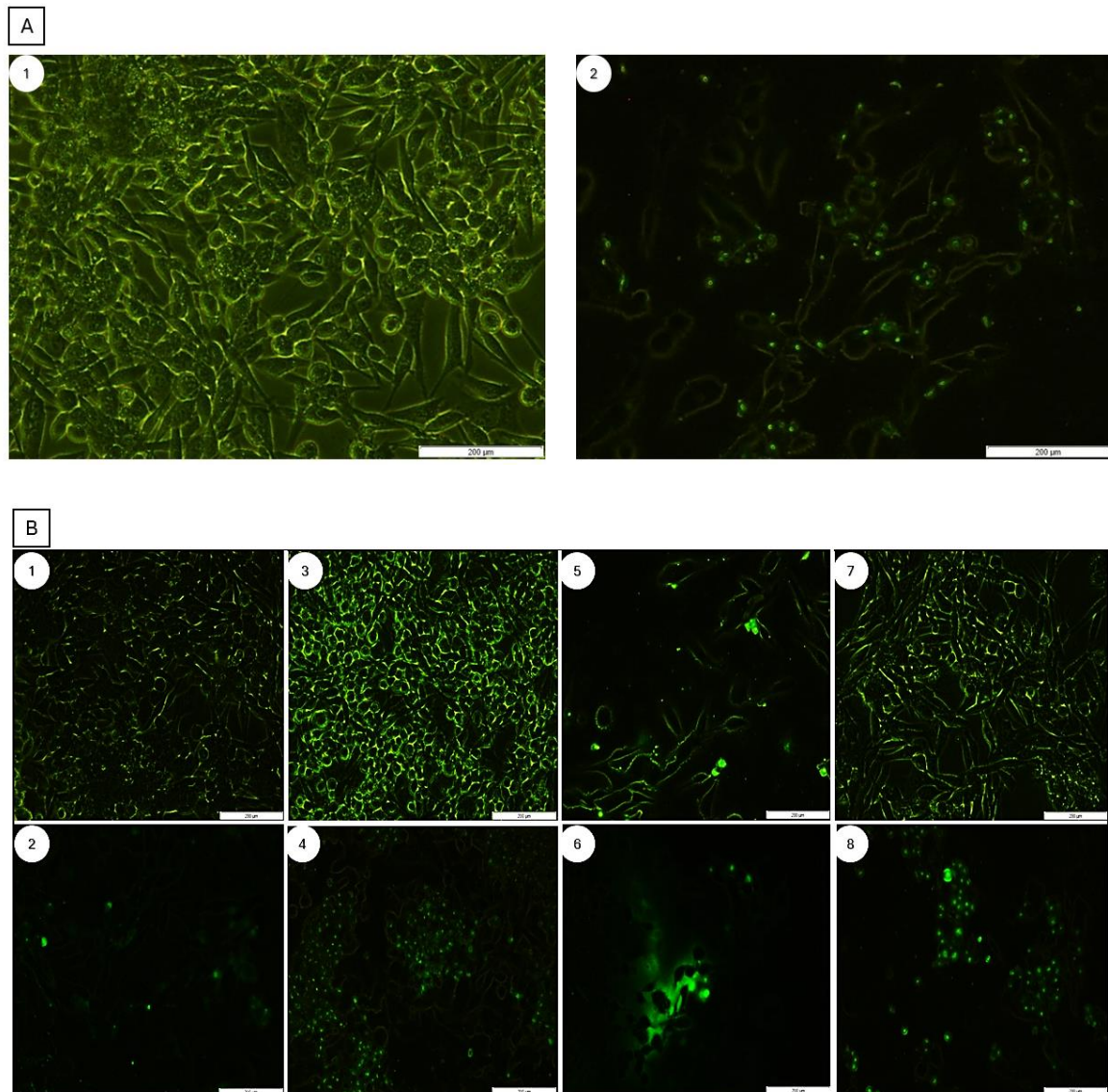


Figure 7.2. Fluorescent images showing cellular uptake in the HEK293 cells. (A1) Control of HEK293 cells not treated with the fluorescent oligo, (A2) Control of naked Block-ITTM oligo not complexed to the SLNPs, (B1 & 2) Oligo: EGB-PLL-SLNPs in a 1:1 (w/w) ratio; (B3 & 4) Oligo: EGB-PLL-SLNPs in a 2:1 (w/w) ratio; (B5 & 6) Oligo:H₂O-PLL-SLNPs in a 1:1 (w/w) ratio; (B7 & 8) Oligo:H₂O-PLL-SLNPs in a 2:1 (w/w) ratio. The cells were visualized at 100x magnification. Scale Bar = 200 μ m.

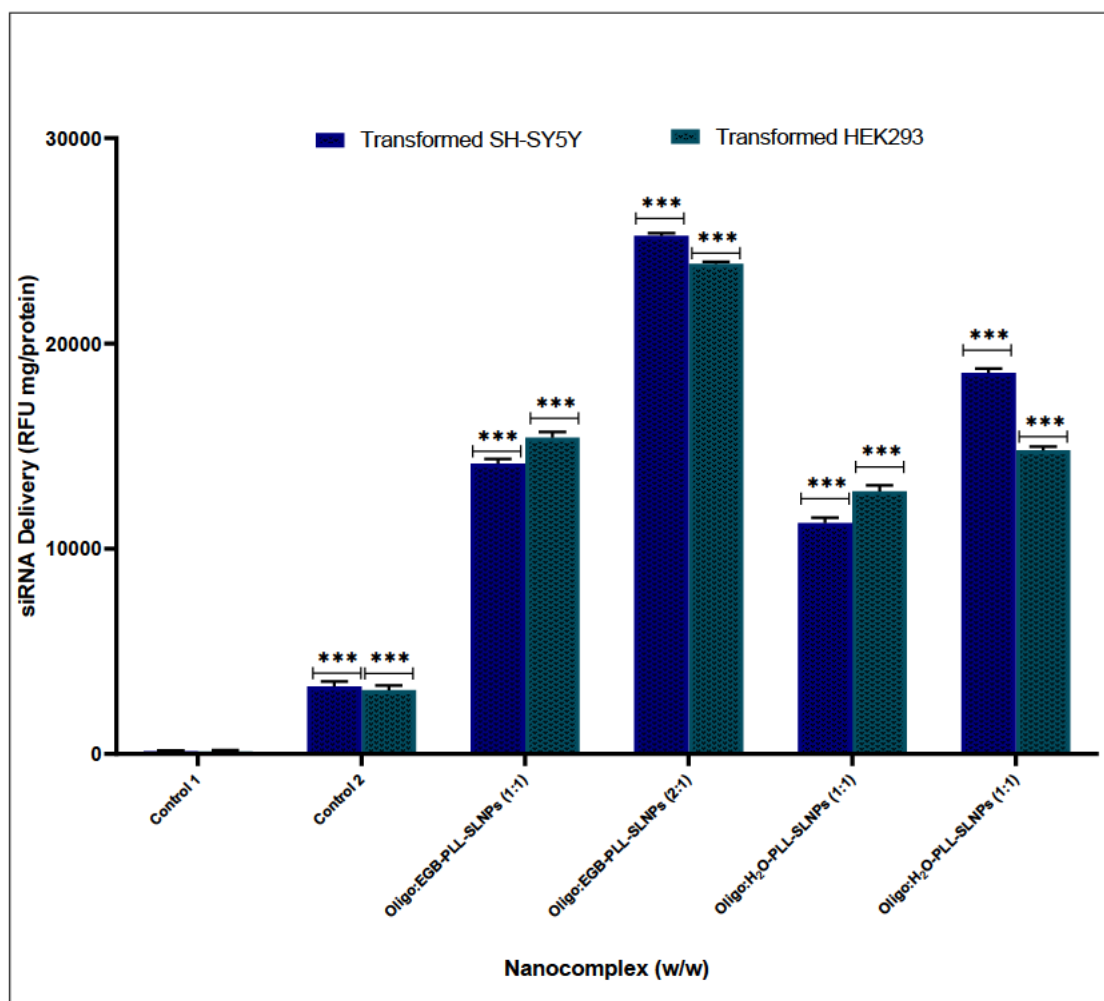


Figure 7.3. The transfection analysis portraying the Control 1 (Transformed HEK293 and SH-SY5Y cells only), control 2 (Naked BLOCK-iT™ Fluorescent Oligo) and the two ratios per PLL-SLNPs therapeutics (***) $p < 0.001$.

7.3.3. siRNA:PLL-SLNPs Safety Profiles

7.3.3.1 The MTT Assay

The MTT assay was employed to quantify cell viability and cytotoxicity, providing a reliable measure of the safety of the synthesized SLNPs on cellular survival. The results indicated that the SLNPs were well tolerated in both SH-SY5Y and HEK293 transformed cells (Figure 7.4).

A notable difference in cellular viability was observed between the EGB-PLL-SLNPs and the H₂O-PLL-SLNPs. In SH-SY5Y cells, the EGB-PLL-SLNPs exhibited a cellular viability greater than 98.37%, while the H₂O-PLL-SLNPs showed a viability of 79.03% (Figure 7.4A). Similarly, in HEK293 cells, the EGB-PLL-SLNPs demonstrated a cellular viability of 92.86%, compared to 87.07% for the H₂O-PLL-SLNPs (Figure 7.4B).

These findings highlight the superior biocompatibility of EGB-PLL-SLNPs, especially in neuroblastoma cells, where they demonstrated the highest cellular viability at the optimal ratio. This emphasizes the safety and efficiency of the biologically synthesized SLNPs, suggesting that EGB not only enhances cellular uptake but also contributes to better cell viability and reduced cytotoxicity.

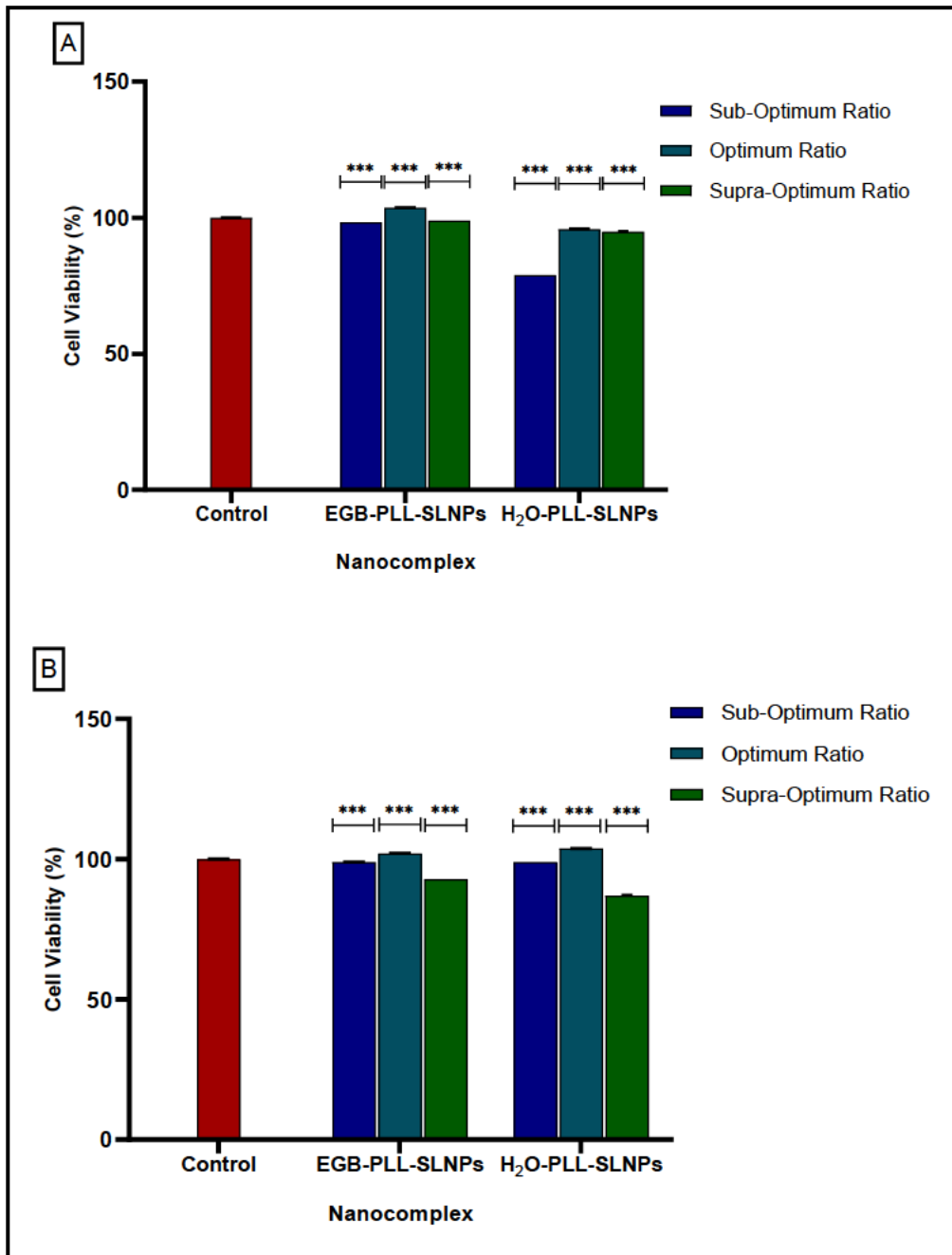


Figure 7.4. The MTT cytotoxicity in the transformed (A) SH-SY5Y and (B) HEK293 cells. Data are represented as means \pm standard deviation ($n = 3$). *** $p < 0.001$ are considered statistically significant between the corresponding means of each suboptimum, optimum, and supra-optimum nanocomplexes and the positive control (Tukey's multiple comparisons test).

7.3.3.2. Caspase 3/7 Assay

The Caspase 3/7 assay was performed to corroborate the results obtained from the MTT assay. This assay quantifies apoptosis associated with the therapeutics by utilizing a substrate that, upon cleavage by active caspase 3/7, promotes a fluorescent signal, allowing for quantification [22]. The cell viability in the SH-SY5Y and HEK293 transformed cells was noted to be >87.15% and 96.55%, respectively (Table 7.1 and Figure 7.5).

In the transformed SH-SY5Y cells (Figure 7.5A), the control group (cells only) showed a baseline viability of 95.90% with 1.90% apoptotic cells. The RNA control group exhibited a significant decline in viability (87.15%) and increased apoptosis (11.10%). Treatment with EGB-PLL-SLNPs significantly improved cell viability (98.55%) and reduced apoptosis (1.45%). In contrast, treatment with H₂O-PLL-SLNPs resulted in lower viability (94.80%) and a higher percentage of apoptosis (2.70%).

In the transformed HEK293 cells (Figure 7.5B), the control group (cells only) exhibited high viability at 98.95% with 1.05% apoptotic cells. Unlike the SH-SY5Y cells, the RNA control group showed increased viability (99.45%) with minimal apoptosis (0.50%). Treatment with EGB-PLL-SLNPs resulted in 99.10% viability and 0.75% apoptosis, indicating excellent cell survival and low apoptosis. In contrast, treatment with H₂O-PLL-SC-SLNPs led to decreased viability (96.55%) and increased apoptosis (2.25%).

The higher apoptotic rates in the H₂O-PLL-SC-SLNPs group underscore the superior efficacy and reduced cytotoxicity of the EGB-PLL-SLNPs (Figure 7.6). These findings further confirm the enhanced safety profile of EGB-PLL-SLNPs as a delivery vehicle, demonstrating their potential for therapeutic applications with minimal cytotoxic effects.

Table 7.1. Caspase 3/7 analysis on the transfected SH-SY5Y and HEK293 cell lines outlining the apoptotic index and cell viability among all therapeutics

Transformed HEK293			
	Live Cells (%)	Dead Cells (%)	Apoptotic Cells (%)
Cells Control	98.95%	0.00%	1.05%
RNA Control	99.45%	0.05%	0.50%
siRNA:EGB-PLL-SLNPs	99.10%	0.15%	0.75%
SiRNA:H₂O-PLL-SLNPs	96.55%	1.20%	2.25%
Transformed SH-SY5Y			
	Live Cells (%)	Dead Cells (%)	Apoptotic Cells (%)
Cells Control	95.90%	2.20%	1.90%
RNA Control	87.15%	11.10%	1.75%

siRNA:EGB-PLL-SLNPs	98.55%	0.00%	1.45%
SiRNA:H ₂ O-PLL-SLNPs	94.80%	2.50%	2.70%

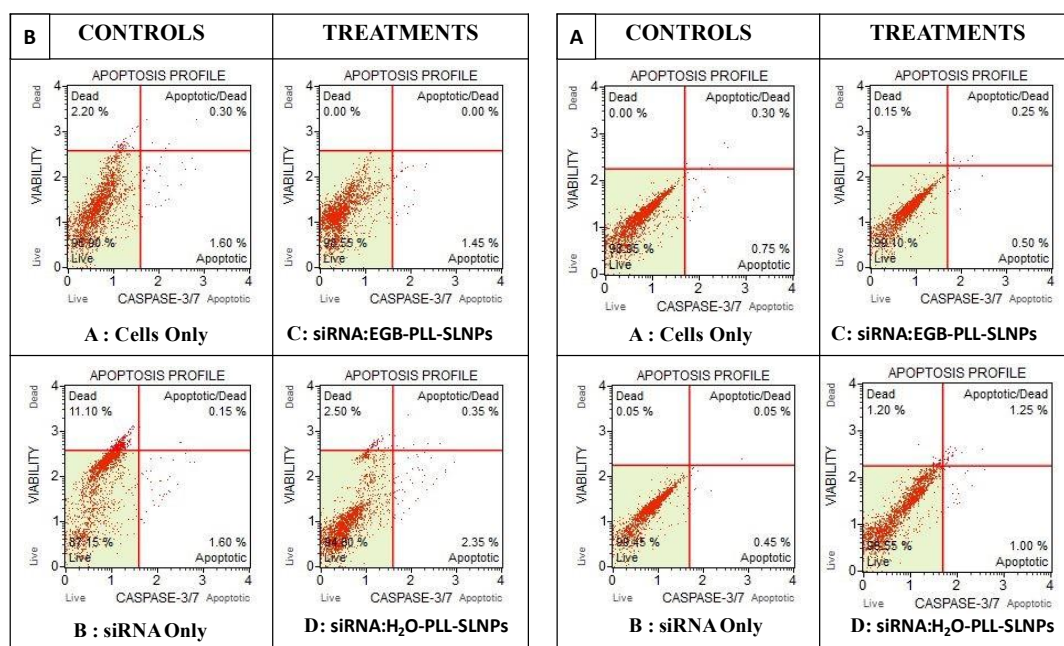


Figure 7.5. Caspase 3/7 Assay of Therapeutic Nanocomplexes in (A) HEK293 and (B) SH-SY5Y Cells. The graph illustrates the apoptotic response of HEK293 and SH-SY5Y cells after treatment with EGB-PLL-SLNPs and H₂O-PLL-SLNPs.

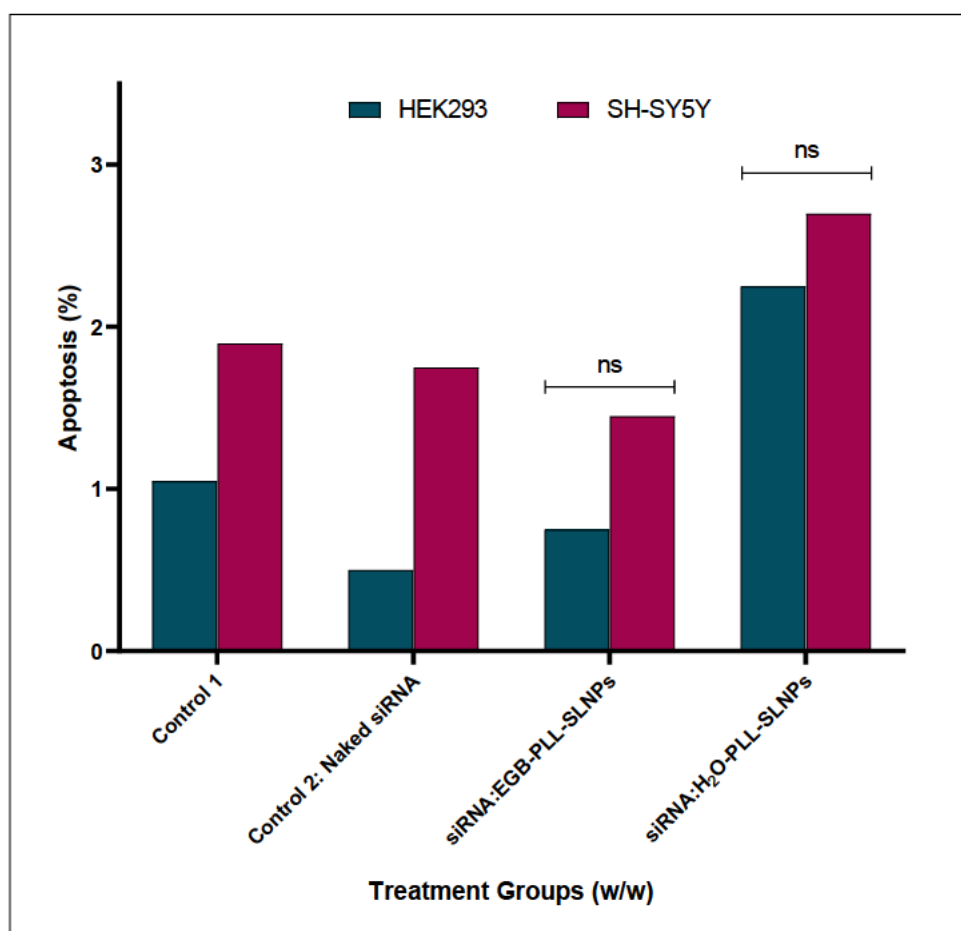


Figure 7.6. Apoptosis rates in HEK293 and SH-SY5Y cells following treatment with the siRNA: PLL-SLNP nanocomplexes (w/w) ratios. Apoptosis levels were determined from the caspase 3/7 activity recorded. No statistical significance (ns) was observed among all groups.

7.3.4. Gene Silencing Studies

7.3.4.1. Kinase Activity Assay

This assay provides evidence for the potential of the therapeutic siRNA-conjugated PLL-SLNPs in targeting and silencing the LRRK2 G2019S mutation. It is well-documented that this mutation causes a pathological increase in kinase activity, contributing to the progression of PD [23].

In the SH-SY5Y cells, the successful transfection with the mutated gene was confirmed by the increased baseline kinase activity in the mutated control groups (cells only) compared to the wild-type cells (Figure 7.7). Specifically, kinase activity increased by 37.57% (from 0.0236 to 0.0378), representing a 1.6-fold change. Treatment with naked siRNA did not result in significant changes in kinase activity, indicating degradation of the siRNA upon entry into the

cells. In contrast, the therapeutic efficacy of EGB-PLL-SLNPs showed a remarkable 56.08% reduction in kinase activity, while H₂O-PLL-SLNPs resulted in a slightly lower reduction of 52.65%.

Similarly, in HEK293 cells, used as a control, a 44.49% increase in kinase activity (1.8-fold change) was observed between the wild-type and transformed cells (Figure 7.7). Naked siRNA was rendered ineffective due to RNase degradation in the cellular environment. However, upon treatment, EGB-PLL-SLNPs achieved a 45.76% reduction in kinase activity, compared to a 38.14% reduction with H₂O-PLL-SLNPs.

The superior efficiency of EGB-PLL-SLNPs is evident from these results, demonstrating normalized kinase activity levels post-treatment in both cell lines, comparable to the baseline wild-type control. This highlights the potential of EGB-PLL-SLNPs as an effective therapeutic approach for mitigating the effects of the LRRK2 G2019S mutation in PD.

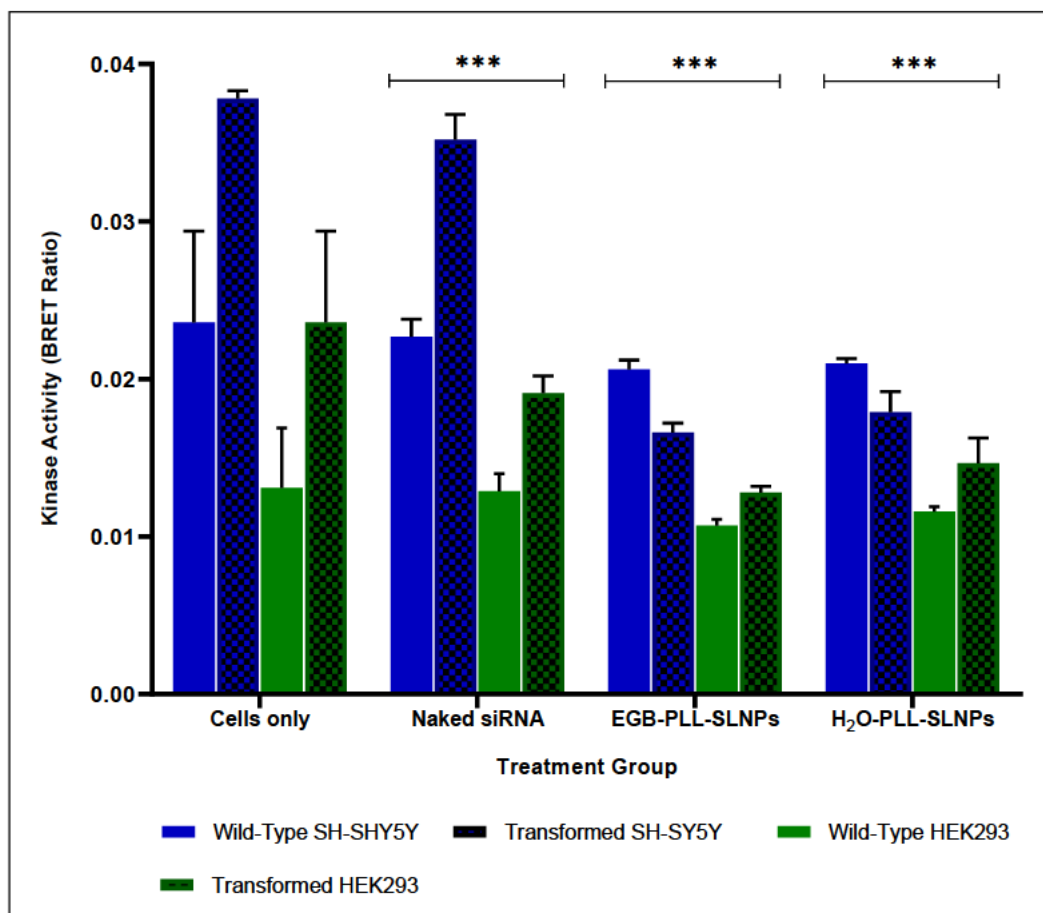


Figure 7.7. Impact of therapeutic siRNA-conjugated EGB-PLL-SLNPs and H₂O-PLL-SLNPs on kinase activity in wild-type and LRRK2 G2019S transformed SH-SY5Y and HEK293 cells.

7.3.4.2. Oxidative Stress

The oxidative stress assay was conducted using the Muse Oxidative Stress Kit in the wild-type and transformed SH-SY5Y (Table 7.2 and Figure 7.8) and HEK293 cells (Table 7.2 and Figure 7.9). In SH-SY5Y wild-type cells, a baseline of 14.22% ROS (+) cells was observed, with a significant decrease following the administration of the nanocomplexes. The EGB-PLL-SLNPs produced the greatest decline in ROS (+) cells to 5.62% (Figure 7.8A). The transformed SH-SY5Y cells showed an increase of 13.58% in ROS (+) control cells. Treatment with the EGB-based nanocomplexes produced a slightly better effect, with a reduction of 13.51% in oxidative stress compared to their H₂O-based counterparts (16.67%). Normalization studies showed that the EGB-based nanocomplexes could reduce oxidative stress to baseline levels following 48 hours of incubation (Figure 7.8B).

The HEK293 cells followed a similar trend to those observed in SH-SY5Y cells. The control cells showed a less pronounced increase in ROS (+) cells from wild-type to transformed cells, with an increase of 7.42% (Figure 7.9A). Although this increase was lower, it was sufficient to validate successful transfection. Here again, the EGB-based nanocomplexes produced a slightly better effect, with a 0.48% reduction in oxidative stress compared to their H₂O-based counterparts (3.06%). These results indicate the nanocomplex's ability to effectively target and silence the LRRK2 G2019S mutation, with the EGB providing improved antioxidant activities and enhancing its potency. Normalization indicated a significant reduction in oxidative stress levels compared to the wild-type baseline (Figure 7.9B).

Table 7.2. Results obtained from the oxidative stress portraying the ROS (-) and ROS (+) cells in the wild type and transformed SH-SY5Y and HEK293 cells.

	ROS (-)		ROS (+)	
	Wild-Type SH-SY5Y	LRRK2 G2019S SH-SY5Y	Wild-Type SH-SY5Y	LRRK2 G2019S SH-SY5Y
Control: Cells Only	84.27%	66.39%	14.22%	27.80%
Control: Naked RNA	85.80%	76.79%	10.23%	19.11%
EGB-SLNPs	87.50%	82.25%	5.62%	13.51%
H₂O-SLNPs	88.97%	64.04%	7.35%	16.67%
	ROS (-)		ROS (+)	
	Wild-Type HEK293	LRRK2 G2019S HEK293	Wild-Type HEK293	LRRK2 G2019S HEK293
Control: Cells Only	93.87%	86.65%	3.46%	10.88%
Control: Naked RNA	94.75%	91.48%	2.25%	6.62%
EGB-SLNPs	96.19%	90.00%	0.79%	0.48%
H₂O-SLNPs	95.00%	88.84%	1.75%	3.06%

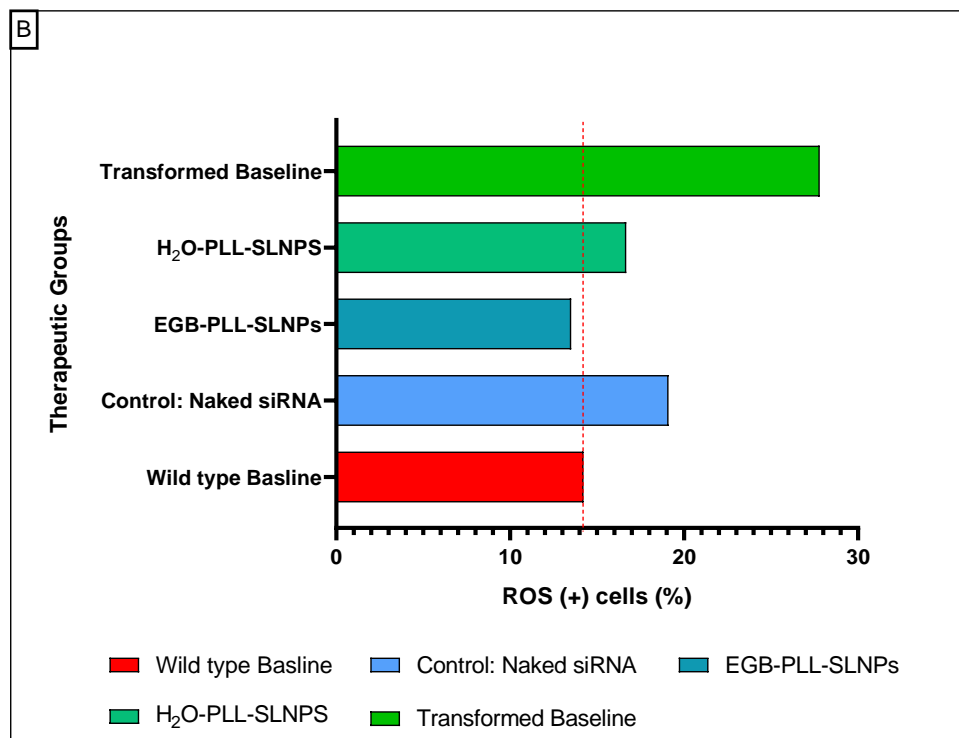
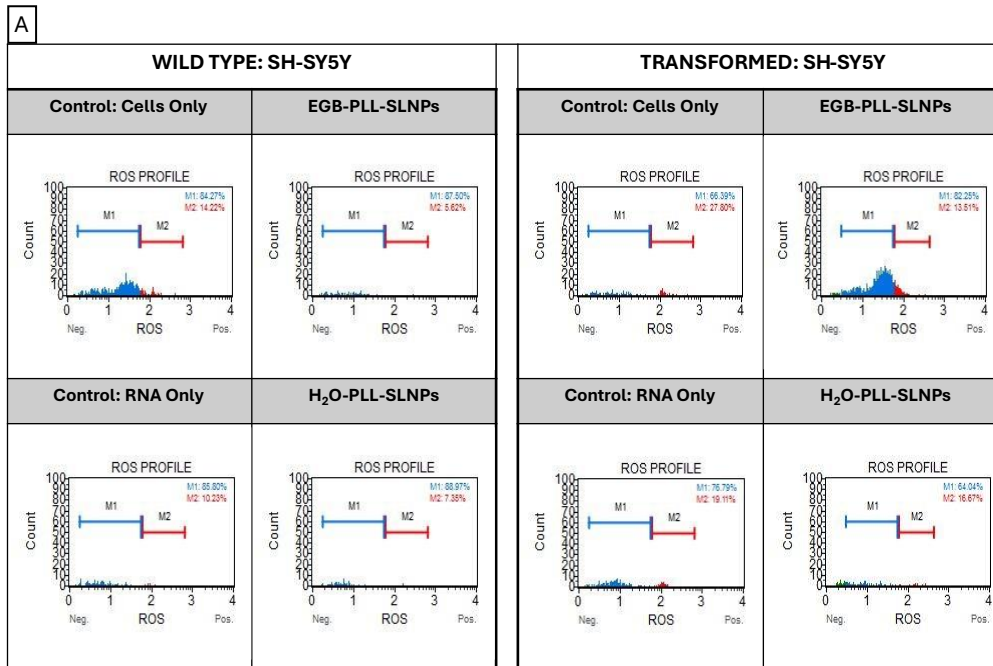


Figure 7.8. (A) The oxidative stress analysis of the therapeutic nanocomplexes on the wild-type and transformed SH-SY5Y cells. (B) The normalization studies showing the comparison of ROS (+) cells between the post-treated transformed SH-SY5Y cells and the wild-type control baseline.

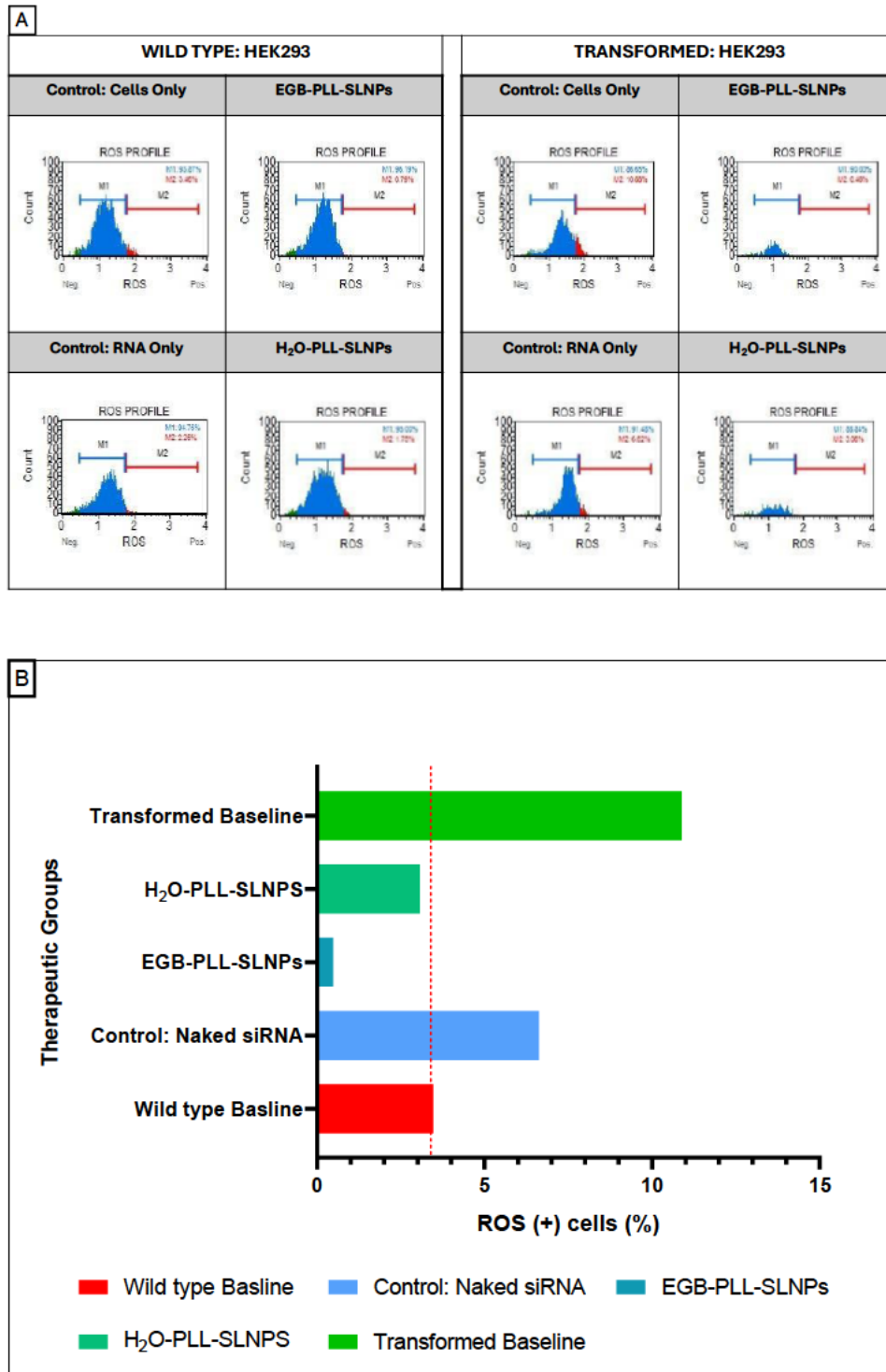


Figure 7.9. (A) The oxidative stress analysis of the various therapeutic groups in the wild type and transformed HEK293 cells. (B) The normalization studies showing the comparison of ROS (+) cells between the post-treated transformed HEK293 cells and the wild-type control baseline.

7.3.4.3. Multi-colour DNA Damage Assay

This assay provides insight into the impact of the mutational event on DNA damage. This assay was conducted on wild-type and transformed SH-SY5Y and HEK293 cells, and the results are presented in Table 3 and Figures 7.10 and 7.11. In the wild-type SH-SY5Y control cells, a baseline DNA damage of 28.42% was observed (Figure 7.10A). This baseline indicated significant DNA damage in the wild-type cells prior to transformation with the LRRK2 G2019S mutation. Treatment with naked siRNA showed a slight but insignificant therapeutic effect, reducing the damage to 26.24%. In comparison, the EGB-nanocomplexes showed lower DNA damage to 20.45% than the H₂O-based nanocomplexes (22.64%).

The same trend was noted in the transformed SH-SY5Y cells (Figure 7.10A), with the baseline control showing a large increase in DNA damage to 48.65%, highlighting the detrimental effect of the mutation on the neuroblastoma cells. Interestingly, treatment with naked siRNA further increased DNA damage to 61.48%. A larger difference was noted between the treatment groups, with EGB-nanocomplexes reducing DNA damage to 33.17%, compared to 44.25% for the H₂O-nanocomplexes. Importantly, an increase in pH2A.X levels to 10.40% in the EGB-nanocomplex treated cells provides insight into the therapeutic's ability to activate DNA repair mechanisms.

In wild-type HEK293 cells, an initial DNA damage of 16.67% was noted, with 0% pH2A.X (Figure 7.11A), indicating no repair mechanisms were activated prior to treatment. A reduction in DNA damage to 16.48% was observed following treatment with naked siRNA. Greater effects were seen with the EGB-nanocomplexes (11.67%) compared to H₂O-nanocomplexes (15.60%). In the transformed HEK293 cells, baseline DNA damage increased to 48.26% (Figure 7.11A), confirming successful transfection. Naked siRNA and H₂O-nanocomplexes performed similarly, with DNA damage levels of 39.39% and 35.82%, respectively. The EGB-nanocomplexes demonstrated the greatest therapeutic efficacy, reducing DNA damage to 18.97%.

Normalization studies in both cell lines showed slight variations. The EGB-nanocomplexes effectively reduced DNA damage to levels only 4.75% above the wild-type neuroblastoma cells (Figure 7.10B) and 2.3% above the wild-type HEK293 cells (Figure 7.11B), indicating almost normalized levels. The H₂O-nanocomplexes also showed a reduction to a lesser extent, with levels of 15.83% above the normalized SH-SY5Y cells (Figure 7.10B) and 19.15% above the normalized HEK293 cells (Figure 7.11B).

Table 7.3. Results obtained from the multi-colour DNA damage assay showing the level of DNA damage in the wild type and transformed SH-SY5Y and HEK293 cells.

Wild Type SH-SY5Y Cells					
	Negative (LL)	pATM (Single Pos) (UL)	DNA Double- strand Breaks (UR)	pH2A.X (single pos) (LR)	Total DNA Damage (UL+UR+LR)
Cells Only	71.58%	8.42%	13.68%	6.32%	28.42%
Naked RNA	73.76%	7.80%	12.77%	5.67%	26.24%
EGB-PLL-SLNPs	79.55%	6.82%	4.55%	9.09%	20.45%
H₂O-PLL-SLNPs	77.36%	9.42%	5.66%	7.55%	22.64%
LRRK2 G2019S Mutated SH-SY5Y Cells					
	Negative (LL)	pATM (Single Pos) (UL)	DNA Double- strand Breaks (UR)	pH2A.X (single pos) (LR)	Total DNA Damage (UL+UR+LR)
Cells Only	33.78%	48.65%	16.22%	1.35%	66.22%
Naked RNA	38.15%	51.41%	9.64%	0.80%	61.85%
EGB-PLL-SLNPs	66.83%	13.86%	8.91%	10.40%	33.17%
H₂O-PLL-SLNPs	55.75%	16.37%	21.24%	6.64%	44.25%
Wild Type HEK293 Cells					
	Negative (LL)	pATM (Single Pos) (UL)	DNA Double- strand Breaks (UR)	pH2A.X (single pos) (LR)	Total DNA Damage (UL+UR+LR)
Cells Only	83.33%	13.89%	2.78%	0.00%	16.67%
Naked RNA	83.52%	13.19%	2.20%	1.10%	16.48%
EGB-PLL-SLNPs	88.33%	10.00%	0.00%	1.67%	11.67%
H₂O-PLL-SLNPs	84.40%	7.34%	0.92%	7.34%	15.60%
LRRK2 G2019S Mutated HEK293 Cells					
	Negative (LL)	pATM (Single Pos) (UL)	DNA Double- strand Breaks (UR)	pH2A.X (single pos) (LR)	Total DNA Damage (UL+UR+LR)
Cells Only	51.74%	1.74%	0.29%	46.22%	48.26%
Naked RNA	60.61%	39.39%	0.00%	0.00%	39.39%
EGB-PLL-SLNPs	81.03%	17.24%	1.72%	0.00%	18.97%
H₂O-PLL-SLNPs	64.18%	2.64%	0.00%	33.19%	35.82%

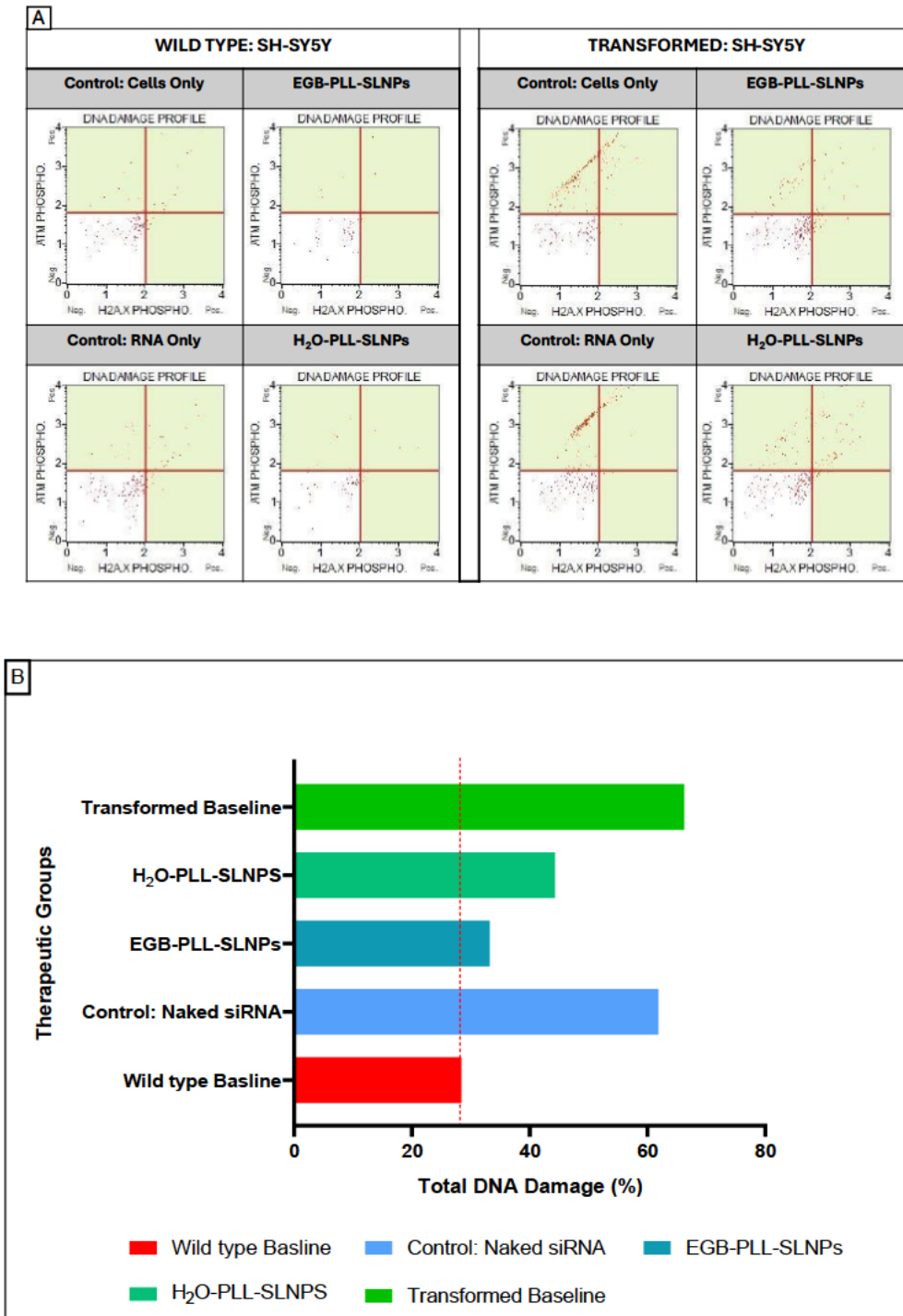


Figure 7.10. (A) The multi-colour DNA damage analysis pertaining to the various therapeutic groups in the wild type and transformed SH-SY5Y cells. (B) The normalization studies portraying the comparison of total DNA damaged (%) cells between the post-treated transformed SH-SY5Y cells and the wild-type control baseline.

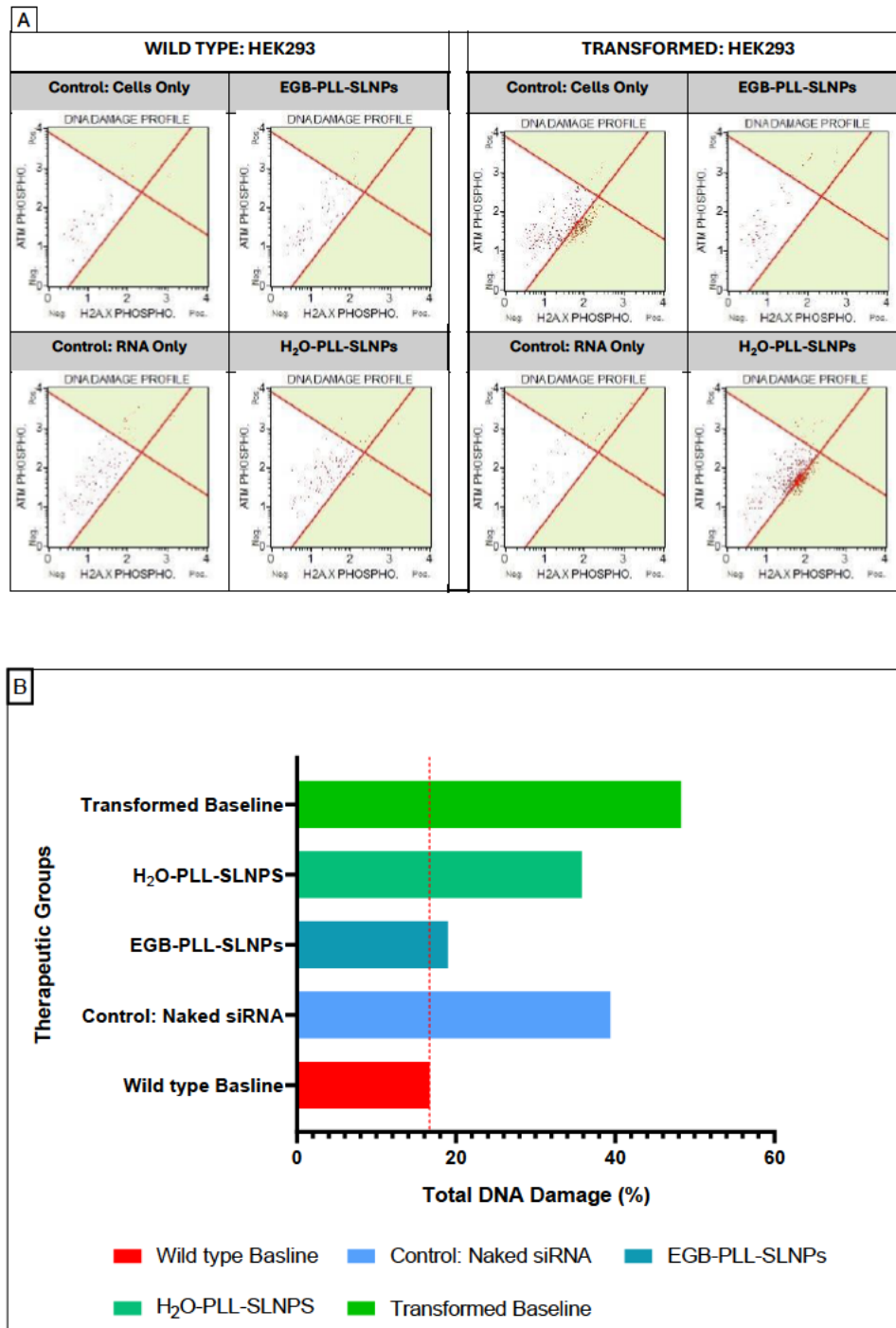


Figure 7.11. (A) The multi-colour DNA damage analysis pertaining to the various therapeutic groups in the wild type and transformed HEK293 cells. (B) The normalization studies portraying the comparison of total DNA damaged (%) cells between the post-treated transformed HEK293 cells and the wild-type control baseline.

7.3.4.4. Mitopotential Assay

The LRRK2 G2019S mutation is known to induce mitochondrial stress, leading to significant cellular damage. The MitoPotential assay assesses mitochondrial health and stress in both transformed and wild-type cells and evaluates the impact of therapeutics on improving this health status (Table 7.4).

In SH-SY5Y cells (Figure 7.12A), the control group (wild-type cells only) showed 68.87% live cells with a total depolarization cell count of 28.97%, serving as a baseline for comparison of therapeutic outcomes. Treatment with naked siRNA showed no significant improvement, with a depolarized cell count of 28.15%. Treatment with the EGB- and H₂O-nanocomplexes reduced mitochondrial damage to 22.5% and 25.22%, respectively, with no major differences in therapeutic efficacy between these groups.

The transformed SH-SY5Y cells (Figure 7.12A) exhibited a significant increase in mitochondrial dysregulation, with an alarming 75.55% of depolarized cells and only 23.35% of live cells. This control highlights the detrimental impact of the mutation on overall cellular health. The naked siRNA group showed a 5.40% decline in depolarized cells. Both treatment groups were effective in decreasing the level of damage to around 40%. These results were between 10-12 % above the wild-type control baseline, indicating excellent mitochondrial recovery (Figure 7.12B).

The wild-type HEK293 cells (Figure 7.13A), showed similar results to the SH-SY5Y cells, with a 26.10% depolarized cell count in the control group. The naked siRNA did not show any substantial reduction in damage (23.55%), while the nanocomplexes demonstrated similar reductions around 21%.

A lower initial depolarization was noted in transformed HEK293 cells (Figure 7.13A) compared to SH-SY5Y cells. However, the increase in depolarization to 36.61% validated the successful transfection. The naked siRNA did not significantly improve mitochondrial health (33.25%), with the nanocomplex treatments showing similar levels (26 -27%). These results were observed to be less than 2% above the wild-type baseline, respectively, indicating almost normalized mitopotential following treatment (Figure 7.13B).

Table 7.4. Results obtained from the MitoPotential assay depicting the levels of live and depolarized cells in wild-type and transformed SH-SY5Y and HEK293 cells.

Wild type: SH-SY5Y					
	Live	Depolarized/ Live	Depolarized/ Dead	Dead Cells	Total Depolarized
Cells Only	68.67%	18.03%	10.94%	2.36%	28.97%
Naked siRNA	70.67%	17.27%	10.88%	1.19%	28.15%
EGB-PLL-SLNPs	77.50%	18.00%	4.50%	0.00%	22.50%
H₂O-PLL-SLNPs	74.49%	22.03%	3.19%	0.29%	25.22%
Transformed SH-SY5Y					
	Live	Depolarized/ Live	Depolarized/ Dead	Dead Cells	Total Depolarized
Cells Only	23.35%	55.20%	20.35%	1.10%	75.55%
Naked siRNA	28.20%	63.55%	6.60%	1.65%	70.15%
EGB-PLL-SLNPs	59.60%	27.40%	12.40%	0.60%	39.80%
H₂O-PLL-SLNPs	57.23%	27.41%	13.55%	1.81%	40.96%
Wild type: HEK293					
	Live	Depolarized/ Live	Depolarized/ Dead	Dead Cells	Total Depolarized
Cells Only	72.85%	23.60%	2.50%	1.05%	26.10%
Naked siRNA	75.17%	2.94%	20.61%	1.28%	23.55%
EGB-PLL-SLNPs	78.94%	2.92%	17.93%	0.22%	20.84%
H₂O-PLL-SLNPs	77.98%	6.17%	15.02%	0.82%	21.19%
Transformed HEK293					
	Live	Depolarized/ Live	Depolarized/ Dead	Dead Cells	Total Depolarized
Cells Only	61.61%	12.50%	24.11%	1.79%	36.61%
Naked siRNA	65.75%	29.45%	3.80%	1.00%	33.25%
EGB-PLL-SLNPs	72.67%	5.81%	20.35%	1.16%	26.16%
H₂O-PLL-SLNPs	70.19%	5.11%	22.75%	1.94%	27.87

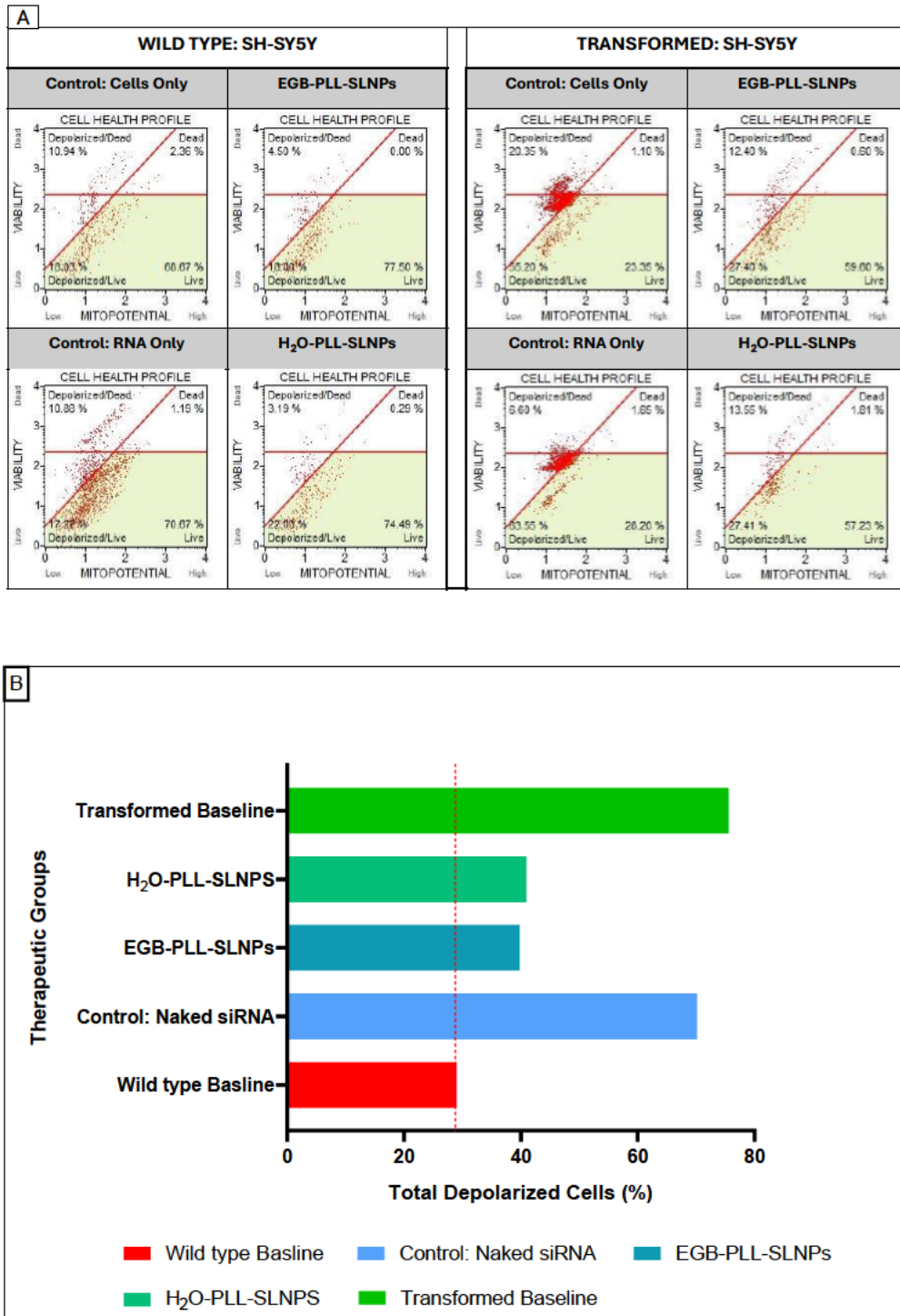


Figure 7.12. (A) The MitoPotential analysis pertaining to the various therapeutic groups in the wild-type and transformed SH-SY5Y cells. (B) The normalization studies portraying the comparison of total depolarized (%) cells between the post-treated transformed SH-SY5Y cells and the wild-type control baseline.

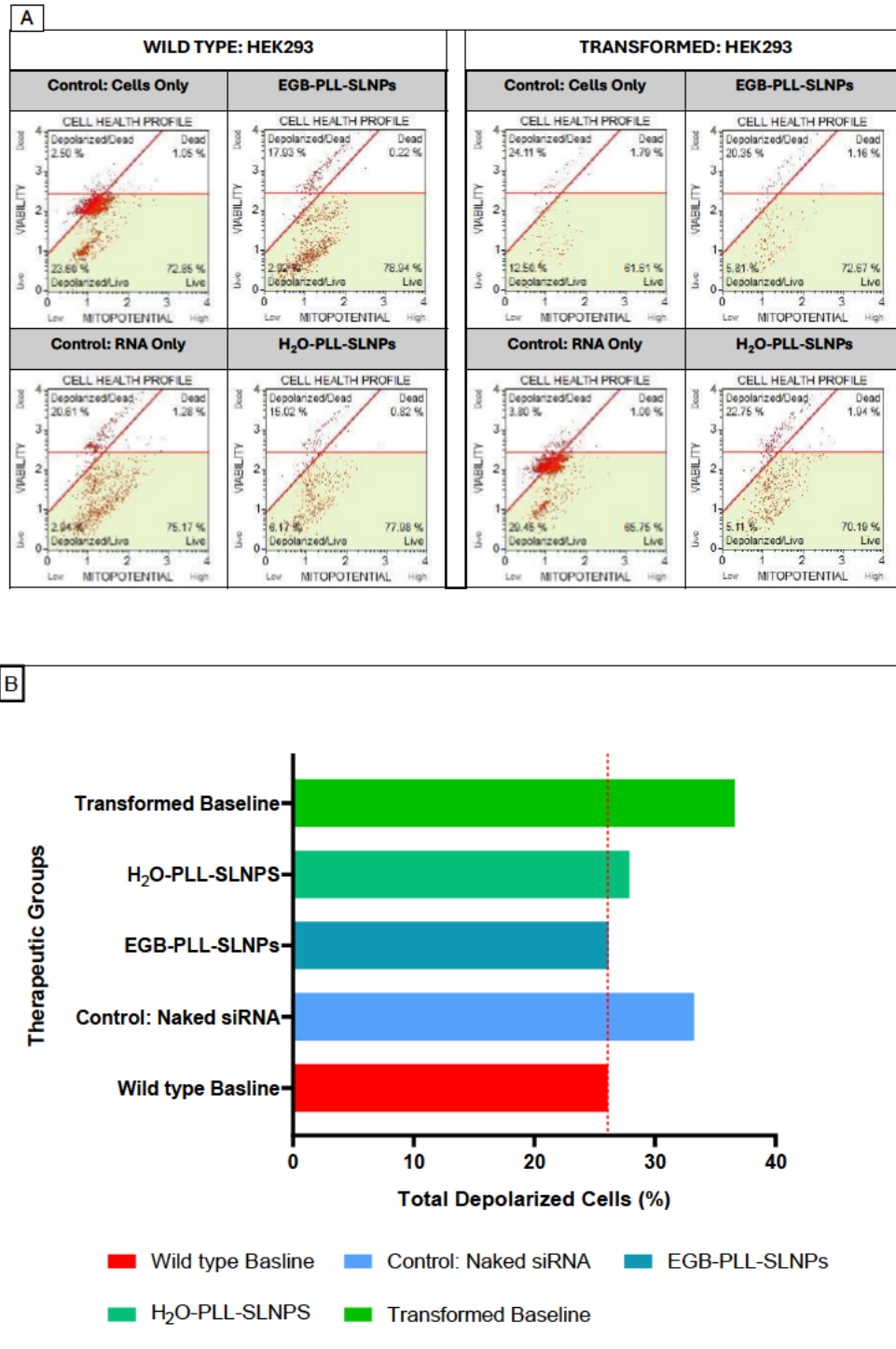


Figure 7.13. (A) The MitoPotential analysis pertaining to the various therapeutic groups in the wild-type and transformed HEK293 cells. (B) The normalization studies portraying the comparison of total depolarized (%) cells between the post-treated transformed HEK293 cells and the wild-type control baseline.

7.3.4.5. Summary of inhibition of LRRK2 G2019S activity

The study aimed to assess the gene silencing efficacy of various therapeutics targeting the LRRK2 G2019S mutation in Parkinson's Disease (PD). The primary endpoints included reductions in kinase activity, reactive oxygen species (ROS) levels, mitochondrial potential, and DNA damage. Treatments evaluated were siRNA:EGB-PLL-SLNPs and H₂O-PLL-SLNP nanocomplexes, and naked siRNA, compared against control cells (untreated).

The siRNA:EGB-PLL-SLNPs demonstrated substantial gene silencing across all assays. In the SH-SY5Y cells, the kinase activity was significantly reduced compared to cells treated with naked siRNA. The reduction in kinase activity was also significant in the HEK293 cells (figure 7.14A). The siRNA:H₂O-PLL-SLNPs also showed a reduction in kinase activity, with fold changes (Figure 14B) in both cells but to a lesser extent than the siRNA:EGB-PLL-SLNPs. ROS levels, which are a marker of oxidative stress, are usually elevated in PD. A notable reduction in ROS levels was observed in both cell lines, demonstrating the efficacy of these nanocomplexes in reducing oxidative stress.

DNA damage, which contributes to neuronal death in PD, was significantly reduced with both nanocomplexes in both cell lines compared to the naked siRNA. Here again, the superior protection offered by the siRNA: EGB-PLL-SLNPs against DNA damage is highlighted (Figure 7.14 A and B). The mito-potential, a critical indicator of cellular health in PD, was also evaluated. In both SH-SY5Y and HEK293 cells, the EGB-based nanocomplexes performed better than the other treatments and naked siRNA, further confirming their high efficacy in maintaining mitochondrial integrity.

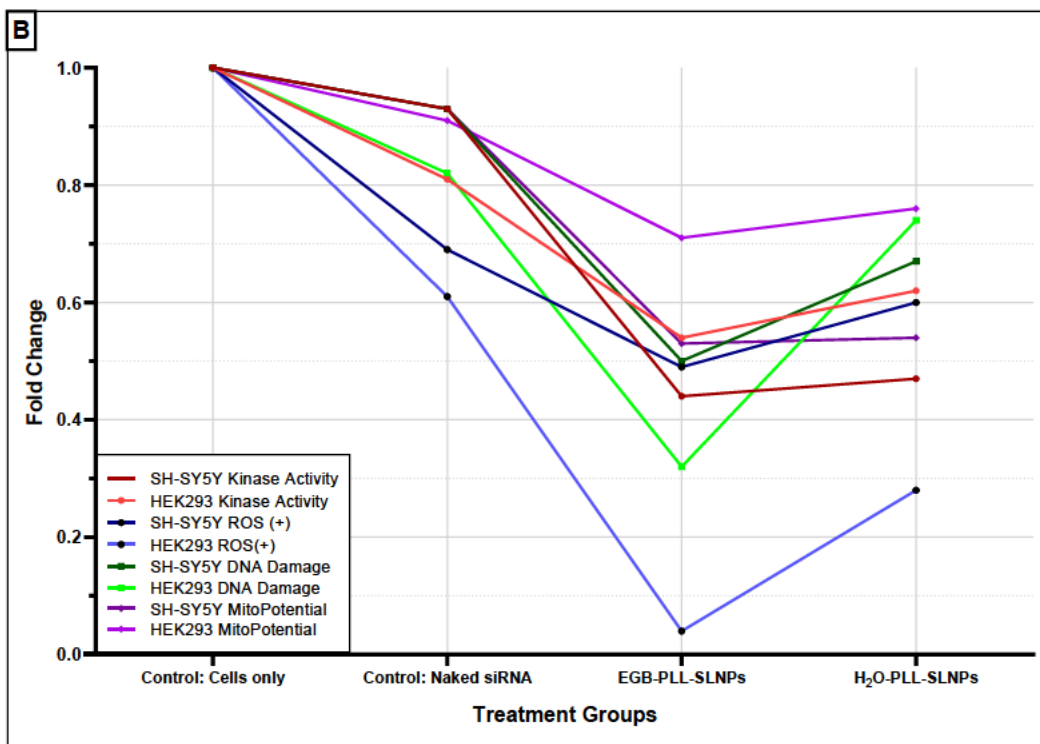
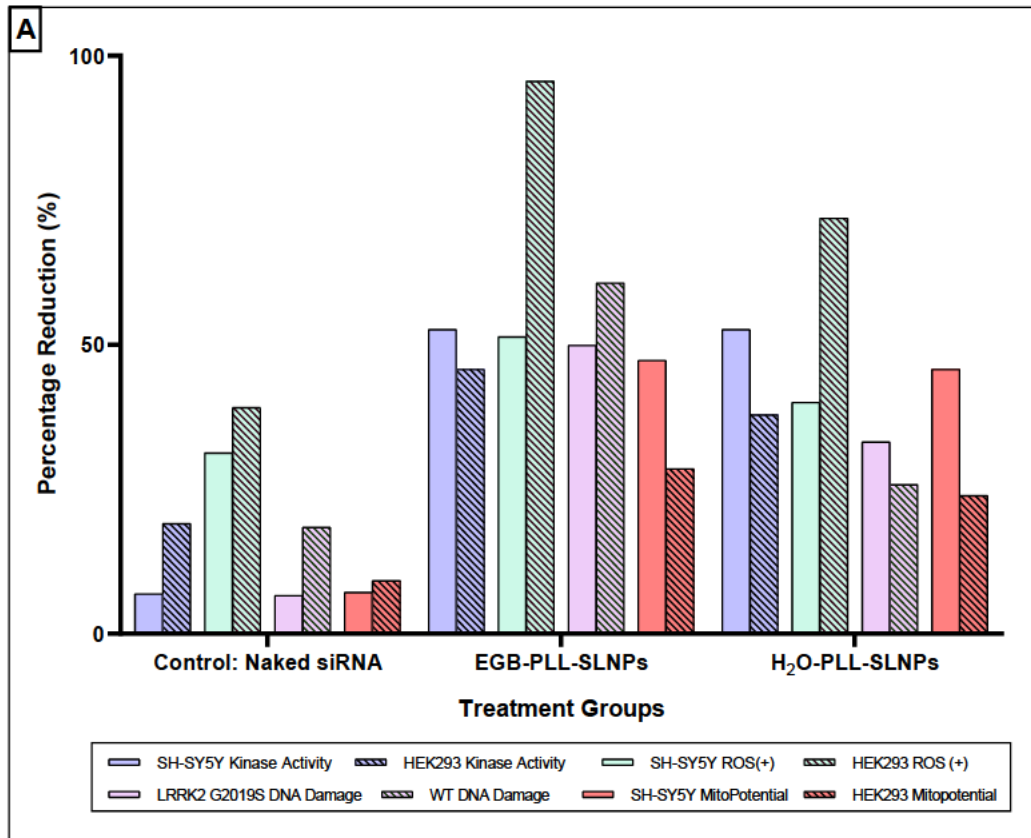


Figure 7.14. A comprehensive overview of the therapeutic efficiency to silence the LRRK2 G2019S by assessing various pivotal indicators of cellular health in PD, including kinase activity, oxidative stress, DNA damage, and MitoPotential and shown as (A) Percentage reduction and (B) Fold change. These were generated through the comparison of the post-treated cells with the control of untreated cells.

7.4. Discussion

The successful synthesis of the SLNPs has been outlined in Chapter 6, section 6.4 and characterized using UV-vis and FTIR spectroscopy, TEM, and DLS. Briefly, the SLNPs are less than 150 nm in size, with high zeta potentials (> 35 mV). This suggested that the SLNPs were of a favourable size and stability for biomedical applications. UV-vis and FTIR analysis were able to confirm the successful synthesis and functionalization of the SLNPs with PLL. These results, together with successful siRNA binding and protection studies, confirmed the potential of these SLNPs for gene delivery.

Following the cellular uptake studies, both qualitative and quantitative results demonstrated the superior ability of the EGB-PLL-SLNPs to facilitate better uptake than the H₂O-PLL-SLNPs. The increased uptake at the 1:2 (w/w) ratio underscores the dose-dependent nature of the SLNP internalization in both neuroblastoma and embryonic kidney cells. For the biosynthesized SLNPs, this could be attributed to the bioactive components of EGB, such as flavonoids and terpenoids, that possess the ability to integrate into lipid bilayers, increasing the fluidity and permeability of the membrane [24] and enhancing cellular uptake. Additionally, the stimulation of endocytosis is facilitated by the presence of ginkgolides in the EGB, which modulate this process, leading to increased internalization of the SLNPs [25]. Moreover, compounds such as quercetin and kaempferol can interact with cell surface receptors, facilitating uptake through receptor-mediated endocytosis and rendering a more targeted and efficient uptake while reducing off-target effects [26].

The comparison between cellular uptake in wild-type and transformed cells revealed interesting insights. The mutated cell lines exhibited greater uptake of the SLNPs compared to the wild-type cells. This can be attributed to alterations in cellular pathways and increased metabolic activity associated with the LRRK2 G2019S mutation, especially the increase in kinase activity that enhances normal endocytic and intracellular trafficking processes [27, 28]. This enhancement is due to the increased formation and trafficking of extracellular vesicles (EVs), including exosomes [29,30]. These small membrane-bound vesicles play a crucial role in intracellular communication and transport of molecular cargo. The mutation upregulates genes such as RAB27B that are involved in the biogenesis and secretion of EVs [29,30]. Furthermore, there is an alteration in the formation of multivesicular bodies (MVBs), resulting in smaller MVBs. As a result, more docking sites are available for the NPs, thus increasing uptake [31,32]. Moreover, enhanced cellular metabolic activity drives the energy-intensive processes of vesicle

trafficking, formation, and fusion with target membranes, facilitating more efficient internalization and distribution of the therapeutic SLNPs.

The combined results obtained from the MTT and Caspase 3/7 assays provide a comprehensive overview of the SLNP's cytotoxicity and apoptotic profiles in addition to their therapeutic potential. The results from the transformed cells are compared to those from the proof-of-principle study on wild-type cells, as outlined in the previous chapter. The SLNPs performed best under optimal binding conditions, highlighting the need to inhibit cytotoxicity at higher concentrations [25]. The EGB-PLL-SLNPs portrayed high cellular viabilities and low apoptotic indices in the neuroblastoma and embryonic kidney cells, respectively. This was in contrast to the H₂O-PLL-SLNPs that produced an increase in the apoptotic index.

These positive results highlight the effect of the bioactive compounds in EGB, which confer anti-apoptotic properties to the SLNPs. These compounds exert multiple protective mechanisms at a cellular level, contributing to the observed reduction in apoptosis and improvement in cell viability. This is achieved by the terpenoids, namely the ginkgolides, which inhibit the release of cytochrome c from the mitochondria, which is a crucial step in the intrinsic apoptotic pathway. This prevents the activation of key apoptosis executioners such as caspase-3 and 7 [33]. Furthermore, EGB downregulates the expression of pro-apoptotic proteins, including Bax, and upregulates anti-apoptotic proteins, such as Bcl-2. Shifting the balance between anti- and pro-apoptotic proteins enhances cell survival and reduces apoptosis initiation [34]. Importantly, the activation of nuclear factor-kappa B (NF-κB), a transcription factor that promotes the expression of pro-apoptotic and pro-inflammatory genes, is inhibited by EGB, thus reducing inflammation-induced apoptosis. This is particularly beneficial in neurodegenerative diseases such as PD [35].

The results from the H₂O-PLL-SLNPs further highlight the beneficial properties of EGB. It can be inferred that due to the lack of bioactive compounds, these SLNPs may induce apoptosis through various mechanisms. This could be due to poor *in vitro* stability and siRNA protection, resulting in premature release and degradation of the therapeutic [25]. Additionally, SLNPs without the anti-inflammatory properties exhibited by the EGB could induce an inflammatory response upon successful uptake and internalization, thereby inducing apoptotic events [35]. Overall, these studies have shown the favourable properties of the formulated SLNPs, promoting their use in downstream applications, such as gene silencing.

The LRRK2 G2019S mutation is reported to cause an increase in kinase activity, contributing to the progression of PD [23]. The mutation's substitution of glycine with serine at position 2019 enhances the intrinsic catalytic activity of the kinase through structural alterations, conformational changes, and increased autophosphorylation at several residues [27,28]. Consequently, the increase in kinase activity promotes neuroinflammation, synaptic defects, and mitochondrial dysfunction, leading to the loss of dopaminergic neurons, characteristic of PD [23,27]. The kinase activity assay was conducted using the NanoBRET TE intracellular kinase assay kit, providing compelling evidence of the therapeutic potential of the PLL-SLNPs.

Successful transfection was noted by an increase in kinase activity in the SH-SY5Y and HEK293 cells, with a significant reduction of >50% in the transformed SH-SY5Y cells and >37% in the transformed HEK293 cells. These results indicate that the siRNA was able to limit the genetic aberrations caused by the mutation, with the EGB providing beneficial properties in this process. These properties are evident in their direct ability to inhibit kinase activity through the quercetin, kaempferol, and isorhamnetin components. These compounds bind to active sites of kinases, minimizing their ability to phosphorylate substrates, leading to a significant reduction in kinase activity [36]. Furthermore, the extract has been noted to modulate various signaling pathways, such as the PI3K/Akt pathway, which intersects with kinase activity. This specific pathway is involved in cell survival and proliferation, and its inhibition leads to a reduction in the activation of downstream kinases [37]. As previously evidenced, EGB has the ability to infiltrate the cellular membrane for efficient internalization. This allows for enhanced therapeutic ability of the siRNA, as observed in the present assay, with the siRNA showing an enhanced effect on kinase activity when synergized with the EGB. The protective nature of the delivery vehicles ensured a larger concentration of intact therapeutic siRNA being delivered into the cells, enhancing gene silencing. The EGB-PLL-SLNPs proved effective in silencing the LRRK2 G2019S mutation by reducing kinase activity close to the wild-type baseline.

Overall, the study demonstrated a pronounced reduction in kinase activity. A study by Nichols *et al.* (2009) reported using traditional kinase inhibitors, which reduced kinase activity by 30% [28]. This was corroborated by a study conducted by Lee *et al.* (2012), who used a nano-based delivery system and achieved a 35% reduction in kinase activity [39]. Furthermore, two independent studies by Pedro *et al.* (2013) and Chen *et al.* (2012) using siRNA to target LRRK2 noted a 50% and 40-50% decline in kinase activity upon treatment [40,41]. These results align

with the current study's findings, highlighting a slight improvement in kinase activity reduction using the siRNA: EGB-PLL-SLNP nanoformulation.

The enhanced kinase activity due to the LRRK2 G2019S mutation leads to elevated oxidative stress due to increased ROS production, thereby contributing to neuronal damage in PD [42,43]. In the SH-SY5Y wild-type cells, the percentage of ROS (+) increased from 14.22% to 27.80% in the transformed cells, validating the effective transformation and introduction of the mutation into the cellular genome. It is important to note that the elevated ROS levels in the wild-type cells are due to the cancerous state of the neuroblastoma cells, which inherently exhibit elevated oxidative stress due to increased metabolic activity [44]. This serves as a baseline for comparative purposes. Once again, the EGB-PLL-SLNPs outperformed the H₂O-PLL-SLNPs, reducing ROS (+) levels to 13.51% versus 16.67%. This trend was further observed in the HEK293 cells. The post-therapeutic outcome showed that these SLNPs decreased ROS (+) levels to near-normal levels compared to the wild-type baseline, highlighting the potent therapeutic effect of the siRNA in silencing the gene of interest and normalizing elevated pathogenic levels.

Synergistically with the effect of the siRNA, EGB has been shown to effectively scavenge free radicals, thereby reducing the concentration of ROS (+) in the cells. This plays a crucial role in its neuroprotective effects in the context of PD. The extract's potent antioxidants (terpenoids and flavonoids) neutralize ROS via electron donation, thus mitigating oxidative stress within the cells [42,43]. These compounds enhance cellular antioxidant defense mechanisms through upregulation of enzymes such as superoxide dismutase (SOD) and glutathione peroxidase (GPx), further detoxifying ROS [44].

Studies on varied treatments for PD, with regard to decreasing oxidative stress, have shown varying degrees of effectiveness. Traditional antioxidant therapies, such as coenzyme Q10, showed a 10% reduction of ROS in clinical trials, which was not substantial enough to yield clinical benefits [45]. Furthermore, vitamin E supplementation showed modest effects, reducing these levels by 8% [46]. An increase in efficacy was noted by Zhang *et al.* (2010), with a 25% reduction noted by using NP-encapsulated antioxidants [25]. In the present study, a 51.39% reduction was observed for the SiRNA:EGB-PLL-SLNPs, which produced significantly greater efficacy in reducing ROS to normal levels.

The multi-color DNA damage assay highlighted the differences associated with the mutational event. The elevated levels of pATM, double-stranded DNA breaks (DSBs), and pH2A.X in the

mutated SH-SY5Y and HEK293 cells suggested heightened genomic instability. The LRRK2 G2019S mutation is known for impairing DNA repair pathways, increasing susceptibility to DNA damage, and permitting the onset of PD through neuronal loss [47]. The impairment in DNA repair pathways fails to effectively resolve this damage, leading to persistent activation of DNA damage checkpoints and neuronal apoptosis, resulting in genomic instability related to PD [48]. In the transformed SH-SY5Y cells, there were markedly higher levels of pATM, DSBs, and pH2A.X, indicating persistent activation of DNA damage responses, genomic instability, and ongoing DNA damage and repair. In contrast, the transformed HEK293 cells showed a significant elevation in damage, noted more in pH2A.X levels, with a reduction in pATM and DSBs [49]. It can be inferred that upon transformation with the mutation, inactivation of DNA responses was noted, thus requiring external intervention.

The EGB-PLL-SLNPs were successful in reducing DNA damage in the SH-SY5Y and HEK293 cells by > 50%. In contrast, the H₂O-PLL-SLNPs total DNA damage in both cells was lower (25-33%). These results provide further evidence of the gene silencing effects through the synergism of EGB and siRNA. In the mutated SH-SY5Y cells, a reduction in pATM and DSBs indicated a reduced activation of DNA damage response levels owing to significant DNA repair mechanisms. Interestingly, increased pH2A.X levels indicated the heightened activation of DNA repair mechanisms due to DNA damage [49]. In contrast, pH2A.X levels were abolished for the siRNA:H₂O-PLL-SLNPs, indicating an effective repair mechanism.

While the siRNA itself does not directly repair DNA damage, the repair mechanisms align with the properties exhibited by the SLNPs and EGB components. Apart from the extract's aforementioned benefits, they have been shown to modulate chromatin remodeling and facilitate access of repair enzymes to damaged DNA sites [44]. Theoretically, the extract enhances ATP-dependent chromatin remodeling complexes such as the SWI/SNF complex. These complexes alter chromatin structure by displacing nucleosomes and recruiting DNA repair proteins to the damage sites [50,48]. The properties exhibited by EGB provide a robust defense against genomic instability and associated neurodegenerative conditions [51].

The MitoPotential assay provided insights into the health of the mitochondria following the induction of the mutation into the genome. The MitoPotential, or mitochondrial membrane potential, is a vital indicator of mitochondrial function, reflecting the maintenance of an electrochemical gradient [52]. Due to the increased kinase activity of the mutation, normal mitochondrial function becomes impaired due to fragmentation, resulting in an increase in ROS

production [53,54]. Mitochondrial trafficking and biogenesis are affected, disrupting the mitochondria along the neuronal axons and resulting in energy deficits at synaptic terminals and impaired neuronal function. These effects increase the vulnerability of dopaminergic neurons to degeneration in PD [55].

In the SH-SY5Y cells, a total depolarization from 28 to 75% was noted after mutation. The therapeutic formulations were successful in reducing this damage, with 12% for the siRNA:EGB-PLL-SLNPs and 13 % for the siRNA:H₂O-PLL-SLNPs. This result was consistent with the HEK293 cells, though to a lesser extent, with depolarization ranging from 26 to 36 % in the control. For the nanoformulations, the EGB-PLL-SLNPs performed the best. These results validate previous findings on the efficacy of the siRNA in silencing the genetic mutation, as well as the synergism with EGB-PLL-SLNPs in enhancing therapeutic efficiency.

Quercetin and kaempferol from the extract enhance mitochondrial function through the stabilization of the mitochondrial membrane, thus promoting ATP production [56]. Quercetin has been identified to enhance the activity of complexes I and III of the electron transport chain, simultaneously maintaining the mitochondrial membrane and reducing its dysfunction [57]. Additionally, kaempferol protects the mitochondria through the promotion of antioxidant enzymes [58]. It is also noted that the compounds in the extract can upregulate the expression of genes involved in mitochondrial biogenesis and function. This involves the activation of the PGC-1 α pathway, a signaling pathway that leads to an increased expression of nuclear and mitochondrial genes essential for the replication, growth, and function of mitochondria [49]. The production of new mitochondria and improvements in overall functionality and energy production capacity of the cells are enhanced [59].

The siRNA primarily reduces the impact on mitochondrial health by mitigating the detrimental effects of the mutant protein. The siRNA-mediated silencing of the LRRK2 G2019S mutation decreases kinase activity, creating a cascade effect on other factors influenced by this mutation. This silencing effect complements the antioxidant effect of the EGB, providing a dual therapeutic approach for the protection of the mitochondria and the prevention of neuronal loss.

7.5. Conclusion

This study demonstrated that the siRNA delivery system utilizing EGB-PLL-SLNPs effectively silenced the LRRK2 G2019S mutation and mitigated its adverse effects. The LRRK2 G2019S mutation leads to increased kinase activity, mitochondrial dysfunction, elevated ROS production, impaired DNA repair mechanisms, and ultimately promoted neuronal loss in PD.

The EGB-PLL-SLNPs delivery system exhibited remarkable efficacy in targeting and silencing the LRRK2 G2019S gene, as evidenced by substantial improvements in mitochondrial health and a marked increase in cell viability. Moreover, the system achieved a favourable reduction in ROS levels, DNA damage, and kinase activity. The superior performance of the EGB-PLL-SLNPs can be attributed to the synergistic effects of the EGB's bioactive compounds, namely, quercetin and kaempferol, which stabilize mitochondrial membrane potential, enhance ATP production, and upregulate genes involved in mitochondrial biogenesis. This dual therapeutic effect by combining the protective and antioxidant properties of EGB with the gene-silencing capabilities of siRNA, offered a robust and promising approach for managing the pathogenic effects of the LRRK2 G2019S mutation in PD. This study provides compelling evidence supporting the use of EGB-PLL-SLNPs as a potent and innovative nanosystem with significant therapeutic outcomes compared to traditional delivery systems and opens up an avenue for advancement in the treatment of PD.

7.6. Future Recommendation

Future research should focus on optimizing the formulation and delivery of EGB-PLL-SLNPs to further enhance their therapeutic efficacy and specificity in targeting the LRRK2 G2019S mutation. Investigating the long-term effects and stability of these SLNPs *in vivo* will provide valuable insights into their potential clinical applications. Additionally, exploring the combination of EGB-PLL-SLNPs with other therapeutic agents or treatment modalities could produce a novel treatment strategy for PD. The precise mechanisms by which the bioactive compounds in EGB contribute to the observed therapeutic benefits should be investigated. It would be beneficial to expand this research to include other neurodegenerative diseases with similar pathological mechanisms to assess the broader applicability of this approach. Finally, *in vivo* studies in animal models are essential to validate the safety and efficacy of EGB-PLL-SLNPs, paving the way for their eventual adoption in a clinical setting.

References

1. Winter, V.S.; Karayel, O.; Strauss, M.T.; Padmanabhan, S.; Surface, M.; Merchant, K.; Alcalay, R.N.; Mann, M. Urinary proteome profiling for stratifying patients with familial Parkinson's disease. *EMBO Mol Med.*, **2021**, 13. doi: 10.15252/emmm.202013257.
2. Przedborski, S. The two-century journey of Parkinson disease research. *Nat Rev Neurosci.*, **2017**, 18, 251-259.

3. Schapira, A.H.V.; Chaudhuri, K.R.; Jenner, P. Non-motor features of Parkinson disease. *Nat Rev Neurosci.*, **2017**, *18*, 435-450.
4. Deng, H.; Wang, P.; Jankovic, J. The genetics of Parkinson disease. *Ageing Res Rev.*, **2018**, *42*, 72-85. doi: 10.1016/j.arr.2017.12.007.
5. Walter, J.; Bolognin, S.; Poovathingal, S.K.; *et al.* The Parkinson's-disease-associated mutation LRRK2-G2019S alters dopaminergic differentiation dynamics via NR2F1. *Cell Rep.*, **2021**, *37*, 109864. doi: 10.1016/j.celrep.2021.109864.
6. Croce, J.C.; McClay, D.R. Evolution of the Wnt pathways. *Methods Mol Biol.*, **2008**, *469*, 3-18. doi: 10.1007/978-1-60327-469-7_1.
7. Funayama, M.; Hasegawa, K.; Kowa, H.; Saito, M.; Tsuji, S.; Obata, F. A new locus for Parkinson's disease (PARK8) maps to chromosome 12p11.2-q13.1. *Ann Neurol.*, **2002**, *51*, 296-301.
8. Paisán-Ruiz, C.; Jain, S.; Evans, E.W.; *et al.* Cloning of the gene containing mutations that cause PARK8-linked Parkinson's disease. *Neuron.*, **2004**, *44*, 595-600.
9. Zimprich, A.; Biskup, S.; Leitner, P.; *et al.* Mutations in LRRK2 cause autosomal-dominant parkinsonism with pleomorphic pathology. *Neuron.*, **2004**, *44*, 601-607.
10. Orenstein, S.J.; Kuo, S-H.; Tasset, I.; *et al.* Interplay of LRRK2 with chaperone-mediated autophagy. *Nat Neurosci.*, **2013**, *16*, 394-406. doi: 10.1038/nn.3350.
11. Migheli, R.; Del Giudice, M.G.; Spissu, Y.; Sanna, G.; Xiong, Y.; Dawson, T.M.; *et al.* LRRK2 affects vesicle trafficking; neurotransmitter extracellular level and membrane receptor localization. *PLoS ONE.*, **2013**, *8*. doi: 10.1371/journal.pone.0077198.
12. Juárez-Flores, D.L.; González-Casacuberta, I.; Ezquerra, M.; *et al.* Exhaustion of mitochondrial and autophagic reserve may contribute to the development of LRRK2G2019S-Parkinson's disease. *J Transl Med.*, **2018**, *16*, 160. doi: 10.1186/s12967-018-1526-3.
13. Nguyen, H.N.; Byers, B.; Cord, B.; *et al.* LRRK2 Mutant iPSC-Derived DA Neurons Demonstrate Increased Susceptibility to Oxidative Stress. *Cell Stem Cell.*, **2011**, *8*, 267-280. doi: 10.1016/j.stem.2011.01.013.
14. Hu, Y.; Deng, H.; Xu, S.; Zhou, Y.; Nie, H.; Liang, D. LRRK2 inhibition for Parkinson's disease treatment: current progress and perspectives. *BMC Med.*, **2023**, *21*, 78. doi: 10.1186/s12916-023-02745-7.
15. Wu, Y.C.; Sonninen, T.M.; Peltonen, S.; Koistinaho, J.; Lehtonen, Š. Blood–Brain Barrier and Neurodegenerative Diseases—Modeling with iPSC-Derived Brain Cells. *Int J Mol Sci.*, **2021**, *22*, 7710. doi: 10.3390/ijms22147710.
16. Daneman, R.; Prat, A. The Blood–Brain Barrier. *Cold Spring Harb Perspect Biol.*, **2015**, *7*
17. Jagaran, K.; Singh, M. Lipid Nanoparticles: Promising Treatment Approach for Parkinson's Disease. *Int J Mol Sci.*, **2022**, *23*, 9361. doi: 10.3390/ijms23169361.

18. Paliwal, R.; Paliwal, S.R.; Kenwat, R.; Kurmi, B.D.; Sahu, M.K. Solid lipid nanoparticles: A review on recent perspectives and patents. *Expert Opin Ther Pat.*, **2020**, 30, 179-194. doi: 10.1080/13543776.2020.1720649.
19. Kim, H.J.; Choi, H.S.; Chang, M.J. Sphingomyelin synthase 1 (SMS1) is an upstream regulator of PTEN for sphingomyelin-enriched membrane domain formation. *J Lipid Res.*, **2020**, 61, 393-403. doi: 10.1194/jlr.M093294.
20. Ariga, T. Role of sphingolipids in the nervous system. *Neurochem Res.*, **2017**, 42, 251-261. doi: 10.1007/s11064-016-2097-4.
21. Ahmad, M.; Saleem, S.; Ahmad, A.S.; Yousuf, S.; Ansari, M.A.; Khan, M.B.; Ishrat, T.; Chaturvedi, R.K.; Agrawal, A.K.; Islam, F. *Ginkgo biloba* affords dose-dependent protection against 6-hydroxydopamine-induced parkinsonism in rats: Neurobehavioural; neurochemical and immunohistochemical evidences. *J Neurochem.*, **2005**, 93, 94-104. doi: 10.1111/j.1471-4159.2005.03000.x.
22. Lugli, E.; Roederer, M.; Cossarizza, A. Data analysis in flow cytometry: the future just started. *Cytometry A.*, **2015**, 87, 785-787. doi: 10.1002/cyto.a.22611.
23. Greggio, E., Cookson, M.R., Savitt, J.M., Campbell, K., Blackinton, J., Farrer, M.J., Katsanis, N., Zhuang, X., & Hardy, J. The Parkinson disease-associated leucine-rich repeat kinase 2 (LRRK2) is a dimer that undergoes intra-molecular autophosphorylation. *J Biol Chem.*, **2006**, 281, 21067-21077.
24. Jiang, H.; Wang, J.; Rogers, J.; Xie, J. *Ginkgo biloba* extract in Alzheimer's disease: From action mechanisms to medical practice. *Int J Mol Sci.*, **2011**, 12, 764-797.
25. Zhang, H.; Nie, S.; Wan, Y. Nanoparticles in therapeutics: Targeted delivery for cancer and neurodegenerative disorders. *Nanomedicine.*, **2010**, 5, 205-220.
26. He, Y.; Yu, H.; Bao, Y.; Pan, Y. Nanoparticle-mediated gene therapy for neurological disorders. *Front Mol Neurosci.*, **2018**, 11, 320.
27. West, A.B., Moore, D.J., Biskup, S., Bugayenko, A., Smith, W.W., Ross, C.A., Dawson, V.L., Dawson, T.M. Parkinson's disease-associated mutations in LRRK2 link enhanced GTP-binding and kinase activities to neuronal toxicity. *Hum Mol Genet.*, **2007**, 16, 223-232.
28. Cookson, M.R. The role of leucine-rich repeat kinase 2 (LRRK2) in Parkinson's disease. *Nat Rev Neurosci.*, **2010**, 11, 791-797.
29. Andreu, Z.; Yáñez-Mó, M. Tetraspanins in extracellular vesicle formation and function. *Front Immunol.*, **2014**, 5, 442.
30. Chiasserini, D., van Weering, J.R., Piersma, S.R., Pham, T.V., Malekzadeh, A., Teunissen, C.E., de Wit, H., Breen, G., Jimenez, C.R. Proteomic analysis of cerebrospinal fluid extracellular vesicles: a comprehensive dataset. *J Proteomics.*, **2014**, 106, 191-204.
31. Jacquet, A.; Tancredi, J.L.; Lemire, A.L.; DeSantis, M.C.; Li, W-P.; O'Shea, E.K. The LRRK2 G2019S mutation alters astrocyte-to-neuron communication via extracellular vesicles and

- induces neuron atrophy in a human iPSC-derived model of Parkinson's disease. *eLife.*, **2021**. doi: 10.7554/eLife.73062.
32. Lin, C-H.; Tsai, P-L.; Wu, R-M.; Chien, C-T. LRRK2 G2019S Mutation Induces Dendrite Degeneration through Mislocalization and Phosphorylation of Tau by Recruiting Autoactivated GSK3 β . *J Neurosci.*, **2010**, 30, 13138-13149. doi: 10.1523/JNEUROSCI.1737-10.2010.
 33. Smith, J.V.; Luo, Y. Studies on molecular mechanisms of *Ginkgo biloba* extract. *Appl Microbiol Biotechnol.*, **2004**, 64, 465-472. doi: 10.1007/s00253-003-1516-z.
 34. Nasr, P. Neuroprotective effects of *Ginkgo biloba* extract in Parkinson's disease: A review. *J Neurochem.*, **2014**, 130, 780-795. doi: 10.1111/jnc.12718.
 35. Kudoh, C., Inoue, M., Hirano, R., Honda, K., Yoshikawa, T., Yamaguchi, R., Furukawa, S., Sawada, M. Inhibition of NF- κ B activation by *Ginkgo biloba* extract in human neuronal cells: A potential mechanism for neuroprotection. *J Neuroinflammation.*, **2014**, 11, 12. doi: 10.1186/1742-2094-11-12.
 36. Kang, N.J.; Lee, K.W.; Lee, D.E.; Rogozin, E.A.; Bode, A.M.; Dong, Z. Quercetin inhibits UV-induced phosphorylation of mitogen-activated protein kinases and cellular transformation in mouse epidermal cells. *J Biol Chem.*, **2011**, 286, 17435-17444. doi: 10.1074/jbc.M111.242420.
 37. Ahlemeyer, B.; Krieglstein, J. Neuroprotective effects of *Ginkgo biloba* extract. *Cell Mol Life Sci.*, **2003**, 60, 1779-1792. doi: 10.1007/s00018-003-3084-7.
 38. Nichols, R.J.; Dzamko, N.; Hutti, J.E.; Cantley, L.C.; Deak, M.; Moran, J.; Alessi, D.R. Substrate specificity and inhibitors of LRRK2; a protein kinase mutated in Parkinson's disease. *Biochem J.*, **2009**, 424, 47-60. doi: 10.1042/BJ20091271.
 39. Lee, S.; Kim, J.; Park, S. Nanoparticle-mediated gene delivery for Parkinson's disease treatment. *Biomaterials.*, **2012**, 33, 6878-6886. doi: 10.1016/j.biomaterials.2012.05.044.
 40. Bravo-San Pedro, J.M., Niso-Santano, M., Gómez-Sánchez, R., Pizarro-Estrella, E., Aiausti, A., Gorostidi, A., Climent, V., López de Maturana, R., Sanchez-Pernaute, R., López-Otín, C., Kroemer, G., Galluzzi, L., Fueyo, R., Zubiarrain, I., Alberdi, E., Ruiz-Martinez, J., Berganzo, K., López de Munain, A. The LRRK2 G2019S mutant exacerbates basal autophagy through activation of the MEK/ERK pathway. *Cell Mol Life Sci.*, **2013**, 70, 121-136. doi: 10.1007/s00018-012-1069-y.
 41. Chen, C.Y., Weng, Y.H., Chien, K.Y., Lin, K.J., Yeh, T.H., Cheng, Y.P., Lu, C.S., Wang, H.L., Hsu, I.W., Wu, Y.R. (G2019S) LRRK2 activates the MKK4-JNK pathway and causes degeneration of SN dopaminergic neurons in a transgenic mouse model of PD. *Cell Death Differ.*, **2012**, 19, 1623-1633. doi: 10.1038/cdd.2012.41.
 42. Tanaka, K.; S-Galduroz, F.R.; Gobbi, T.B.L.; Galduroz, C.F.J. *Ginkgo biloba* Extract in an Animal Model of Parkinson's Disease: A Systematic Review. *Curr Neuropharmacol.*, **2013**, 11, 430-435. doi: 10.2174/1570159X11311040006.

43. Lejri, I.; Agapouda, A.; Grimm, A.; Eckert, A. Mitochondria- and Oxidative Stress-Targeting Substances in Cognitive Decline-Related Disorders: From Molecular Mechanisms to Clinical Evidence. *Oxid Med Cell Longev.*, **2019**, 2019, 1-12. doi: 10.1155/2019/9695412.
44. Liu, X.; Qin, W.; Decker, Y.; Wang, Y.; Burkart, M.; Schötz, M.; Menger, M.D.; Fassbender, K.; Liu, Y. Long-term treatment with *Ginkgo biloba* extract EGB 761 improves symptoms and pathology in a transgenic mouse model of Alzheimer's disease. *Brain Behav Immun.*, **2015**, 46, 121. doi: 10.1016/j.bbi.2015.02.003.
45. Beal, M.F. Mitochondria take center stage in aging and neurodegeneration. *Ann Neurol.*, **2005**, 58, 495-505. doi: 10.1002/ana.20624.
46. Schults, C.W. Ongoing clinical trials of coenzyme Q10 in Parkinson's disease. *BioFactors.*, **2000**, 9, 235-239. doi: 10.1002/biof.5520090233.
47. Ruo Tong, S.; Foo, C.N.; Lin, Y.E.; Chien, C.T.; Lim, Y.M. Molecular Pathways Involved in LRRK2-Linked Parkinson's Disease: A Systematic Review. *Int J Mol Sci.*, **2022**, 23, 11744. doi: 10.3390/ijms231911744.
48. van Attikum, H.; Gasser, S.M. Crosstalk between histone modifications during the DNA damage response. *Trends Cell Biol.*, **2009**, 19, 207-217. doi: 10.1016/j.tcb.2009.03.001.
49. Wang, X.; Zhang, Y.; Li, P. The role of non-homologous end joining and homologous recombination in DNA repair. *Cancer Res.*, **2019**, 79, 890-899. doi: 10.1158/0008-5472.CAN-18-2339.
50. Hoeijmakers, J.H.J. Genome maintenance mechanisms for preventing cancer. *Nature.*, **2001**, 411, 366-374. doi: 10.1038/35077232.
51. Tian, Z.; Tang, C.; Wang, Z. Neuroprotective effect of ginkgetin in experimental cerebral ischemia/reperfusion via apoptosis inhibition and PI3K/Akt/mTOR signaling pathway activation. *J Cell Biochem.*, **2019**, 120, 18487-18496. doi: 10.1002/jcb.28989.
52. Nicholls, D.G.; Ferguson, S.J. Bioenergetics. *Academic Press.*, **2013**.
53. Di Maio, R.; Hoffman, E.K.; Rocha, E.M.; *et al.* LRRK2 activation in idiopathic Parkinson's disease. *Sci Transl Med.*, **2018**, 10. doi: 10.1126/scitranslmed.aar5429.
54. Trancikova, A.; Mamais, A.; Webber, P.J.; *et al.* Phosphorylation of LRRK2: from pathogenesis to therapeutic intervention. *Biochem Soc Trans.*, **2012**, 40, 1112-1118. doi: 10.1042/BST20120124.
55. Papkovskaia, T.D.; Chau, K.Y.; Inesta-Vaquera, F.; *et al.* G2019S LRRK2 mutant linked to increased kinase activity and microtubule-binding sensitivity in familial Parkinson's disease. *Proc Natl Acad Sci U S A.*, **2012**, 109, 6929-6934. doi: 10.1073/pnas.1117299109.
56. Zhou, Y.; Zheng, J.; Li, S.; Zhou, T.; Zhang, P.; Li, H.B. Flavonoids and mitochondrial function in human cells. *Pharmacol Res.*, **2019**, 139, 83-92. doi: 10.1016/j.phrs.2018.10.006.
57. Liobikas, J.; Trumbeckaite, S.; Pauziene, N.; Deduchovas, O.; Borutaite, V.; Morkunas, E.; Barauskaite, J.; Brown, G.C. Quercetin protects mitochondrial function in the experimental

model of Parkinson's disease. *Neurochem Res.*, **2011**, 3, 1876-1885. doi: 10.1007/s11064-011-0494-8.

58. Chen, C., Jiang, X., Lai, Y., Tang, H., Liang, J., Guo, X., Sun, X. Protective effects of kaempferol against oxidative stress-induced mitochondrial dysfunction in human neuroblastoma SH-SY5Y cells. *Mol Med Rep.*, **2018**, 18, 328-340. doi: 10.3892/mmr.2018.8948.
59. Yao, L., Chen, H., Wu, Q., Xie, K., Xiao, Q., Zhang, W., Hu, J. The role of PGC-1 α in mitochondrial biogenesis and function. *Exp Cell Res.*, **2020**, 391, 111955. doi: 10.1016/j.yexcr.2020.111955.

Refer to Appendix C5 for the Turnitin Report.

Chapter 8:
**Summary, Conclusions, Limitations and Future
Recommendations**

8.1. Summary

The overarching aim of this thesis was to develop and evaluate a bio-inspired solid lipid nanoparticle (SLNP) system for the targeted delivery of small interfering RNA (siRNA) to suppress the LRRK2 G2019S mutation, a key contributor to the pathogenesis of Parkinson's disease (PD). Current treatments for PD are primarily palliative, addressing only the symptoms rather than the genetic causes of the disease. Thus, this project sought to establish a therapeutic strategy that could intervene at a molecular level, offering both gene silencing and symptomatic relief.

The theory behind this research is grounded in the role of the LRRK2 G2019S mutation, which increases kinase activity and disrupts cellular homeostasis, leading to neurodegeneration in PD. This mutation is one of the most common genetic causes of PD, making it a promising target for therapeutic intervention. siRNA provides a mechanism for silencing this mutation, but it requires an effective delivery vehicle to overcome challenges such as degradation in circulation and poor uptake across the blood-brain barrier (BBB). To address this, the study used *Ginkgo biloba* extract (EGB) as a reducing agent to biosynthesize SLNPs, taking advantage of EGB's properties that enhance BBB permeability, while also offering antioxidant and neuroprotective effects.

The SLNPs were designed using a sphingomyelin-cholesterol matrix, functionalized with poly-L-lysine (PLL), to enhance siRNA binding and facilitate its cellular uptake. In Chapter 6, these nanoparticles were characterized extensively using techniques such as UV-visible (UV-vis) spectroscopy, transmission electron microscopy (TEM), dynamic light scattering (DLS), and Fourier-transform infrared spectroscopy (FTIR). Results demonstrated the successful synthesis of nanoparticles with desirable size (~200 nm), surface charge (-30 mV to +20 mV depending on functionalization), and stability. siRNA binding studies, including the ethidium bromide intercalation assay and band shift electrophoresis, confirmed efficient complexation of siRNA with the SLNPs. Binding efficiency peaked at a 2:1 PLL ratio, ensuring the stability and protection of siRNA from enzymatic degradation.

In terms of biological evaluation, the cytotoxicity of the NPs was assessed in the wild-type and LRRK2 G2019S mutated SH-SY5Y cells using the MTT and caspase 3/7 assays. Cell viability remained above 87% for all therapeutic doses, indicating high biocompatibility of the SLNPs. Cellular uptake studies using BLOCK-iT™ fluorescent oligos demonstrated efficient NP internalization, indicating enhanced delivery in the mutated disease model.

Chapter 7 expanded on these findings by exploring the therapeutic efficiency of the SLNPs in mediating gene silencing. EGB-PLL-SLNPs significantly reduced kinase activity, a key measure of LRRK2 mutation-related dysfunction, was reduced by 56.08% with EGB-PLL-SLNPs, surpassing the performance of H₂O-based counterparts. The oxidative stress assay showed a reduction in ROS (+) levels to 13.51% in the LRRK2 G2019S mutated cells compared to 16.67 % observed for the H₂O-PLL-SLNPs, and 27.80% ROS (+) noted in the control group. The reduction in total DNA damage was similarly notable, with EGB-PLL-SLNPs reducing DNA damage by 49.90%, compared to 33.17% for H₂O-PLL-SLNPs. In addition, the MitoPotential assay revealed that EGB-PLL-SLNP treatment led to a 47.31% reduction in depolarized cells, indicating a restoration of mitochondrial function, which is often compromised in PD due to excessive oxidative stress.

This study successfully evaluated a novel bio-inspired SLNP delivery system for targeted gene therapy in PD. The EGB-PLL-SLNPs provided dual functionality, acting as both a gene silencing agent and a neuroprotective therapeutic, making them a promising candidate for future clinical applications in the treatment of PD and other neurodegenerative diseases involving genetic mutations. This thesis thus contributes significantly to the field of nanomedicine and gene therapy, providing a foundation for future personalized medicine approaches tailored to the genetic and molecular profiles of individual patients.

8.2. Limitations of the Study

Despite the promising findings of this study, several limitations must be acknowledged. One primary limitation is the *in vitro* nature of the experiments. While cellular models provide valuable insights into the therapeutic efficacy of the SLNPs for siRNA delivery, they do not fully replicate the complex *in vivo* environment. The blood-brain barrier (BBB), potential off-target effects and immune responses must be further evaluated in animal models before clinical applications can be considered.

Another limitation is noted in the variability of natural extracts, such as Ginkgo biloba, which can exhibit batch-to-batch variations in bioactive compound composition. This variability could impact the consistency of the synthesized SLNPs, necessitating stringent quality control measures.

Furthermore, the long-term effects of SLNPs on overall brain function with a focus on neuronal health and metabolism are yet to be determined. Extended exposure studies are required to assess potential cytotoxicity and unintended side effects of chronic nanotherapeutic

administration. The pharmacokinetics and biodistribution of these nanoparticles must also be evaluated using in vivo models to optimize dosing strategies and minimize systemic side effects.

Lastly, this study focused on the LRRK2 G2019S mutation, a key genetic contributor to Parkinson's disease (PD). However, PD is a multifactorial disease with other genetic and environmental influences. Future studies should explore SLNPs to be adapted to target other genetic variants and neurodegenerative pathways.

8.3. Conclusion and future recommendations

The study presented a comprehensive evaluation of *Ginkgo biloba* extract-functionalized sphingomyelin-cholesterol solid lipid nanoparticles (EGB-PLL-SLNPs) as a novel therapeutic approach for targeting the LRRK2 G2019S mutation in PD. This research not only showcased the potential of using natural extract-based nanoparticle systems for gene therapy but also highlighted the advantages of combining traditional medicine with advanced nanotechnology.

The initial phase of the study successfully demonstrated the synthesis and functionalization of EGB-PLL-SLNPs, characterized by high biocompatibility and efficient cellular uptake, with cell viability exceeding 90% in wild-type SH-SY5Y cells. This proof of principle study established the foundational properties required for effective therapeutic delivery systems. The second phase focused on evaluating the therapeutic efficacy of EGB-PLL-SLNPs in LRRK2 G2019S mutated SH-SY5Y cells, yielding promising results. EGB-PLL-SLNPs significantly reduced oxidative stress, DNA damage, and kinase activity compared to H2O-PLL-SLNPs. Specifically, EGB-PLL-SLNPs reduced reactive oxygen species (ROS) levels by 51.39%, decreased total DNA damage by 49.90%, and lowered kinase activity by 52.65%, surpassing the reductions achieved by H2O-PLL-SLNPs.

The gene silencing efficiency of EGB-PLL-SLNPs was particularly notable, effectively silencing the LRRK2 G2019S gene and resulting in a significant reduction in kinase activity and associated cellular dysfunction. These findings underscore the enhanced delivery and efficacy provided by the *Ginkgo biloba* extract, which not only facilitated better cellular uptake and siRNA delivery but also offered additional antioxidant and DNA repair benefits. The consistent efficacy of the EGB-PLL-SLNPs highlights their potential as a highly effective therapeutic approach for managing PD, particularly in cases involving the LRRK2 G2019S mutation. This innovative approach underscores the importance of natural extract-based

therapies in advancing personalized medicine, promoting environmental safety, reduced toxicity, and cost-effectiveness.

The utilization of the *Ginkgo biloba* extract, a natural product, ensures better biocompatibility and reduces the risk of long-term adverse effects compared to synthetic compounds. From an economic perspective, the use of readily available natural extracts like *Ginkgo biloba* can lower production costs, making these advanced therapies more accessible. The principles and methodologies established in this research can be extrapolated to other neurodegenerative diseases and genetic disorders, broadening the scope of gene-silencing technologies. Moving forward, further investigations, including in vivo studies, are necessary to assess the pharmacokinetics, biodistribution, and long-term toxicity of EGB-PLL-SLNPs in animal models, with potential progression to clinical trials to determine efficacy and safety in human subjects. Optimizing the system for crossing the blood-brain barrier, enhancing cellular uptake, and targeting additional genetic mutations implicated in PD, such as SNCA, PARK2, and DJ-1, could further expand its applicability.

Beyond PD, this innovative NP system holds promise for treating other neurodegenerative and genetic diseases, such as Alzheimer's, Huntington's, and amyotrophic lateral sclerosis (ALS), where targeted delivery and gene silencing could yield substantial benefits. The versatility of bio-inspired SLNPs may extend to addressing genetic mutations in cancers and metabolic disorders, illustrating the broad therapeutic potential of this approach. Emphasizing personalized medicine, where treatments are tailored to individual genetic profiles, will enhance therapeutic efficacy and minimize adverse effects, paving the way for more effective and customized healthcare solutions. This study thus not only advances PD research but also lays the groundwork for transformative applications in the broader medical field, advocating for continued exploration and innovation in personalized and sustainable healthcare.

Beyond this, recent advances in AI and ML offer transformative potential in optimizing siRNA-based nanomedicine for Parkinson's disease. AI-driven algorithms can aid in the rational design of lipid nanoparticles (LNPs) by predicting optimal compositions, surface modifications, and encapsulation efficiencies, thereby enhancing the precision of therapeutic delivery (Witten et al., 2024).

Machine learning models can be utilized to predict binding efficiency, siRNA stability as well as off-target effects. Resultingly, this improves the selection of gene silencing sequences with minimal side effects and higher specificity (Liu et al., 2024). Novel biomarkers have also been

identified by means of deep learning approaches, permitting early diagnosis and personalized treatment strategies (Jia et al., 2025). Through the integration of AI with high-throughput screening, researchers possess the capability to expedite the discovery of more effective siRNA formulations that cross the BBB and achieve efficient intracellular delivery.

Furthermore, AI-driven simulations can predict nanoparticle interactions within biological systems, thus providing greater insights into cellular uptake, pharmacokinetics and biodistribution. These optimized nanoparticle formulations will reduce costs and accelerate translational research (Bhange and Telange., 2025). In addition to therapeutic applications, AI and ML play a crucial role in PD patient management. AI-powered wearable technologies, together with mobile applications, allow the tracking of motor symptoms, providing real-time feedback in detecting disease progression, and allowing for personalized treatment adjustments. Such innovations, combined with siRNA-based nanotherapies, could revolutionize precision medicine approaches for PD.

References:

1. Witten, J., Raji, I., Manan, R. S., Beyer, E., Bartlett, S., Tang, Y., Ebadi, M., Lei, J., Nguyen, D., Oladimeji, F., Jiang, A. Y., MacDonald, E., Hu, Y., Mughal, H., Self, A., Collins, E., Yan, Z., Engelhardt, J. F., Langer, R., & Anderson, D. G. Artificial intelligence-guided design of lipid nanoparticles for pulmonary gene therapy. *Nature Biotechnology*, **2024**. DOI: 10.1038/s41587-024-02490-y.
2. Liu, B., Yuan, Y., Pan, X., Shen, H.-B., & Jin, C. AttSiOff: a self-attention-based approach on siRNA design with inhibition and off-target effect prediction. *Med-X*, **2024**, 2, 5. DOI: 10.1007/s44258-024-00019-1.
3. Jia, J., Niu, L., Feng, P., Liu, S., Han, H., Zhang, B., Wang, Y., & Wang, M. Identification of Novel Biomarkers for Ischemic Stroke Through Integrated Bioinformatics Analysis and Machine Learning. *Journal of Molecular Neuroscience*, **2025**, 75, 13. DOI: 10.1007/s12031-025-02309-8.
4. Bhange, M., & Telange, D. Convergence of nanotechnology and artificial intelligence in the fight against liver cancer: a comprehensive review. *Discover Oncology*, **2025**, 16, 77. DOI: 10.1007/s12672-025-01821-y.

Appendix A1

Published Paper: Jagaran, K., Singh, M*. Nanomedicine for Neurodegenerative Disorders: Focus on Alzheimer's and Parkinson's Diseases. *Int. J. Mol. Sci.*, 2021, 22(16), 9082. DOI: <https://doi.org/10.3390/ijms22169082>



Review

Nanomedicine for Neurodegenerative Disorders: Focus on Alzheimer's and Parkinson's Diseases

Keelan Jagaran and Moganavelli Singh *

Nano-Gene and Drug Delivery Group, Discipline of Biochemistry, University of KwaZulu-Natal, Private Bag X54001, Durban 4000, South Africa; 215055447@stu.ukzn.ac.za
* Correspondence: singhm1@ukzn.ac.za; Tel.: +27-31-260-7170

Abstract: Neurodegenerative disorders involve the slow and gradual degeneration of axons and neurons in the central nervous system (CNS), resulting in abnormalities in cellular function and eventual cellular demise. Patients with these disorders succumb to the high medical costs and the disruption of their normal lives. Current therapeutics employed for treating these diseases are deemed palliative. Hence, a treatment strategy that targets the disease's cause, not just the symptoms exhibited, is desired. The synergistic use of nanomedicine and gene therapy to effectively target the causative mutated gene/s in the CNS disease progression could provide the much-needed impetus in this battle against these diseases. This review focuses on Parkinson's and Alzheimer's diseases, the gene/s and proteins responsible for the damage and death of neurons, and the importance of nanomedicine as a potential treatment strategy. Multiple genes were identified in this regard, each presenting with various mutations. Hence, genome-wide sequencing is essential for specific treatment in patients. While a cure is yet to be achieved, genomic studies form the basis for creating a highly efficacious nanotherapeutic that can eradicate these dreaded diseases. Thus, nanomedicine can lead the way in helping millions of people worldwide to eventually lead a better life.



Citation: Jagaran, K.; Singh, M. Nanomedicine for Neurodegenerative Disorders: Focus on Alzheimer's and Parkinson's Diseases. *Int. J. Mol. Sci.* **2021**, *22*, 9082. <https://doi.org/10.3390/ijms22169082>

Academic Editor: Szilvia Veszelka

Received: 28 July 2021

Accepted: 20 August 2021

Published: 23 August 2021

Publisher's Note: MDPI stays neutral with regard to jurisdictional claims in published maps and institutional affiliations.



Copyright: © 2021 by the authors. Licensee MDPI, Basel, Switzerland. This article is an open access article distributed under the terms and conditions of the Creative Commons Attribution (CC BY) license (<https://creativecommons.org/licenses/by/4.0/>).

Keywords: neurodegenerative disorders; gene therapy; nanomedicine; Parkinson's disease; Alzheimer's disease

1. Introduction

Neurodegenerative disorders, through the subsequent immune activation of the central nervous system (CNS), impose substantial burdens on the public and health sectors. While immune activation may aid in regeneration and repair, together with various other mechanisms such as the limitation of neurotropic viral infections and the removal of necrotic cells, it can also lead to the development of neurodegeneration, ischaemia, infections, and immune-mediated disorders. Neurodegeneration is defined as the slow but gradual degeneration of neurons and axons in the CNS that results in abnormalities in cellular function and, consequently, cellular demise [1]. The ensuing symptoms stem from the degeneration stage, beginning with a loss of coordination and memory, to a complete loss of the ability to function as a normal healthy individual. The three major neurodegenerative disorders have been identified as Alzheimer's disease (AD), Parkinson's disease (PD), and amyotrophic lateral sclerosis (ALS) [2]. These diseases are closely linked to environmental cues, disordered immunity, advancing age, and the genetic make-up of the affected individual [3].

Although over 50 million people are believed to be affected by AD globally, these numbers are progressively increasing due to the increased average lifespan and genetic and environmental factors. An estimated 152 million of the population are projected to be affected by the year 2050 [4]. This will create an immense global economic strain in the years to come. Beyond AD, and based on the Parkinson's Foundation Prevalence Project, approximately 10 million individuals have presented with PD, with about one million belonging to the United States of America (USA) alone. These patients succumb

Appendix A2

Jagaran, K., Singh, M*. Lipid Nanoparticles: Promising Treatment Approach for Parkinson's Disease. *Int. J. Mol. Sci.*, 2022, 23(16), 9361. DOI: <https://doi.org/10.3390/ijms23169361>



Review

Lipid Nanoparticles: Promising Treatment Approach for Parkinson's Disease

Keelan Jagaran and Moganavelli Singh *

Nano-Gene and Drug Delivery Laboratory, Discipline of Biochemistry, University of KwaZulu-Natal, Private Bag X54001, Durban 4000, South Africa

* Correspondence: singhm1@ukzn.ac.za; Tel: +27-31-2607170

Abstract: Parkinson's disease (PD), a neurodegenerative disorder, is a life-altering, debilitating disease exhibiting a severe physical, psychological, and financial burden on patients. Globally, approximately 7–10 million people are afflicted with this disease, with the number of cases estimated to increase to 12.9 million by 2040. PD is a progressive movement disorder with nonmotor symptoms, including insomnia, depression, anxiety, and anosmia. While current therapeutics are available to PD patients, this treatment remains palliative, necessitating alternative treatment approaches. A major hurdle in treating PD is the protective nature of the blood–brain barrier (BBB) and its ability to limit access to foreign molecules, including therapeutics. Drugs utilized presently are nonspecific and administered at dosages that result in numerous adverse side effects. Nanomedicine has emerged as a potential strategy for treating many diseases. From the array of nanomaterials available, lipid nanoparticles (LNPs) possess various advantages, including enhanced permeability to the brain via passive diffusion and specific and nonspecific transporters. Their bioavailability, nontoxic nature, ability to be conjugated to drugs, and targeting moieties catapult LNPs as a promising therapeutic nanocarriers for PD. While PD-related studies are limited, their potential as therapeutics is evident in their formulations as vaccines. This review is aimed at examining the roles and properties of LNPs that make them efficient therapeutic nanodelivery vehicles for the treatment of PD, including therapeutic advances made to date.

Keywords: Parkinson's disease; lipid nanoparticles; drug delivery; blood–brain barrier; nanomedicine

Citation: Jagaran, K.; Singh, M. # Lipid Nanoparticles: Promising Treatment Approach for Parkinson's Disease. *Int. J. Mol. Sci.* 2022, 23, 9361. <https://doi.org/10.3390/ijms23169361>

Academic Editor: Maryam Ardalan

Received: 28 July 2022

Accepted: 18 August 2022

Published: 19 August 2022

Publisher's Note: MDPI stays neutral with regard to jurisdictional claims in published maps and institutional affiliations.



Copyright: © 2022 by the authors. Licensee MDPI, Basel, Switzerland. This article is an open access article distributed under the terms and conditions of the Creative Commons Attribution (CC BY) license (<https://creativecommons.org/licenses/by/4.0/>).

1. Introduction

Parkinson's disease (PD) presents itself as a life-altering and debilitating disease that primarily affects the neuronal make-up of the brain. It is deemed a neurodegenerative disorder. It is estimated that 7–10 million people are afflicted with this disease worldwide, with a prevalence rate of 41 in 100,000 people. Notably, the prevalence rate increases to 1900 people per 100,000 in individuals over 80 years old [1]. This growing health issue is postulated to see an increased prevalence to 12.9 million cases by 2040 [2].

Clinically, PD is a progressive movement disorder with various nonmotor symptoms, including sleep disturbance, constipation, depression, anxiety, and anosmia [3,4]. This disease manifests in two forms: (i) sporadic (idiopathic), which is caused by a gene–environment interaction, and (ii) familial, which is genetically inherited in either an autosomal recessive or dominant manner [5,6]. Genetic mutations that cause the disease are noted in some genes, such as the *LRRK2*, *PARK7*, *PINK1*, *PRKN*, and *SNCA*. The resulting manifestation of parkinsonian symptoms is due to a pathological effect, which is observed as loss of dopaminergic neurons in the substantia nigra and presence of various protein aggregates (including α -synuclein), called Lewy bodies, in the midbrain [7].

Appendix B1

Zeta Potential Report (ZetaSizer): GBE-SC-SLNPs

Zeta Potential Report

v2.3



Malvern Instruments Ltd - © Copyright 2008

Sample Details

Sample Name: GBE-SC-SLNPs
SOP Name: mansettings.nano
General Notes:

File Name: SLNPs.dts
Record Number: 42
Date and Time: Thursday, 23 June 2022 14:12:18
Dispersant Name: Water
Dispersant RI: 1,330
Viscosity (cP): 0,8872
Dispersant Dielectric Constant: 78,5

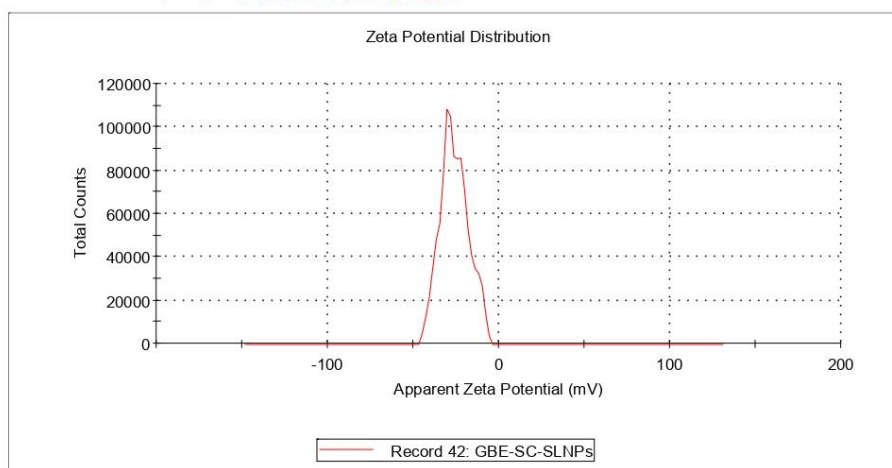
System

Temperature (°C): 25,0
Count Rate (kcps): 75,4
Cell Description: Zeta dip cell
Zeta Runs: 12
Measurement Position (mm): 4,50
Attenuator: 7

Results

	Mean (mV)	Area (%)	St Dev (mV)
Zeta Potential (mV): -25,9	Peak 1: -30,9	58,8	4,97
Zeta Deviation (mV): 8,22	Peak 2: -18,4	41,2	4,94
Conductivity (mS/cm): 0,00872	Peak 3: 0,00	0,0	0,00

Result quality : See result quality report



Appendix B2

Zeta Potential Report (ZetaSizer): GBE-PLL-SC-SLNPs

Zeta Potential Report

v2.3



Malvern Instruments Ltd - © Copyright 2008

Sample Details

Sample Name: GBE-PLL-SC-SLNPs

SOP Name: mansettings.nano

General Notes:

File Name: SLNPs.dts	Dispersant Name: Water
Record Number: 36	Dispersant RI: 1,330
Date and Time: Thursday, 23 June 2022 14:30:26	Viscosity (cP): 0,8872
	Dispersant Dielectric Constant: 78,5

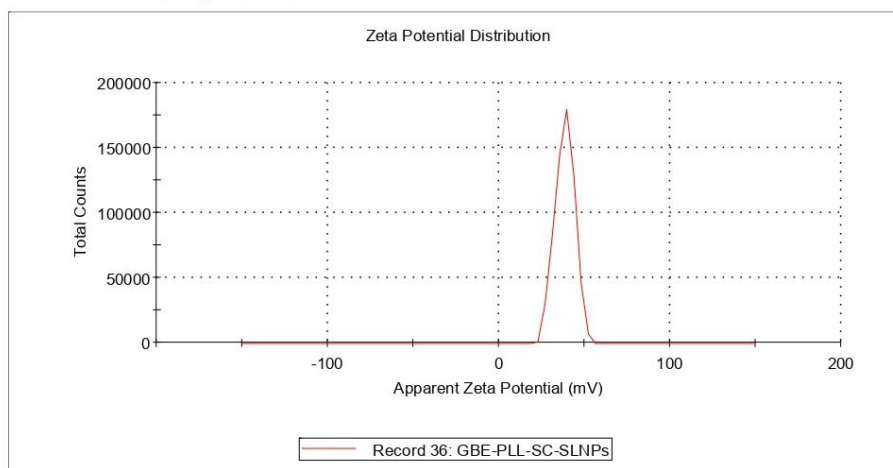
System

Temperature (°C): 25,0	Zeta Runs: 12
Count Rate (kcps): 135,8	Measurement Position (mm): 4,50
Cell Description: Zeta dip cell	Attenuator: 7

Results

	Mean (mV)	Area (%)	St Dev (mV)
Zeta Potential (mV): 38,4	Peak 1: 38,4	100,0	5,63
Zeta Deviation (mV): 5,63	Peak 2: 0,00	0,0	0,00
Conductivity (mS/cm): 0,0276	Peak 3: 0,00	0,0	0,00

Result quality : **Good**



Appendix B3

Zeta Potential Report (ZetaSizer): GBE-PLL-SC-SLNPs:siRNA

Zeta Potential Report

v2.3



Malvern Instruments Ltd - © Copyright 2008

Sample Details

Sample Name: GBE-PLL-SC-SLNPs-siRNA

SOP Name: mansettings.nano

General Notes:

File Name: SLNPs.dts	Dispersant Name: Water
Record Number: 38	Dispersant RI: 1,330
Date and Time: Thursday, 23 June 2022 14:51:18	Viscosity (cP): 0,8872
	Dispersant Dielectric Constant: 78,5

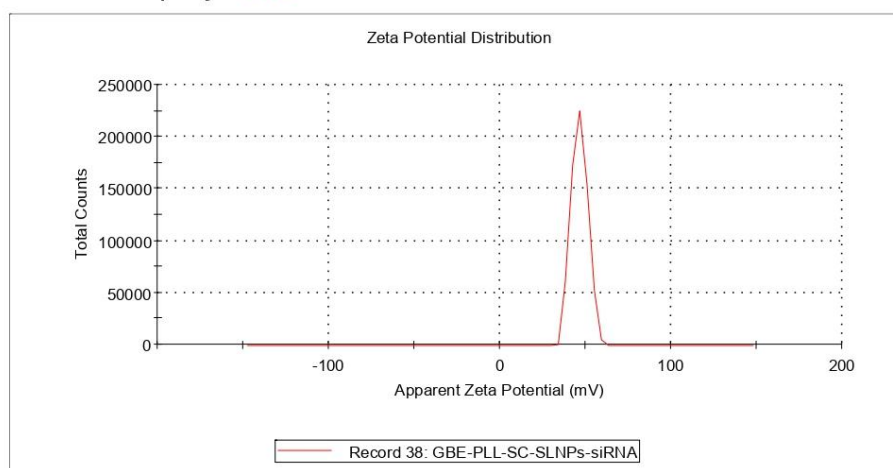
System

Temperature (°C): 25,0	Zeta Runs: 12
Count Rate (kcps): 171,2	Measurement Position (mm): 4,50
Cell Description: Zeta dip cell	Attenuator: 8

Results

	Mean (mV)	Area (%)	St Dev (mV)
Zeta Potential (mV): 46,4	Peak 1: 46,4	100,0	4,71
Zeta Deviation (mV): 4,71	Peak 2: 0,00	0,0	0,00
Conductivity (mS/cm): 0,0883	Peak 3: 0,00	0,0	0,00

Result quality : Good



Appendix B4

Zeta Potential Report (ZetaSizer): H₂O-SC-SLNPs

Zeta Potential Report

v2.3



Malvern Instruments Ltd - © Copyright 2008

Sample Details

Sample Name: H2O-SC-SLNPs
SOP Name: mansettings.nano
General Notes:

File Name: SLNPs.dts
Record Number: 41
Date and Time: Thursday, 23 June 2022 13:54:00
Dispersant Name: Water
Dispersant RI: 1,330
Viscosity (cP): 0,8872
Dispersant Dielectric Constant: 78,5

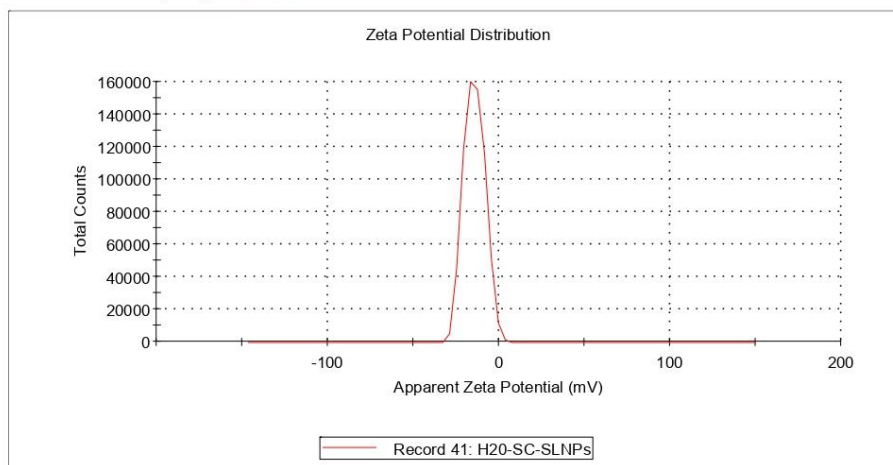
System

Temperature (°C): 25,0
Count Rate (kcps): 121,7
Cell Description: Zeta dip cell
Zeta Runs: 12
Measurement Position (mm): 4,50
Attenuator: 6

Results

	Mean (mV)	Area (%)	St Dev (mV)
Zeta Potential (mV): -14,4	Peak 1: -14,4	100,0	5,99
Zeta Deviation (mV): 5,99	Peak 2: 0,00	0,0	0,00
Conductivity (mS/cm): 0,0331	Peak 3: 0,00	0,0	0,00

Result quality : Good



Appendix B5

Zeta Potential Report (ZetaSizer): H₂O-PLL-SC-SLNPs

Zeta Potential Report

v2.3



Malvern Instruments Ltd - © Copyright 2008

Sample Details

Sample Name: H2O-PLL-SC-SLNPs

SOP Name: mansettings.nano

General Notes:

File Name: SLNPs.dts
Record Number: 37
Date and Time: Thursday, 23 June 2022 14:38:47

Dispersant Name: Water
Dispersant RI: 1,330
Viscosity (cP): 0,8872
Dispersant Dielectric Constant: 78,5

System

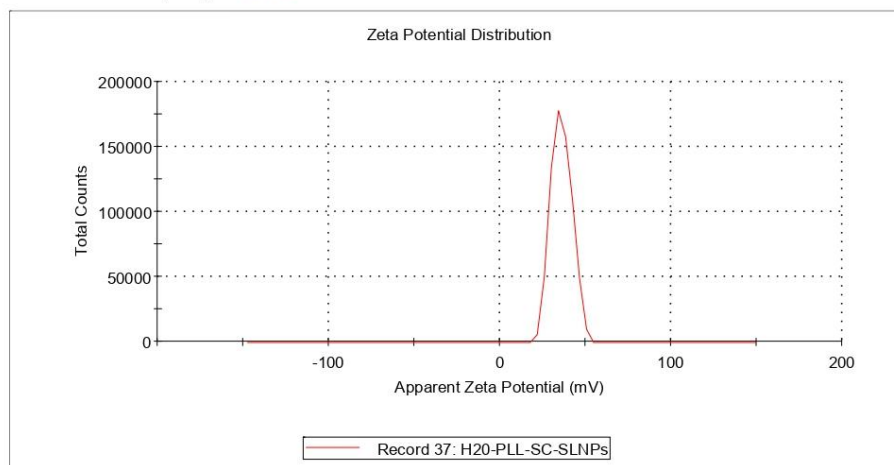
Temperature (°C): 25,0
Count Rate (kcps): 207,6
Cell Description: Zeta dip cell

Zeta Runs: 12
Measurement Position (mm): 4,50
Attenuator: 7

Results

	Mean (mV)	Area (%)	St Dev (mV)
Zeta Potential (mV): 35,9	Peak 1: 35,9	100,0	5,95
Zeta Deviation (mV): 5,95	Peak 2: 0,00	0,0	0,00
Conductivity (mS/cm): 0,0242	Peak 3: 0,00	0,0	0,00

Result quality : **Good**



Appendix B6

Zeta Potential Report (ZetaSizer): H₂O-PLL-SC-SLNPs:siRNA

Zeta Potential Report v2.3



Malvern Instruments Ltd - © Copyright 2008

Sample Details

Sample Name: H2O-PLL-SC-SLNPs-siRNA

SOP Name: mansettings.nano

General Notes:

File Name: SLNPs.dts Dispersant Name: Water
Record Number: 39 Dispersant RI: 1,330
Date and Time: Thursday, 23 June 2022 14:56:13 Viscosity (cP): 0,8872
Dispersant Dielectric Constant: 78,5

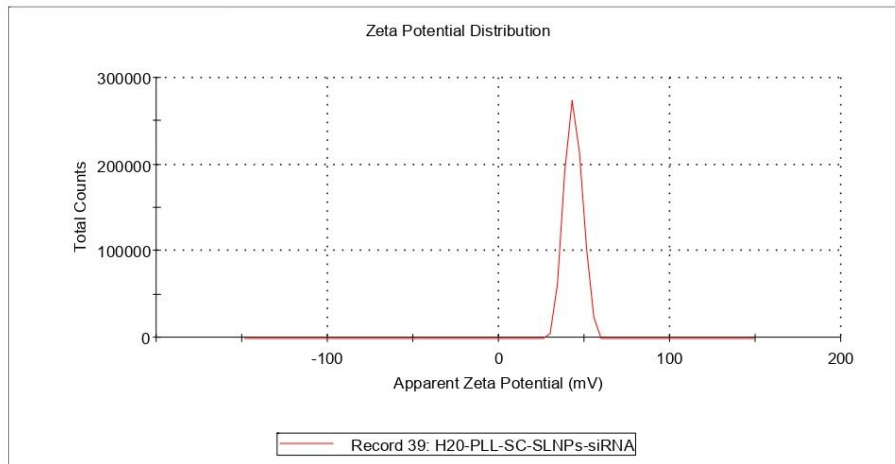
System

Temperature (°C): 25,0 Zeta Runs: 14
Count Rate (kcps): 155,6 Measurement Position (mm): 4,50
Cell Description: Zeta dip cell Attenuator: 8

Results

	Mean (mV)	Area (%)	St Dev (mV)
Zeta Potential (mV): 43,4	Peak 1: 43,4	100,0	5,20
Zeta Deviation (mV): 5,20	Peak 2: 0,00	0,0	0,00
Conductivity (mS/cm): 0,0882	Peak 3: 0,00	0,0	0,00

Result quality : **Good**



Appendix C1

Turnitin Report Chapter 1:

Chapter 1.docx

ORIGINALITY REPORT

15% SIMILARITY INDEX	13% INTERNET SOURCES	9% PUBLICATIONS	5% STUDENT PAPERS
--------------------------------	--------------------------------	---------------------------	-----------------------------

PRIMARY SOURCES

1	www.ncbi.nlm.nih.gov Internet Source	5%
2	www.researchgate.net Internet Source	1%
3	Submitted to Queen Mary and Westfield College Student Paper	1%
4	Submitted to Durban University of Technology Student Paper	1%
5	Submitted to University of Surrey Student Paper	1%
6	Ronald F. Pfeiffer, Zbigniew K. Wszolek, Manuchair Ebadi. "Parkinson's Disease", CRC Press, 2019 Publication	1%
7	Submitted to University of Strathclyde Student Paper	1%
8	www.nature.com Internet Source	1%

9	Submitted to University of Leeds Student Paper	1 %
10	Submitted to IDEA Leadership & Management Institute Student Paper	1 %
11	pubmed.ncbi.nlm.nih.gov Internet Source	1 %
12	www.science.gov Internet Source	1 %
13	www.frontiersin.org Internet Source	1 %
14	www.mdpi.com Internet Source	1 %
15	encyclopedia.pub Internet Source	<1 %
16	mpace.lib.umanitoba.ca Internet Source	<1 %

Exclude quotes On

Exclude matches Off

Exclude bibliography On

Appendix C2

Turnitin Report Chapter 4:

Chapter 4.docx

ORIGINALITY REPORT

9%	4%	8%	1%
SIMILARITY INDEX	INTERNET SOURCES	PUBLICATIONS	STUDENT PAPERS

PRIMARY SOURCES

1	Anurag Kumar Singh, Vivek K. Chaturvedi, Jay Singh. "Nanoarchitectonics for Brain Drug Delivery", CRC Press, 2024 Publication	1%
2	Mantosh Kumar Satapathy, Ting-Lin Yen, Jing-Shiun Jan, Ruei-Dun Tang, Jia-Yi Wang, Rajeev Taliyan, Chih-Hao Yang. "Solid Lipid Nanoparticles (SLNs): An Advanced Drug Delivery System Targeting Brain through BBB", Pharmaceutics, 2021 Publication	1%
3	Ronald F. Pfeiffer, Zbigniew K. Wszolek, Manuchair Ebadi. "Parkinson's Disease", CRC Press, 2019 Publication	1%
4	www.frontiersin.org Internet Source	1%
5	Rajesh Pahwa, Kelly E. Lyons. "Handbook of Parkinson's Disease", CRC Press, 2019 Publication	<1%

www.omicsdi.org

6	Internet Source	<1 %
7	Wenyi Liang, Wei Xu, Jing Zhu, Yadong Zhu et al. "Ginkgo biloba extract improves brain uptake of ginsenosides by increasing blood-brain barrier permeability via activating A1 adenosine receptor signaling pathway", Journal of Ethnopharmacology, 2020 Publication	<1 %
8	www.lusofarmaco.it Internet Source	<1 %
9	network.bepress.com Internet Source	<1 %
10	Submitted to Harrisburg University of Science and Technology Student Paper	<1 %
11	Submitted to Leyton Sixth Form College Student Paper	<1 %
12	Daniela Oliveira, Cheryl Latimer, Pier Parpot, Chris I. R. Gill, Rui Oliveira. "Antioxidant and antigenotoxic activities of Ginkgo biloba L. leaf extract are retained after in vitro gastrointestinal digestive conditions", European Journal of Nutrition, 2019 Publication	<1 %
13	www.pubfacts.com Internet Source	<1 %

14	Ibai Tamayo, Carlos Gamazo, Juliana de Souza Rebouças, Juan M. Irache. "Topical immunization using a nanoemulsion containing bacterial membrane antigens", <i>Journal of Drug Delivery Science and Technology</i> , 2017 Publication	<1 %
15	Ikumi Tamai. "Transporter-mediated permeation of drugs across the blood-brain barrier", <i>Journal of Pharmaceutical Sciences</i> , 11/2000 Publication	<1 %
16	www.researchgate.net Internet Source	<1 %
17	Ying Mak, Maria Wai, David Yew. "The Neuroprotective Effect of Ginkgo biloba Leaf Extract and its Possible Mechanism", <i>Central Nervous System Agents in Medicinal Chemistry</i> , 2007 Publication	<1 %
18	digitalcommons.wayne.edu Internet Source	<1 %
19	journals.plos.org Internet Source	<1 %
20	www.crookstontimes.com Internet Source	<1 %

21	"Lysosomal Storage Disorders", Wiley, 2022 Publication	<1 %
22	James E. Frampton. "Pramipexole Extended-Release: A Review of Its Use in Patients with Parkinson's Disease", Drugs, 2014 Publication	<1 %
23	K MacLennan. "The CNS effects of Ginkgo biloba extracts and ginkgolide B", Progress in Neurobiology, 2002 Publication	<1 %
24	Ahmad, M.. "Attenuation by Nardostachys jatamansi of 6-hydroxydopamine-induced parkinsonism in rats: behavioral, neurochemical, and immunohistochemical studies", Pharmacology, Biochemistry and Behavior, 200601 Publication	<1 %
25	Colin R. Martin, Victor R. Preedy, Ross J. Hunter. "Nanomedicine and the Nervous System", CRC Press, 2019 Publication	<1 %
26	Robert A. Peattie, Robert J. Fisher, Joseph D. Bronzino, Donald R. Peterson. "Transport Phenomena in Biomedical Engineering - Principles and Practices", CRC Press, 2019 Publication	<1 %
27	www.ncbi.nlm.nih.gov	

Internet Source

<1%

28

Rajesh Pahwa, Kelly E. Lyons, William Koller.
"Therapy of Parkinson's Disease", CRC Press,
2019

Publication

<1%

Exclude quotes On

Exclude matches Off

Exclude bibliography On

Appendix C3

Turnitin Report Chapter 5:

Chapter 5.docx

ORIGINALITY REPORT

11 %	7 %	10 %	2 %
SIMILARITY INDEX	INTERNET SOURCES	PUBLICATIONS	STUDENT PAPERS

PRIMARY SOURCES

1	www.ncbi.nlm.nih.gov Internet Source	3 %
2	www.frontiersin.org Internet Source	1 %
3	Chao Ren, Yu Ding, Shizhuang Wei, Lina Guan, Caiyi Zhang, Yongqiang Ji, Fen Wang, Shaohua Yin, Peiyuan Yin. "G2019S Variation in LRRK2: An Ideal Model for the Study of Parkinson's Disease?", <i>Frontiers in Human Neuroscience</i> , 2019 Publication	1 %
4	Tutu Kalita, Saba Abbasi Dezfouli, Lalit M. Pandey, Hasan Uludag. "siRNA Functionalized Lipid Nanoparticles (LNPs) in Management of Diseases", <i>Pharmaceutics</i> , 2022 Publication	1 %
5	Camilla Hald Albertsen, Jayesh Kulkarni, Dominik Witzigmann, Marianne Lind, Karsten Petersson, Jens B. Simonsen. "The role of lipid components in lipid nanoparticles for	<1 %

vaccines and gene therapy", Advanced Drug
Delivery Reviews, 2022

Publication

-
- | | | |
|----|--|------|
| 6 | Submitted to October University for Modern Sciences and Arts (MSA)
Student Paper | <1 % |
| 7 | "Novel Therapeutic Approaches to the Treatment of Parkinson's Disease", Springer Science and Business Media LLC, 2016
Publication | <1 % |
| 8 | Xu Tang, Shuaishuai Xing, Mingkang Ma, Ziwei Xu et al. "The Development and Design Strategy of Leucine-Rich Repeat Kinase 2 Inhibitors: Promising Therapeutic Agents for Parkinson's Disease", Journal of Medicinal Chemistry, 2023
Publication | <1 % |
| 9 | Md. Shariful Islam, Darren J. Moore. "Mechanisms of LRRK2-dependent neurodegeneration: role of enzymatic activity and protein aggregation", Biochemical Society Transactions, 2017
Publication | <1 % |
| 10 | Submitted to The University of Texas at Tyler
Student Paper | <1 % |
| 11 | www.intechopen.com
Internet Source | <1 % |
-

12	Submitted to Associatie K.U.Leuven Student Paper	<1 %
13	Submitted to Monash University Student Paper	<1 %
14	Antonio Sánchez-Rodríguez, Cristina Tirnauca, Diana Salas-Gómez, Mario Fernández-Gorgojo et al. "Sensor-based gait analysis in the premotor stage of LRRK2 G2019S-associated Parkinson's disease", Parkinsonism & Related Disorders, 2022 Publication	<1 %
15	Qiuyang Zhang, Xiaojuan Cheng, Wei Wu, Siyu Yang, Hanlin You, Zucheng Ye, Nan Liu, Xiaochun Chen, Xiaodong Pan. "Age-related LRRK2 G2019S Mutation Impacts Microglial Dopaminergic Fiber Refinement and Synaptic Pruning Involved in Abnormal Behaviors", Journal of Molecular Neuroscience, 2021 Publication	<1 %
16	Submitted to University of Reading Student Paper	<1 %
17	Wallings, Rebecca, Claudia Manzoni, and Rina Bandopadhyay. "Cellular processes associated with LRRK2 function and dysfunction", FEBS Journal, 2015. Publication	<1 %

18	Borkwei Ed Nignpense, Boris Budiono, Nidhish Francis, Christopher Blanchard, Abishek Bommannan Santhakumar. "The Effect of In Vitro Digestion on the Anti-allergic, Anti-Inflammatory and Antioxidant Properties of Purple Rice and Purple Barley Phenolic Extracts in Caco-2 and RBL-2H3 Cells", Food Bioscience, 2024 Publication	<1 %
19	Submitted to King's College Student Paper	<1 %
20	ia801006.us.archive.org Internet Source	<1 %
21	Submitted to Durban University of Technology Student Paper	<1 %
22	Andreia Ascenso, Sandra Simões, Helena Ribeiro. "Carrier-Mediated Dermal Delivery - Applications in the Prevention and Treatment of Skin Disorders", CRC Press, 2017 Publication	<1 %
23	hal.archives-ouvertes.fr Internet Source	<1 %
24	preview-bmcmolbiol.biomedcentral.com Internet Source	<1 %
25	"Symposia", Journal of Neurochemistry, 2019 Publication	<1 %

<1 %

26

Qiting Yao, Qing Yang, Zhenyu Li, Fan Wu, Shi Duan, Mengxi Cao, Xinhua Chen, Xueping Zhong, Qingchun Zhou, Haobin Zhao. "Methylosome protein 50 is necessary for oogenesis in medaka", Comparative Biochemistry and Physiology Part D: Genomics and Proteomics, 2024

Publication

<1 %

27

Sarwar Beg, Mahfoozur Rahman, Syed Sarim Imam, Nabil K. Alruwaili, Majed Al Robaian, Sunil Kumar Panda. "Pharmaceutical Drug Product Development and Process Optimization - Effective Use of Quality by Design", CRC Press, 2020

Publication

<1 %

28

www.omicsdi.org

Internet Source

<1 %

29

www.sciencegate.app

Internet Source

<1 %

30

www.tandfonline.com

Internet Source

<1 %

31

Aurelie de Rus Jacquet, Jenna L Tancredi, Andrew L Lemire, Michael C DeSantis, Wei-Ping Li, Erin K O'Shea. "The LRRK2 G2019S mutation alters astrocyte-to-neuron

<1 %

communication via extracellular vesicles and induces neuron atrophy in a human iPSC-derived model of Parkinson's disease", Cold Spring Harbor Laboratory, 2021

Publication

32 Ga Ram Jeong, Byoung Dae Lee. "Pathological Functions of LRRK2 in Parkinson's Disease", Cells, 2020 <1 %

Publication

33 Mirza Hasanuzzaman, Masayuki Fujita, Hirosuke Oku, M. Tofazzal Islam. "Plant Tolerance to Environmental Stress - Role of Phytoprotectants", CRC Press, 2019 <1 %

Publication

34 Sylvie Delcambre, Jenny Ghelfi, Nassima Ouzren, Léa Grandmougin et al. "Mitochondrial Mechanisms of LRRK2 G2019S Penetrance", Frontiers in Neurology, 2020 <1 %

Publication

Exclude quotes On

Exclude matches Off

Exclude bibliography On

Appendix C4

Turnitin Report Chapter 6:

DM20240654 Revised Version .docx

ORIGINALITY REPORT

17 %	14 %	15 %	9 %
SIMILARITY INDEX	INTERNET SOURCES	PUBLICATIONS	STUDENT PAPERS

PRIMARY SOURCES

1	Submitted to University of KwaZulu-Natal Student Paper	3 %
2	Aliscia N Daniels, Moganavelli Singh. "Sterically stabilized siRNA:gold nanocomplexes enhance silencing in a breast cancer cell model ", Nanomedicine, 2019 Publication	3 %
3	Jeaneen Venkatas, Moganavelli Singh. "Curcumin-reduced gold nanoparticles facilitate delivery to a cervical cancer cell model ", Nanomedicine, 2023 Publication	2 %
4	researchspace.ukzn.ac.za Internet Source	2 %
5	gmd.copernicus.org Internet Source	1 %
6	mdpi-res.com Internet Source	1 %
7	www.mdpi.com Internet Source	1 %

8	www.ncbi.nlm.nih.gov Internet Source	1 %
9	Jeaneen Venkatas, Moganavelli Singh. "Chemical and green synthesis of gold nanoparticles for mRNA delivery in vitro", <i>Advances in Natural Sciences: Nanoscience and Nanotechnology</i> , 2024 Publication	1 %
10	Tanzimjahan A. Saiyed, Jerry O. Adeyemi, Moganavelli Singh, Sunday N. Okafor, Damian C. Onwudiwe. "Synthesis, characterization, and biological evaluation of some metal complexes containing N and S donor atoms", <i>Results in Chemistry</i> , 2023 Publication	<1 %
11	www.toxicology.org Internet Source	<1 %
12	www.frontiersin.org Internet Source	<1 %
13	digitalcommons.wpi.edu Internet Source	<1 %
14	Maryam Amidi, Stefan G. Romeijn, Gerrit Borchard, Hans E. Junginger, Wim E. Hennink, Wim Jiskoot. "Preparation and characterization of protein-loaded N-trimethyl chitosan nanoparticles as nasal delivery system", <i>Journal of Controlled Release</i> , 2006	<1 %

Publication

15	www2.mdpi.com Internet Source	<1 %
16	Submitted to University of Ulsan Student Paper	<1 %
17	ruor.uottawa.ca Internet Source	<1 %
18	etheses.whiterose.ac.uk Internet Source	<1 %
19	www.researchgate.net Internet Source	<1 %
20	www.rsc.org Internet Source	<1 %
21	www.sfstore.org Internet Source	<1 %
22	P. Plevka, S. Hafenstein, K. G. Harris, J. O. Cifuentes et al. "Interaction of Decay-Accelerating Factor with Echovirus 7", <i>Journal of Virology</i> , 2010 Publication	<1 %
23	Chick, Helen Elizabeth, Ali Nowrouzi, Raffaele Fronza, Robert McDonald, Nicole Kane, Raul Alba, Christian Delles, William C. Sessa, Manfred Schmidt, Adrian Thrasher, and Andrew H Baker. "Integrase-deficient lentiviral	<1 %

vectors mediate efficient gene transfer to human vascular smooth muscle cells with minimal genotoxic risk", Human Gene Therapy, 2012.

Publication

24 Dongyou Liu. "Handbook of Nucleic Acid Purification", CRC Press, 2019 <1 %

Publication

25 Femi Olawale, Mario Ariatti, Moganavelli Singh. "Ocimum tenuiflorum L mediated green synthesis of silver and selenium nanoparticles: antioxidant activity, cytotoxicity and density functional theory studies", Advances in Natural Sciences: Nanoscience and Nanotechnology, 2022 <1 %

Publication

26 Kirill A. Afonin, Morgan Chandler. "Therapeutic RNA Nanotechnology - Immunomodulation and Dynamicity", Jenny Stanford Publishing Pte. Ltd., 2021 <1 %

Publication

27 Sina Katharina Goetzfried, Matthijs L. A. Hakkennes, Anja Busemann, Sylvestre Bonnet. "Treatment of Glioblastoma tumors using photoactivated chemotherapy", American Chemical Society (ACS), 2024 <1 %

Publication

28	Unnati Patel, Kavini Rathnayake, Nirupama Singh, Emily C. Hunt. "Dual Targeted Delivery of Liposomal Hybrid Gold Nano-Assembly for Enhanced Photothermal Therapy against Lung Carcinomas", ACS Applied Bio Materials, 2023 Publication	<1 %
29	library2.usask.ca Internet Source	<1 %
30	pure.rug.nl Internet Source	<1 %
31	researchspace.csir.co.za Internet Source	<1 %
32	www.dovepress.com Internet Source	<1 %
33	www.science.gov Internet Source	<1 %
34	www.spandidos-publications.com Internet Source	<1 %
35	Knox Van Dyke, Christopher Van Dyke, Karen Woodfork. "Luminescence Biotechnology - Instruments and Applications", CRC Press, 2019 Publication	<1 %
36	Taosheng Chen. "A Practical Guide to Assay Development and High-Throughput Screening	<1 %

in Drug Discovery", CRC Press, 2019

Publication

Exclude quotes On

Exclude matches Off

Exclude bibliography On

Appendix C5

Turnitin Report Chapter 7:

Chapter 7.docx			
ORIGINALITY REPORT			
5%	3%	3%	0%
SIMILARITY INDEX	INTERNET SOURCES	PUBLICATIONS	STUDENT PAPERS
PRIMARY SOURCES			
1	Jeaneen Venkatas, Moganavelli Singh. "Curcumin-reduced gold nanoparticles facilitate delivery to a cervical cancer cell model ", Nanomedicine, 2023 Publication	1%	
2	hdl.handle.net Internet Source	1%	
3	researchspace.ukzn.ac.za Internet Source	<1%	
4	Delle Monache, Simona, Patrizia Sanità, Elena Trapasso, Maria Rita Ursino, Paola Dugo, Marina Russo, Nadia Ferlazzo, Gioacchino Calapai, Adriano Angelucci, and Michele Navarra. "Mechanisms Underlying the Anti-Tumoral Effects of Citrus bergamia Juice", PLoS ONE, 2013. Publication	<1%	
5	Wanrui Li, Xuanyi Pan, Ming Li, Li ling, MengMeng Zhang, Ziming liu, Ke Zhang, Jiguang Guo, Hongjie Wang. "Impact of age on the rotenone-induced sporadic Parkinson's	<1%	

disease model using *Drosophila melanogaster*", Neuroscience Letters, 2023

Publication

6	en.wikipedia.org Internet Source	<1 %
7	Submitted to University of Western Ontario Student Paper	<1 %
8	Submitted to Trinity College Dublin Student Paper	<1 %
9	pubag.nal.usda.gov Internet Source	<1 %
10	Fabio Candotti. "THE POTENTIAL FOR THERAPY OF IMMUNE DISORDERS WITH GENE THERAPY", Pediatric Clinics of North America, 2000 Publication	<1 %
11	Ping-Kun Tsai, Sheng-Wen Wu, Chen-Yu Chiang, Min-Wei Lee et al. "Evaluation of cytotoxicity, apoptosis, and genotoxicity induced by indium chloride in macrophages through mitochondrial dysfunction and reactive oxygen species generation", Ecotoxicology and Environmental Safety, 2020 Publication	<1 %
12	precisionmedicine.uni.lu Internet Source	<1 %

13	mdpi-res.com Internet Source	<1 %
14	repository.ubn.ru.nl Internet Source	<1 %
15	scholarworks.uvm.edu Internet Source	<1 %
16	www.pharmaceutical-technology.com Internet Source	<1 %
17	Damilare Emmanuel Rotimi, Marvellous A. Acho, Babatunde Michael Falana, Tomilola Debby Olaolu et al. "Oxidative Stress-induced Hormonal Disruption in Male Reproduction", <i>Reproductive Sciences</i> , 2024 Publication	<1 %
18	docslib.org Internet Source	<1 %
19	jbc.bj.uj.edu.pl Internet Source	<1 %
20	usiena-air.unisi.it Internet Source	<1 %
21	www.biorxiv.org Internet Source	<1 %
22	www.ncbi.nlm.nih.gov Internet Source	<1 %

- 23 Hrudayanath Thatoi, Swagat Kumar Das, Sonali Mohapatra. "Bioresource Utilization and Management - Applications in Therapeutics, Biofuels, Agriculture, and Environmental Scienc", CRC Press, 2021
Publication <1 %
-
- 24 Long Chen, Qiushi Li, Hao Wang, Quan Chen, Yuanyuan Wu, You Shang. "Paeoniflorin attenuated bupivacaine-induced neurotoxicity in SH-SY5Y cells via suppression of the p38 MAPK pathway", Journal of Cellular Biochemistry, 2018
Publication <1 %
-
- 25 d-nb.info
Internet Source <1 %
-
- 26 ruja.ujaen.es
Internet Source <1 %
-
- 27 www.science.gov
Internet Source <1 %
-
- 28 Sushil Sharma. "Charnolophagy in Health and Disease - With Special Reference to Nanotheranostics", CRC Press, 2021
Publication <1 %
-
- 29 Jiahao Zheng, Boran Li, Lanxin Jia, Jiayou Zhang et al. "Tumorigency decrease in Bcl-xL deficient MDCK cells ensuring the safety for <1 %

influenza vaccine production", Cold Spring Harbor Laboratory, 2024

Publication

30

Rajesh Pahwa, Kelly E. Lyons Ph.D..
"Handbook of Parkinson's Disease", CRC
Press, 2019

Publication

<1%

Exclude quotes On

Exclude matches Off

Exclude bibliography On